Alma Mater Studiorum – Università degli Studi di Bologna

FACOLTÀ DI SCIENZE MATEMATICHE, FISICHE E NATURALI
Dipartimento di Chimica "G. Ciamician"

DOTTORATO DI RICERCA IN
SCIENZE CHIMICHE
Ciclo XXIII

Settore scientifico-disciplinare di afferenza: CHIM 03

POLYMORPHS SOLVATES AND CO-CRYSTALS OF MOLECULAR MATERIALS

Presentata da:
Dott.ssa
ELENA DICHIARANTE

Relatore:
Chiar.mo Prof.
DARIO BRAGA

Coordinatore Dottorato:
Chiar.mo Prof.
GIULIANO LONGONI

Esame finale - Anno 2011

INDEX

PREFACE

It is a fact of Nature that the solid phase of a material may exhibit different structures (carbon, silica, ice, etc. as well as very many molecular crystals). In addition to different crystal structures called *polymorphs,* which are characterized by long range order, a material may appear as an amorphous solid phase characterized by the lack of long range order. Different solid state structures manifest themselves in different properties. The formal recognition of the phenomenon of *crystal polymorphism* is generally credited to E. Mitscherlich,[1]even though the existence of different crystal forms of calcium carbonate (calcite, vaterite and aragonite) was identified much earlier by M. H. Klaproth in 1788.[2]

The phenomenon of *polymorphism* is ubiquitous in the solid state and involves all sort of crystalline solids, from purely covalent, where directional sigma bonds between atoms are the exclusive interactions (i.e. silica at atmospheric pressure can exist as low quartz, high quartz, tridymite and cristobalite), to "purely molecular", where dispersive non-covalent interactions are the only sources of stability for the crystal (i.e. S_8sulphur exists as α, β and γ phases) and in between the plethora of molecular solids formed by all combination of directional and semi-directional non covalent interactions coupled with covalent skeletons and/or with ionic contributions arising from charge transfer. Each of these crystals may show polymorphism, depending on the conditions of investigation, or preparation or treatment.

However, as the scientific and utilitarian interest on the structure-property relationships of crystals, especially molecular crystals, expands and attracts new adepts from the communities of supramolecular, materials, nanomaterials, biomaterials, and theoretical chemists, the term "polymorphism" appears to be too specific to account for the breadth of the field. Take a molecule M: beside potentially forming single entity polymorphs, M may crystallize with various numbers of solvent molecules, M can form co-crystals with a number of partners, and these co-crystals may also be solvates, M may forms salts (e.g. when proton

transfer is possible), and these salts may carry solvent molecules in the crystal structure, etc..Furthermore, any of these additional crystal forms of M may show crystal polymorphism [3]i.e. exhibit alternative crystal structures for the same chemical composition.

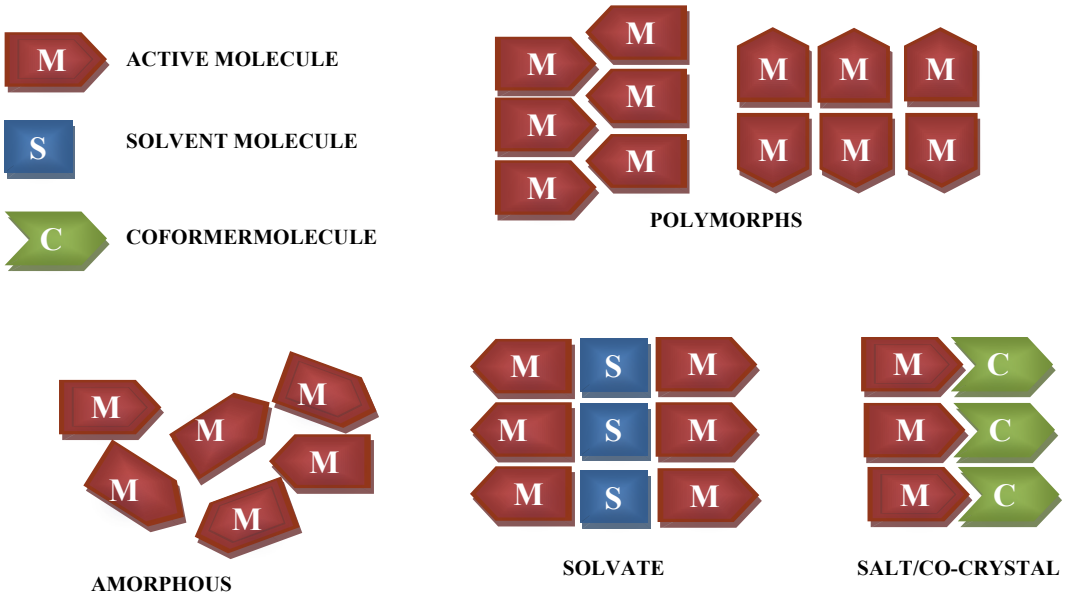

Figure 1. Scheme of various types of solid forms.

Solvates and hydrates are crystal forms that have different properties from those of the corresponding solvent-free species.[4] One can use desolvation/dehydration processes to generate new crystal forms of lower solvates/hydrates or of the solvent-free crystals.[5]

Crystals containing solvent molecules (solvates) are often formed unpredictably. Whether a given molecule will precipitate out of a solvent, say water, with one or more molecules of water in the unit cell is not foreseeable. Nor is it predictable whether the hydrate will be more stable or less stable of the corresponding anhydrous forms, or whether other sub- or super-hydrates, let alone non-stoichiometric hydrates stable over a range of compositions, will be formed. The practical consequences of this "uncertainty principle" are enormous as they impact on stability, processability, and reproducibility, even transport and manufacture conditions, hence on the market potentials, of any chemical species.

Co-crystals represent a means to further expand the variability of crystal forms and to access new solid-state properties. The great potential of co-crystals resides in their different properties (solubility, dissolution rate, melting point, color, etc.) with respect to those of the single entity crystals. At the same time the process of co-crystal formation does not alter the chemical integrity of the component of interest, such as an active pharmaceutical ingredient. In fact, co-crystals are at the forefront of the quest for novel crystal forms, mainly, but not only, because of the interest in the pharmaceutical field and in all areas where the final products are commercialized and utilized in their solid state forms.[6] In the academic world co-crystals are intensively investigated because they provide new insights into the mechanisms of recognition, assembly and packing.[7]The very definition of a co-crystal is still controversial, because the borderline between solvates, molecular salts (e.g. when proton transfer along a hydrogen bond is involved) and molecular complexes is somewhat difficult to define.[8,9]

However, we can define a co-crystal as a multiple-component crystal in which two or more molecules that are solids under ambient conditions coexist through a hydrogen bond.[10]

Complementary supramolecularsynthons[11] that seem to favor formation of co-crystals are exemplified by carboxylic acid-pyridine[12], carboxylic acid- amide [13] and alcohol-pyridine.[14] Co-crystals involving these supramolecular synthons are usually synthesized by slow evaporation from a solution containing stoichiometric amounts of the components (co-crystal formers); however, sublimation, growth from the melt, grinding of two solid co-crystal formers in a ball mill and solvent-drop grinding (addition of a small amount of suitable solvent to the ground mixture to accelerate co-crystallization)[15] are also suitable methodologies.

Co-crystals in the pharmaceutical field offer opportunities to modify the properties (solubility, stability, hygroscopicity and dissolution rate) of an API without the modification of molecular structure. Furthermore a co-crystal might be used to isolate or purify an API during manufacturing and to separate enantiomers.[16]Another application of co-crystals in the pharmaceutical field is due to the possibility to obtain pharmaceutical co-crystals involving two or more

APIs[6b,17] overcoming the problem associated with traditional combination drugs[18] where two or more APIs are produced in a single tablets.[19] Multi-API co-crystals, in fact, represent unique solid forms of APIs and display physical and chemical properties different from their parent APIs. These advantages together with simple and convenient preparation methods favor multi-API co-crystals as potential combination drugs.[20]

The scope of my research project is to produce and characterize new crystalline forms of organic compounds, focusing the attention on co-crystals and then transferring these notions on APIs to produce co-crystals of potential interest in the pharmaceutical field.

In the first part of this work co-crystallization experiments were performed using as building blocks the family of aliphatic dicarboxylic acids HOOC-$(CH_2)_n$-COOH, with n= 2-8. This class of compounds has always been an object of study because it is characterized by an interesting phenomenon of alternation of melting points: the acids with an even number of carbon atoms show a melting point higher than those with an odd one.[21]

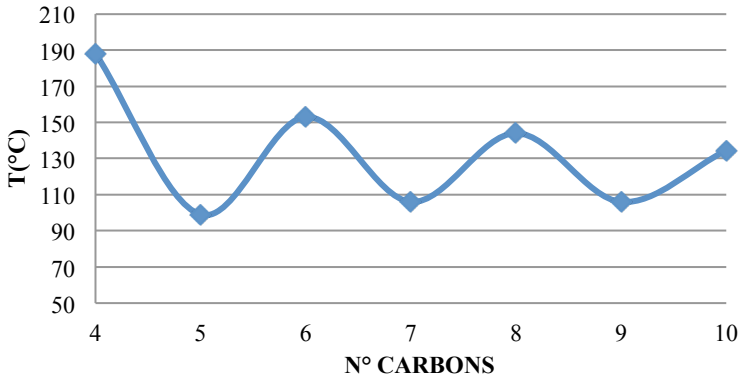

Figure 2. Melting point trend of aliphatic dicarboxylic acids HOOC-(CH2)n-COOH, with n= 2-8.

The acids were co-crystallized with four dipyridyl molecules (formed by two pyridine rings with a different number of bridging carbon atoms) through the formation of intermolecular interactions N···(H)O.

The bases used were (Scheme 1): 4,4'-bipyridine (BPY), 1,2-bis(4-pyridyl)ethane (BPA),1,2-(di-4-pyridyl)ethylene (BPE)and1,2-bis(4-pyridyl)propane (BPP). The co-crystals obtained by solution synthesis were characterized by different solid-state techniques to determine the structure and to see how the melting points in co-crystals change.

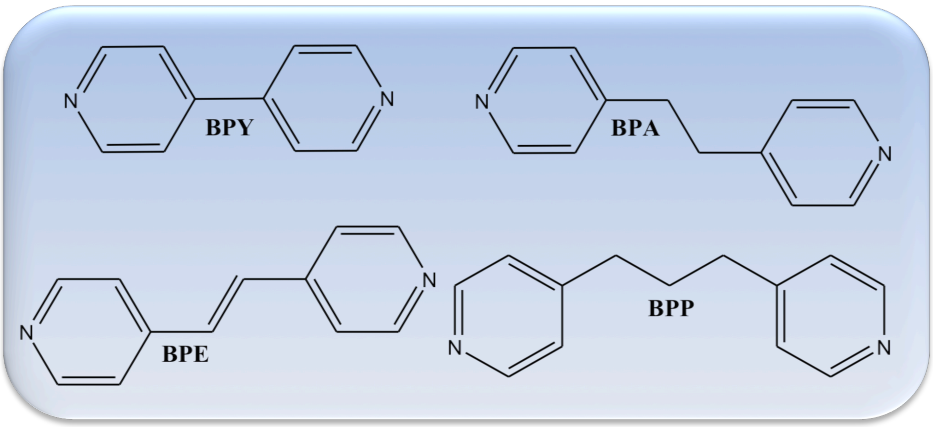

Scheme 1.

In the second part of this study we tried to obtain new crystal forms of compounds of pharmaceutical interest. The APIs studied (Scheme 2) are: O-desmethylvenlafaxine (**ODV**), Lidocaine (**1**), Nalidixic Acid (**2**) and Sulfadiazine (**3**).

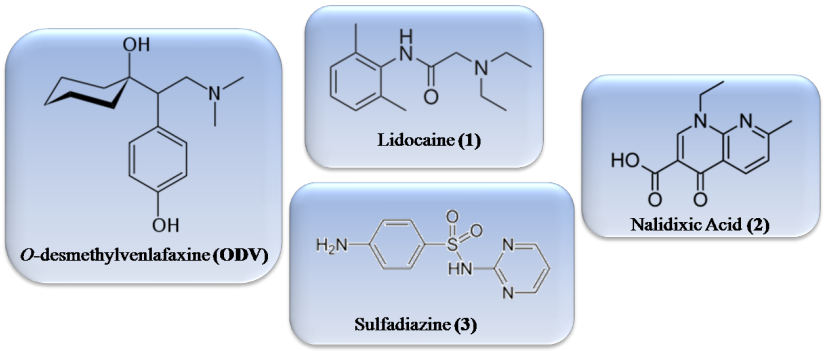

Scheme 2.

Each API was subjected to Polymorph Screening[22] (using the solvents summarized in Table 1) and Salt/Co-crystal Screening[23]experiments to identify new crystal forms characterized by different properties.

SOLVENT
DIETHYL ETHER
DICHLOROMETHANE
ACETONE
CHLOROFORM
METHANOL
n-HEXANE
ETHYL ACETATE
ETHANOL
ACETONITRILE
1,2-DIMETHOXYETHANE
1-PROPANOL
WATER
1,4-DIOXANE
NITROMETHANE
1-BUTANOL
2-METHOXY ETHANOL
p-XYLENE
DMF
DMSO

Table1. Solvents used in experiments of polymorph screening.

In a typical Salt/Co-crystal Screening the sample was made to react with a co-former (solid or liquid) through different methods: crystallization by solution, grinding, kneading and solid-gas reactions.[24]

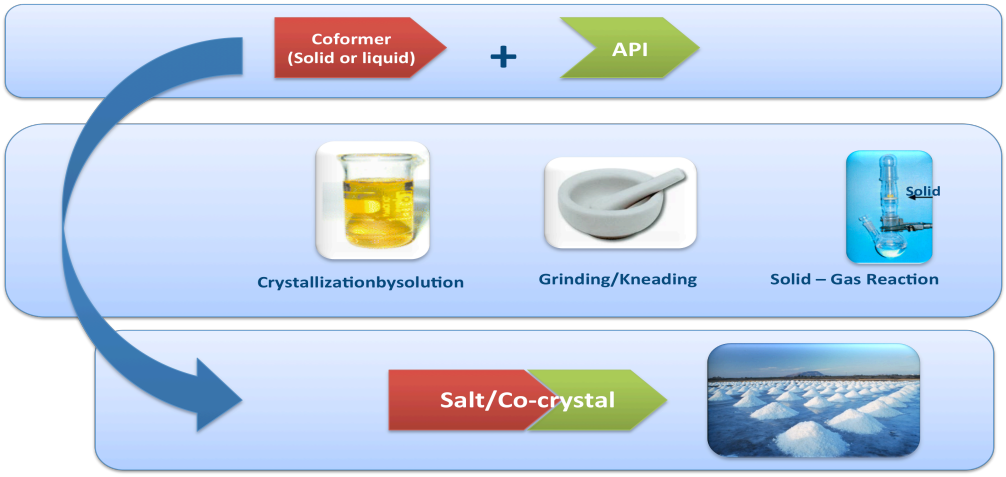

Figure 3. Methods used to prepare pharmaceutical co-crystals.

The co-formers are acids and bases chosen among the ones listed in the pharmaceutical handbook of salts on the basis of their properties (solubility, pKa). The pKa values are generally reliable indicators of salt formation when the ΔpKa (pKa of base – pKa of acid) is greater than 3, and they predict co-crystal formation when the ΔpKa is negative, while their predictive power is poor in the ΔpKa range 0-3. In this latter range, complexes between acids and bases can still form, although they can be salts or co-crystals or can contain shared protons or mixed ionization states that cannot be assigned to either category.[25] The new crystal forms obtained were characterized by different solid state techniques:

- X-ray single crystal diffraction (SC-XRD)
- X-ray powder diffraction (XRPD)
- Differential Scanning Calorimetry (DSC)
- Thermogravimetric Analysis (TGA)
- Evolved gas analysis(EGA)
- FT-IR – ATR
- Solid State N.M.R.

BASES	ACIDS	ACIDS
L-Arginine	Acetic Acid (d=1.05)	Oxalic Acid
CalciumHydroxide	Adipic Acid	Phosphoric Acid(M=14,65;d=1,689)
N-methyl-Glucamine	L-Aspartic Acid	Salicylic Acid
Imidazole	Citric Acid	Sebacic Acid
L-Lysine	Formic Acid (99%, d=1,22)	Succinic Acid
MagnesiumHydroxide	Fumaric Acid	L-Tartaric Acid
Piperazine	L-Glutamic Acid	Glutaric Acid
PotassiumHydroxide	Glycolic Acid	Cinnamic Acid
SodiumHydroxide (0,1 N)	Hippuric Acid	Folic acid
Triethanolamine (85% d=1,124)	Hydrochloric acid (0.1 N)	Ascorbic Acid
NH_3 (d=0,9)	Maleic Acid	Nicotinic Acid
Diethanolamine(d=1)	L-Malic Acid	
Diethylamine(d=0,704)	Malonic Acid	
Morpholine (d=1)	DL-Mandelic Acid	
Pyrrolidine (d=0,86)	DL-Mandelic Acid	
Adenine	MethanesulfonicAc (d=1,48)	

Table 2. List of acids and bases used in the Salt/Co-crystal Screening.

References

1. E. Mitscherlich, *Abhl. Akad. Berlin*, **1823**, 43-48.
2. M. H. Klaproth, *Bergmannische J.* I, **1798**, 294-299.
3. D. Braga, F. Grepioni, L. Maini, *Chem.Commun.*, **2010**, *46*, 6232-6242.
4. a) U. Griesser in *Polymorphism: in the Pharmaceutical Industry* (Ed.: R. Hilfiker), Wiley VCH, Weinheim, **2006**, pp. 211-234; b)R. K. Khankari, D. J. W. Grant, *Thermochim. Acta*, **1995**, *248*, 61.
5. J. K. Guillory in *Polymorphism in Pharmaceutical Solids*, *Vol. 95* (Ed.: H. G. Brittain), Marcel Dekker, Inc, New York, **1999**, pp. 183-226.
6. a) N. Schultheiss, A. Newman, *Cryst. Grow. Des.*, **2009**, *9*, 2950-2967; b) P. Vishweshwar, J. A. McMahon, M. L. Peterson, M. B. Hickey, T. R. Shattock, M. J. Zaworotko, *Chem.Commun.*, **2005**, 4601-4603.
7. See for instance: a) S. L. Childs, M. J. Zaworotko, *Cryst. Grow. Des.*, **2009**, *9*, 4208-4211; b) C. B. Aakeroy, D. J. Salmon, M. M. Smith, J. Desper, *CrystEngComm*, **2009**, *11*, 439-443; c) S. Eppel, J. Bernstein, *Cryst. Grow. Des.*, **2009**, *9*, 1683-1691; d) D. Braga, G. Palladino, M. Polito, K. Rubini, F. Grepioni, M. R. Chierotti, R. Gobetto, *Chem. Eur. J.*, **2008**, *14*, 10149-10159; e) M. Polito, E. D'Oria, L. Maini, P. G. Karamertzanis, F. Grepioni, D. Braga, S. L. Price, *CrystEngComm*, **2008**, *10*, 1848-1854.
8. a) A. D. Bond, *CrystEngComm*, **2007**, *9*, 833-834; b) S. Mohamed, D. A. Tocher, M. Vickers, P. G. Karamertzanis, S. L. Price, *Cryst. Grow. Des.*, **2009**, *9*, 2881-2889; c) S. L. Childs, G. P. Stahly, A. Park, *Mol. Pharmaceutics*, **2007**, *4*, 323-338; d) G. P. Stahly, *Cryst. Growth Des.*, **2007**, *7*, 1007-1026; e) C. B. Aakeroy, D. J. Salmon, *CrystEngComm,* **2005**, *7*, 439-448; f) P. Vishweshwar, J. A. McMahon, J. A. Bis, M. J. Zaworotko, *J. Pharm. Sci.*, **2006**, *95*, 499-516; g) G. R. Desiraju, *CrystEngComm*, **2003**, *5*, 466-467; h) J. D. Dunitz, *CrystEngComm*, **2003**, *5*, 506.
9. D. Braga, S. D'Agostino, E. Dichiarante, L. Maini, F. Grepioni, *Chem. Asian J.*, submitted.

10. O. Almarsson, M. J. Zaworotko, *Chem. Commun*., **2004**, 1889-1896.
11. G. R. Desiraju, *Angew. Chem.*, Int. Ed. Engl., **1995**, *34*, 2311-2327.
12. a) P. Vishweshwar, A. Nangia, V. M. Lynch, *J. Org. Chem.*, **2002**, *67*, 556-565; b) B. R. Bhogala, A. Nangia, *Cryst. Growth Des.*, **2003**, *3*, 547-554; c) A. D. Bond, *Chem.Commun.*, **2003**, 250-251.
13. a) S. Harkema, J. W. Bats, A. M. Weyenberg, D. Feil, *ActaCrystallogr*., **1972**, *B28*, 1646-1648; b) L. Leiserowitz, F. Nader, *ActaCrystallogr*., **1977**, *B33*, 2719-2733; c) L. S. Reddy, A. Nangia, V.M. Lynch, *Cryst. Growth Des.*, **2004**, *4*, 89-94; d) C. B. Aakeroy, A. M. Beatty, B. A. Helfrich, M. Nieuwenhuyzen,*Cryst. Growth Des.*,**2003**, *3*, 159-165
14. a) P. Vishweshwar, A. Nangia, V.M. Lynch, *CrystEngComm,* **2003**, *5*, 164-168; b) G. S. Papaefstathiou, M. Nieuwenhuyzen, *Org. Lett.*, **2001**, *3*, 3835-3838; c) K. Biradha, M. J. Zaworotko, *J. Am. Chem. Soc.*, **1998**, *120*, 6431-6432.
15. a) A. V. Trask, W. D. S. Motherwell, W. Jones, *Chem. Commun.,* **2004**, 890-891; b) N. Shan, F. Toda, W. Jones, *Chem. Commun.,* **2002**, 2372-2373.
16. P. Vishweshwar, J. A. McMahon, M. J. Zaworotko in *FRONTIERS IN CRYSTAL ENGINEERING* (Eds. E. R. T. Tiekink, J. J. Vittal), J. Wiley & Sons, Ltd, ***2006,*** pp. 25-49.
17. a) P. Vishweshwar, J. A. McMahon, M. Oliveira, M. L. Peterson, M. J. Zaworotko, *J. Am. Chem. Soc.*, **2005**, *127*, 16802; b) M. R. Caira, *Mol. Pharm.,* **2007**, *4*, 310; c) S. L. Childs, int. pat. Number, WO 2007/067727 A2, **2007**; d) N. Shan, M. J. Zaworotko, *Drug Discovery Today,* **2008**, *13*, 440-446.
18. a) A. I. Wertheimer, A. Morrison, *P&*T, **2002**, *27*, 44; b) K. K. Bucci, C. J. Possidente, *Am. J. Health. Syst. Pharm.,* **2006***, 63,* 1654; c) S. Frantz, *Nat. Rev.*, **2006**, *5*, 881.
19. U.S. Food and Drug Administration, Office of Combination Products, www.fda.gov/oc/combination/, 21 CFR Part 3.2.
20. S. Aitipamula, P. S. Chow, R. B. H. Tan, *CrystEngComm*, **2009***, 11,* 1823-1827.

21. V. R. Thalladi, M. Nusse, R. Boese, *J. Am. Chem. Soc.,* **2000**, *122,* 9227-9236.
22. R. Hilfiker, S. M. De Paul, M. Szelagiewicz in *Polymorphism: in the Pharmaceutical Industry* (Ed.: R. Hilfiker), Wiley VCH, Weinheim, **2006**, pp. 287-308.
23. M. J. Bowker in *Handbook of Pharmaceutical Salts: Properties, Selection, and Use* (Eds.: P. H. Stahl, C. G. Wermuth), Wiley VCH, Weinheim, **2008**, pp. 160-189.
24. D. Braga, M. Curzi, E. Dichiarante, S. L. Giaffreda, F. Grepioni, L. Maini, G. Palladino, A. Pettersen, M. Polito in *Engineering of Crystalline Materials Properties* (Eds. J. J. Novoa, D. Braga, L. Addadi), Springer, **2008**, pp. 131-156.
25. S. L. Childs, G. P. Stahly, A. Park, *Molecular Pharmaceutics,* **2007**, *Vol. 4,* No. 3, 323-338.

1. REMARKABLE REVERSAL OF MELTING POINT ALTERNATION BY CO-CRYSTALLIZATION

1.1. Introduction

Co-crystal is an interesting route to change the physical properties of single entity crystals, without altering the chemical integrity of the component. Although the main interest is in the pharmaceutical field, we would like to focus the attention of the reader on a more academic problem.[1]

The phenomenon of melting point alternation in n-alkanes and in most end-substituted n-alkanes has been known for decades.[2] Physical properties such as solubility and sublimation enthalpy, that are related to the solid state, also exhibit an alternating pattern,[3] whereas those related to the liquid state show monotonic behaviours. There is vast literature on this phenomen, various structural models have been put forward to explain the melting point alternation in n-alkane derivates.[4] Organic di-acids of the type $HOOC(CH_2)_nCOOH$ are also known to show melting point alternation[5] depending on the number of carbon atoms in the chain. The only examples of variations in the melting point alternation induced by co-crystallization have been reported in a paper by A. Bond et al.,[6] in which co-crystals of n-alkyl carboxylic acids with pyrazine show a steady increase in their melting temperatures for $n(CH_2) \geq 5$, and in a paper by Callear et al.,[7] in which co-crystals of imidazole derivatives with α,ω-alkanedicarboxylic acids ($HOOC(CH_2)_nCOOH$, n = 0–6) show a different behaviour in the melting point when $n(CH_2) = 4$.

In the course of our crystal engineering efforts to prepare molecular co-crystals and salts by means of mechanical and other non-solution methods, we have synthesised and structurally characterized several families of acid-base adducts.[8]

In particular, in 2003, we reported the first observation of melting point alternation in co-crystals.[8a]In the course of the investigation of mechanochemically prepared hydrogen bonded co-crystals of DABCO ($N(CH_2CH_2)_3N$) and dicarboxylic acids $HOOC(CH_2)_nCOOH$ (n= 1-7) we

noticed that, irrespective of the salt (proton transfer from the acid to DABCO) or molecular (no proton transfer) nature of the products, the melting points of the even-acid adducts were systematically higher than those of the odd-acid adducts.[1]

In this project, the melting point behaviour of acid-base pairs was investigated for several bases belonging to the family of the dipyridyl molecules, which are constituted of two pyridine rings with a different number of bridging carbon atoms. The bases are labelled as BPA(1,2-bis(4-pyridyl)ethane), BPP (1,2-bis(4-pyridyl)propane), BPY (4,4'-bipyridine) and BPE (1,2-(di-4-pyridyl)ethylene), see Scheme 1, and we refer to the diacids by the total number of carbon atoms in the molecule (C4 corresponding to succinic acid, C5 to glutaric acid, etc.), hence the adducts are identified as BPA·C4 ÷ BPA·C10, BPP·C4 ÷ BPP·C10, BPY·C4 ÷ BPY·C10 and BPE·C4 ÷ BPE.

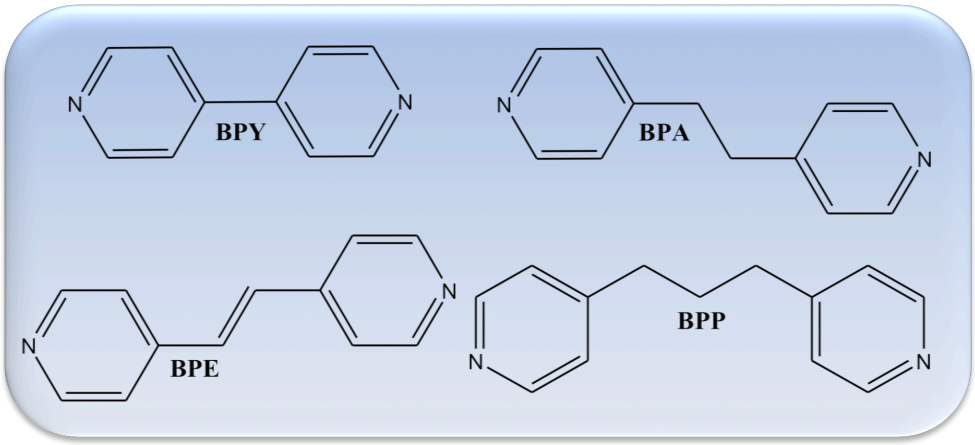

Scheme 1

1.2. Experimental

All reactants and solvents were purchased from Sigma Aldrich and used without further purification.

1.2.1. Solution syntheses of BPA C_n (n = 4-10), BPP C_n (n = 4,5,7,8,9,10), BPY C_n (n = 4,5,6,7,9,10), BPE C_7

Crystalline powder and single crystals were obtained by reaction in methanol solution. The reagents (0.5mmol of acid and 0.05mmol of base) were added to ca. 10-15 mL of methanol, the solution was heated until complete dissolution and left to evaporate slowly at ca. 4°C.

1.2.2. Solution synthesis of BPP C_6

Crystalline powder and single crystals were obtained by reaction in water solution. The reagents (0.5mmol of acid and 0.05mmol of base) were added to ca. 10-15 mL of bidistilled water, the solution was heated until complete dissolution and left to evaporate slowly at ca. 4°C.

1.2.3. Solution synthesis of BPY C_8

Crystalline powder and single crystals were obtained by reaction in ethanol solution. The reagents (0.5mmol of acid and 0.05mmol of base) were added to ca. 10-15 mL of ethanol, the solution was heated until complete dissolution and left to evaporate slowly at ca. 4°C.

1.2.4. Solution syntheses of BPE C_n (n = 4, 5, 6, 8, 9, 10)

Crystalline powder and single crystals were obtained by reaction in acetone-ethanol solution. The reagents (0.5mmol of acid and 0.05mmol of base) were added to ca. 10-15 mL of a mixture acetone-ethanol (2-1), the solution was heated until complete dissolution and left to evaporate slowly at ca. 4°C.

1.2.5. **Differential Scanning Calorimetry (DSC)**

Differential scanning calorimetry was used to measure the melting point of all compounds and to detect the presence of additional crystalline phases. In some cases solid-solid phase transitions to higher temperature polymorphs were also observed before melting (**BPA**·C6, 133 °C (onset), **BPA**·C8, 131 °C (onset), **BPA**·C9, 123 °C (onset).

Calorimetric measurements were performed using a Perkin Elmer Pyris Diamond DSC differential scanning calorimeter equipped with a model ULSP 90 intra-cooler. The instrument was calibrated with high-purity standards (indium and cyclohexane) at 5 K min^{-1}. The samples (2–4 mg) were placed in aluminium closed pans, and heating was carried out at 5°C min^{-1} .

1.2.6. **X-Ray diffraction**

Single-crystal data were collected on an Oxford X'Calibur S CCD diffractometer equipped with a graphite monochromator (MoKα radiation, λ = 0.71073) and operated at room temperature. The structures were solved by direct methods and refined by full-matrix least-squares on F2 with SHELX97[9a] program package.

A calculated XRPD pattern was generated for Cu radiation using Mercury v 1.4 or. PowderCell 2.2[9d]and the atomic coordinates, space group, and unit cell parameter from the single crystal data.

MERCURY and SCHAKAL99 [9b] were used for the graphical representation of the results and PLATON [9c] was used for hydrogen bonding analysis.

X-ray powder diffractograms were collected on a Panalytical X'Pert Pro automated Diffractometer equipped with X'Celerator, CuKα, using a glass sample holder. The tube voltage and amperage were set to 40 kV and 40 mA, respectively. The program used for data collection was set to record only the data points within the 2θ range 3 – 40 deg.

1.2.7. **Solid-state Nuclear Magnetic Resonance (SS NMR) spectroscopy**

SS NMR experiments were recorded on a Bruker Avance II 400 instrument. The spectra were collected and interpretated by the Research Group of Prof. Roberto Gobettoo at the University of Torino.

1.3. Results and discussion

In this project, the melting point behaviour of acid-base pairs was investigated for several bases belonging to the family of the dipyridyl molecules, which are constituted of two pyridine rings with a different number of bridging carbon atoms.

All co-crystals have been investigated by a combination of solid state techniques, namely single crystal [except for: **BPY**·Cn(n=5, 6, 7, 10), **BPE**·Cn(n=4, 6), **BPP**·C4, whose structures were already known[10], and **BPY**·C9, **BPP**·Cn(n=8, 9), **BPE**·Cn(n=7, 9, 10) for which no good single crystals were obtained] and powder X-ray diffraction, differential scanning calorimetry and solid-state NMR spectroscopy (SS NMR).

This latter in particular has been instrumental not only to the definition of the nature of the crystals, whether molecular or salts, resulting from the positioning of the acid protons in the O···H···N interactions,[8a,11] but also to the definition of the packing features in the adducts (BPP Cn), for which no single crystal X-ray data could be obtained.

All compounds were crystallized by slow evaporation from different solvents. Correspondence between the structures determined by single crystal X-ray diffraction and those of the bulk materials was checked by comparing calculated and measured powder patterns (See supplementary material). All compounds are characterized by the presence of infinite chains constituted of alternating base and acid units (Figure 1 and Figure 2), joined together via N···(H)O and C(H)···O hydrogen bonds in the series with BPA and BPP.Crystal data and details of measurements are summarized in Table 1, Table 2 and Table 3. Relevant hydrogen bonding distances (in Å) for all the compounds structurally characterized in this chapter are summarized in Table 4.

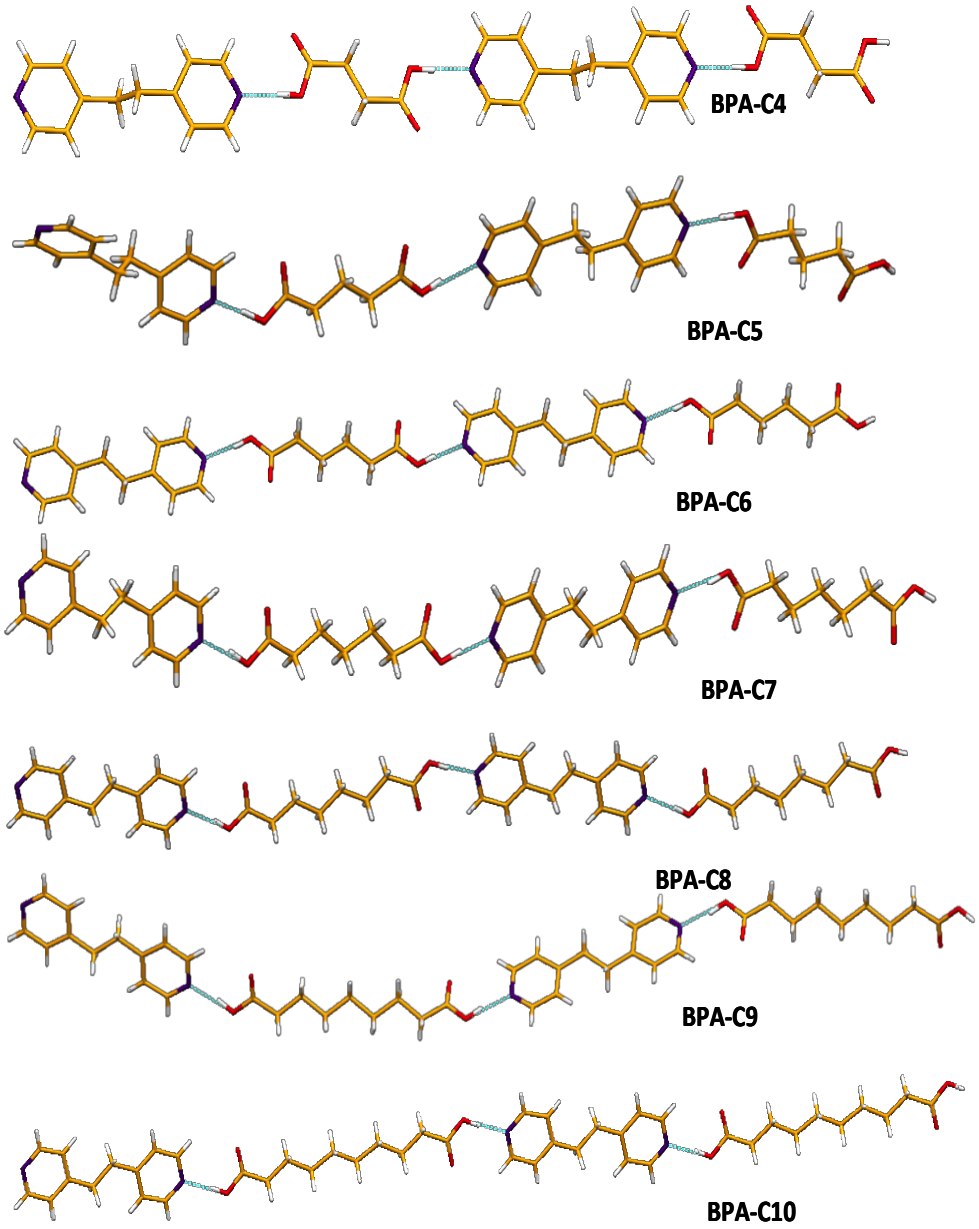

Figure 1. N···(H)O hydrogen bonded chains of base and acid units in (from top to bottom) crystalline **BPA·C4**, **BPA·C5**, **BPA·C6**, **BPA C7**, **BPA C8**, **BPA C9**, **BPA C10**.

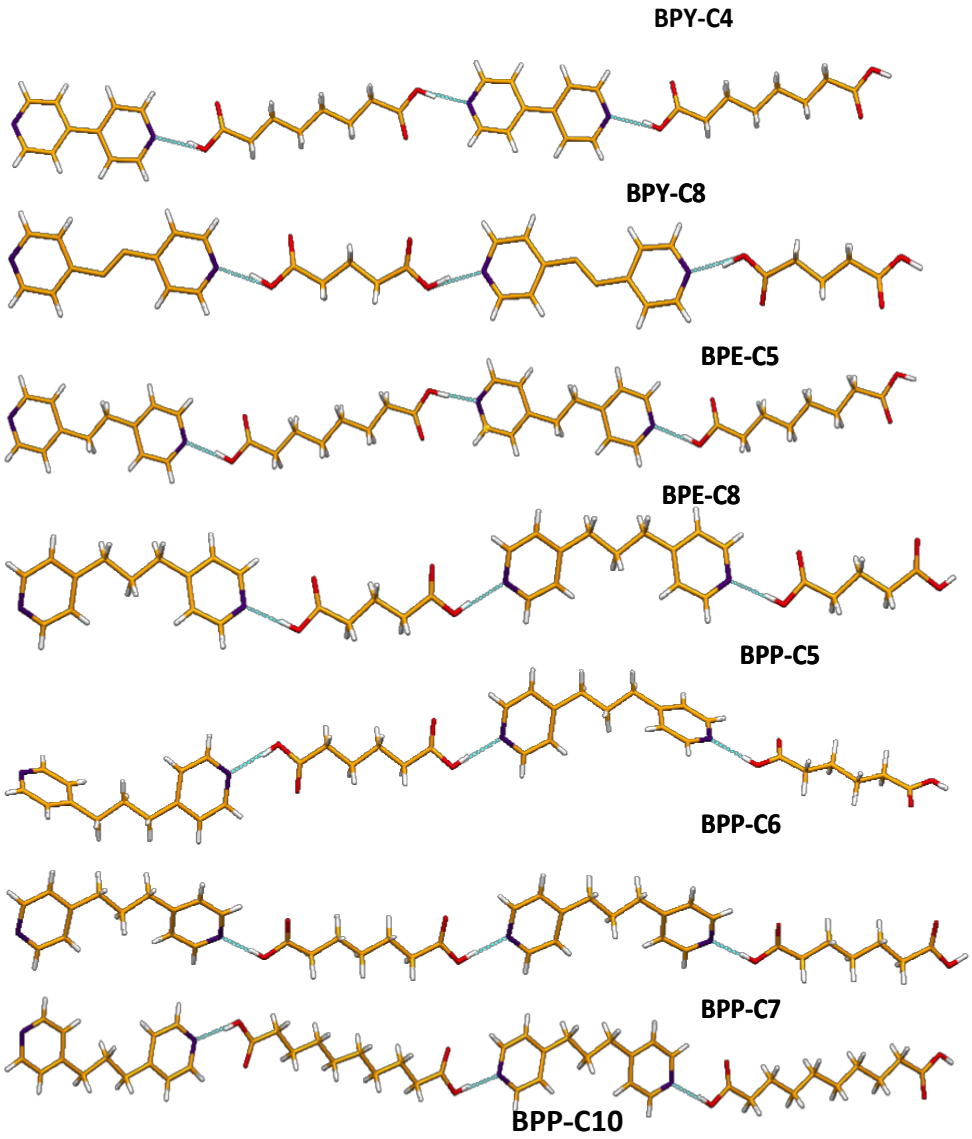

Figure 2. N···(H)O hydrogen bonded chains of base and acid units in (from top to bottom) crystalline **BPY·C4**, **BPY·C8**, **BPE·C5**, **BPE C8**, **BPP C5**, **BPP C6**, **BPP C7**, **BPP C10**.

Table 1. Crystal Data and Details of Measurements for compounds **BPY**·C4, **BPY**·C8, **BPE**·C5 and **BPE**·C8.

compound	BPY C4	BPY C8	BPE C5	BPE C8
Formula	$C_{14}H_{14}N_2O_4$	$C_{18}H_{22}N_2O_4$	$C_{17}H_{18}N_2O_4$	$C_{20}H_{22}N_2O_4$
M_r	274.27	330.38	314.34	354.22
system	Triclinic	Triclinic	Monoclinic	Triclinic
space group	P-1	P-1	C2/c	P-1
***a* [Å]**	7.3603(6)	8.9882(5)	15.750(3)	5.8000(3)
***b* [Å]**	9.2459(8)	9.6220(5)	10.3012(1)	8.8127(4)
***c* [Å]**	11.0608(9)	11.2238(4)	9.5812(1)	9.5299(5)
α [°]	98.951(7)	81.035(4)	90.00	76.389(4)
β [°]	106.043(7)	72.146(5)	90.393(1)	89.748(4)
γ[°]	110.453(7)	65.971(5)	90.00	76.804(4)
***V* [Å³]**	650.68(9)	843.33(7)	1554.5(4)	460.30(4)
Z	2	2	4	1
d_{calc}[g mm^{-3}]	1.4	1.301	1.343	1.278
***F*(000)**	288	352	664	188
μ($Mo_{K\alpha}$) [mm^{-1}]	0.104	0.092	0.097	0.090
θ_{max} [°]	25	28.88	24.63	29.09
measuredreflns	4513	7764	2077	10063
uniquereflns	2203	3785	973	2202
refined parameters	189	225	109	118
GOF on F^2	1.204	1.143	1.223	1.064
***R*1 [on *F*, $I>2\sigma(I)$]**	0.0860	0.0901	0.0557	0.0540
***wR*2(onF^2,all data)**	0.1648	0.1768	0.1652	0.1340

Table 2. Crystal Data and Details of Measurements for compounds BPA·C4 to BPA·C10

compound	Succinic acid 1C4	Glutaric acid 1C5	Adipic acid 1C6	Pimelic acid 1C7	Suberic acid 1C8	Azelaic acid 1C9	Sebacic acid 1C10
Formula	$C_{16}H_{18}N_2O_4$	$C_{17}H_{20}N_2O_4$	$C_{18}H_{22}N_2O_4$	$C_{19}H_{24}N_2O_4$	$C_{20}H_{26}N_2O_4$	$C_{21}H_{28}N_2O_4$	$C_{22}H_{28}N_2O_4$
M_r	302.32	316.35	330.38	344.40	358.43	372.45	384.46
system	Monoclinic	Monoclinic	Triclinic	Monoclinic	Monoclinic	Monoclinic	Triclinic
space group	C2/c	$P2_1/c$	P -1	$P2_1/c$	$P2_1/c$	C2/c	P-1
a [Å]	21.121(2)	12.2889(4)	7.2159(6)	11.138(1)	11.6701(5)	10.656(3)	6.9363(4)
b [Å]	4.9224(3)	11.1400(5)	7.3354(7)	47.332(5)	20.9348(7)	8.429(1)	6.9574(4)
c [Å]	16.6376(1)	24.3454(1)	8.8449(7)	14.436(2)	12.9988(5)	22.310(2)	12.0029(8)
α [°]	90.00	90.00	90.210(7)	90.00	90.00	90.00	77.230(5)
β [°]	119.752(6)	96.933(4)	93.428(6)	105.832(1)	114.656(5)	99.851(4)	73.739(6)
γ[°]	90.00	90.00	115.808(9)	90.00	90.00	90.00	71.192(6)
V [Å³]	1501.7(2)	3308.5(2)	420.49(6)	7322(1)	2886.2(2)	1974.3(6)	520.90(5)
Z	4	8	1	16	6	4	1
d_{calc}	1.337	1.270	1.305	1.250	1.137	1.253	1.226
F(000)	640	1344	176	2944	1152	800	206
$\mu(Mo_{K\alpha})$ [mm^{-1}]	0.097	0.091	0.093	0.088	0.086	0.087	0.084
θ_{max} [°]	29	28	29	28	28.4	25	29
measuredreflns	3714	18988	4004	60898	13402	1768	4579
uniquereflns	1728	7286	1907	16573	6159	1720	2332
refined parameters	104	427	112	934	365	127	144
GOF on F^2	0.954	0.900	0.916	0.986	1.035	1.006	0.862
$R1$ [on F, $I>2\sigma(I)$]	0.0427	0.0827	0.0499	0.0827	0.0793	0.0424	0.0545
$wR2$(onF^2,all data)	0.1136	0.2049	0.1370	0.2987	0.2062	0.1291	0.1505

Table 3. Crystal Data and Details of Measurements for compounds **BPP**·C5, **BPP**·C6, **BPP**·C7 and **BPP**·C10

compound	BPP C5	BPP C6	BPP C7	BPP C10
Formula	$C_{18}H_{22}N_2O_4$	$C_{19}H_{24}N_2O_4$	$C_{20}H_{26}N_2O_4$	$C_{23}H_{32}N_2O_4$
M_r	330.38	344.4	358.43	400.51
system	Monoclinic	Monoclinic	Triclinic	Monoclinic
space group	$P2_1/c$	C2/c	P-1	C2/c
a [Å]	5.43048(2)	13.7629(8)	7.1246(4)	12.661(3)
b [Å]	20.7179(7)	5.3869(4)	11.1403(4)	10.129(1)
c [Å]	15.4813(6)	24.640(2)	12.9265(7)	17.361(2)
α [°]	90.00	90.00	81.099(4)	90
β [°]	92.205(3)	95.597(6)	84.868(5)	93.13(1)
γ[°]	90.00	90.00	71.717(4)	90
V [Å³]	1740.6(1)	1818.1(2)	961.54(8)	2223.1(6)
Z	4	4	2	4
d_{calc}[g mm^{-3}]	1.261	1.258	1.238	1.197
F(000)	704	736	384	864
$\mu(Mo_{K\alpha})$ [mm^{-1}]	0.090	0.089	0.086	0.082
θ_{max} [°]	26	25	26	25
measuredreflns	15427	4312	7249	5603
uniquereflns	3411	1586	3687	1935
refined parameters	239	114	243	132
GOF on F^2	1.159	1.099	0.911	1.023
$R1$ [on F, $I>2\sigma(I)$]	0.0882	0.0647	0.0580	0.0934
$wR2$(onF^2,all data)	0.1685	0.1429	0.1333	0.2667

Table 4. Relevant hydrogen bonding distances (in Å) for all the compounds structurally characterized in this paper

compound	**BPY C4**	**---**	**---**	**---**	**BPY C8**	**---**	**---**
N···(H)O[a]	2.629(4)				2.675(4) 2.658(4)		
C(H)···O[b]	---				---		
compound	**BPA C4**	**BPA C5**	**BPA C6**	**BPA C7**	**BPA C8**	**BPA C9**	**BPA C10**
N···(H)O[a]	2.607(2)	2.650(4) 2.631(5) 2.656(5) 2.649(5)	2.613(2)	2.611(4) 2.642(4) 2.629(4) 2.633(4) 2.643(4)	2.645(3) 2.629(3) 2.620(3)	2.653(2)	2.654(2)
C(H)···O[b]	3.345(3)	3.295(6) 3.272(6)	3.330(2)	3.195(6) 3.294(6) 3.190(5) 3.250(5) 3.239(6) 3.245(5) 3.258(5)	3.336(4) 3.238(3) 3.437(4)	3.413(2)	3.355(3)
compound	**---**	**BPE C5**	**---**	**---**	**BPE C8**	**---**	**---**
N···(H)O[a]		2.616(4)			2.670(2)		
C(H)···O[b]		---			---		
compound	**---**	**BPP C5**	**BPP C6**	**BPP C7**	**---**	**---**	**BPP C10**
N···(H)O[a]		2.624(3) 2.653(3)	2.676(3)	2.645(3) 2.644(3)			2.660(5)
C(H)···O[b]		3.321(4) 3.467(4) 3.334(4)	3.290(3)	3.269(3) 3.436(3) 3.346(3)			

a) N···O < 3.0 Å ; b) C···O < 3.5 Å

Table 5 and Figure 3 collect all information on the melting points as determined by differential scanning calorimetry. The melting points of the dicarboxylic acids[6] are also reported for comparison.

Table 5. Melting points (°C) for pure diacids[6] and co-crystals (n is the total number of C atoms in the acid).

Cn	pure acid	BPY·Cn	BPA·Cn	BPE·Cn	BPP·Cn	pure base
C4	188	229.18	169.3	261.83	155.8	
C5	99	145.33	134.2	192.75	131.3	
C6	153	174.32	173.7[a]	213.28	112.6	
C7	106	141.1	145.1	156.68	138.1	
C8	144	178.72	180.9[a]	183.49	110.8	
C9	106	137.1	131.1[a]	143.08	131.1	
C10	134.5	168.58	160.1[a]	169.31	101.1	
						BPY 110-114[b]
						BPA 110-112[b]
						BPE 148-152[d]
						BPP 53-56[c]

a) The DSC trace shows also the presence of an endothermic solid-to-solid phase transition at lower temperature (see ESI); b) Sigma-Aldrich; c) Alfa Aesar, d) Fluka.

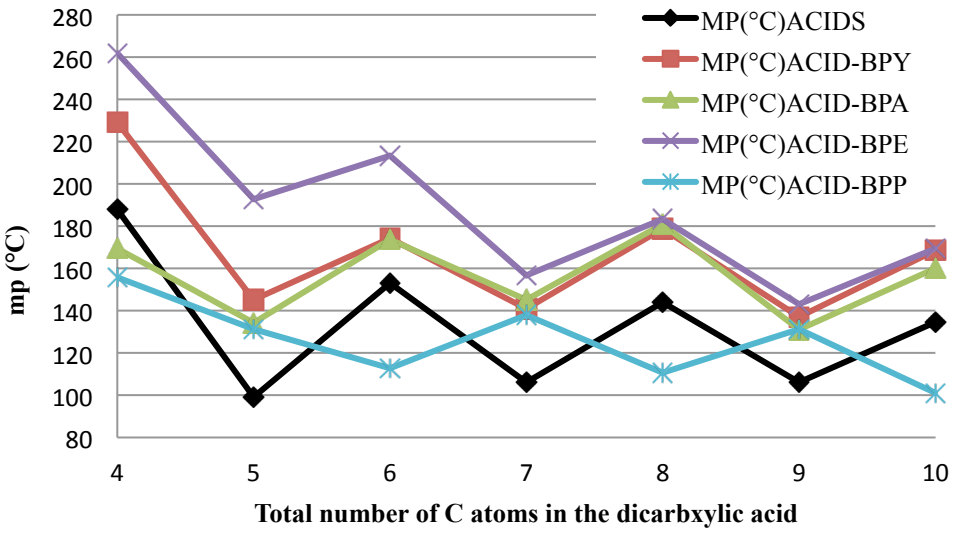

Figure 3. Melting point alternation for pure acids, **BPY**·Cn, **BPA**·Cn,**BPE**·Cn and **BPP**·Cn series (n in the range 4 to 10 corresponding to succinic, glutaric, adipic, pimelic, suberic, azelaic and sebacic, respectively).

Figure 3 allows the following observations: i) the melting points of the co-crystals with BPY, BPA and BPE, except for **BPA·C4,** are invariably higher than those of the starting dicarboxylic acids and of the co-crystals with BPP; ii) the co-crystals with BPY, BPA and BPE follow the same alternating trend as the diacids *i.e*. higher melting points are shown by the co-crystals with even carbon atom chains (succinic, adipic, suberic, and sebacic); iii) the co-crystals with BPY and BPA have very similar melting points except for the co-crystals of **BPA·C4**and **BPA·C5**that show a melting point lower than those with BPY; iv) the co-crystals of BPE with C8, C9 and C10 present a very close melting point to those with BPY and BPA; v) the co-crystals with BPP present an inverse trend, *i.e.* higher melting points are shown by the co-crystals with glutaric, pimelic and azelaic acid thus demonstrating that it is the overall number of carbon atoms in the repeating units along the hydrogen bonded chains that matters, irrespective of the supramolecular nature of the interactions within such repeating unit; vi) an exception to this behaviour is represented by the co-crystal **BPP·C4** (succinic acid) which shows a melting point of ca. 156°C, still lower than that of the corresponding succinic acid itself, but higher than that of **BPP C5**.It is also interesting to note that the difference in the melting points of BPY (110-114°C), BPA (100–110°C), BPE (148-152°C) and BPP (57–60°C) is somehow reflected in the fact that, on average, the melting points for the **BPY·Cn**, **BPA·Cn** and **BPE·Cn** co-crystals are higher than those of the **BPP·Cn** co-crystals. It can be seen that for co-crystals with BPY, BPA and BPE the trend is comparable to those of pure dicarboxylic acids $HOOC(CH_2)_nCOOH$ (n = 2-8).

SS NMR spectroscopy has been able to detect the similarity of all structures in terms of the main packing feature, i.e. chains of alternating base and acid units; in addition to this, it shows that the melting point alternation is consistent with the length of the chain repeating unit rather than on conformational features or global crystal packing.[12] The co-crystal nature of all the adducts has been ascertained by means of ^{13}C and in some case (BPA and BPP series)^{15}N CPMAS NMR spectra (spectra ^{15}N and chemical shifts are reported in ESI Figures and Tables). Both sets of data confirm that no proton

transfer took place in any adducts: the ^{13}C carboxylic chemical shifts (around 175-178 ppm) are typical of COOH rather than COO^- groups and the ^{15}N pyridine chemical shifts for BPA and BPP adducts (around 250-260 ppm) are in the region of the pyridine rather than the pyridinium anion.[13] Numbers and relative intensities of COOH and N signals in each spectrum are in agreement with the presence in the unit cell of different carboxylic and pyridine environments (See supplementary material).

The presence and strength of a hydrogen bond can be evaluated with ^1HMAS SS NMR spectra. Indeed, the signals of hydrogen atoms involved in hydrogen bonds are at high values of chemical shift, away from the aliphatic and aromatic regions. Moreover, since its chemical shift depends on the polarization of the XH covalent bond, the stronger the interaction, the greater the polarization of the bond and the higher the value of chemical shift[14](Figure 4).

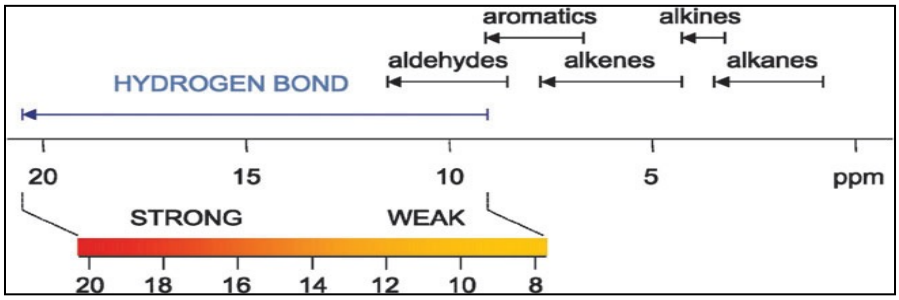

Figure 5: Strengthof thehydrogen bondinan1HNMRspectrum.

The ^1H hydrogen bond signals are summarized in Table 6 and the comparison of all spectra of the four co-crystals series is shown in supplementary material.

^{13}C	ACID-BPY	ACID-BPE	ACID-BPA	ACID-BPP
Succinic	15.7	15.8	16.7	16.3
Glutaric	14.9	15.5	16.4-14.7[a]	15.4
Adipic	14.9	15.4	16.9	14.6
Pimelic	14.4	14.9	16.0	16.2
Suberic	14.6	14.3	16.4	16.1
Azelaic	15.0	14.6	15.2	16.3
Sebacic	15.0	14.4	15.5	15.0

Table6: ^1Hchemical shift data (ppm) of co-crystals series with BPY, BPA, BPE and BPP.
a) In agreement with the presence of various N···O environments.

For each set of co-crystals, the comparison between the hydrogen bond ^{1}H chemical shift and the melting points reported in figure 7 shows the following features: i) in the co-crystals with BPY the chemical shift trend follows that of the melting points but for sample C9 BPY; ii) in the co-crystals with BPE the chemical shift trend does not follow that of the melting points but it is observed that an overall decrease in the melting points, increasing the length of acid chain, corresponds to a decrease in the strength of hydrogen bonds and in the ^{1}H chemical shift values; iii) in the co-crystals with BPA and BPP the chemical shift trend strictly resembles the melting point behaviour, furthermore, a low-frequency shift is observed by increasing the acid chain length in agreement with N···O (See supplementary material) distances and with the previously reported dicarboxylic acid-dabco series.[8a,15]

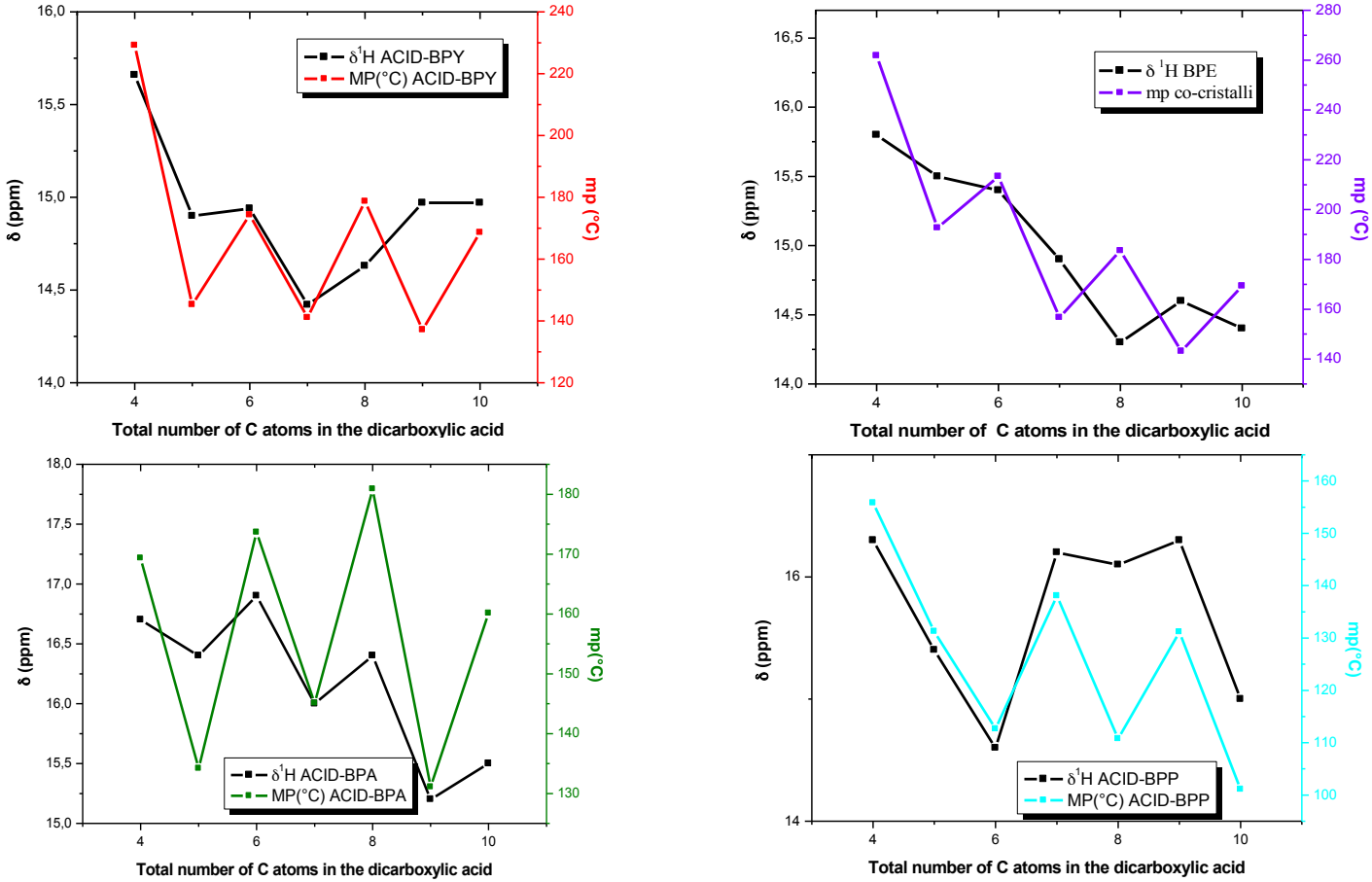

Figure 7: Comparison between melting points trend and chemical shift trend for each set of co-crystals.

1.4. Conclusion

In summary, we have shown that the melting point alternation phenomenon *propagates* also via hydrogen bonding interactions. Our experiments with the co-crystals of the dicarboxylic acids with BPA and BPP[16]indicate that it is the sum of the carbon atoms in the repeating unit that correlates with the melting points measured on these two classes of compounds, and the reason for the alternation has to be found in the number and type of hydrogen bonding intermolecular interactions, responsible for packing efficiency and thus for lattice energy; we have also provided further evidence on the molecular nature of crystals in cases where the difference depends solely on the positioning of the proton along an H-bond,[17] and does not affect a bulk physical property of solid materials such as the melting point. The hydrogen bond strength, on the other hand, seems to be one the parameters influencing this physical property since, at least from an NMR point of view, the highest melting points are associated in most cases to strong hydrogen bond interactions and *vice versa*.

1.5. Supplementary Material

Legenda

BPY C4 = BPY-Succinic Acid
BPY C5 = BPY-Glutaric Acid
BPY C6 = BPY-Adipic Acid
BPY C7 = BPY-Pimelic Acid
BPY C8 = BPY-Suberic Acid
BPY C9 = BPY-Azelaic Acid
BPY C10 = BPY-Sebacic Acid

BPAC4 = BPA-Succinic Acid
BPAC4 = BPA-Succinic Acid
BPAC4 = BPA-Succinic Acid
BPAC4 = BPA-Succinic Acid
BPAC4 = BPA-Succinic Acid
BPAC4 = BPA-Succinic Acid
BPAC4 = BPA-Succinic Acid

BPEC4 = BPY-Succinic Acid
BPEC5 = BPY-Glutaric Acid
BPEC6 = BPY-Adipic Acid
BPEC7 = BPY-Pimelic Acid
BPEC8 = BPY-Suberic Acid
BPEC9 = BPY-Azelaic Acid
BPEC10 = BPY-Sebacic Acid

BPPC4 = BPA-Succinic Acid
BPPC4 = BPA-Succinic Acid
BPPC4 = BPA-Succinic Acid
BPPC4 = BPA-Succinic Acid
BPPC4 = BPA-Succinic Acid
BPPC4 = BPA-Succinic Acid
BPPC4 = BPA-Succinic Acid

1.5.1. **Thermal behavior – BPY**

Differential scanning calorimetry measurements for the **BPY**·C4, **BPY**·C5,**BPY**·C6, **BPY**·C7, **BPY**·C8, **BPY**·C9 and **BPY**·C10 adducts.

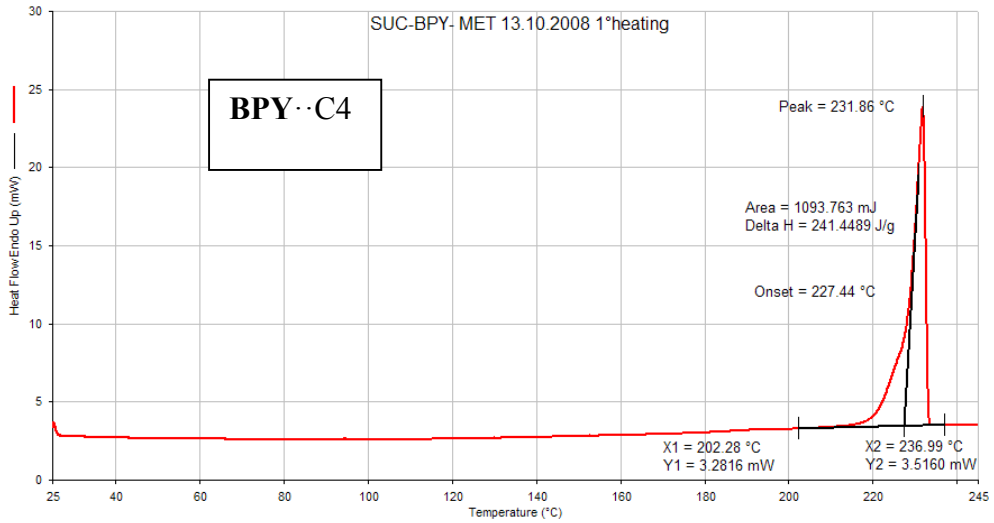

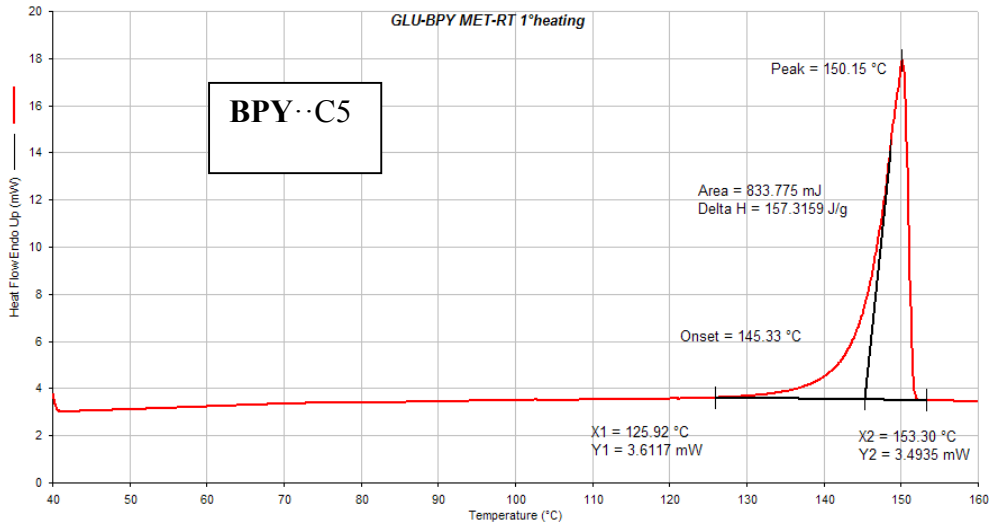

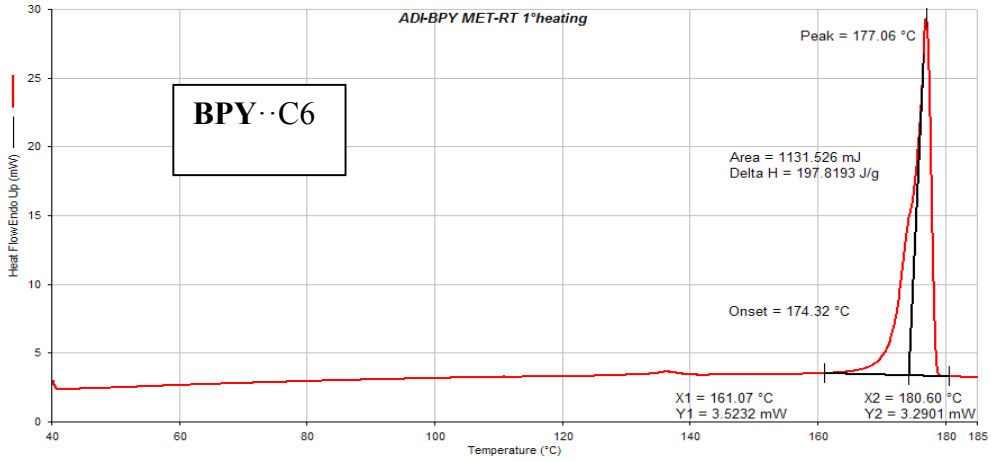
ADI-BPY MET-RT 1°heating
BPY··C6
Peak = 177.06 °C
Area = 1131.526 mJ
Delta H = 197.8193 J/g
Onset = 174.32 °C
X1 = 161.07 °C
Y1 = 3.5232 mW
X2 = 180.60 °C
Y2 = 3.2901 mW
Heat Flow Endo Up (mW)
Temperature (°C)

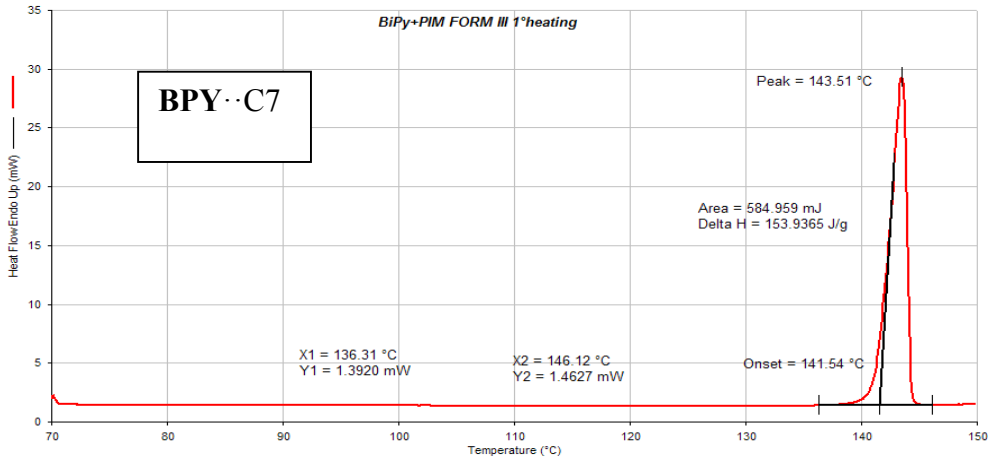
BiPy+PIM FORM III 1°heating
BPY··C7
Peak = 143.51 °C
Area = 584.959 mJ
Delta H = 153.9365 J/g
X1 = 136.31 °C
Y1 = 1.3920 mW
X2 = 146.12 °C
Y2 = 1.4627 mW
Onset = 141.54 °C
Heat Flow Endo Up (mW)
Temperature (°C)

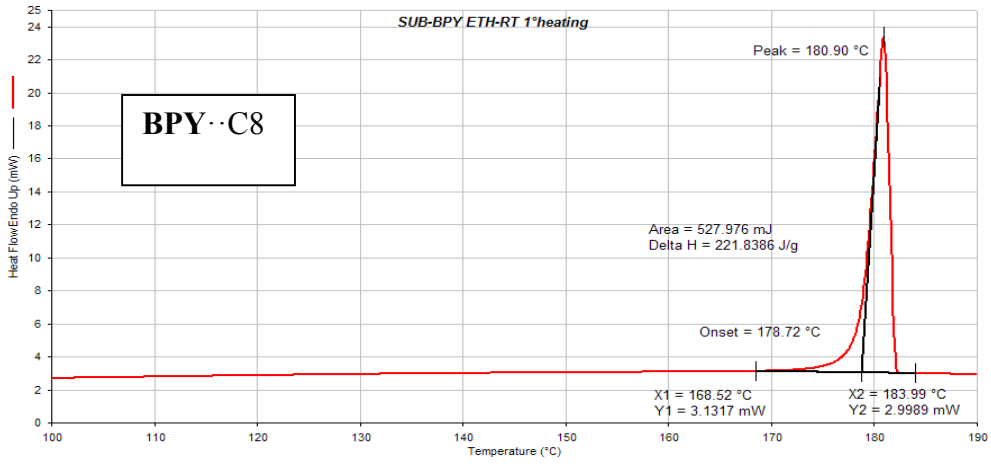
SUB-BPY ETH-RT 1°heating
BPY··C8
Peak = 180.90 °C
Area = 527.976 mJ
Delta H = 221.8386 J/g
Onset = 178.72 °C
X1 = 168.52 °C
Y1 = 3.1317 mW
X2 = 183.99 °C
Y2 = 2.9989 mW
Heat Flow Endo Up (mW)
Temperature (°C)

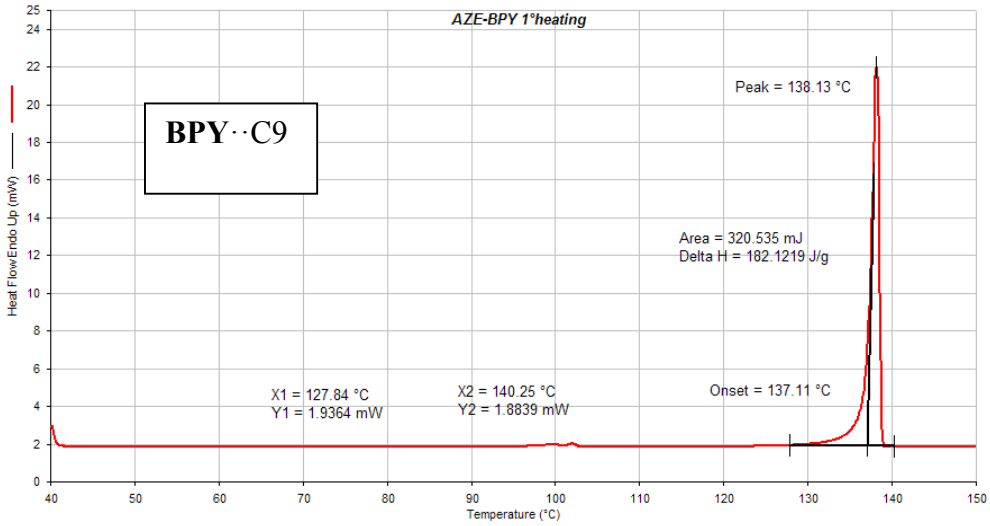
AZE-BPY 1°heating
BPY··C9
Peak = 138.13 °C
Area = 320.535 mJ
Delta H = 182.1219 J/g
X1 = 127.84 °C
Y1 = 1.9364 mW
X2 = 140.25 °C
Y2 = 1.8839 mW
Onset = 137.11 °C
Heat Flow Endo Up (mW)
Temperature (°C)

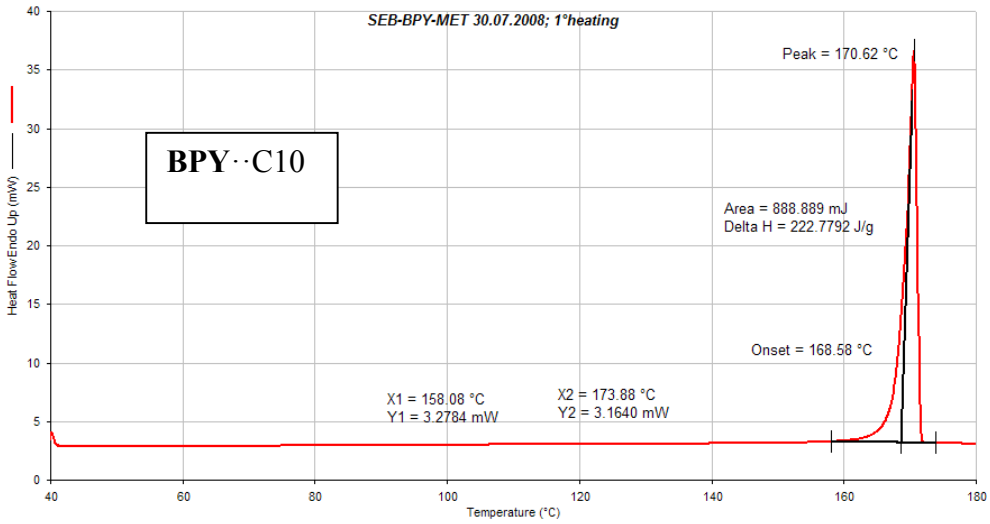
SEB-BPY-MET 30.07.2008; 1°heating
BPY··C10
Peak = 170.62 °C
Area = 888.889 mJ
Delta H = 222.7792 J/g
Onset = 168.58 °C
X1 = 158.08 °C
Y1 = 3.2784 mW
X2 = 173.88 °C
Y2 = 3.1640 mW
Heat Flow Endo Up (mW)
Temperature (°C)

1.5.2. **Thermal behavior - BPA**

Differential scanning calorimetry measurements for the **BPA**·C4, **BPA**·C5,**BPA**·C6, **BPA**·C7, **BPA**·C8, **BPA**·C9 and **BPA**·C10 adducts.

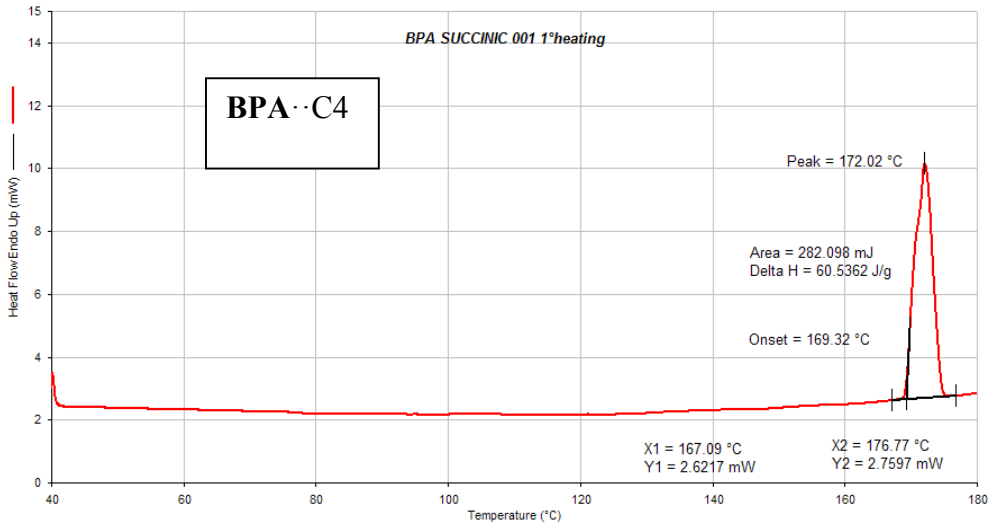

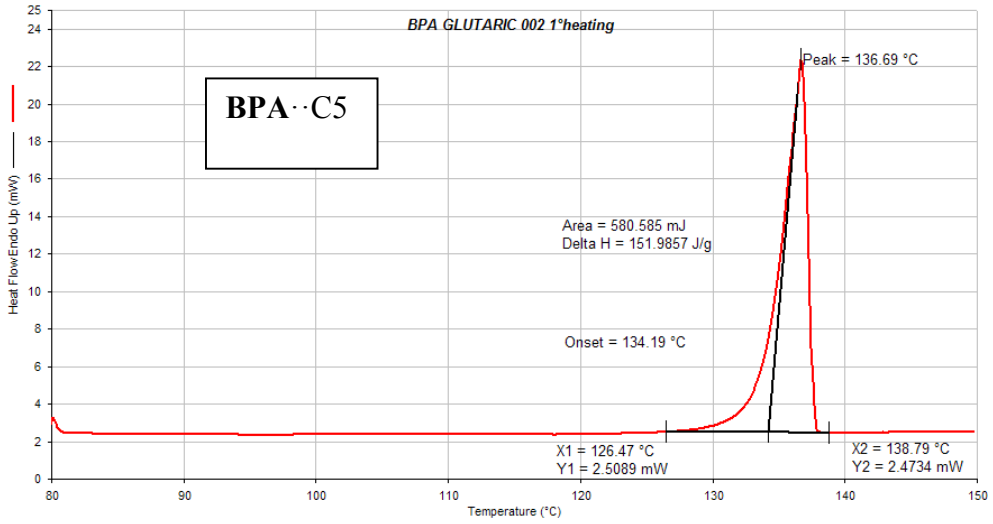

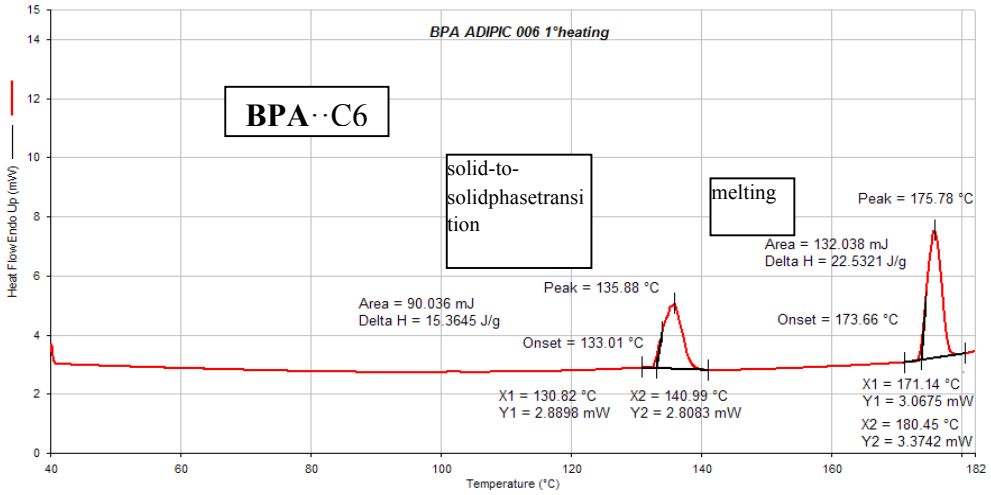
BPA ADIPIC 006 1°heating
BPA··C6
solid-to-solidphasetransition
melting
Peak = 175.78 °C
Area = 132.038 mJ
Delta H = 22.5321 J/g
Peak = 135.88 °C
Area = 90.036 mJ
Delta H = 15.3645 J/g
Onset = 173.66 °C
Onset = 133.01 °C
X1 = 130.82 °C
Y1 = 2.8898 mW
X2 = 140.99 °C
Y2 = 2.8083 mW
X1 = 171.14 °C
Y1 = 3.0675 mW
X2 = 180.45 °C
Y2 = 3.3742 mW
Heat FlowEndo Up (mW)
Temperature (°C)

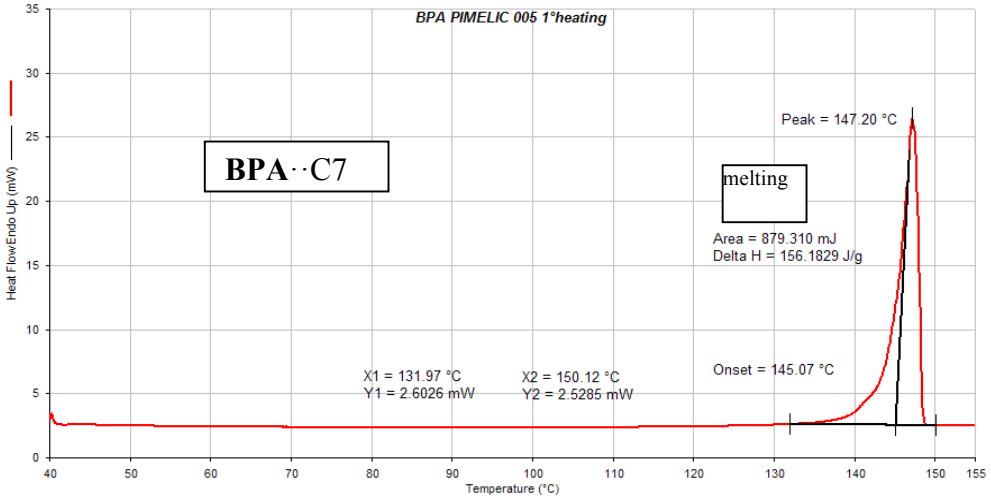
BPA PIMELIC 005 1°heating
BPA··C7
Peak = 147.20 °C
melting
Area = 879.310 mJ
Delta H = 156.1829 J/g
X1 = 131.97 °C
Y1 = 2.6026 mW
X2 = 150.12 °C
Y2 = 2.5285 mW
Onset = 145.07 °C
Heat FlowEndo Up (mW)
Temperature (°C)

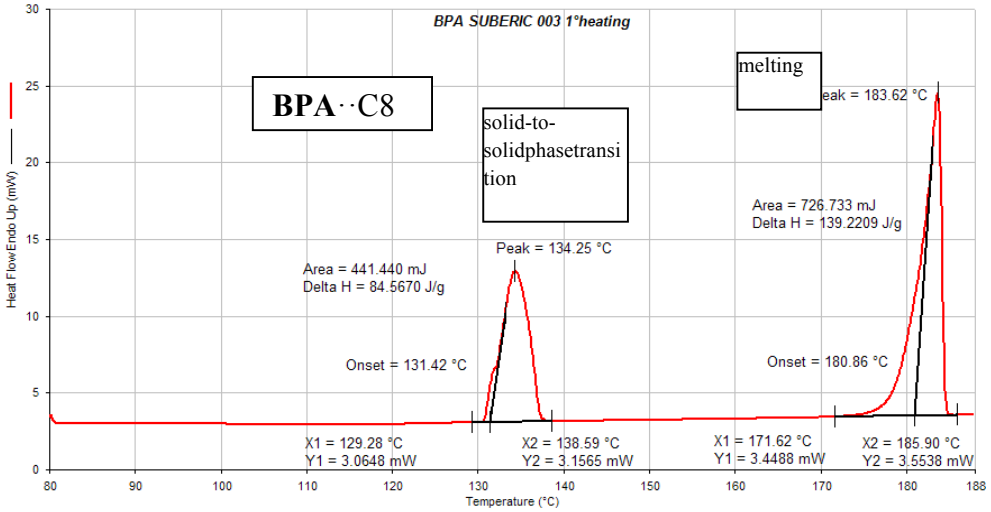
BPA SUBERIC 003 1°heating
BPA··C8
melting
eak = 183.62 °C
solid-to-solidphasetransition
Area = 726.733 mJ
Delta H = 139.2209 J/g
Peak = 134.25 °C
Area = 441.440 mJ
Delta H = 84.5670 J/g
Onset = 131.42 °C
Onset = 180.86 °C
X1 = 129.28 °C
Y1 = 3.0648 mW
X2 = 138.59 °C
Y2 = 3.1565 mW
X1 = 171.62 °C
Y1 = 3.4488 mW
X2 = 185.90 °C
Y2 = 3.5538 mW
Heat FlowEndo Up (mW)
Temperature (°C)

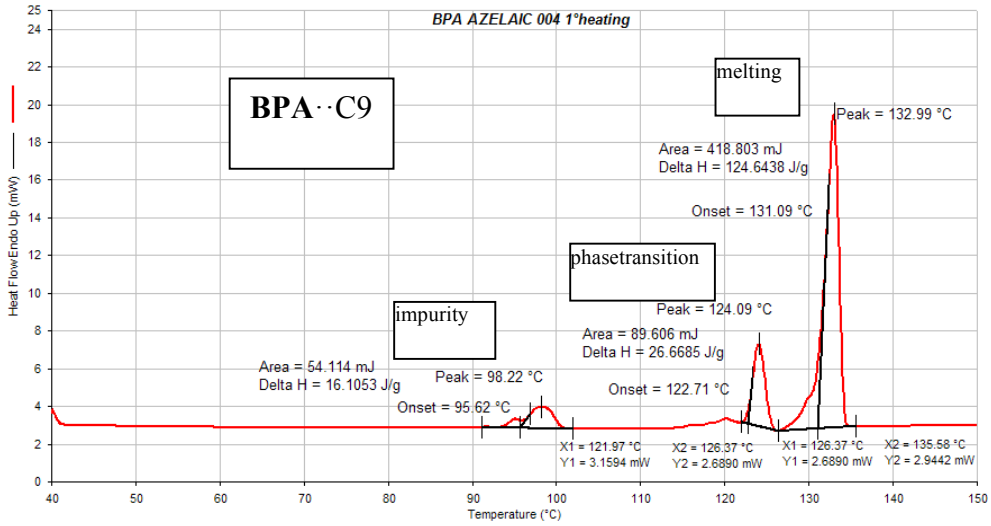
BPA AZELAIC 004 1°heating
BPA··C9
melting
Peak = 132.99 °C
Area = 418.803 mJ
Delta H = 124.6438 J/g
Onset = 131.09 °C
phasetransition
Peak = 124.09 °C
Area = 89.606 mJ
Delta H = 26.6685 J/g
Onset = 122.71 °C
impurity
Area = 54.114 mJ
Delta H = 16.1053 J/g
Peak = 98.22 °C
Onset = 95.62 °C
X1 = 121.97 °C
Y1 = 3.1594 mW
X2 = 126.37 °C
Y2 = 2.6890 mW
X1 = 126.37 °C
Y1 = 2.6890 mW
X2 = 135.58 °C
Y2 = 2.9442 mW
Heat FlowEndo Up (mW)
Temperature (°C)

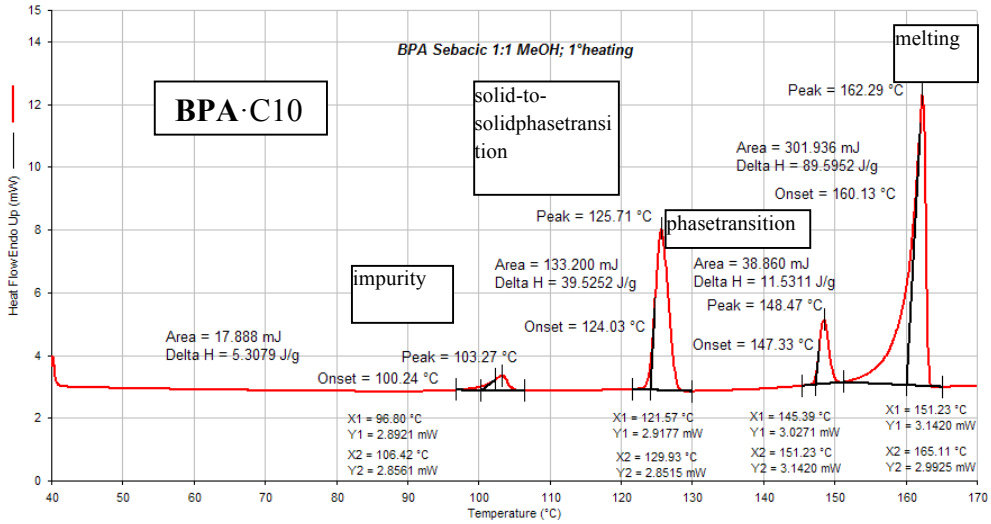
BPA Sebacic 1:1 MeOH; 1°heating
BPA·C10
melting
Peak = 162.29 °C
solid-to-solidphasetransition
Area = 301.936 mJ
Delta H = 89.5952 J/g
Onset = 160.13 °C
Peak = 125.71 °C
phasetransition
Area = 133.200 mJ
Delta H = 39.5252 J/g
Area = 38.860 mJ
Delta H = 11.5311 J/g
Peak = 148.47 °C
impurity
Onset = 124.03 °C
Onset = 147.33 °C
Area = 17.888 mJ
Delta H = 5.3079 J/g
Peak = 103.27 °C
Onset = 100.24 °C
X1 = 96.80 °C
Y1 = 2.8921 mW
X2 = 106.42 °C
Y2 = 2.8561 mW
X1 = 121.57 °C
Y1 = 2.9177 mW
X2 = 129.93 °C
Y2 = 2.8515 mW
X1 = 145.39 °C
Y1 = 3.0271 mW
X2 = 151.23 °C
Y2 = 3.1420 mW
X1 = 151.23 °C
Y1 = 3.1420 mW
X2 = 165.11 °C
Y2 = 2.9925 mW
Heat FlowEndo Up (mW)
Temperature (°C)

1.5.3. **Thermal behavior – BPE**

Differential scanning calorimetry measurements for the **BPE**·C4, **BPE**·C5,**BPE**·C6, **BPE**·C7, **BPE**·C8, **BPE**·C9 and **BPE**·C10 adducts.

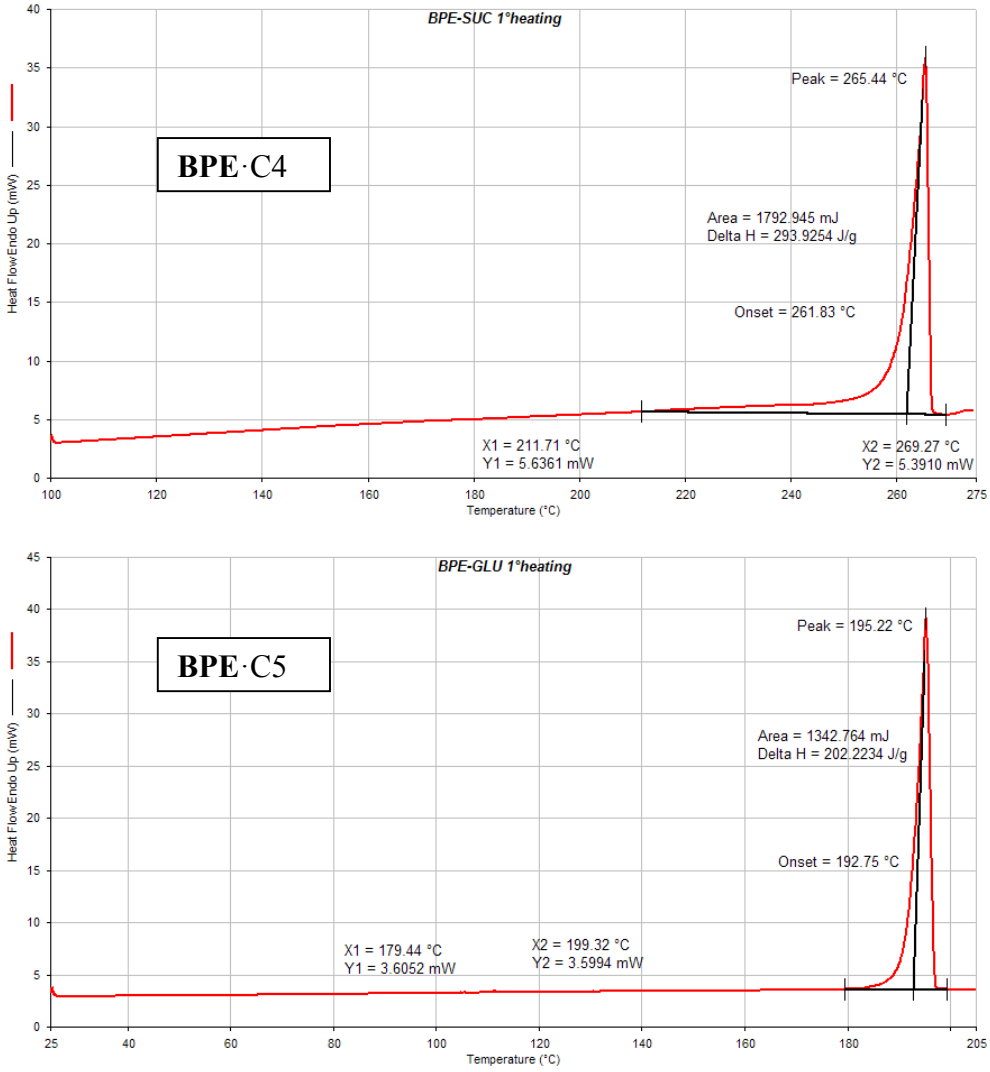

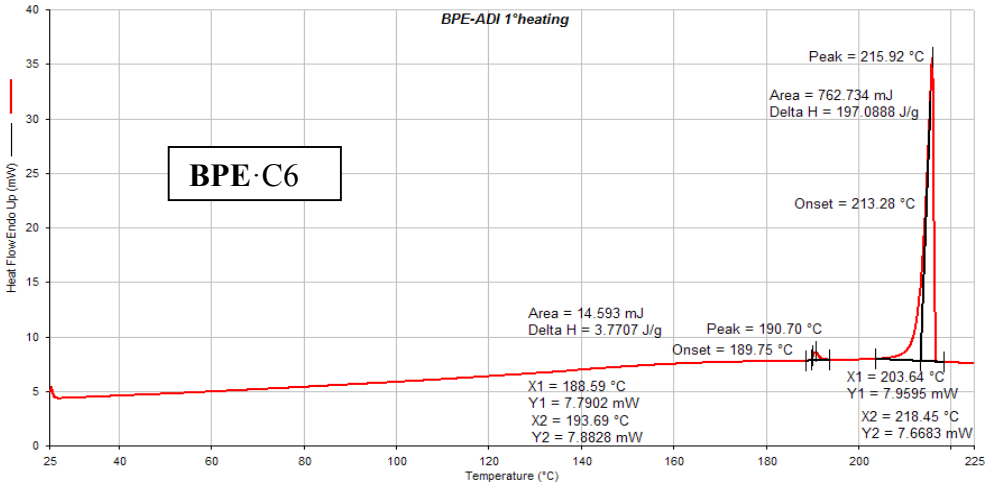
BPE-ADI 1°heating
BPE·C6
Peak = 215.92 °C
Area = 762.734 mJ
Delta H = 197.0888 J/g
Onset = 213.28 °C
Area = 14.593 mJ
Delta H = 3.7707 J/g
Peak = 190.70 °C
Onset = 189.75 °C
X1 = 188.59 °C
Y1 = 7.7902 mW
X2 = 193.69 °C
Y2 = 7.8828 mW
X1 = 203.64 °C
Y1 = 7.9595 mW
X2 = 218.45 °C
Y2 = 7.6683 mW
Heat Flow Endo Up (mW)
Temperature (°C)

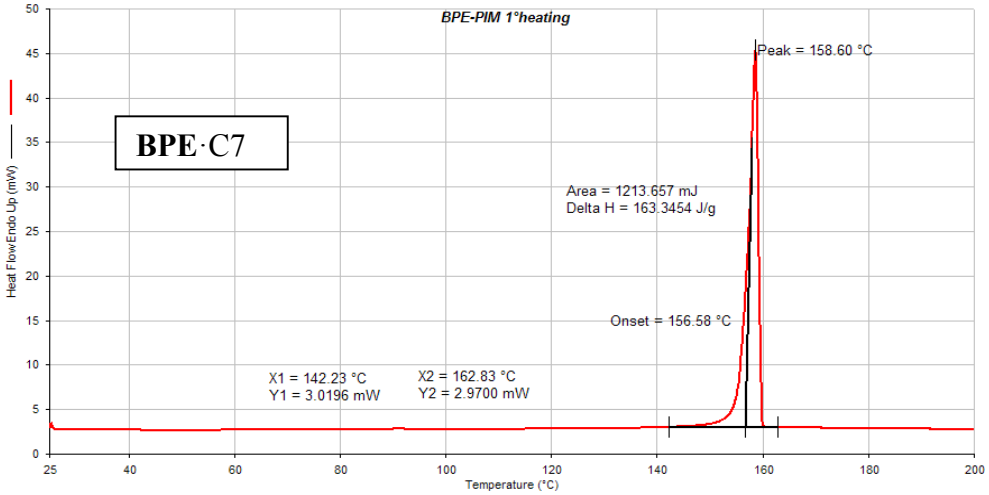
BPE-PIM 1°heating
BPE·C7
Peak = 158.60 °C
Area = 1213.657 mJ
Delta H = 163.3454 J/g
Onset = 156.58 °C
X1 = 142.23 °C
Y1 = 3.0196 mW
X2 = 162.83 °C
Y2 = 2.9700 mW
Heat Flow Endo Up (mW)
Temperature (°C)

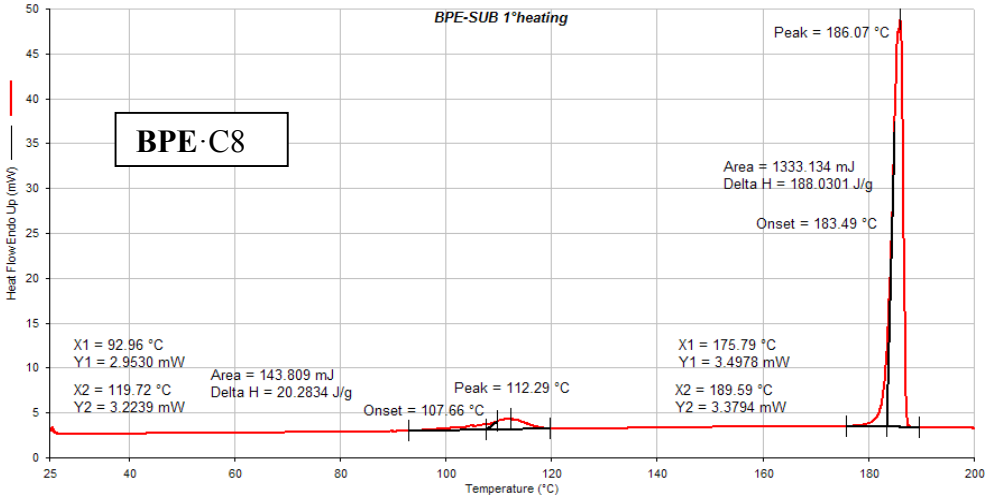
BPE-SUB 1°heating
BPE·C8
Peak = 186.07 °C
Area = 1333.134 mJ
Delta H = 188.0301 J/g
Onset = 183.49 °C
X1 = 92.96 °C
Y1 = 2.9530 mW
X2 = 119.72 °C
Y2 = 3.2239 mW
Area = 143.809 mJ
Delta H = 20.2834 J/g
Peak = 112.29 °C
Onset = 107.66 °C
X1 = 175.79 °C
Y1 = 3.4978 mW
X2 = 189.59 °C
Y2 = 3.3794 mW
Heat Flow Endo Up (mW)
Temperature (°C)

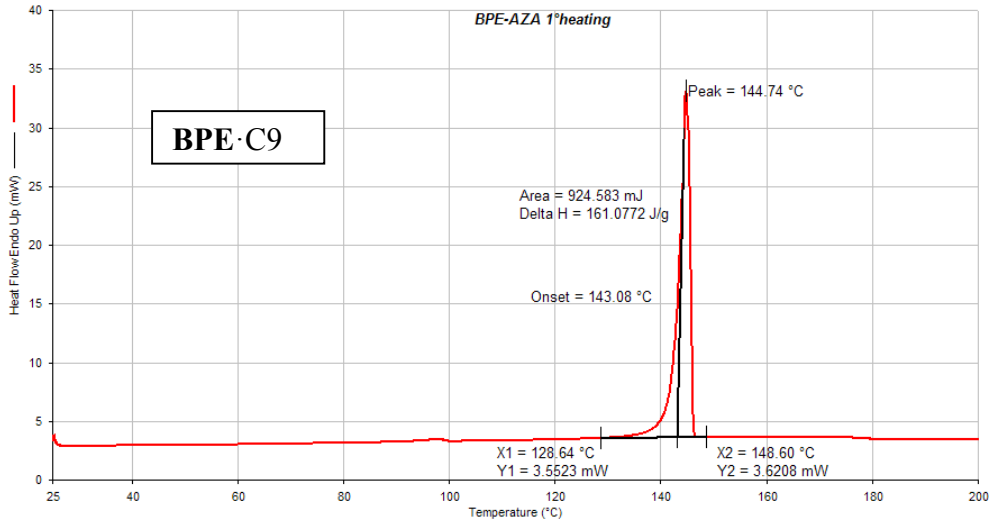
BPE-AZA 1°heating
BPE·C9
Peak = 144.74 °C
Area = 924.583 mJ
Delta H = 161.0772 J/g
Onset = 143.08 °C
X1 = 128.64 °C
Y1 = 3.5523 mW
X2 = 148.60 °C
Y2 = 3.6208 mW
Heat Flow Endo Up (mW)
Temperature (°C)

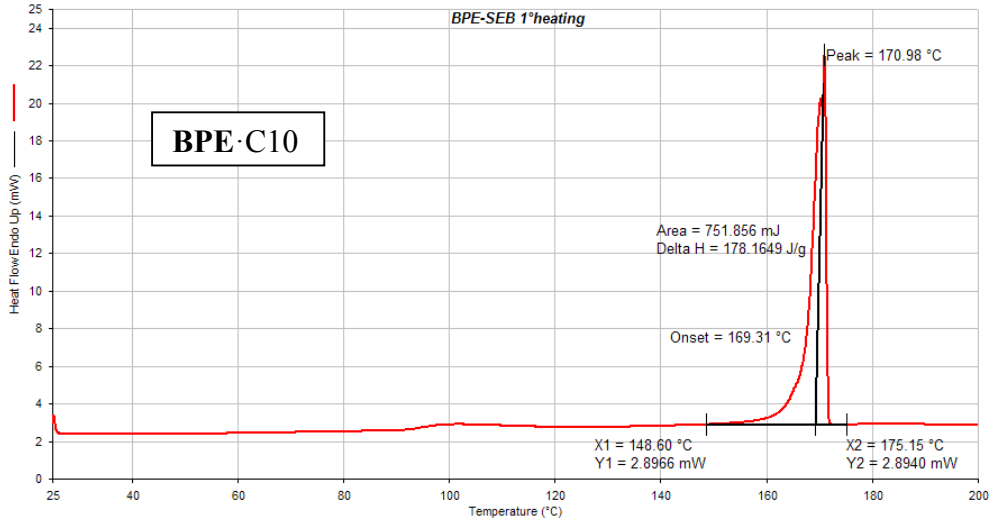
BPE-SEB 1°heating
BPE·C10
Peak = 170.98 °C
Area = 751.856 mJ
Delta H = 178.1649 J/g
Onset = 169.31 °C
X1 = 148.60 °C
Y1 = 2.8966 mW
X2 = 175.15 °C
Y2 = 2.8940 mW
Heat Flow Endo Up (mW)
Temperature (°C)

1.5.4. **Thermal behavior – BPP**

Differential scanning calorimetry measurements for the **BPP**·C4, **BPP**·C5,**BPP**·C6, **BPP**·C7, **BPP**·C8, **BPP**·C9 and **BPP**·C10 adducts.

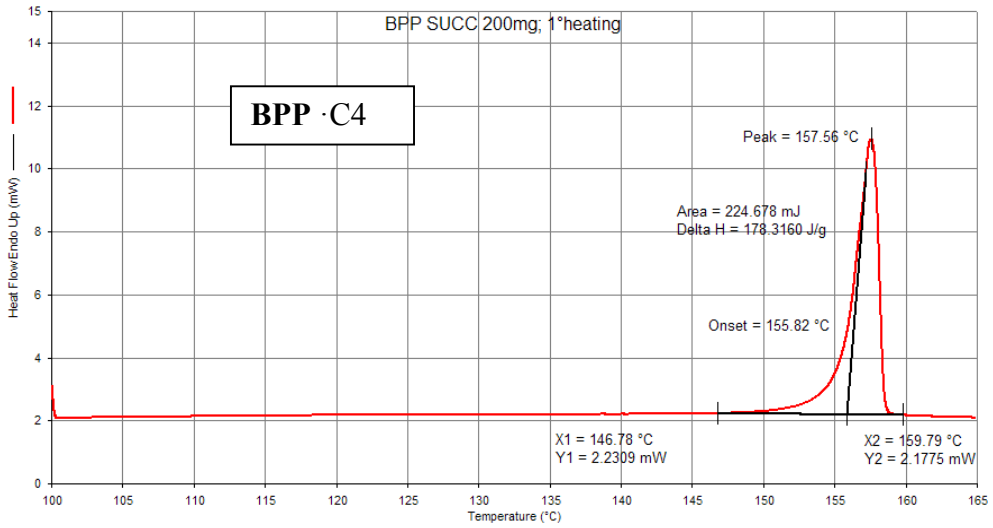

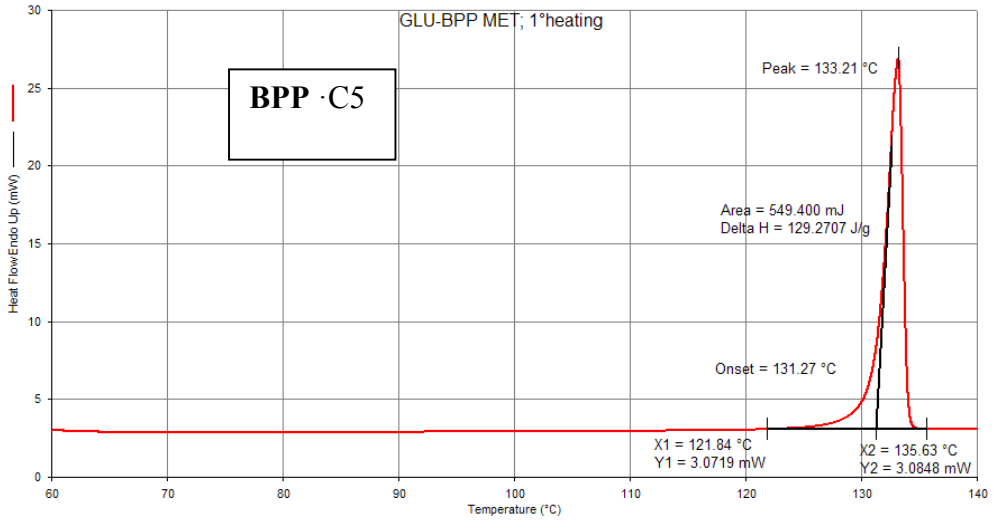

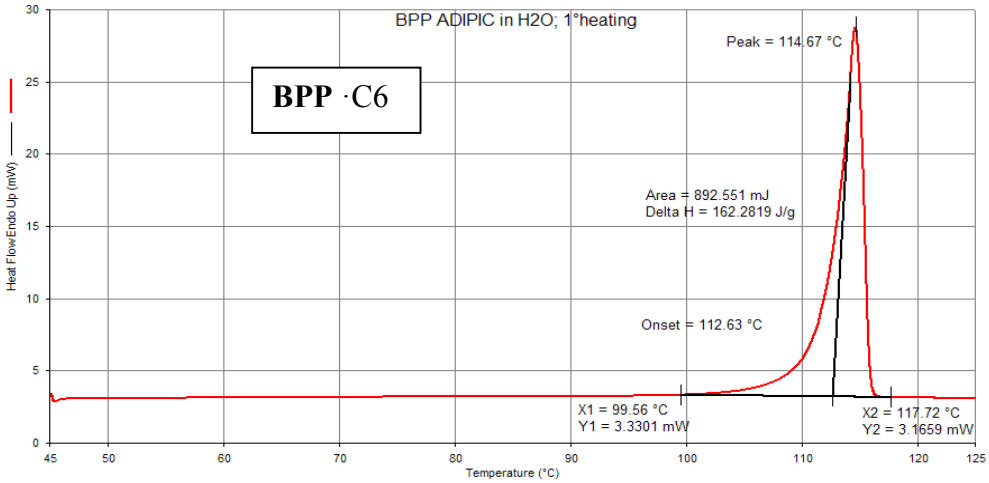
BPP ADIPIC in H2O; 1°heating
BPP ·C6
Peak = 114.67 °C
Area = 892.551 mJ
Delta H = 162.2819 J/g
Onset = 112.63 °C
X1 = 99.56 °C
Y1 = 3.3301 mW
X2 = 117.72 °C
Y2 = 3.1659 mW
Heat FlowEndo Up (mW)
Temperature (°C)

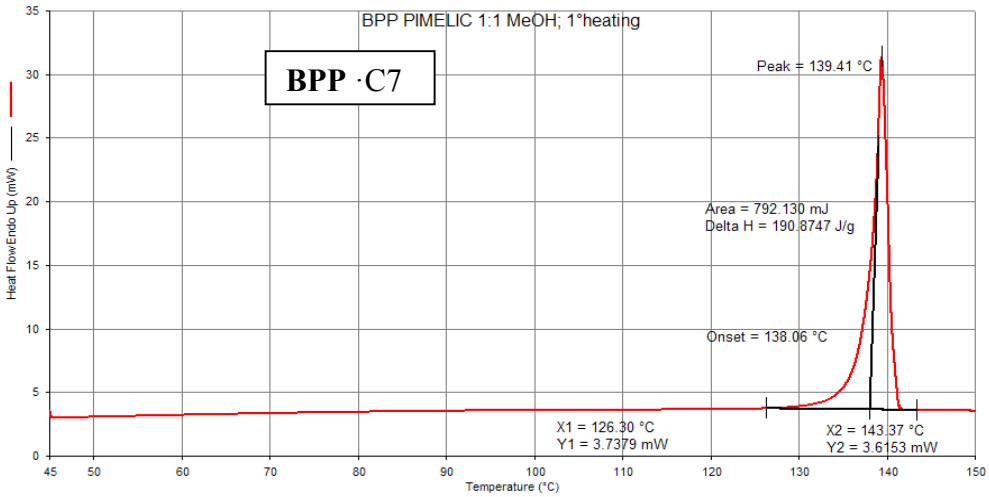
BPP PIMELIC 1:1 MeOH; 1°heating
BPP ·C7
Peak = 139.41 °C
Area = 792.130 mJ
Delta H = 190.8747 J/g
Onset = 138.06 °C
X1 = 126.30 °C
Y1 = 3.7379 mW
X2 = 143.37 °C
Y2 = 3.6153 mW
Heat FlowEndo Up (mW)
Temperature (°C)

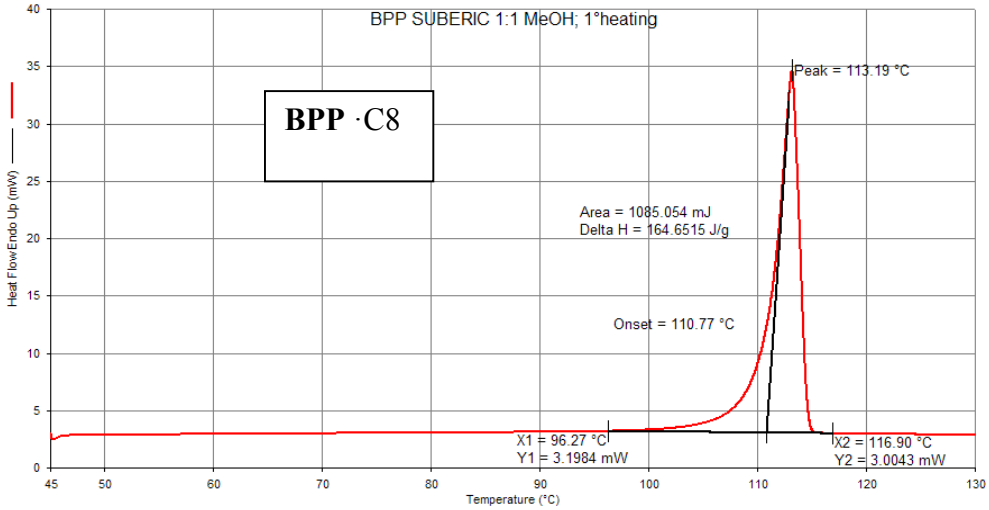
BPP SUBERIC 1:1 MeOH; 1°heating
BPP ·C8
Peak = 113.19 °C
Area = 1085.054 mJ
Delta H = 164.6515 J/g
Onset = 110.77 °C
X1 = 96.27 °C
Y1 = 3.1984 mW
X2 = 116.90 °C
Y2 = 3.0043 mW
Heat FlowEndo Up (mW)
Temperature (°C)

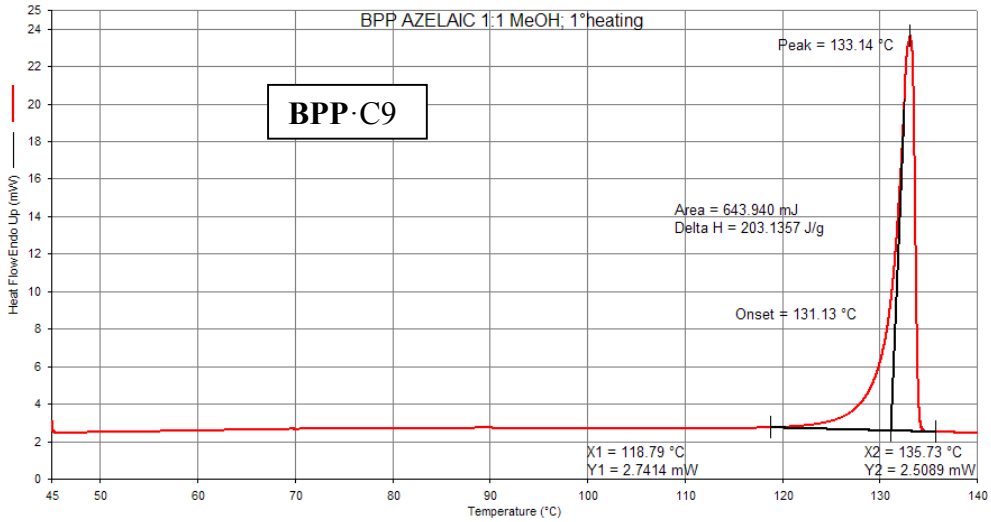
BPP AZELAIC 1:1 MeOH; 1°heating
BPP·C9
Peak = 133.14 °C
Area = 643.940 mJ
Delta H = 203.1357 J/g
Onset = 131.13 °C
X1 = 118.79 °C
Y1 = 2.7414 mW
X2 = 135.73 °C
Y2 = 2.5089 mW
Heat Flow Endo Up (mW)
Temperature (°C)

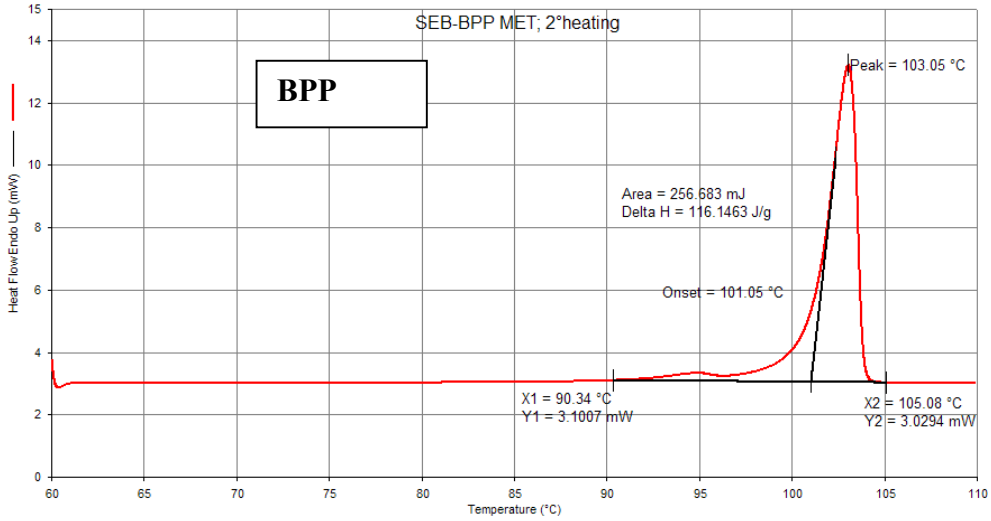
SEB-BPP MET; 2°heating
BPP
Peak = 103.05 °C
Area = 256.683 mJ
Delta H = 116.1463 J/g
Onset = 101.05 °C
X1 = 90.34 °C
Y1 = 3.1007 mW
X2 = 105.08 °C
Y2 = 3.0294 mW
Heat Flow Endo Up (mW)
Temperature (°C)

1.5.5. **XRPD Patterns - BPY:acid**

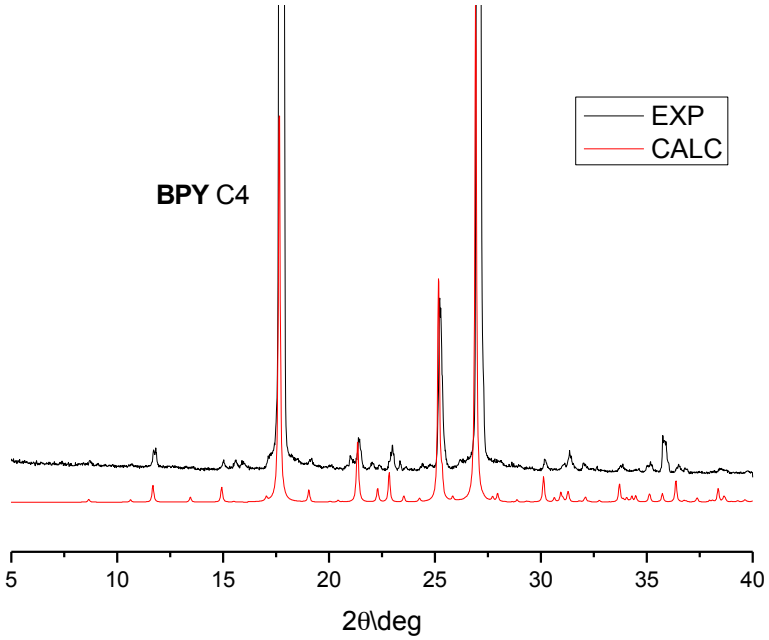

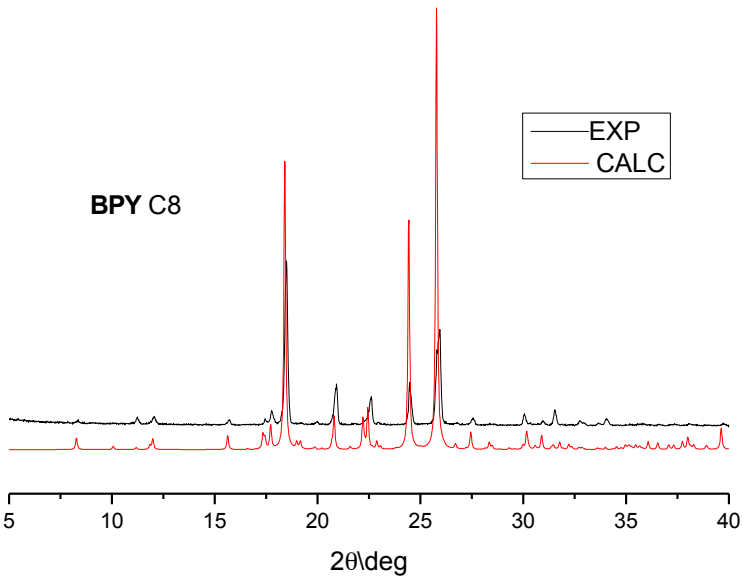

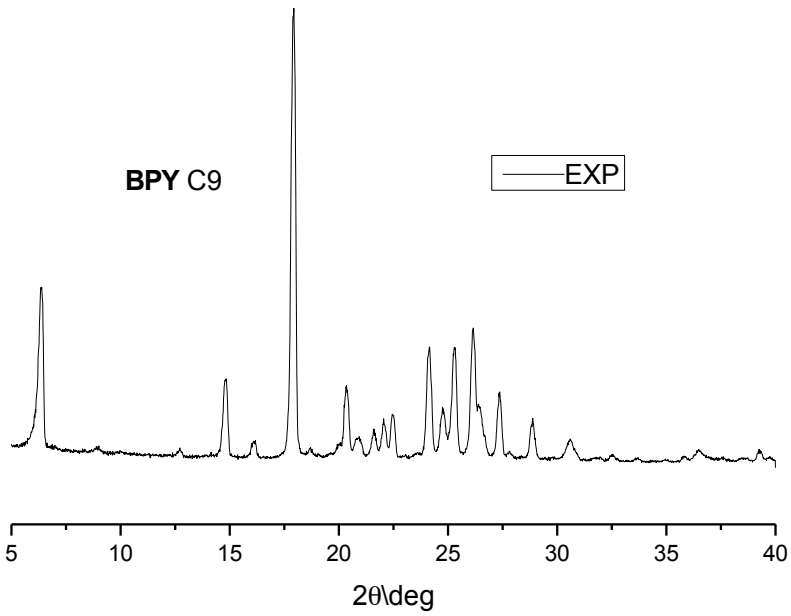
BPY C9
EXP
5
10
15
20
25
30
35
40
2θ\deg

1.5.6. **XRPD Patterns - BPA:acid**

BPA C4

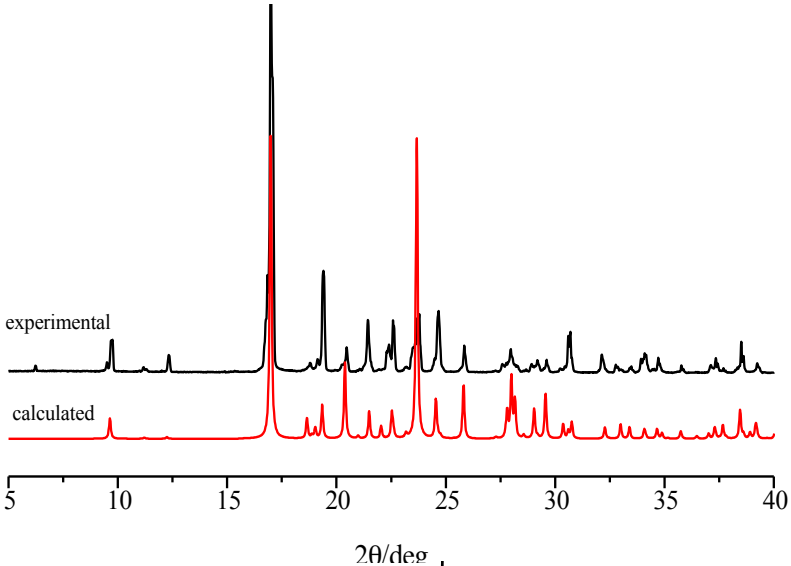

BPA C5

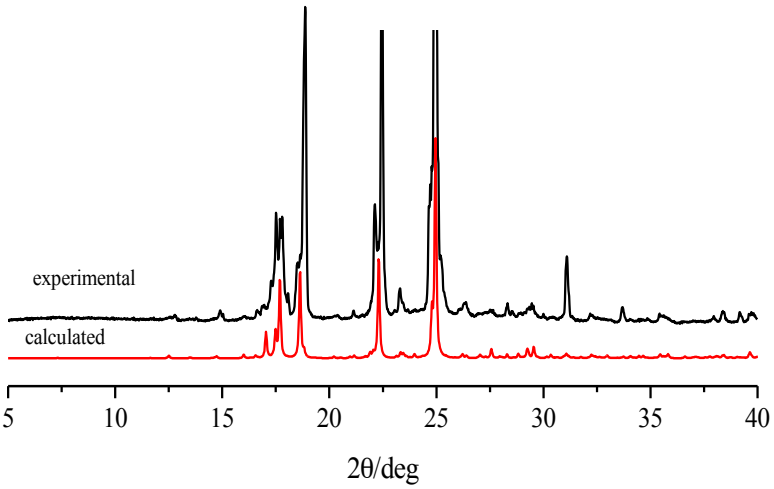

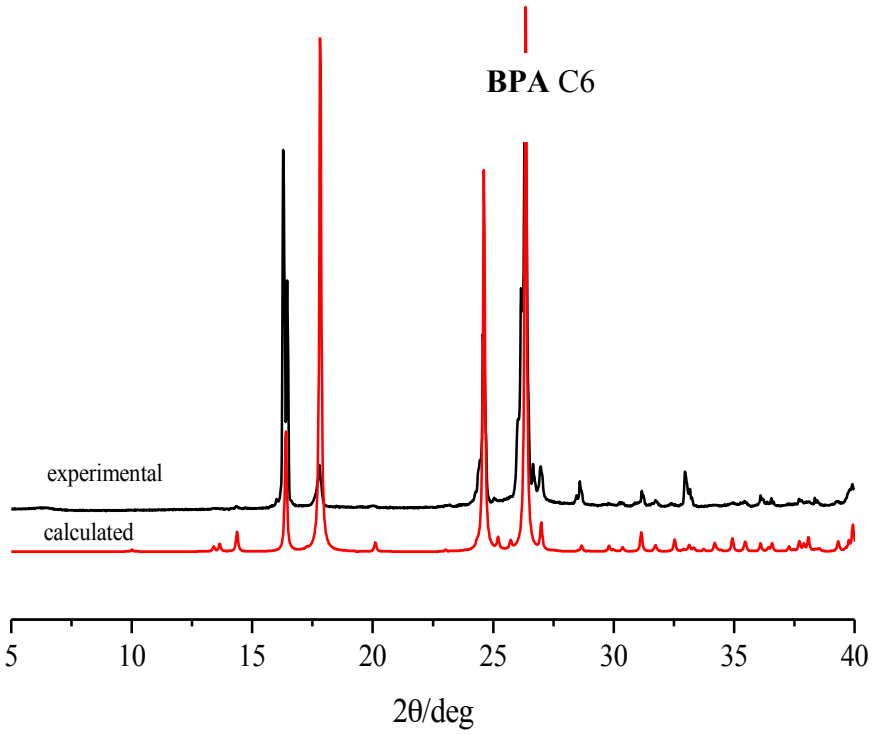
BPA C6
experimental
calculated
5
10
15
20
25
30
35
40
2θ/deg

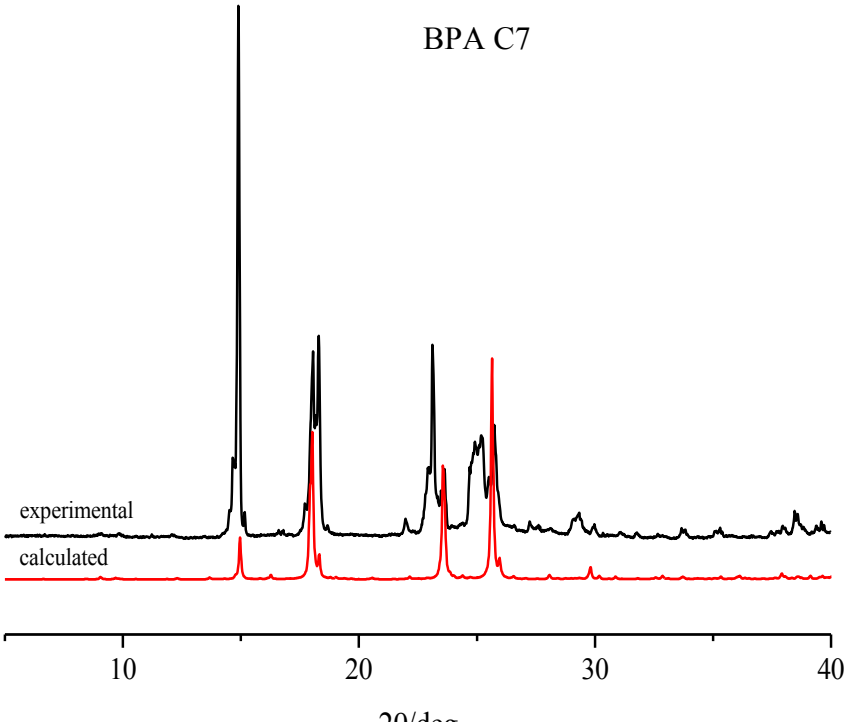
BPA C7
experimental
calculated
10
20
30
40

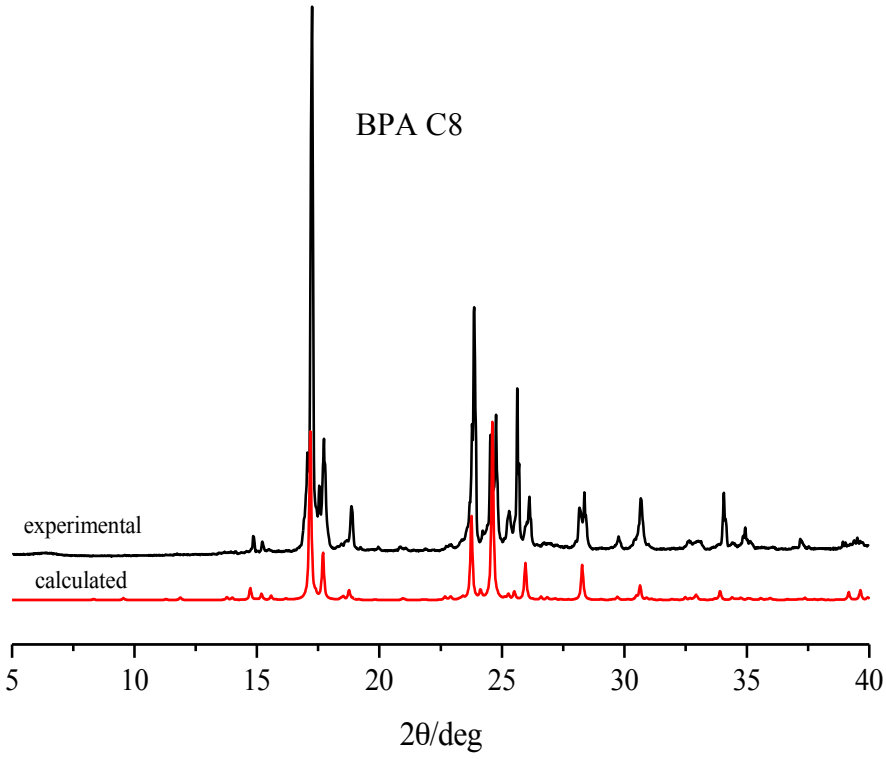
BPA C8
experimental
calculated
5
10
15
20
25
30
35
40
2θ/deg

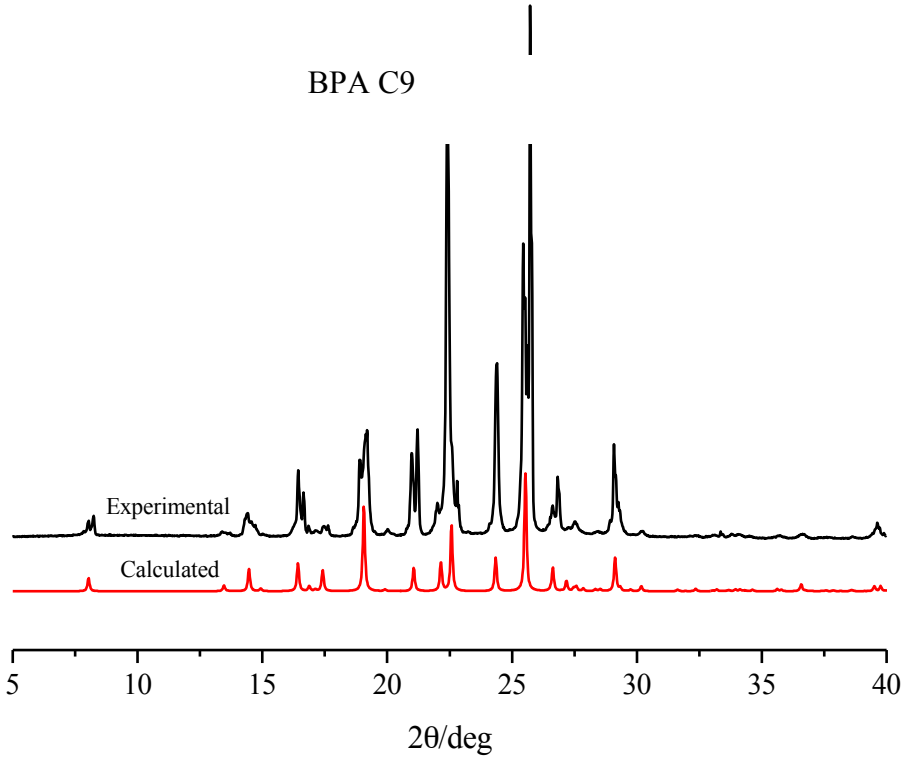
BPA C9
Experimental
Calculated
5
10
15
20
25
30
35
40
2θ/deg

BPA C10

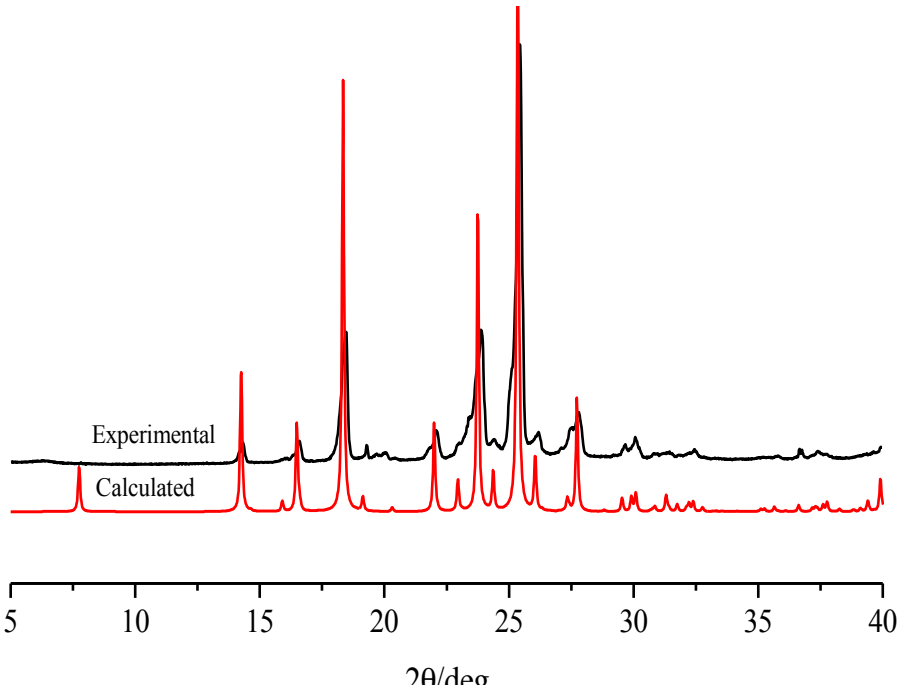

1.5.7. **XRPD Patterns - BPE:acid**

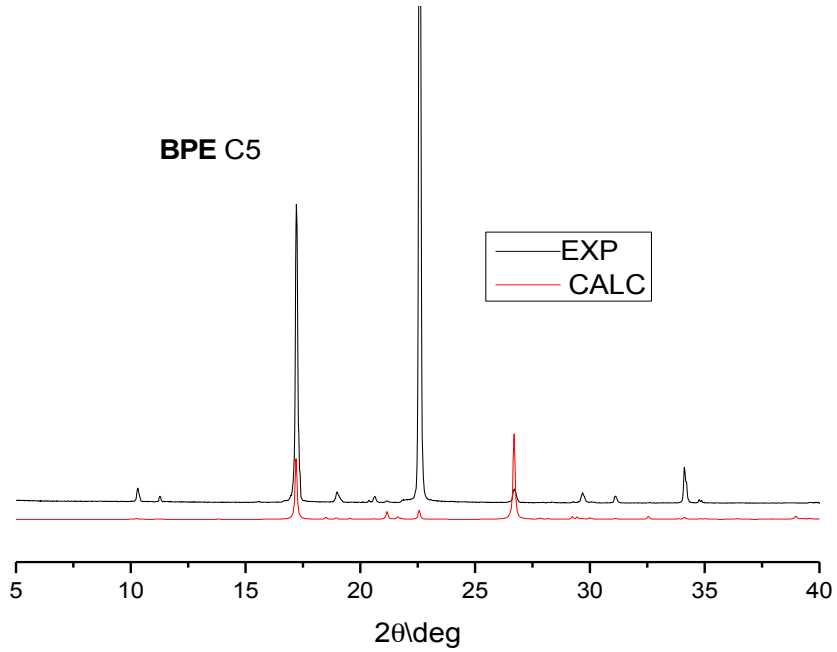

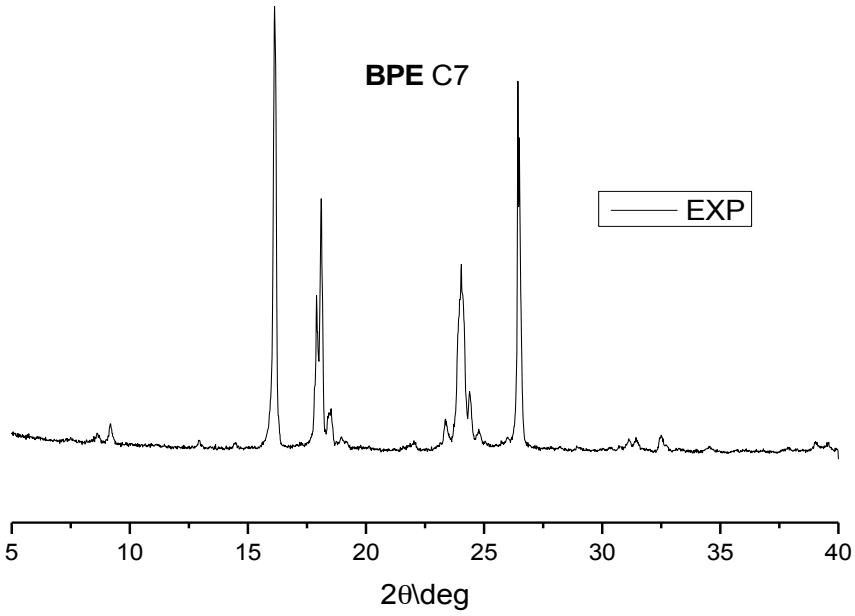

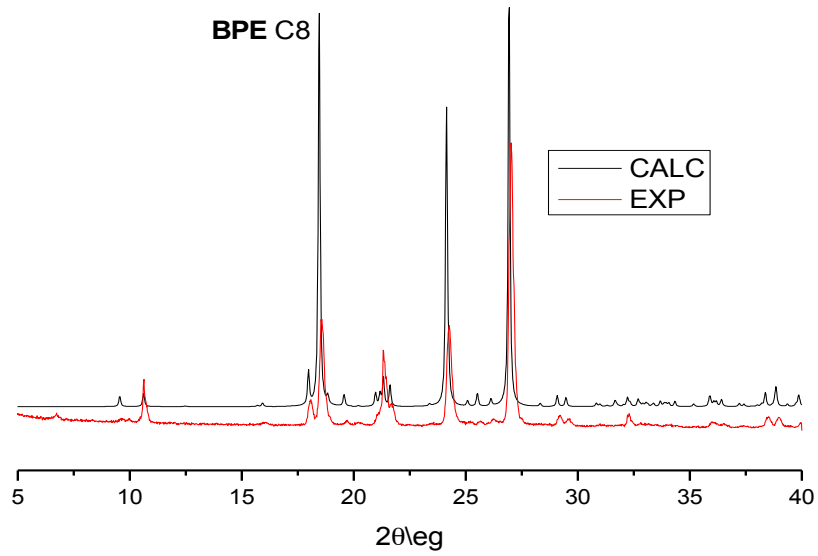
BPE C8
CALC
EXP
5
10
15
20
25
30
35
40
2θ\eg

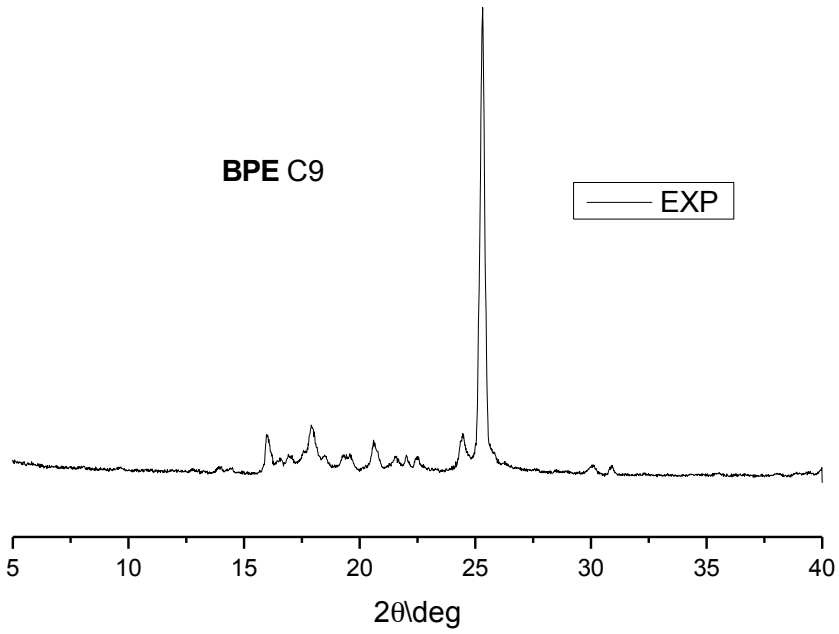
BPE C9
EXP
5
10
15
20
25
30
35
40
2θ\deg

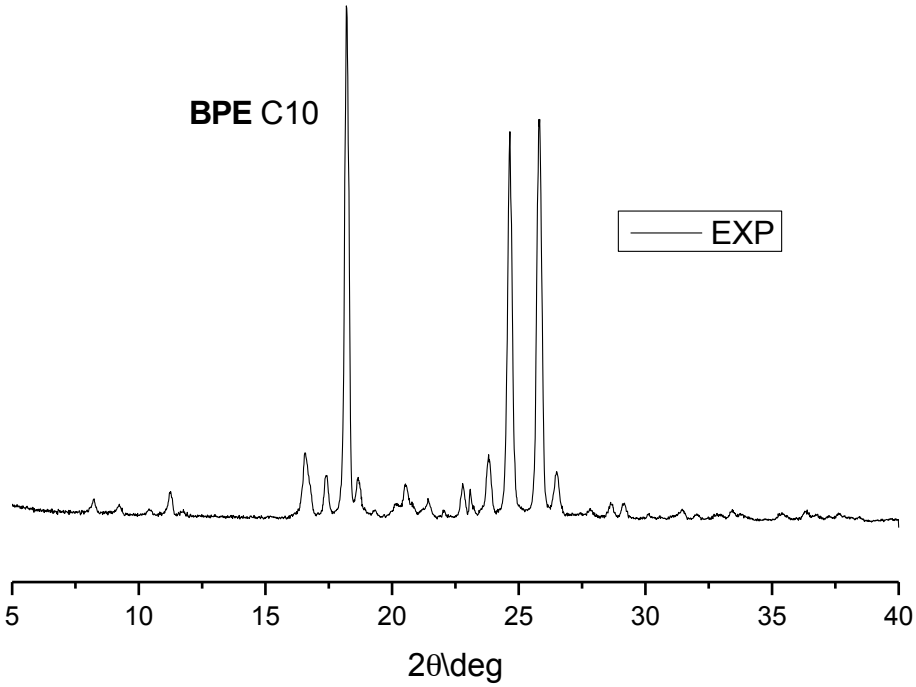
BPE C10
EXP
5
10
15
20
25
30
35
40
2θ\deg

1.5.8. **XRPD Patterns - BPP:acid**

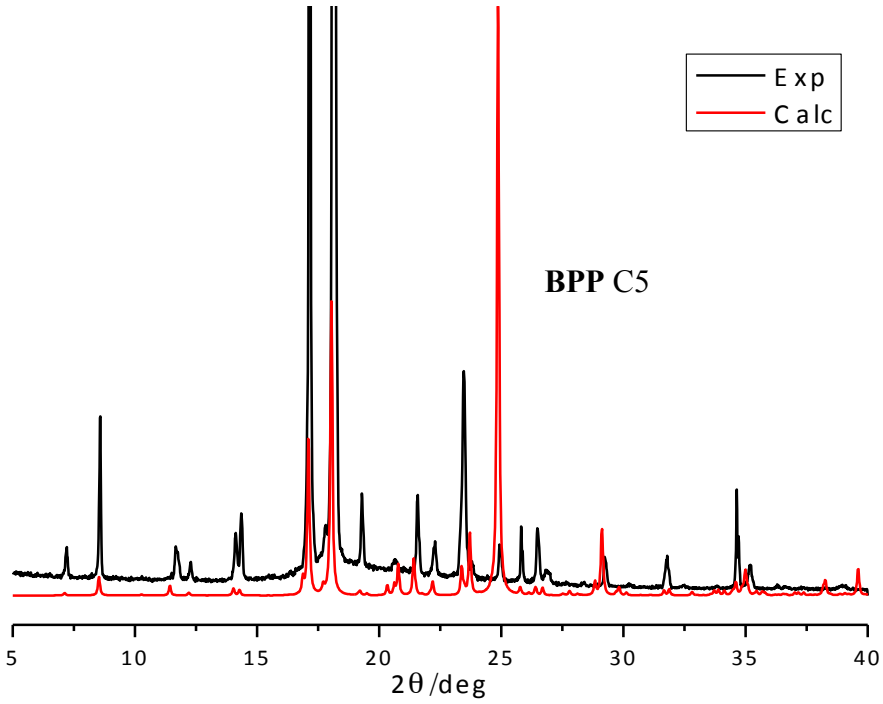

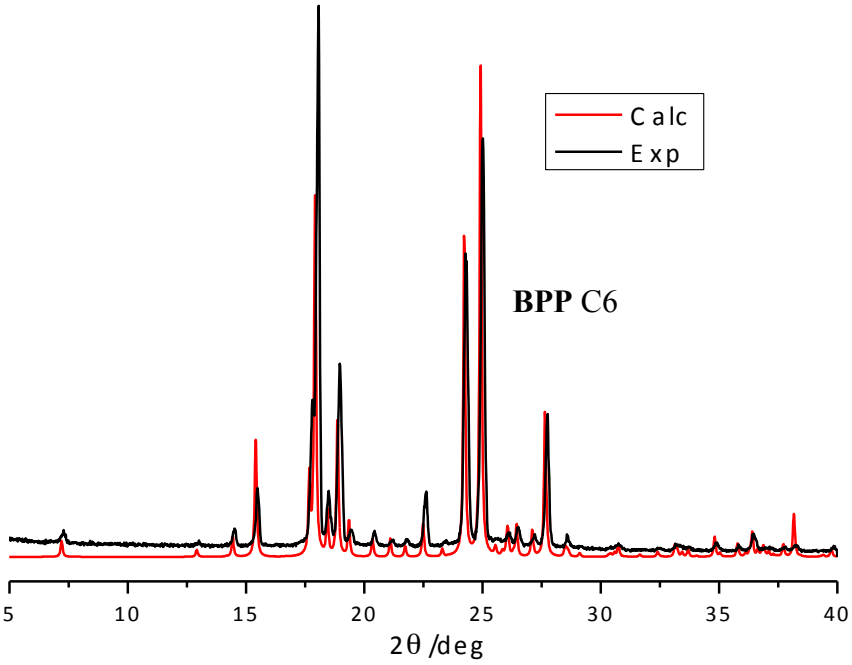

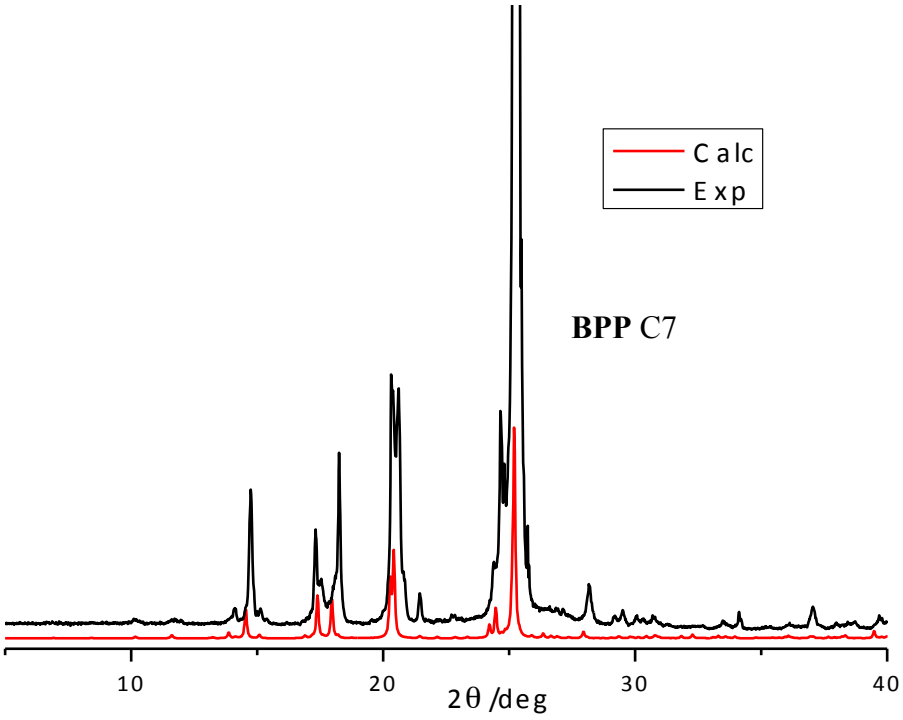
Calc
Exp
BPP C7
10
20
30
40
2θ /deg

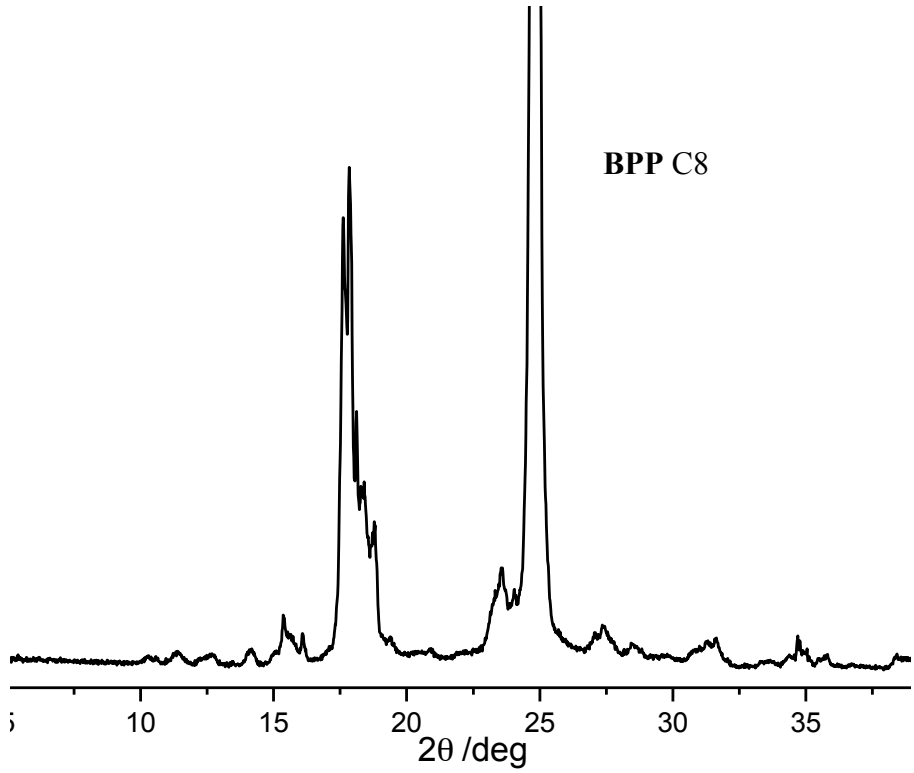
BPP C8
10
15
20
25
30
35
2θ /deg

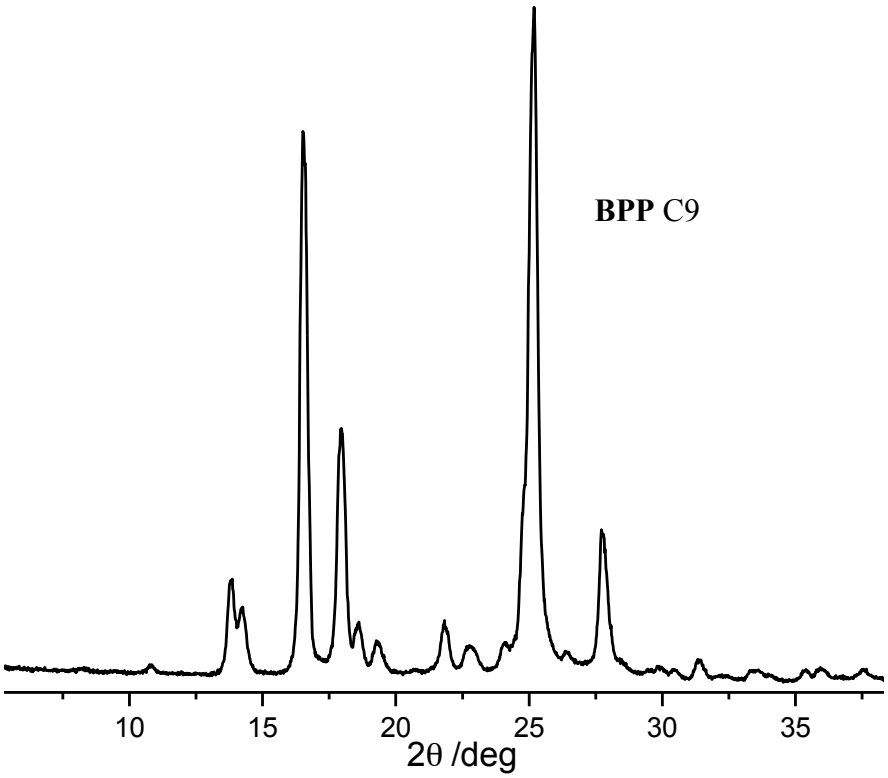
BPP C9
10
15
20
25
30
35
2θ /deg

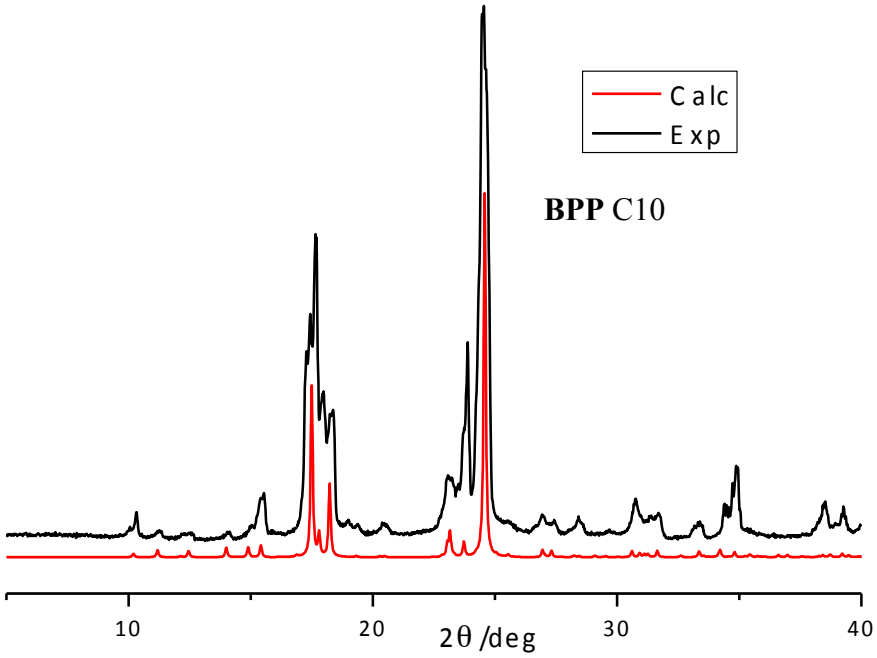
Calc
Exp
BPP C10
10
20
30
40
2θ /deg

1.5.9. **Solid-state NMR**

The spectra were collected and interpretated by the Research Group of Prof. Roberto Gobetto of Torino University.

The chemical shift of pure dicarboxylic acids are slightly higher than the average value of a COOH group. This is because they form the typical cyclical centrosymmetric dimerization of carboxyl function which creates a resonance between the bond sleading to an intermediate chemical shift value between carboxylic and carboxylate.

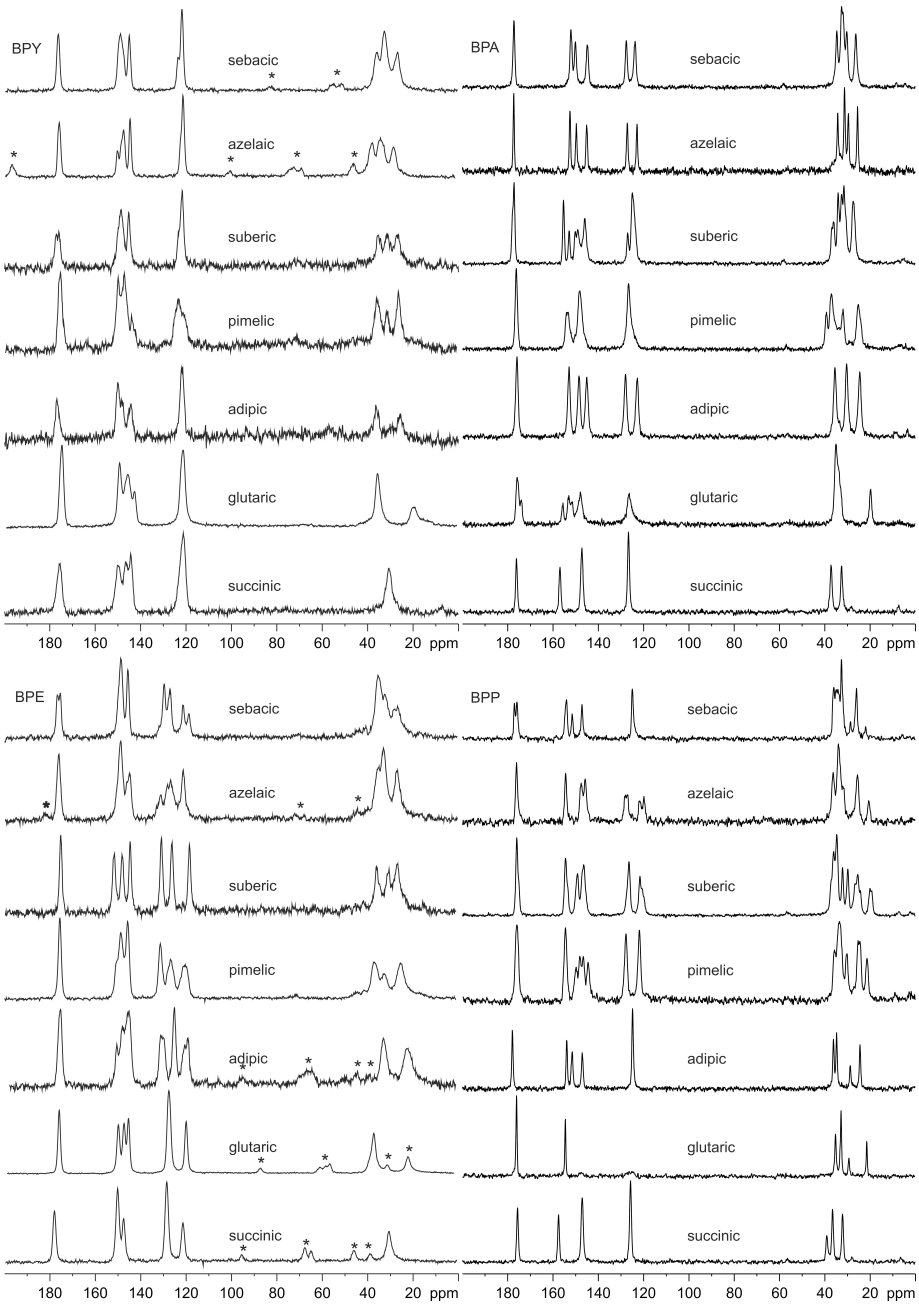

Figure 1: ^{13}C CPMAS NMR spectra of the co-crystals series with BPY, BPA, BPE and BPP recorded with a spinning speed of 12 kHz.

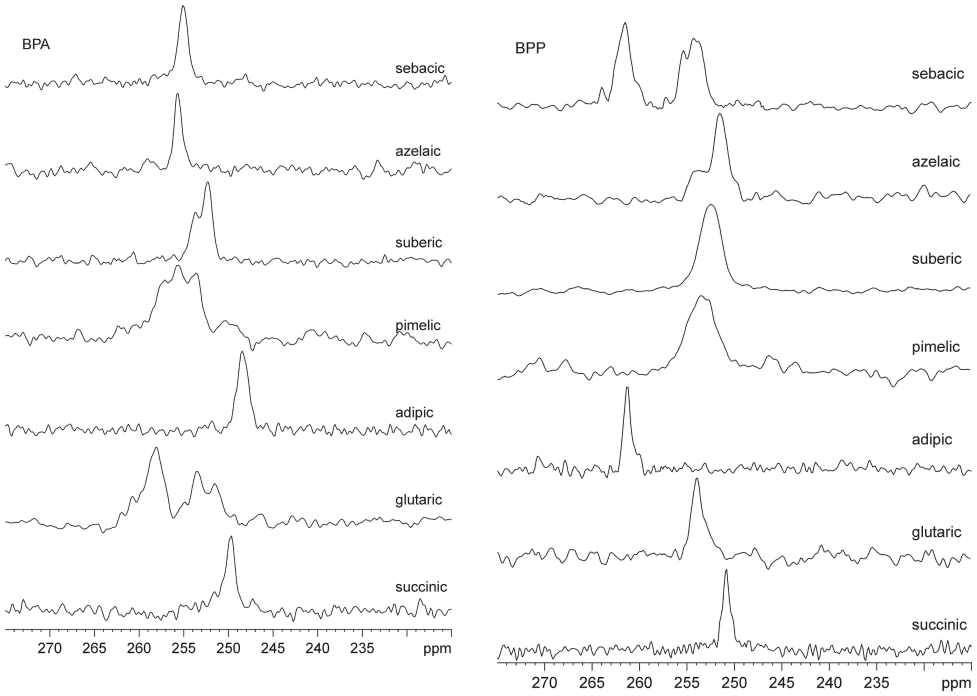

Figure 2: ^{15}N CPMAS NMR spectra of the acid-BPA and acid-BPPseries recorded with a spinning speed of 6 kHz.

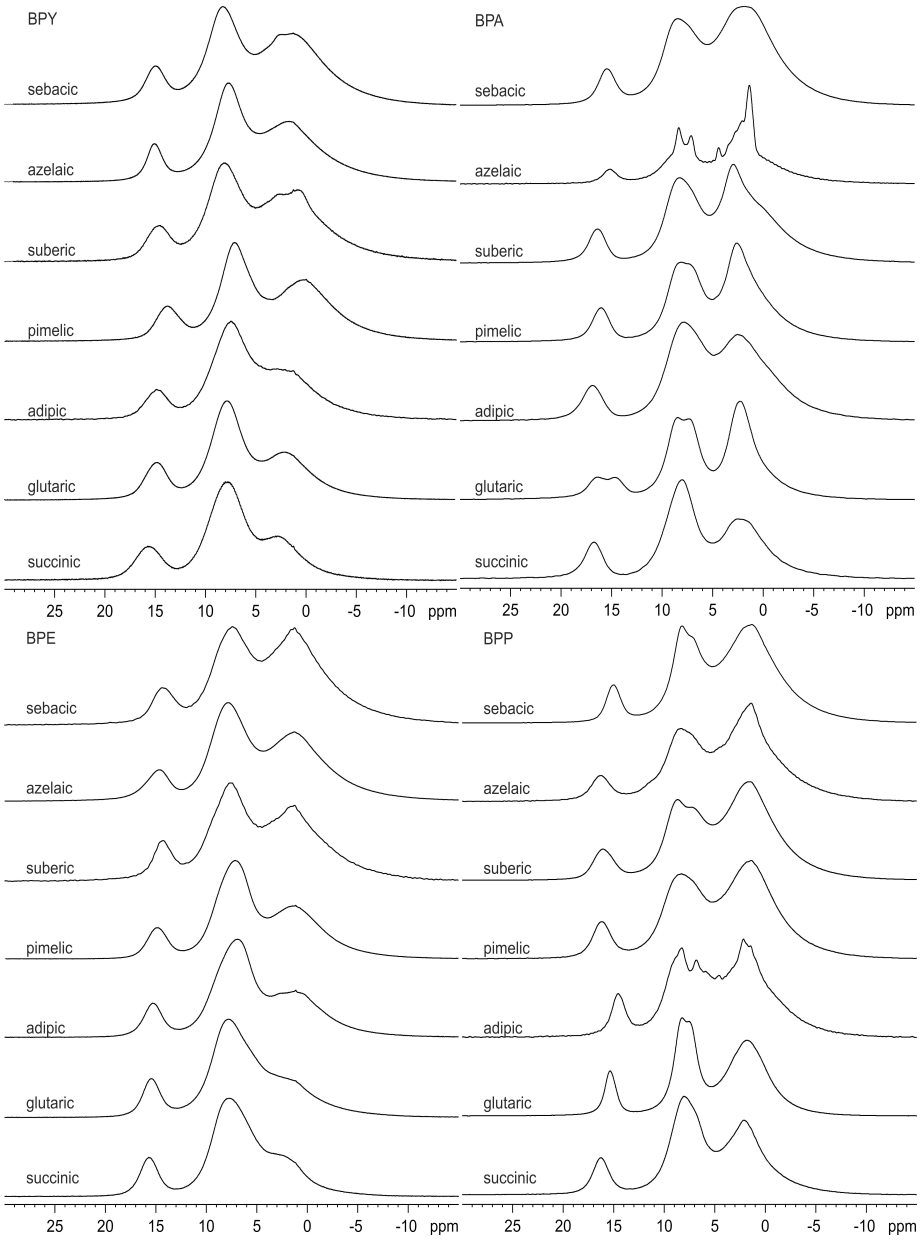

Figure 3: ^{1}H MAS NMR spectra of the co-crystals series with BPY, BPA, BPE and BPP recorded with a spinning speed of 32 kHz.

1.6. References

1. D. Braga, S. D'Agostino, E. Dichiarante, L. Maini, F. Grepioni, *Chem. Asian J.*, submitted.
2. a) F. L. Breusch, *Fortschr. Chem. Forsch.*, 1969, **12**, 119; A. I. Kitaigorodskii, *Molecular Crystals and Molecules*, Academic Press, New York, 1973;b) Feng Tao and Steven L. Bernasek, *Chem. Rev.*, 2007**, 107**, 1408.
3. M. Bilde, B. Svenningsson, J. Mønster and T. Rosenørn, *Environ. Sci. Technol.*, 2003, **37**, 1371.
4. a) R. Boese, H. C. Weissand D. Bläser, *Angew. Chem.,* 1999, **111**, 1042; b) R. Boese, H. C. Weissand D. Bläser, *Angew. Chem. Int. Ed*. 1999, **38**, 988; c) A. D. Bond, *New. J. Chem.*, 2004, **28**, 104; d) E. Badea, G. Della Gatta, D. D'Angelo, B. Brunettiand Z. Recˇkova´, *J. Chem. Thermodynamics,* 2006, **38**, 1546; e) V. R. Thalladi, R. Boese and H. C. Weiss, *Angew. Chem. Int. Ed*., 2000, **39**, 918; f) P. Vishweshwar, A. Nangia and V. M. Lynch, *Cryst. Growth & Des.*, 2003, **3**, 783;g) E. Badea, I. Blanco and G. Della Gatta, *J. Chem. Thermodynamics*, 2007, **39**, 1392; h) K. Uno, Y. Ogawa and N. Nakamura, *Crystal Growth & Design,* 2008, **8**, 593;i) V. R. Thalladi, R. Boese and H. C. Weiss, *J. Am. Chem. Soc.*, 2000, **122**, 1186.
5. V. R. Thalladi, M. Nüsse and R. Boese, *J. Am. Chem. Soc.*, 2000, **122**, 9227.
6. A. D. Bond, *CrystEngComm,* 2006, **8**, 333.
7. Samantha K. Callear, Michael B. Hursthouse and Terence L. Threlfall, *CrystEngComm*, 2010, DOI: 10.1039/b917191f.
8. a) D. Braga, L. Maini, G. de Sanctis, K. Rubini, F. Grepioni, M. R. Chierotti and R. Gobetto, *Chem. Eur. J.*, 2003, **9**, 5538; b) D. Braga, S. L. Giaffreda, F. Grepioni, G. Palladino and M. Polito, *New J. Chem.*, 2008, **32**, 820.
9. a) G. M. Sheldrick, *SHELX97*, *Program for Crystal Structure Determination*; University of Göttingen: Göttingen, Germany, 1997; b) E. Keller, SCHAKAL99, Graphical Representation of Molecular Models,

University of Freiburg, Germany, 1999; c)A. L. Speck, PLATON; *ActaCrystallogr*., *Sect*. *A*, 1990, **46**, C34; d) PowderCell programmed by W. Kraus and G. Nolze (BAM Berlin) © subgroups derived by Ulrich Müller (Gh Kassel).

10. a) V.R.Pedireddi, S.Chatterjee, A.Ranganathan, C.N.R.Rao, *Tetrahedron,* 1998, **54**, 9457; b) D. Braga, G. Palladino, F. Grepioni, M. Polito, K. Rubini, M. R. Chierotti, R. Gobetto, *Chem. Eur. J.,* 2008**,** **14***,* 10149-10159*;*c) Bin Yu, Xiao-qing Wang, Ru-Ji Wang, Guang-Qiu Shen, De-Zhong Shen, *Acta Crystallogr., Sect.E:Struct.Rep.Online,* 2006, **62**, 2757; d) Jing Zhang, Lixin Wu, Yuguo Fan, *J.Mol.Struct.*, 2003,**660**,119; e) B. R. Bhogala, S. Basavoju and A. Nangia, *CrystEngComm*, 2005, **7**, 551-582.
11. a) D. Braga, F. Grepioni, M. Polito, M. R. Chierotti, S. Ellena and R. Gobetto, *Organometallics*, 2006, **25**, 4627; b) D. Braga, L. Maini, C. Fagnano, P. Taddei, M. R. Chierotti and R. Gobetto, *Chem. Eur. J.*, 2007, **13**, 1222.
12. a) S. P. Brown and H. W. Spiess, Chem. Rev., 2001, **101**, 4125; b) D. Braga,G. Palladino, M. Polito, K. Rubini, F. Grepioni, M. R. Chierotti andR. Gobetto, Chem.–Eur. J., 2008, **14**, 10149.
13. R. Gobetto, C. Nervi, M. R. Chierotti, D. Braga, L. Maini,F. Grepioni, R. K. Harris and P. Hodgkinson, Chem.–Eur. J., 2005,**11**, 7461.
14. M. R. Chierotti and R. Gobetto, Chem. Commun., 2008, 1621.
15. R. Gobetto, C. Nervi, E.Valfr_e, M. R. Chierotti, D. Braga, L. Maini,F. Grepioni, R. K. Harris and P. Y. Ghi, Chem. Mater., 2005, **17**,1457.
16. D. Braga, E. Dichiarante,G. Palladino, F. Grepioni, M. R. Chierotti, R. Gobetto, L. Pellegrino,*CrystEngComm,*2010,*DOI: 10.1039/c0ce00253d*.
17. S. L. Childs, G. P.Stahly and A. Park, *Mol. Pharm.*, 2007, **4**, 323.

2. CRYSTAL FORMS OF THE NOVEL OXALATE SALT OF O-DESMETHYLVENLAFAXINE

2.1. Introduction

The pharmaceutical industry relies predominantly on solid, possibly crystalline forms for the delivery of active pharmaceutical ingredients (APIs), mainly for reasons of purity, thermal stability, manufacturability, and ease of handling. However, problems associated with the solid form of many drugs exist, including polymorphic conversion, low solubility, and low bioavailability for crystalline solids, and the tendency of amorphous forms to spontaneously crystallize into more stable crystalline forms.[1] For these reasons, but also for the considerable financial interests caused by legal ramifications, a constant screening for new drug solid forms, including salts, solvates and co-crystals, is ongoing.[2] More than 50% of the drugs on the market today are sold as organic salts[3]. The interest in salt formation has grown greatly over the past decades and, in recent years, it has become the most commonly used technique to improve the property of an API[4]. Salification of a drug substance, a crucial step in drug development, can have a huge impact on its properties, including solubility, dissolution rate, hygroscopicity, stability, impurity profile and particle characteristics[5]. The investigation of crystal forms represents nowadays a large portion of the experimental and theoretical work in the domain of crystal engineering, with considerable ramifications in different areas of solid state chemistry[6].

O-Desmethylvenlafaxine is a selective serotonin and norepinephrine reuptake inhibitor useful for the treatment of depression. The fumarate salt of O-Desmethylvenlafaxine is known and has poor physiochemical and permeability characteristics (See US Patent 4,535,186). US Patent 7,291,347 discloses that the succinate salt of O-Desmethylvenlafaxine has a much more improved solubility as compared to the fumarate salt and thus has improved bioavailability. It is reported to exist in four crystalline forms one of which is a monohydrate form characterized by single crystal X-ray diffraction[7]. In the course of our studies we discovered a new salt of O-Desmethylvenlafaxine,

oxalate salt (WO 2009/155488 A2), with similar stability and significantly improved solubility compared with the fumarate and succinate salts of O-Desmethylvenlafaxine (ODV). The new salt is labelled as ODV-OX (Scheme 1).

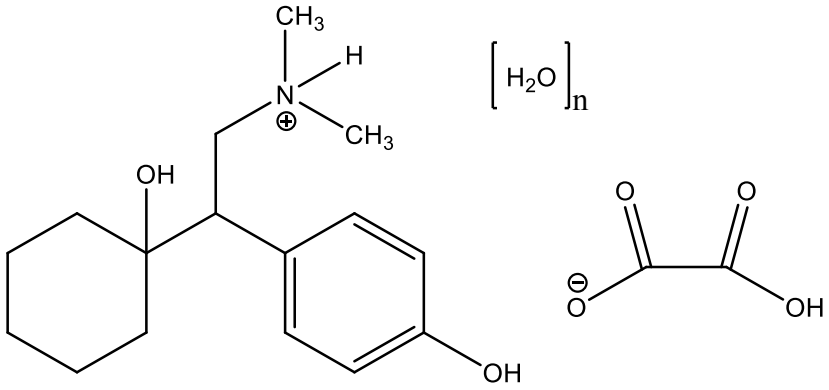

Scheme 1. Structure of ODV-OX (0 › n ‹ 2.5).

2.2. Experimental section

2.2.1. Synthesis of ODV

The synthesis of ODV is taken from the patent US 2008/0015259 A1.
4 g of Venlafaxine were dissolved in 10 mL of N-methyl-pirrolidone with 2 g of Na_2S in N_2 atmosphere. The N_2 flux was closed and solution was heated to 175°C in 1 hr. The solution was left at 175°C for 3 hrs and after was cooled to 90°C. 12 mL of water were added to solution that after was cooled at room temperature and left at 4°C for approx. 12 hrs. The suspension was filtered and washed with water.

2.2.2. Solution synthesis of ODV-OX Form A

ODV-OX Form A was prepared dissolving 4 mmol of Des-Methyl-Venlafaxine and 4 mmol of Oxalic acid (stoichiometric ratio 1:1) in 4 mL of boiling water. The solution,concentrated and purified by filtration, was left to evaporate at 60°C or room temperature.

2.2.3. Solution synthesis of ODV-OX Form B

ODV-OX FORM B was obtained by dissolving 0.200 g of ODV-OX Form A in 2 mL of Acetone. The suspension was left under stirring for three days at room temperature and filtered on a Whatman filter.

2.2.4. Solution synthesis of ODV-OX Form C

ODV-OX FORM C was obtained by evaporation of an acetonitrile solution of ODV-OX FORM A. The solution was prepared dissolving 0.05 g of ODV-OX Form A in 4mL acetonitrile. The solution was left under stirring at room temperature, filtered with a Whatman filter and left to evaporate at 60°C.

2.2.5. **Solution synthesis of ODV-OX Form D**

ODV-OX FORM D was obtained by evaporation of a water solution of ODV-OX FORM A. The solution was prepared dissolving 0.05 g of ODV-OX Form A in 4 mL water. The solution was left under stirring at room temperature, filtered with a Whatman filter and left to evaporate at 4°C. Single crystal of Form D was obtained.

2.2.6. **Solution synthesis of ODV-OX Form E**

ODV-OX Form E was obtained by dissolving 1 g of ODV-OX in 15 mL of 1-Propanol. The suspension was stirred for seven days at room temperature, and filtered on a Whatman filter. The sample was dried at 90-100 degrees for 1 hrs.

2.2.7. **Solution synthesis of ODV-OX Form F (Form B-100D in the Patent WO 2009/155488 A2)**

ODV-OX FORM F was obtained by dissolving 0.200 g of ODV-OX FORM A in 2 mL of acetone. The suspension was stirred for three days at room temperature, and filtered on a Whatman filter. The sample was dried at 90-100 °C for 1 hrs.

2.2.8. **Thermal behaviour**

Thermogravimetric analyses were performed using a simultaneus STA 409 PC Luxx® Netzsch equipped with a thermocouple for the direct measurament of DSC signal, and a thermobalance for the measurament of TGA signal. The samples (5-15 mg) were placed in aluminium pierced pans, and the heating was carried out at 10°C min^{-1} in N_2 atmosphere (See supplementary material). Calorimetric measurements were performed using a DSC 200 *F3 Maia*® differential scanning calorimeter equipped with an intra-cooler. The samples (2–4 mg) were placed in aluminium pierced pans, and the heating was carried out at 10°C min^{-1} in N_2 atmosphere(See supplementary material).

2.2.9. **X-Ray diffraction**

Single-crystal data were collected on an Oxford X'Calibur S CCD diffractometer equipped with a graphite monochromator (MoKα radiation, λ= 0.71073) and operated at room temperature. Data collection and refinement details are reported in the supplementary material. The structure was solved by direct methods and refined by full-matrix least-squares on F^2 with SHELX97[8a] program package.

A calculated XRPD pattern was generated for Cu radiation using Mercury v 1.4 and the atomic coordinates, space group and unit cell parameter from the single crystal data.

MERCURY and SCHAKAL99[8b] were used for the graphical representation of the results and PLATON[8c] was used for hydrogen bonding analysis.

X-ray powder diffractograms were collectedon a Panalytical X'Pert Pro automated Diffractometer equipped with X'Celerator, CuKα, using glass sample holder**.** The tube voltage and amperage were set to 40 kV and 40 mA, respectively.The program used for data collection was set to record only the data points within the range 2θ= 3° - 40°. VT-XRPD analyses were performed equipping the diffractometer with an Anton Paar TTK 450 low-temperature camera that was a non-ambient attachment for powder X-ray diffraction studies in reflection geometry from -193 °C to +450 °C.

2.2.10. **FT-IR**

All FT-IR measurements were performed using Nicolet FT-IR 6700 Thermo Fischer equipped with ATR device. The analyses were performed on all samples and for each measurament 32 scans were recorded (See supplementary material).

2.2.11. **Dissolution tests**

The calibration curve was constructed by plotting the absorbance against the concentration for four standard solutions of the sample in a sodium chloride solution 0.9% in standard concentrations. The analyses were performed using a dissolution tester and methods as described in the "*European Pharmacopeia section 2.9.3 pg. 267"*. The detector used was a UV-Vis Cary 50 Varian, equipped with an optic fiber. The program used was "*Concentration*" (Cary 50 WinUV Software V.3) and the measurement for each standard was recorded at a fixed λ. The Kinetic solubilities were performed on a Hanson's Vision Classic 6 dissolution tester coupled with a Varian Cary 50 UV-Vis Spectrophotometer. The program used was "*Kinetic"* (Cary 50 WinUV Software V.3), which recorded continuously the absorbance at fixed λ of a sodium chloride solution 0.9% (80mL) under stirring (250rpm) at 37°C in which were added approx. 10 mg of sample.The values obtained were converted from Abs/min into mol/min and for each sample two measurements were recorded. The thermodynamic solubilities were measured by leaving a sodium chloride solution 0.9% of the sample under stirring at 500 rpm for 24 h at 37°C. Then the suspensions were filtered, opportunly diluited and analyzed by UV-Vis Cary 50 Varian equipped with an optic fiber. The results were obtained using the calibration curves built in the first part of the experiment. For each sample two measurements were taken. Dissolution tests details are reported in the supplementary material.

2.3. Results and discussion

The new salt, named ODV-OX Form A, was synthesized dissolving Des-methyl-venlafaxine (synthesis taken from patent US2008,0015259A1) and oxalix acid in stoichiometric amount (1:1) in boiling water. The solution was filtered and left to evaporate at 60°C or at room temperature.

ODV-OX Form A was subjected to a polymorph screening to identify the possible different crystal forms. It was recrystallized from different solvents by evaporation experiments in different conditions: at room temperature, at 4°C, at 60°C and at low pressure. Also slurry experiments were performed in different solvents. In addition to ODV-OX Form A (hydrate) other five different crystal forms (three hydrates and two anhydrous) were found: ODV-OX Form C and Form D were obtained by evaporation experiments and ODV-OX Form B, Form E and Form F were obtained by slurry experiments.

The samples were characterized by different solid-state techniques: X-ray powder diffraction(XRPD), variable temperature XRPD (VT-XRPD), differential scanning calorimetry (DSC), thermogravimetric analysis (TGA), evolved gas analysis (EGA), FT-IR and single crystal X-ray diffraction (SC-XRD) for Form D (See supplementary material for details). The characterization was also implemented with stability tests at 40°C and 75%RH for one week.

The SC-XRD analysis of ODV-OX Form D evidences the presence of four ODV cations, four oxalate anions and ten water molecules in the P-1 unit cell. As shown in figure 1, the amine group of the ODV cation forms hydrogen bonds with the oxalate anion that forms other three hydrogen bonds two of which with two water molecules and the other with another oxalate anion. Another molecule of water coordinates, through hydrogen bonds, the O-H groups of two ODV cation. The packing - Figure 1 - shows a structure that is characterized by chains of oxalate, molecules of water, and chains of ODV held together by hydrogen bonds. The chains of oxalate anions have a characteristic structure composed by dimers of oxalate anions held together by two molecules of water (Figure 1b)

(a)

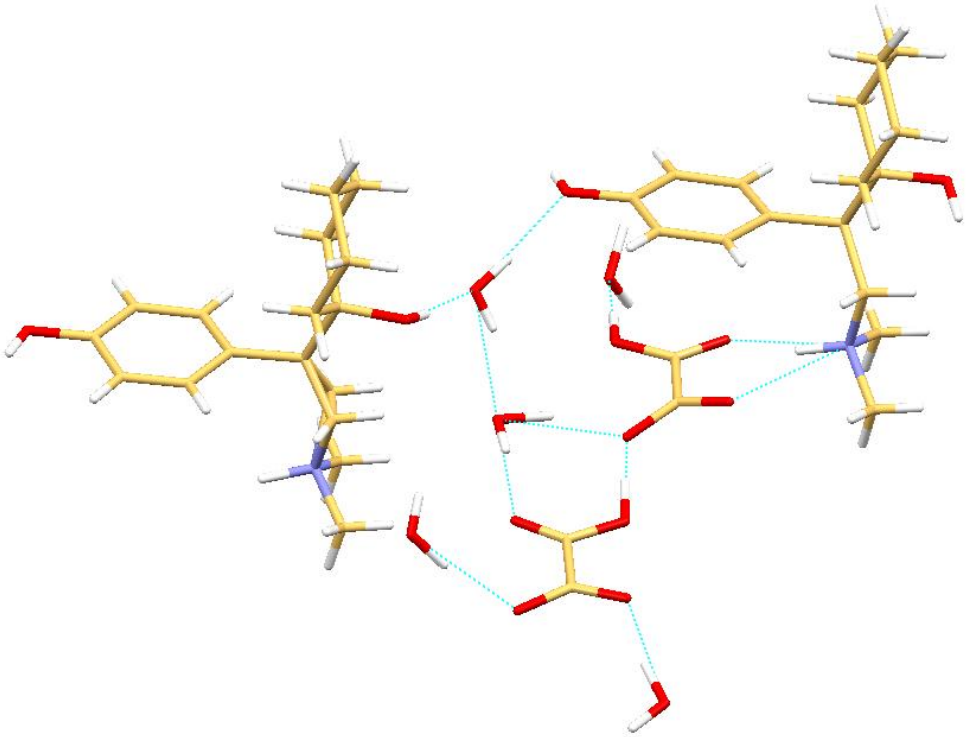

(b)

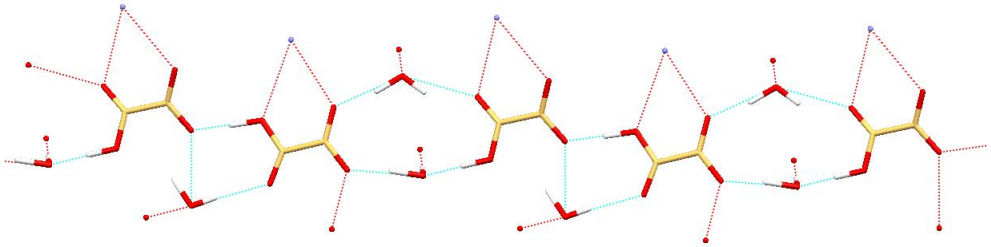

(c)

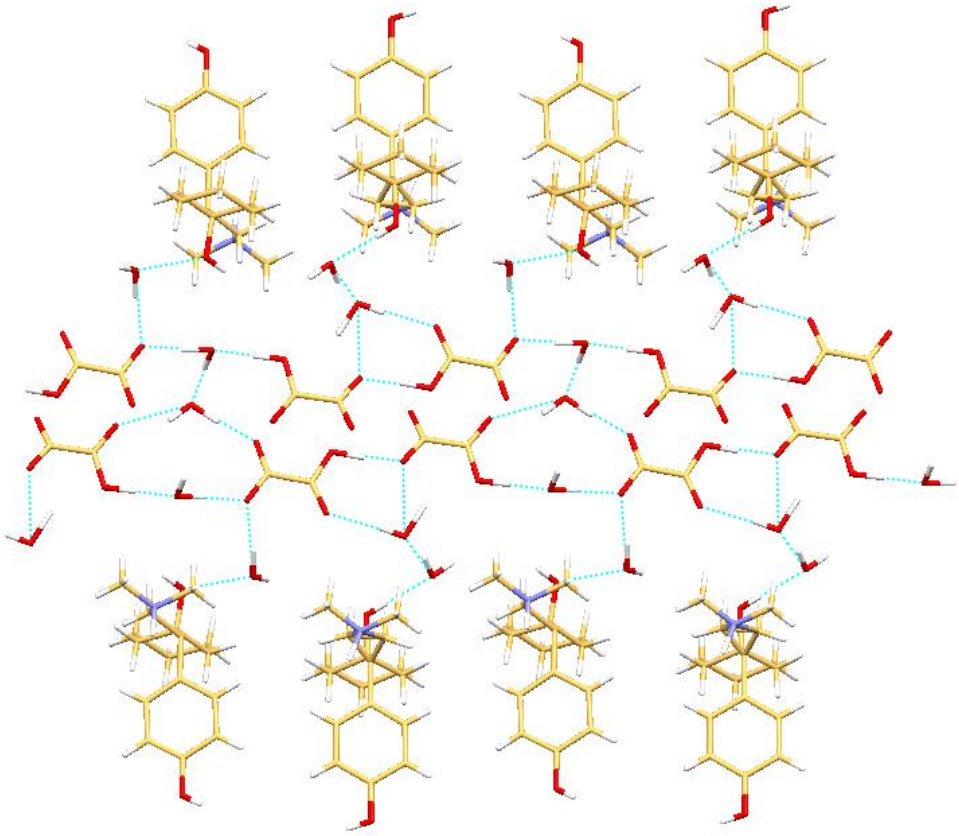

Figure.1 (a) Hydrogen bonds of ODV cations and hydrogen oxalate anions in ODV-OX Form D through the coordination of water molecules; (b)Packing of oxalate anion in ODV-OX Form D;(c) Packing of ODV-OX Form D.

In this case the correspondence of the structure, determined by SC-XRD, and that of bulk material was checked by comparing the calculated pattern with the experimental one (figure 2).

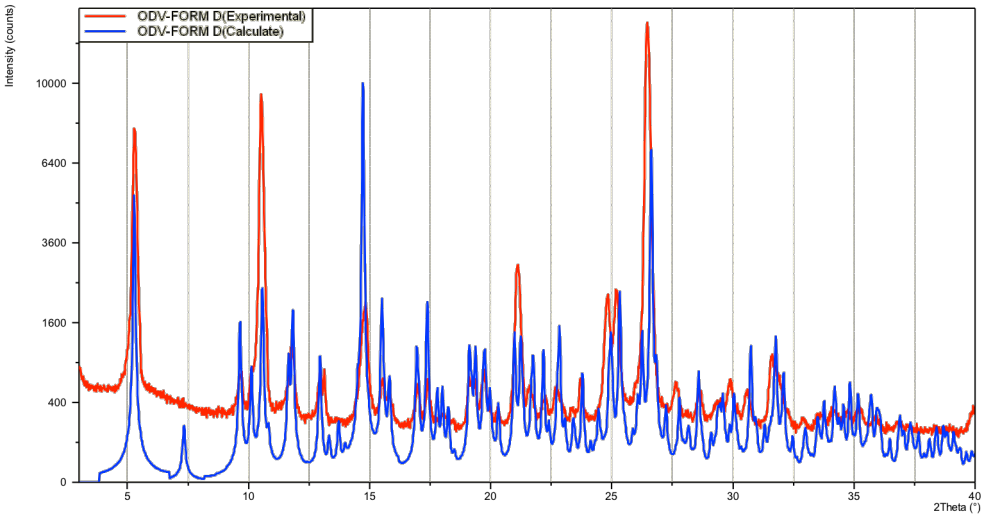

Figure.2 Comparison between XRD patterns of ODV-OX Form D experimental (red line) and calculated (blue line) by SC-XRD data.

Differential scanning calorimetry (DSC) was used to measure the melting point of all compounds and to detect the presence of additional crystalline phases. Thermogravimetric analysis (TGA) was used to measure possible solvent loss. This tecnique was associated with evolved gas analysis (EGA) that measured IR spectra and the kinetic profile of solvent loss during the TGA.

In Table 1 the melting points obtained by DSC analyses, the weight loss obtained by TG analyses and the solvent identification by EG analyses are reported. The TGA results reported in the Table 1 evidence that four of the six different crystal forms found are hydrates and two (Form E and Form F) are anhydrous. The TGA profiles of Form E and Form F show only the degradation of sample after 200°C. The TGA profiles of Form A, Form B, Form C and Form D show weight loss before the degradation. In particular Form A and Form C show a very similar TGA profile with a weight loss of approx. 5% between 70-80°C that corresponds to approx. one molecule of water as evidenced by kinetic profile of water in EGA between 5 and 8 minutes; after 100°C the TGA profile evidences the beginning of the degradation.

The TGA profile of Form B shows a weight loss of 6.9% that in EGA correspondes to water loss. After 100°C the sample is stable and decomposes after 200°C as Form F.

The TGA profile of Form D shows a double loss of 6.02% and 5.5% that in EGA correspondes to water loss. All DSC and TGA profiles are showed in the supplementary material, while the kinetic profiles are showed in Figure 3.

Table 1 Melting point (°C) and weight loss of six crystal form of ODV-OX.

CRYSTAL FORM[a]	DSC Onset (°C)	TGA LOSS (%)	Solvent loss
FORM A	79.5	5.6	water
FORM B	76.4	6.9	water
FORM C	79	4.7	water
FORM D	78.1	6.02-5.5	water
FORM E	128.7	-	-
FORM F	-	-	-

[a] Crystal form of ODV-OX salt.

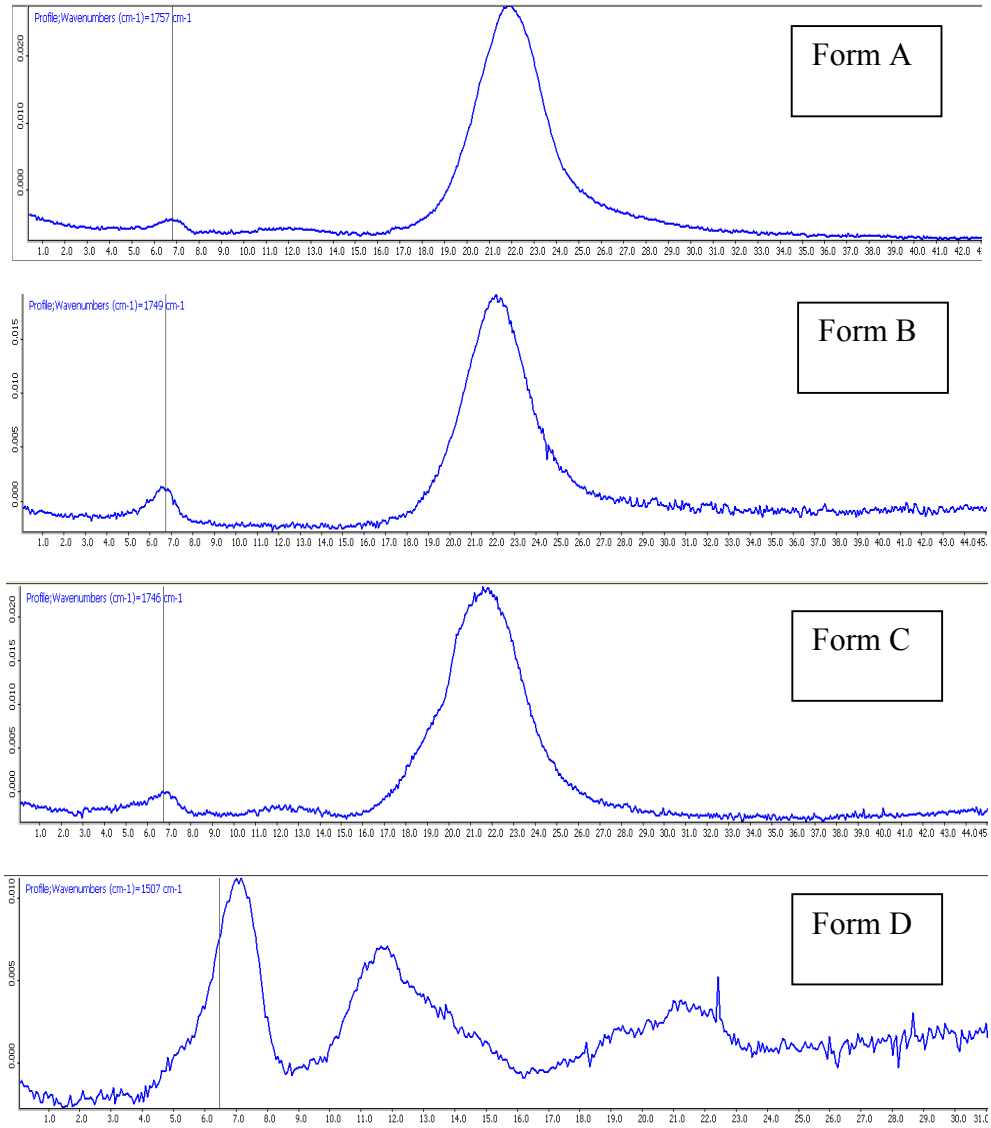

Figure.3 Kinetic profiles of water loss of four hydrate forms of ODV-OX.

ODV-OX Form A, Form B, Form C and Form E were also analyzed by VT-XRPD. Form A and Form C show the same behaviour (Figure 4 and 5): the samples were heated until 100°C and analyzed at 40°C and 80°C, the samples after 80°C begin to melt and at 100°C show the pattern of an amourphous phase.

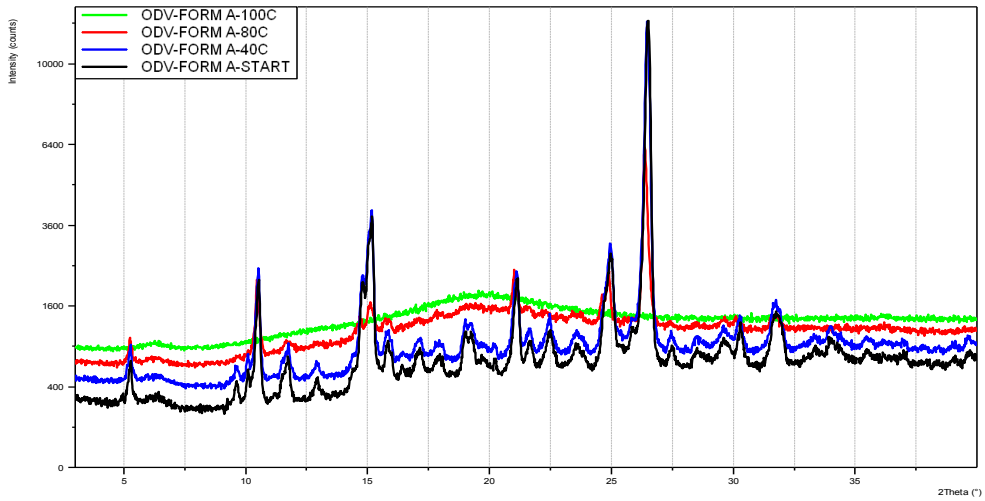

Figure.4 Comparison between XRPD patterns of ODV-OX Form A at RT and sample heated to 40°C, 80°C and 100°C.

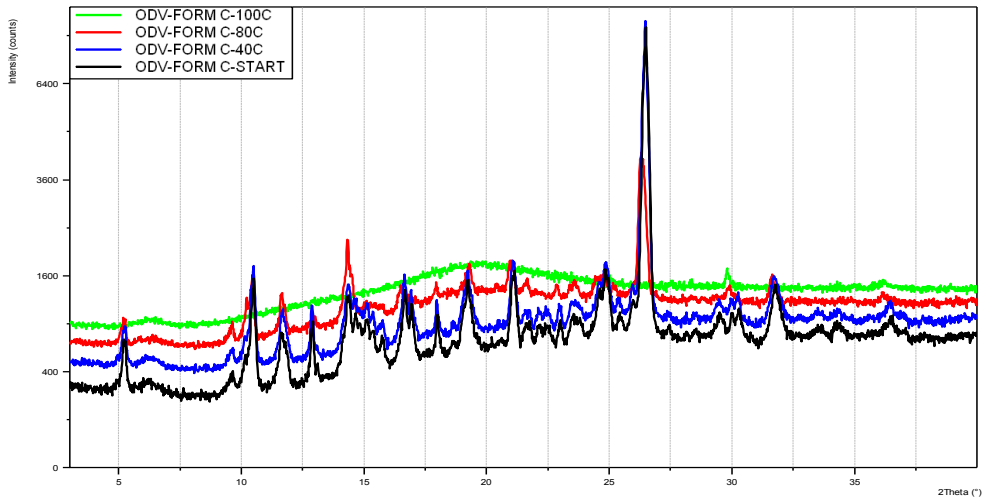

Figure.5 Comparison between XRPD patterns of ODV-OX Form C at RT and sample heated to 40°C, 80°C and 100°C.

Form B was heated until 160°C and measured from 60°C to 130°C every 10°C: the sample after 90°C converts into Form F but in the pattern there is a high amorphous content (Figure 6). After 120°C total conversion into amorphous phase is observed (Figure 7).

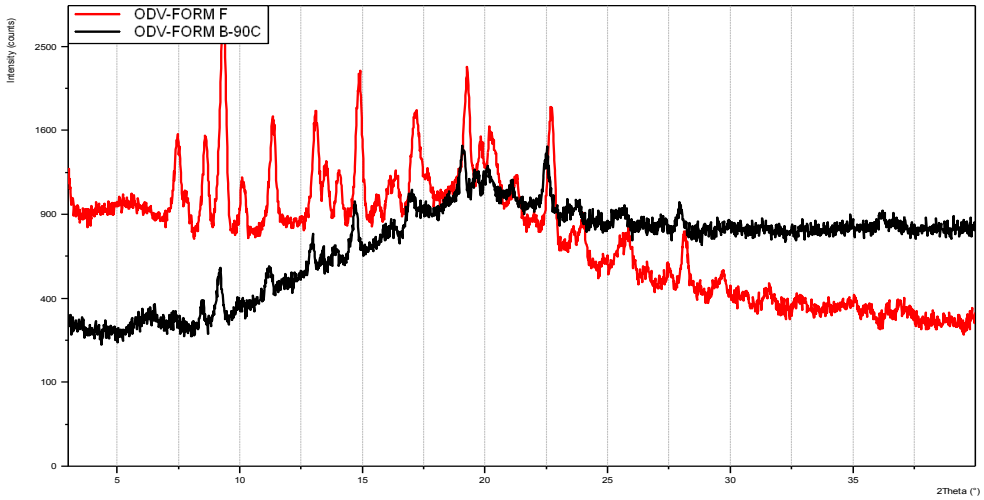

Figure.6 Comparison between XRPD patterns of ODV-OX Form B at 100°C and ODV-OX Form F.

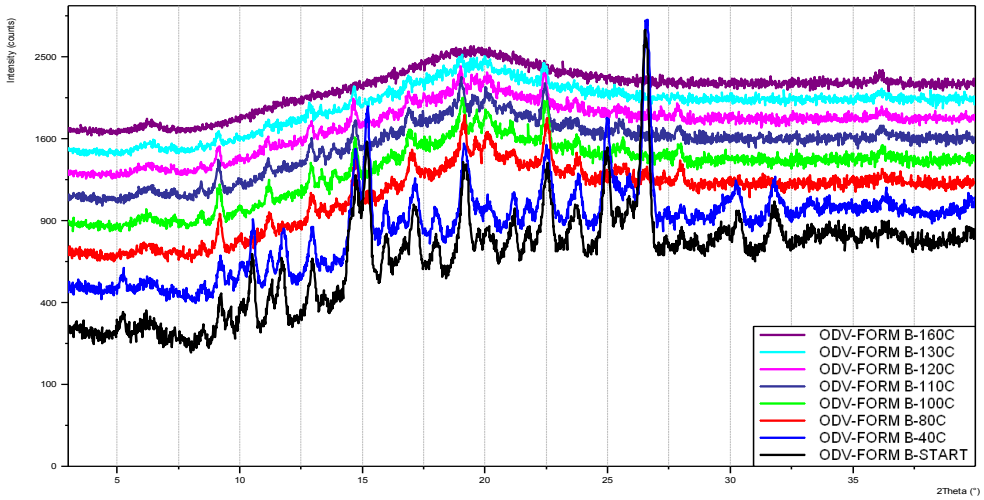

Figure.7 Comparison between XRPD patterns of ODV-OX Form B at RT and sample heated to 40°C, 80°C, 100°C, 110°C, 120°C, 130°C and 160°C.

ODV-OX Form E was heated until 150°C and analyzed at different temperatures: the sample is stable until approx. 120°C and after this temperature converts into amorphous phase (Figure 8).

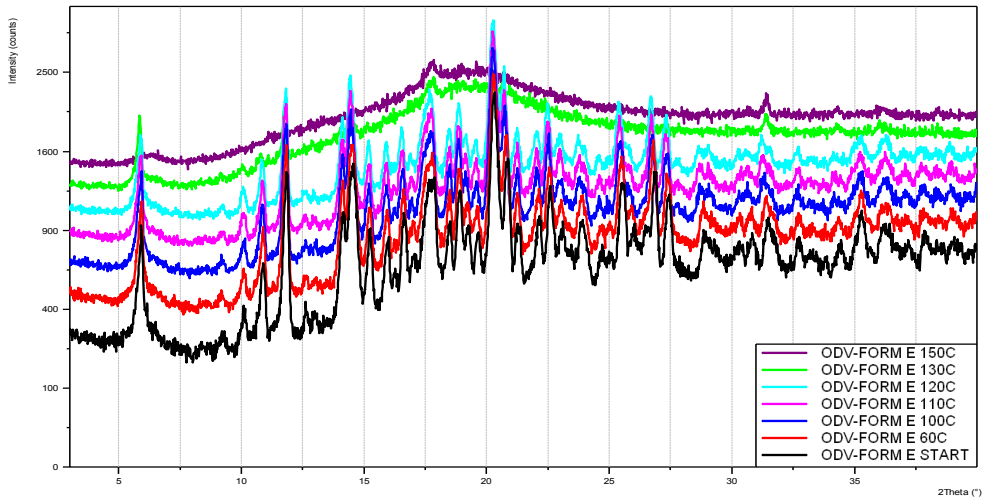

Figure.8 Comparison between XRPD patterns of ODV-OX Form E at RT and sample heated to 40°C, 60°C, 100°C, 110°C, 120°C, 130°C and 150°C.

The six crystal forms of ODV-OX were also subjected to stability test: the samples were stored for one week at 40°C and 75%RH and analyzed by XRPD.The Form A is stable (Figure 9); the Form B is stable for 3 days but after six days converts into Form A (Figure 10); the Form C is stable (Figure 11);the Form D is stable (Figure 12); the Form E converts into Form A (Figure 13) and the Form F converts into Form B (Figure 14).

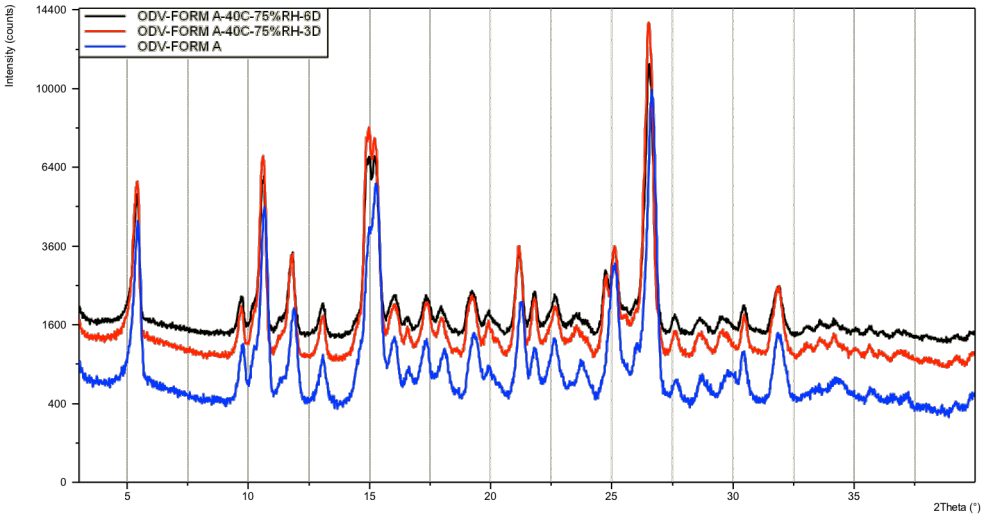

Figure.9 Comparison between XRPD patterns of ODV-OX Form A and Form A stored for three and six days at 40°C and 75%RH.

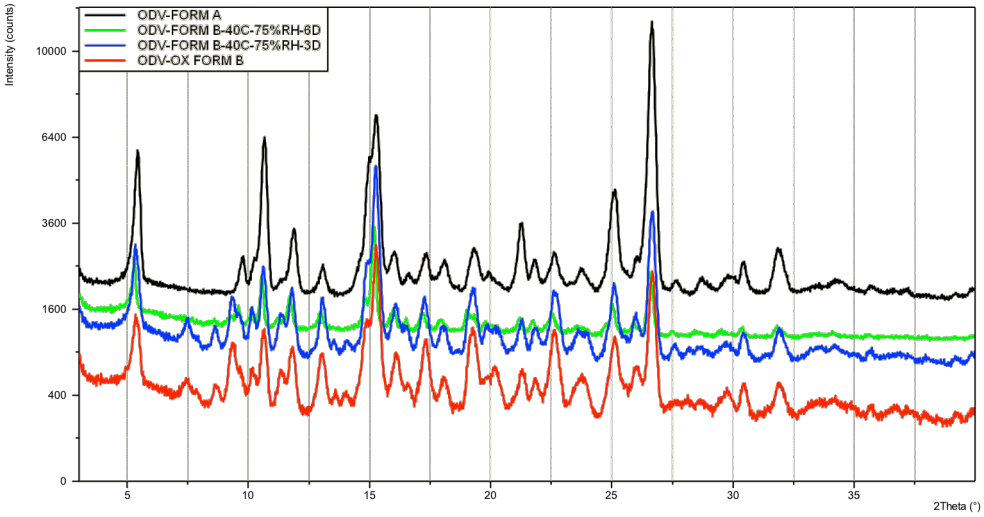

Figure.10 Comparison between XRPD patterns of ODV-OX Form B, Form B stored for three and six days at 40°C and 75%RH and Form A.

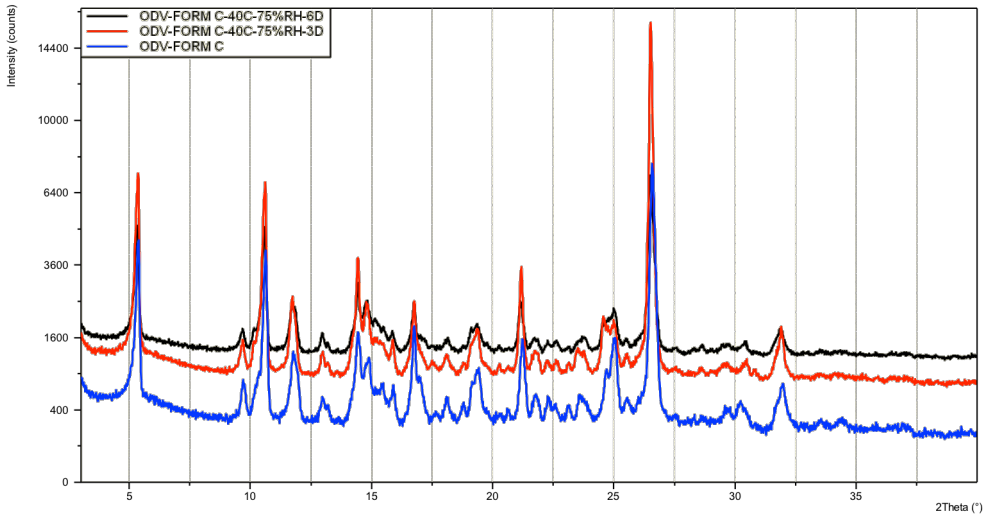

Figure.11 Comparison between XRPD patterns of ODV-OX Form C and Form C stored for three and six days at 40°C and 75%RH.

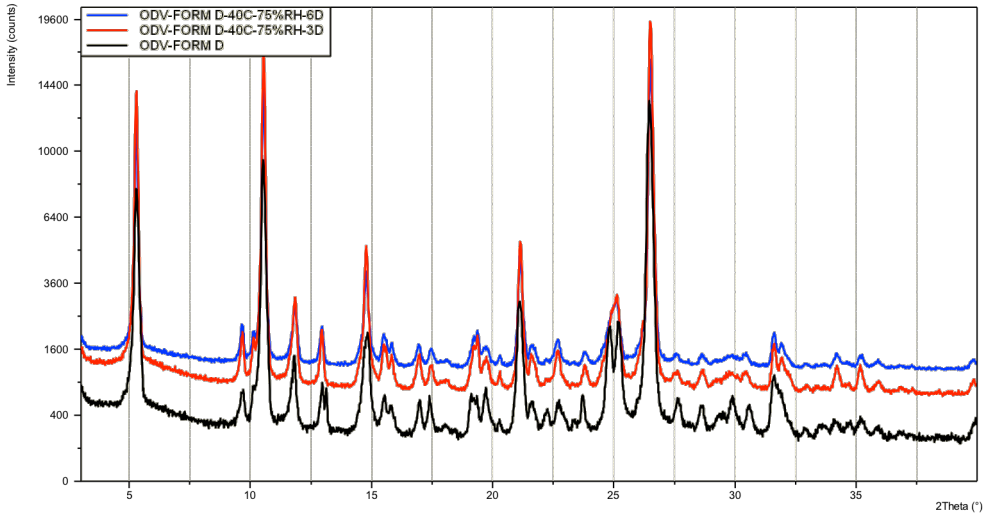

Figure.12 Comparison between XRPD patterns of ODV-OX Form D and Form D stored for three and six days at 40°C and 75%RH.

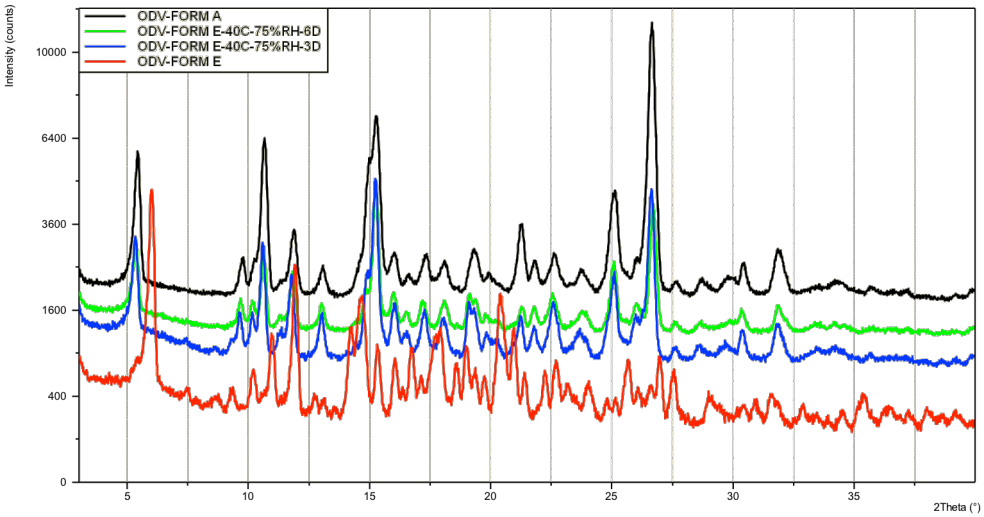

Figure.13 Comparison between XRPD patterns of ODV-OX Form E, Form E stored for three and six days at 40°C and 75%RH and Form A.

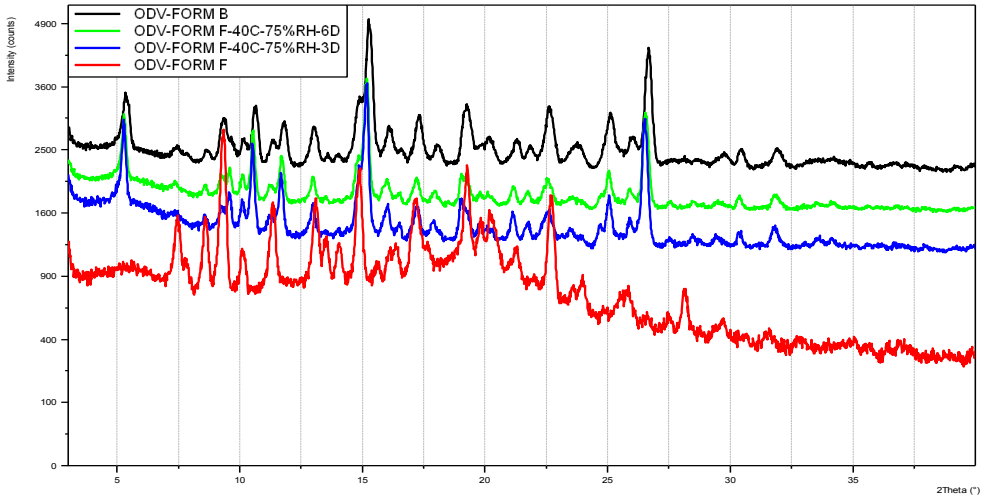

Figure.14 Comparison between XRPD patterns of ODV-OX Form F, Form F stored for three and six days at 40°C and 75%RH and Form B.

Dissolution tests were performed on ODV-OX and ODV-SUCC to compare the behavior of the oxalate and succinate salts of ODV.

A particle size homogenization was performed on both salts (using stable forms) to obtaine reproducible results. The particle size analyses were performed using Beckman-Coulter LS100 Q particle size analyzer equipped with micro-volume cell. The samples were ground to obtain the same particles size distribution as shown in figure 15 and table 2.

Table 2 Particle size results of ODV-OX and ODV-SUCC used for dissolution tests.

Mean[a]	**S.D.**[b]	**Median**[c]	**Mode**[d]	**D10**[e]	**D50**[f]	**D90**[g]
78.68 µm	47.48 µm	77.56 µm	116.3 µm	13.34 µm	77.56 µm	144.0 µm

[a] Mean: described the central location of the data; [b]S.D.: standard deviation described the spread; [c]Median: numeric value separating the higher half of the distribution from the lower half; [d]Mode: the value that occur most frequently in the distribution; [e]D10: the higher value of 10% of particles; [f] D50: the higher value of 50% of particles; [g]D90: the higher value of 90% of particles.

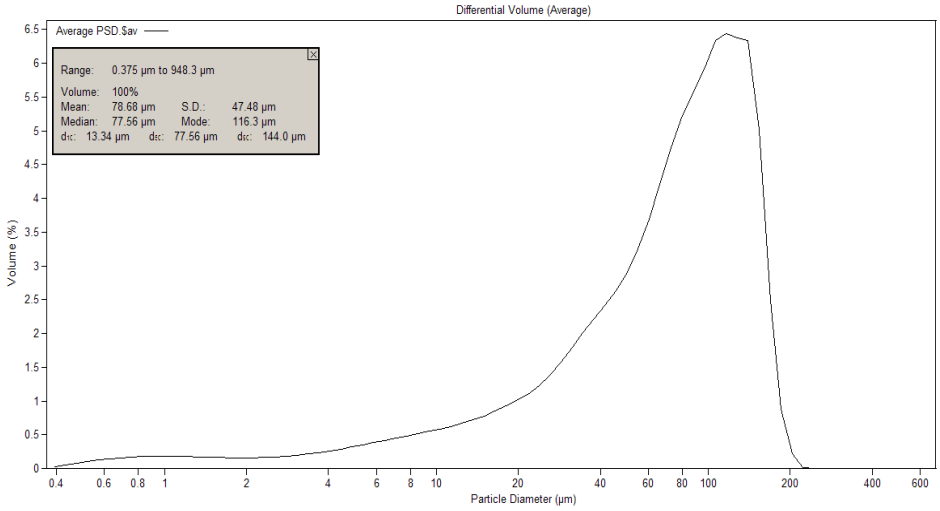

Figure15 Particle size distribution of ODV-OX and ODV-SUCC used for dissolution tests.

The results of thermodynamic and kinetic solubilities, summarized in the table 3, evidence an important increasing in solubility for the oxalate salt compared with the succinate salt.

Table 3 Thermodynamic and kinetic solubility results of ODV oxalate and succinate salts.

Salt	Kinetic solubility Abs/min	Thermodynamic solubility (g\L)
PCL01_OX	1,31	142
PCL01_SUCC	1,00	70

2.4. Conclusion

In conclusion we have reported the preparation of a new salt of o-Desmethylvenlafaxine (ODV): ODV oxalate (Form A) and other five different crystal forms (Form B, Form C, Form D, Form E and Form F). All samples obtained were characterized by a combination of different solid-state technique (XRPD, VT-XRPD, TGA, EGA, DSC, FT-IR). The ODV-OX Form D was also characterized by SC-XRD, this evidences the presence of water molecules in the structure. The TGA analyses evidence that four of the six different crystal forms found are hydrates and two (Form E and Foem F) are anhydrous. VT-XRPD analyses evidence that the monohydrate form A and C, after the water loss at 80-90°C, melt while Form B converts into anhydrous Form F that decomposes after 200°C as Form E. The stability tests performed at 40°C and 75%RH show that Form A, C, and D are stable while B and E convert into Form A; Form F converts into Form B after six days. Comparative dissolution tests, performed after a particle size homogenization of ODV-OX and ODV-SUCC, evidence a significant increasing in solubility for the oxalate salt (142 g/L) compared with the succinate salt (70 g/L).

2.5. Supplementary Material

Legenda

ODV = o-Desmethylvenlafaxine

ODV-OX = o-Desmethylvenlafaxine oxalate salt

ODV-SUCC = o-Desmethylvenlafaxine succinate salt

2.5.1. **Crystal structure determination**

A colourless needle of ODV-OX form D having approximate dimensions of 0.2 x 0.2 x 0.3 mm, was mounted on a glass fibre in random orientation. The sample ODV-OX form D crystallises in a Triclinic system with cell parameter a = 9.4342(6) Å, b = 13.0621(9) Å, c= 18.0686(12) Å, α = 109.701(6) deg., β = 96.728(5) deg., γ = 99.120(5) deg., V = 2034.62 $Å^3$ with space group P-1.

Crystal data and details of measurements are summarized in Table 1.

Table 1.Crystal data and details of measurement for ODV-OX FormD

Identification code	odv_ox
Empirical formula	C36 H64 N2 O17
Formula weight	796.89
Temperature	293(2) K
Wavelength	0.71073 A
Crystal system, space group	Triclinic, P-1
Unit cell dimensions	a = 9.4342(6) A alpha = 109.701(6) deg.
	b = 13.0621(9) A beta = 96.728(5) deg.
	c = 18.0686(12) A gamma = 99.120(5) deg.
Volume	2034.6(2) A^3
Z, Calculated density	2, 1.301 Mg/m^3
Absorption coefficient	0.103 mm^-1
F(000)	860
Crystal size	0.3 x 0.1 x 0.1 mm
Theta range for data collection	2.41 to 29.06 deg.
Limiting indices	-12<=h<=11, -16<=k<=12, -24<=l<=23
Reflections collected / unique	18059 / 8206 [R(int) = 0.0847]
Completeness to theta =	25 89.5 %
Absorption correction	Semi-empirical from equivalents
Refinement method	Full-matrix least-squares on F^2
Data / restraints / parameters	8206 / 0 / 561
Goodness-of-fit on F^2	1.023
Final R indices [I>2sigma(I)]	R1 = 0.1125, wR2 = 0.1320
R indices (all data)	R1 = 0.2874, wR2 = 0.1735
Extinction coefficient	0.0006(5)
Largest diff. peak and hole	0.322 and -0.218 e.A^-3

2.5.2. **Thermal behaviour**

Differential scanning calorimetry measurements (DSC)

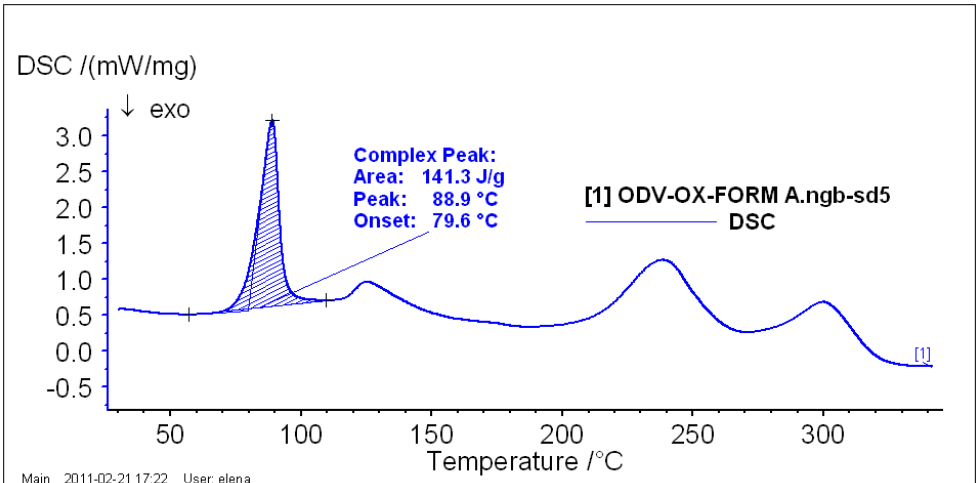

Instrument :	NETZSCH DSC 200F3	**File :**	C:\Documents and Settings\Elena\Desktop\odv-tga-dsc\ODV-OX-FORM A.ngb-sd5		
Project :	PhD	**Reference :**	Al pan,0 mg	**Mode/type of meas. :**	DSC / Sample
Identity :	ODV-OX-FORM A	**Material :**	Pharma	**Segments :**	1/1
Date/time :	17/02/2011 9.02.58	**Corr./temp.cal :**	/ 240-20-492-L.n...	**Crucible :**	Pan Al, pierced lid
Laboratory :	POLYCRYSTALLINE	**Sens.file :**	240-20-492-L.ngb...	**Atmosphere :**	<no gas>/--- / NITROGEN/40 / NITR...
Operator :	ED	**Range :**	20/10.0(K/min)/450	**Corr/m. range :**	000/5000 µV
Sample :	ODV-OX-FORM A, 5....	**Sample car./TC :**	DSC 200F3 t-sen...		

Created with NETZSCH Proteus software

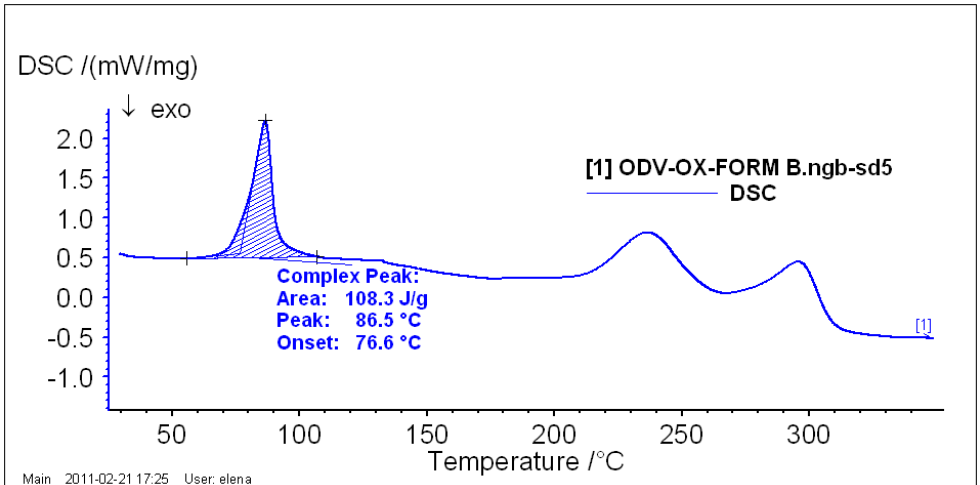

Instrument :	NETZSCH DSC 200F3	**File :**	C:\Documents and Settings\Elena\Desktop\odv-tga-dsc\ODV-OX-FORM B.ngb-sd5		
Project :	PhD	**Reference :**	Al pan,0 mg	**Mode/type of meas. :**	DSC / Sample
Identity :	ODV-OX-FORM B	**Material :**	Pharma	**Segments :**	1/1
Date/time :	16/02/2011 14.38.52	**Corr./temp.cal :**	/ 240-20-492-L.n...	**Crucible :**	Pan Al, pierced lid
Laboratory :	POLYCRYSTALLINE	**Sens.file :**	240-20-492-L.ngb...	**Atmosphere :**	<no gas>/--- / NITROGEN/40 / NITR...
Operator :	ED	**Range :**	20/10.0(K/min)/450	**Corr/m. range :**	000/5000 µV
Sample :	ODV-OX-FORM B, 3....	**Sample car./TC :**	DSC 200F3 t-sen...		

Created with NETZSCH Proteus software

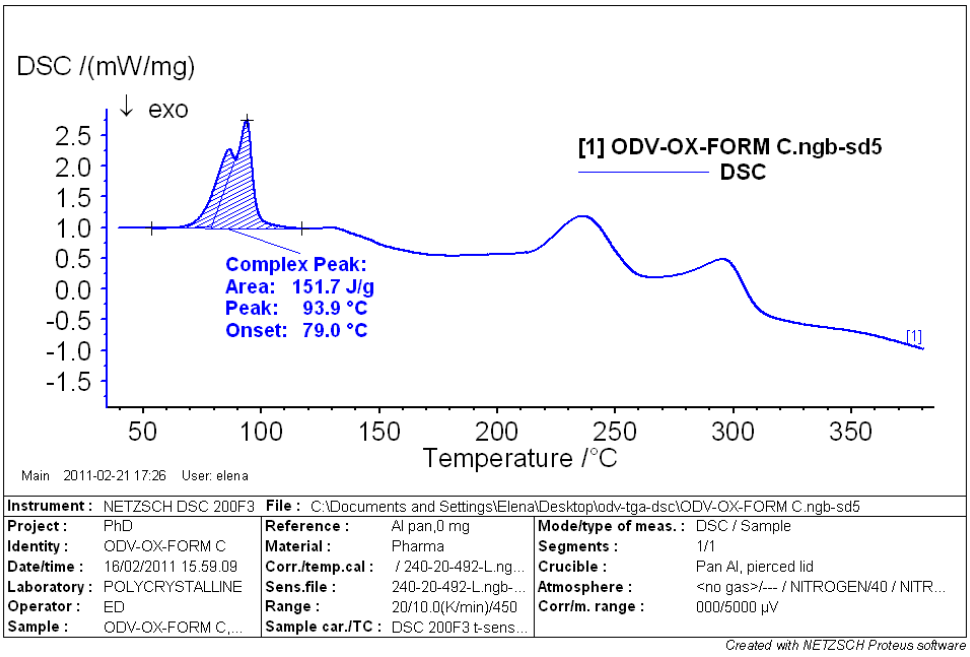

Instrument :	NETZSCH DSC 200F3	**File :**	C:\Documents and Settings\Elena\Desktop\odv-tga-dsc\ODV-OX-FORM C.ngb-sd5		
Project :	PhD	**Reference :**	Al pan,0 mg	**Mode/type of meas. :**	DSC / Sample
Identity :	ODV-OX-FORM C	**Material :**	Pharma	**Segments :**	1/1
Date/time :	16/02/2011 15.59.09	**Corr./temp.cal :**	/ 240-20-492-L.ng...	**Crucible :**	Pan Al, pierced lid
Laboratory :	POLYCRYSTALLINE	**Sens.file :**	240-20-492-L.ngb-...	**Atmosphere :**	<no gas>/--- / NITROGEN/40 / NITR...
Operator :	ED	**Range :**	20/10.0(K/min)/450	**Corr/m. range :**	000/5000 µV
Sample :	ODV-OX-FORM C,...	**Sample car./TC :**	DSC 200F3 t-sens...		

Created with NETZSCH Proteus software

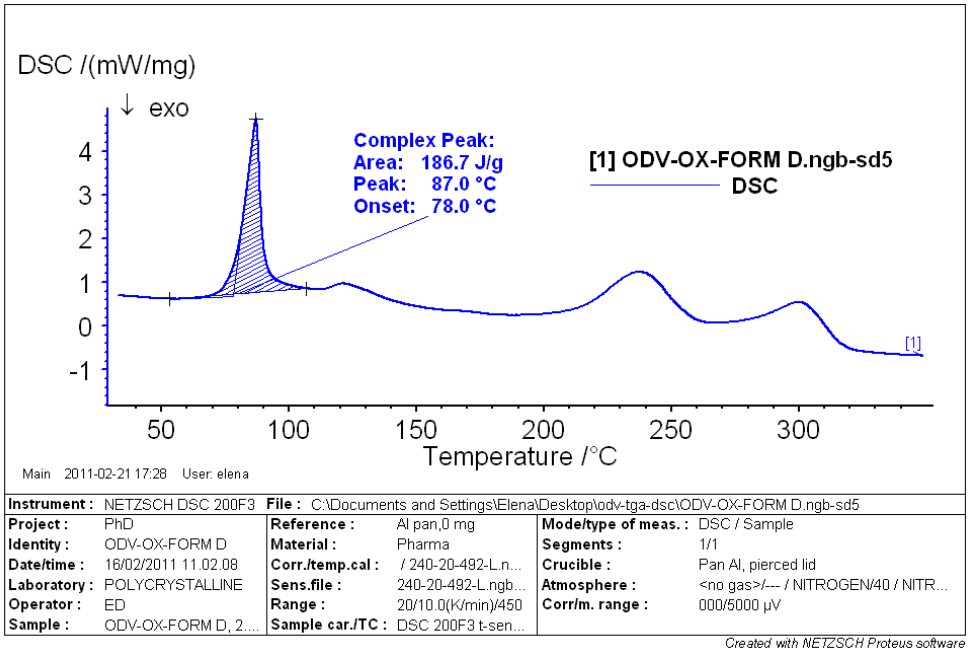

Instrument :	NETZSCH DSC 200F3	**File :**	C:\Documents and Settings\Elena\Desktop\odv-tga-dsc\ODV-OX-FORM D.ngb-sd5		
Project :	PhD	**Reference :**	Al pan,0 mg	**Mode/type of meas. :**	DSC / Sample
Identity :	ODV-OX-FORM D	**Material :**	Pharma	**Segments :**	1/1
Date/time :	16/02/2011 11.02.08	**Corr./temp.cal :**	/ 240-20-492-L.n...	**Crucible :**	Pan Al, pierced lid
Laboratory :	POLYCRYSTALLINE	**Sens.file :**	240-20-492-L.ngb...	**Atmosphere :**	<no gas>/--- / NITROGEN/40 / NITR...
Operator :	ED	**Range :**	20/10.0(K/min)/450	**Corr/m. range :**	000/5000 µV
Sample :	ODV-OX-FORM D, 2....	**Sample car./TC :**	DSC 200F3 t-sen...		

Created with NETZSCH Proteus software

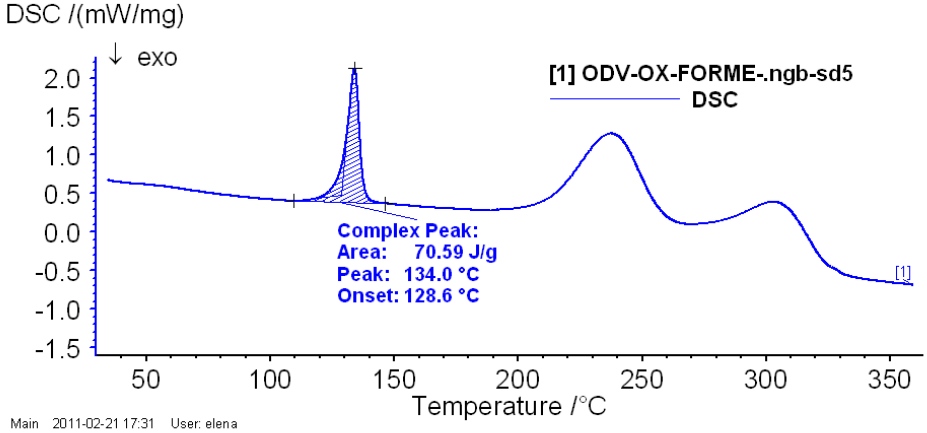

Instrument :	NETZSCH DSC 200F3	**File :**	C:\Documents and Settings\Elena\Desktop\odv-tga-dsc\ODV-OX-FORME-.ngb-sd5		
Project :	PhD	**Reference :**	Al pan,0 mg	**Mode/type of meas. :**	DSC / Sample
Identity :	ODV-OX-FORME	**Material :**	Pharma	**Segments :**	1/1
Date/time :	21/02/2011 14.38.44	**Corr./temp.cal :**	/ 240-20-492-L.ng...	**Crucible :**	Pan Al, pierced lid
Laboratory :	POLYCRYSTALLINE	**Sens.file :**	240-20-492-L.ngb-...	**Atmosphere :**	<no gas>/--- / NITROGEN/40 / NITR...
Operator :	ED	**Range :**	20/10.0(K/min)/450	**Corr/m. range :**	000/5000 µV
Sample :	ODV-OX-FORME, 3...	**Sample car./TC :**	DSC 200F3 t-sens...		

Created with NETZSCH Proteus software

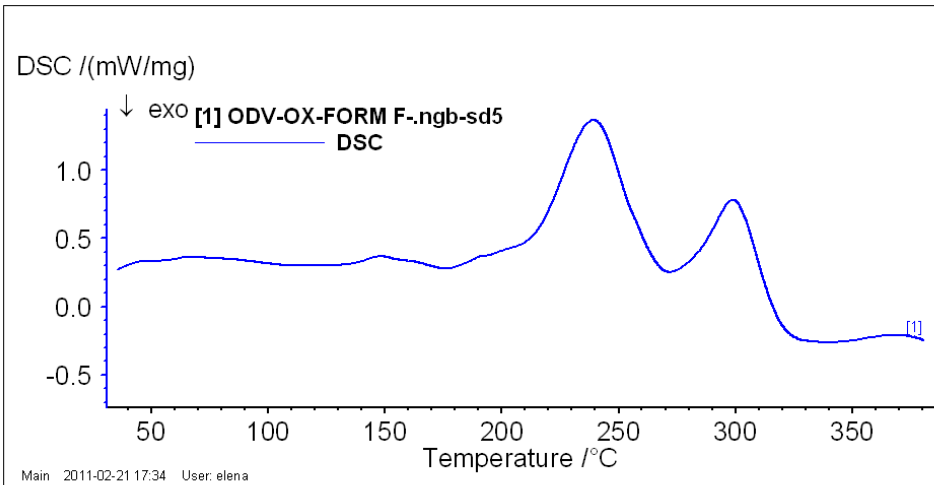

Instrument :	NETZSCH DSC 200F3	**File :**	C:\Documents and Settings\Elena\Desktop\odv-tga-dsc\ODV-OX-FORM F-.ngb-sd5		
Project :	PhD	**Reference :**	Al pan,0 mg	**Mode/type of meas. :**	DSC / Sample
Identity :	ODV-OX-FORM B-100DM02	**Material :**	Pharma	**Segments :**	1/1
Date/time :	17/02/2011 11.41.00	**Corr./temp.cal :**	/ 240-20-492-L....	**Crucible :**	Pan Al, pierced lid
Laboratory :	POLYCRYSTALLINE	**Sens.file :**	240-20-492-L.n...	**Atmosphere :**	<no gas>/--- / NITROGEN/40 / NI...
Operator :	ED	**Range :**	20/10.0(K/min)/...	**Corr/m. range :**	000/5000 µV
Sample :	ODV-OX-FORM B-100DM...	**Sample car./TC :**	DSC 200F3 t-se...		

Created with NETZSCH Proteus software

Thermogravimetric analyses (TGA)

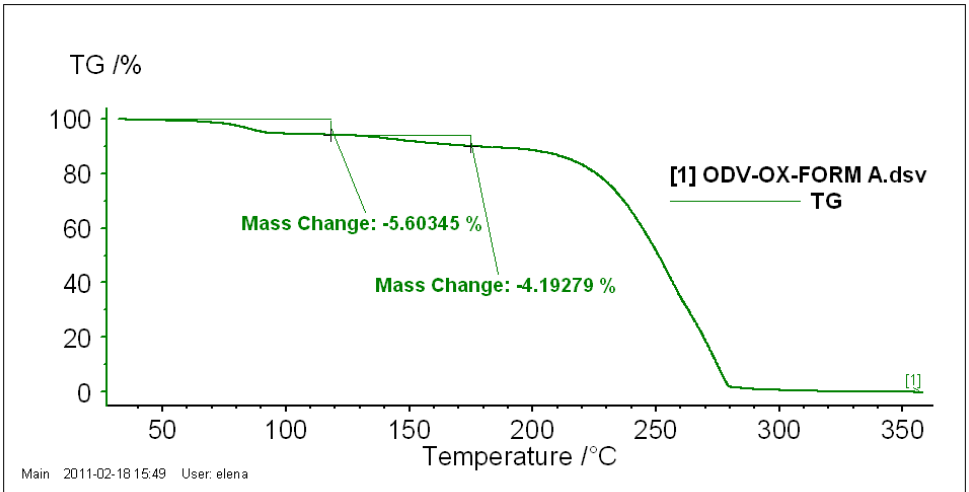

Instrument :	NETZSCH STA 409 PC/PG	**File :**	C:\Documents and Settings\Elena\Desktop\odv-tga-dsc\ODV-OX-FORM A.dsv		
Project :	PhD	**Material :**	Vuoto	**Segments :**	1/1
Identity :	ODV-OX-FORM A	**Correction file :**	CORR_Al_25-590_10K_20110...	**Crucible :**	DSC/TG pan Al
Date/time :	17/02/2011 14.44.00	**Temp.Cal./Sens. Files :**	CalTemp Al 20100723-K.tsv /	**Atmosphere :**	N2/60 / ---/10 / N2 -...
Laboratory :	POLYCRYSTALLI...	**Range :**	25/10.0(K/min)/490	**TG corr./m. range :**	020/30000 mg
Operator :	ED	**Sample car./TC :**	DSC(/TG) MIDDLE RG 2 / K	**DSC corr./m. range :**	020/5000 µV
Sample :	ODV-OX-FORM A...	**Mode/type of meas. :**	TG / sample with correction		

Created with NETZSCH Proteus software

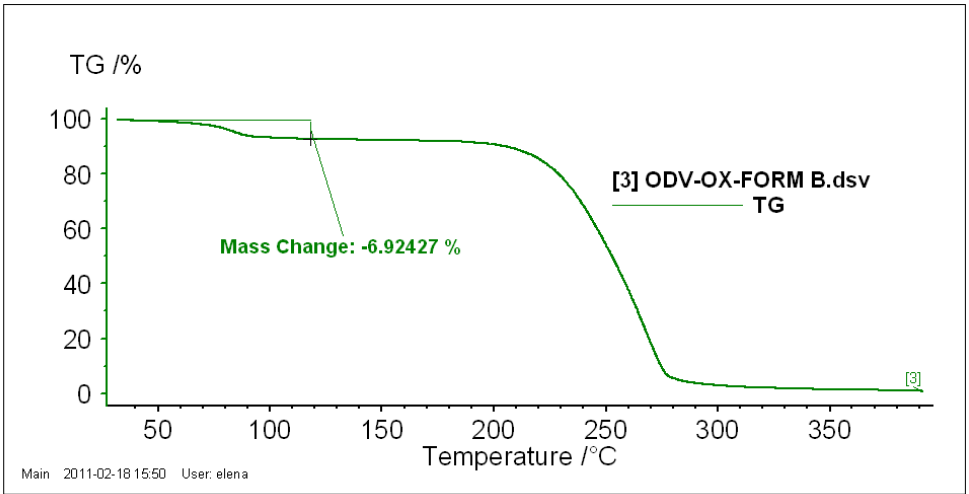

Instrument :	NETZSCH STA 409 PC/PG	**File :**	C:\Documents and Settings\Elena\Desktop\odv-tga-dsc\ODV-OX-FORM B.dsv		
Project :	PhD	**Material :**	Vuoto	**Segments :**	1/1
Identity :	ODV-OX-FORM B	**Correction file :**	CORR_Al_25-590_10K_20110...	**Crucible :**	DSC/TG pan Al
Date/time :	16/02/2011 16.01....	**Temp.Cal./Sens. Files :**	CalTemp Al 20100723-K.tsv /	**Atmosphere :**	N2/60 / ---/10 / N2 -...
Laboratory :	POLYCRYSTALL...	**Range :**	25/10.0(K/min)/490	**TG corr./m. range :**	020/30000 mg
Operator :	ED	**Sample car./TC :**	DSC(/TG) MIDDLE RG 2 / K	**DSC corr./m. range :**	020/5000 µV
Sample :	ODV-OX-FORM...	**Mode/type of meas. :**	TG / sample with correction		

Created with NETZSCH Proteus software

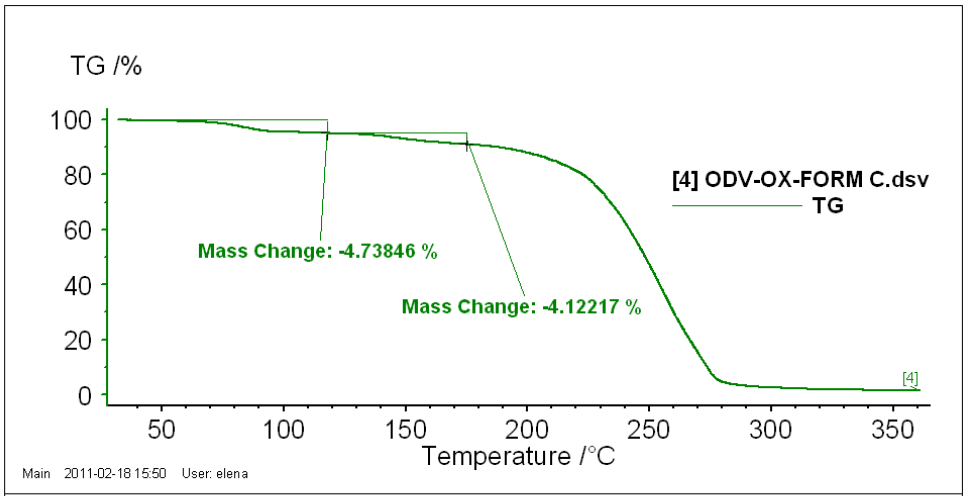

Instrument :	NETZSCH STA 409 PC/PG	**File :**	C:\Documents and Settings\Elena\Desktop\odv-tga-dsc\ODV-OX-FORM C.dsv		
Project :	PhD	**Material :**	Vuoto	**Segments :**	1/1
Identity :	ODV-OX-FORM A	**Correction file :**	CORR_Al_25-590_10K_20110...	**Crucible :**	DSC/TG pan Al
Date/time :	17/02/2011 9.08.37	**Temp.Cal./Sens. Files :**	CalTemp Al 20100723-K.tsv /	**Atmosphere :**	N2/60 / ---/10 / N2 -...
Laboratory :	POLYCRYSTALL...	**Range :**	25/10.0(K/min)/490	**TG corr./m. range :**	020/30000 mg
Operator :	ED	**Sample car./TC :**	DSC(/TG) MIDDLE RG 2 / K	**DSC corr./m. range :**	020/5000 µV
Sample :	ODV-OX-FORM...	**Mode/type of meas. :**	TG / sample with correction		

Created with NETZSCH Proteus software

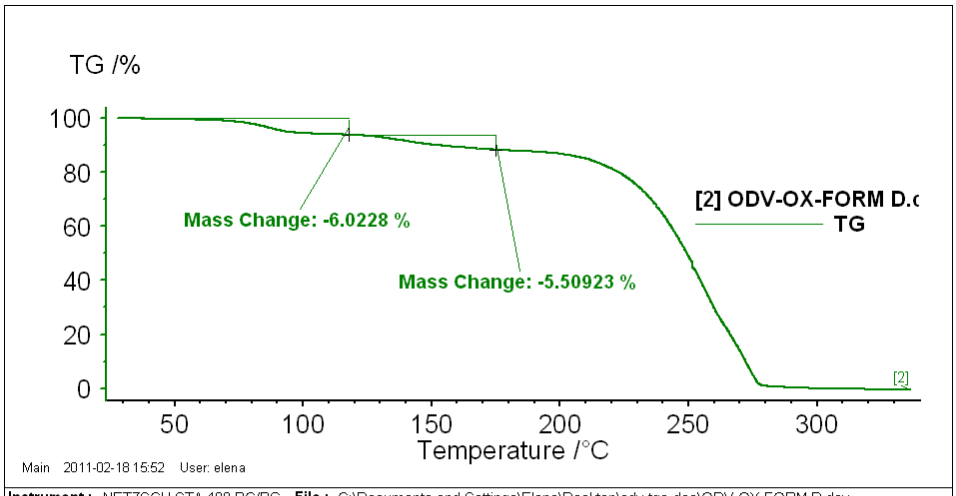

Instrument :	NETZSCH STA 409 PC/PG	**File :**	C:\Documents and Settings\Elena\Desktop\odv-tga-dsc\ODV-OX-FORM D.dsv		
Project :	ODV-OX	**Material :**	Vuoto	**Segments :**	1/1
Identity :	ODV-OX-FORM D	**Correction file :**	CORR_Al_25-590_10K_20110...	**Crucible :**	DSC/TG pan Al
Date/time :	16/02/2011 11.13.40	**Temp.Cal./Sens. Files :**	CalTemp Al 20100723-K.tsv /	**Atmosphere :**	N2/60 / ---/10 / N2 -...
Laboratory :	POLYCRYSTALLI...	**Range :**	25/10.0(K/min)/490	**TG corr./m. range :**	020/30000 mg
Operator :	ED	**Sample car./TC :**	DSC(/TG) MIDDLE RG 2 / K	**DSC corr./m. range :**	020/5000 µV
Sample :	ODV-OX-FORM D...	**Mode/type of meas. :**	TG / sample with correction		

Created with NETZSCH Proteus software

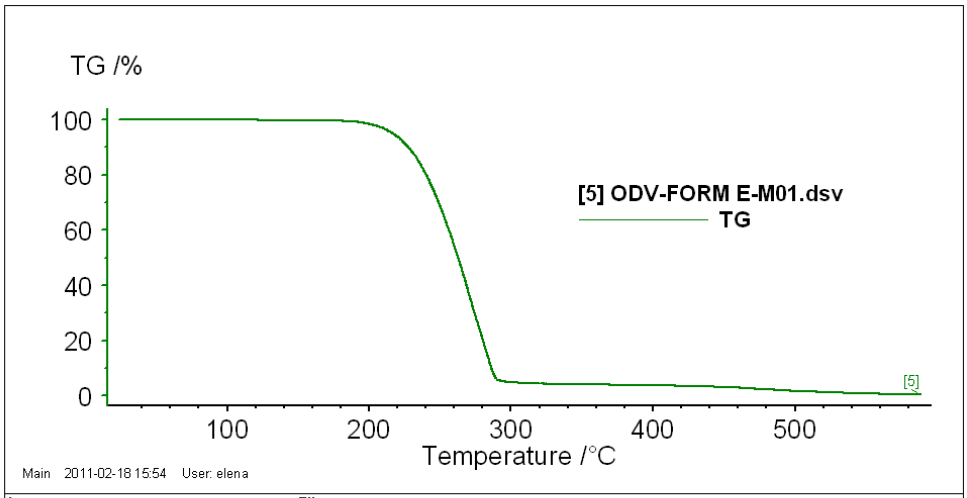

Instrument :	NETZSCH STA 409 PC/PG	**File :**	C:\Documents and Settings\Elena\Desktop\odv-tga-dsc\ODV-FORM E-M01.dsv		
Project :	PCL01	**Material :**	Vuoto	**Segments :**	1/1
Identity :	PCL01-OX-SL-ACT...	**Correction file :**	CORR_Al_25-590_10K_K_2010...	**Crucible :**	DSC/TG pan Al
Date/time :	16/03/2010 11.44.28	**Temp.Cal./Sens. Files :**	CalTemp Al 20090921-K.tsv / Ca...	**Atmosphere :**	N2/60 / ---/10 / N...
Laboratory :	POLYCRYSTALLIN...	**Range :**	25/10.0(K/min)/590	**TG corr./m. range :**	020/30000 mg
Operator :	ED	**Sample car./TC :**	DSC(/TG) MIDDLE RG 2 / K	**DSC corr./m. range :**	020/5000 µV
Sample :	PCL01-OX-SL-ACT...	**Mode/type of meas. :**	DSC-TG / sample with correction		

Created with NETZSCH Proteus software

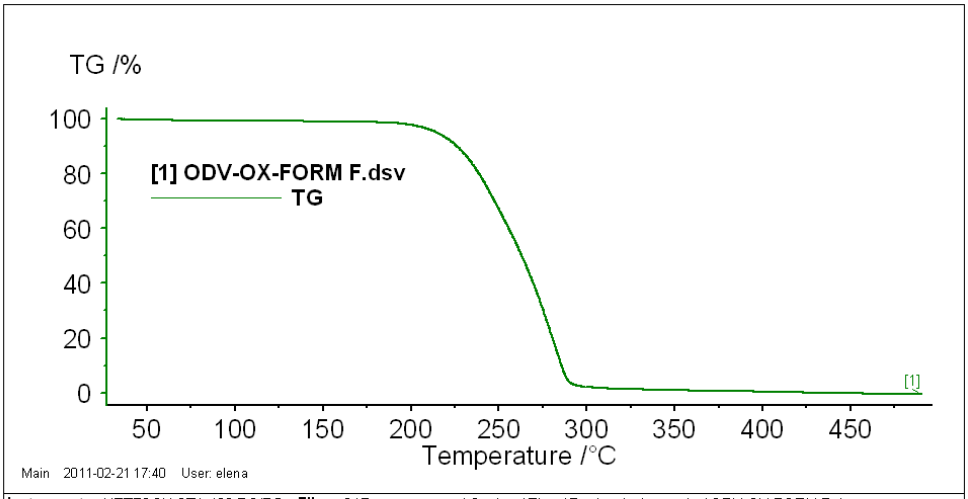

Instrument :	NETZSCH STA 409 PC/PG	**File :**	C:\Documents and Settings\Elena\Desktop\odv-tga-dsc\ODV-OX-FORM F.dsv		
Project :	PhD	**Material :**	Vuoto	**Segments :**	1/1
Identity :	ODV-OX-FORM B-100...	**Correction file :**	CORR_Al_25-590_10K_201...	**Crucible :**	DSC/TG pan Al
Date/time :	17/02/2011 11.47.12	**Temp.Cal./Sens. Files :**	CalTemp Al 20100723-K.tsv /	**Atmosphere :**	N2/60 / ---/10 / N2...
Laboratory :	POLYCRYSTALLINE srl	**Range :**	25/10.0(K/min)/490	**TG corr./m. range :**	020/30000 mg
Operator :	ED	**Sample car./TC :**	DSC(/TG) MIDDLE RG 2 / K	**DSC corr./m. range :**	020/5000 µV
Sample :	ODV-OX-FORM B-100...	**Mode/type of meas. :**	TG / sample with correction		

Created with NETZSCH Proteus software

2.5.3. **XRPD Patterns**

ODV-OX Form A

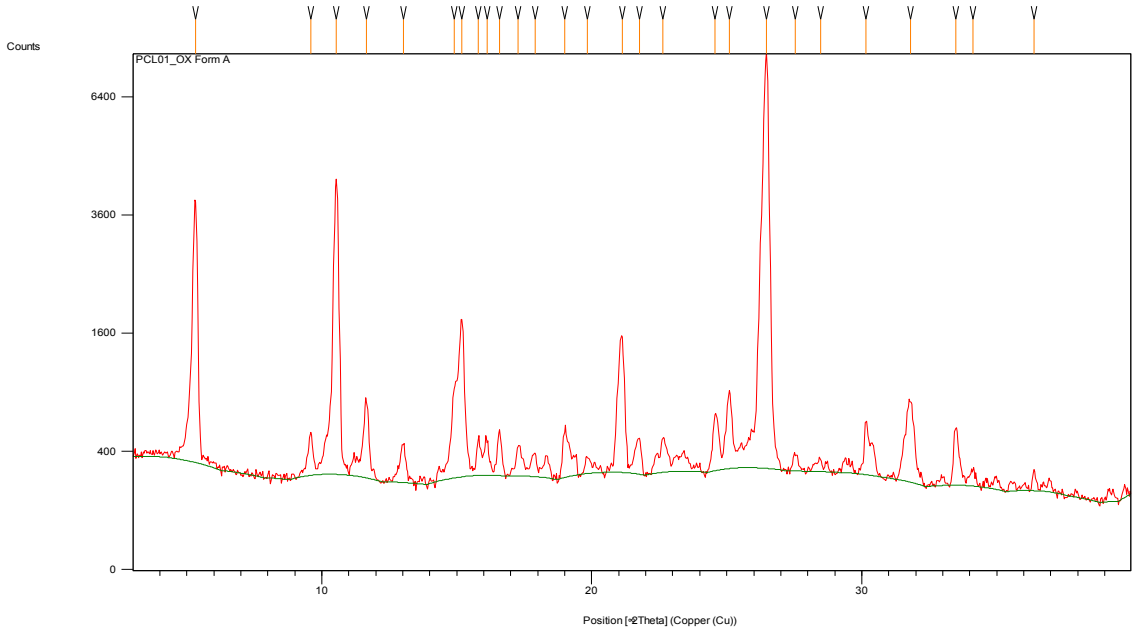

Pos. [°2Th.]	Height [cts]	FWHM [°2Th.]	d-spacing [Å]	Rel. Int. [%]
5,3111	3663,39	0,1624	16,63945	49,54
9,5916	284,79	0,1299	9,22123	3,85
10,5410	4098,59	0,1948	8,39270	55,43
11,6532	578,34	0,1624	7,59410	7,82
13,0162	232,42	0,1299	6,80176	3,14
14,9010	705,17	0,1299	5,94540	9,54
15,1949	1544,07	0,1299	5,83104	20,88
15,8002	247,99	0,0974	5,60901	3,35
16,1124	208,57	0,0974	5,50101	2,82
16,5757	307,87	0,1299	5,34828	4,16
17,2785	184,54	0,1624	5,13231	2,50
17,8960	140,95	0,1624	4,95658	1,91
18,9905	298,60	0,1299	4,67332	4,04
19,8346	98,90	0,1948	4,47630	1,34

21,1225	1312,00	0,2598	4,20618	17,74
21,7703	231,60	0,2273	4,08247	3,13
22,6391	222,85	0,1624	3,92773	3,01
24,5723	407,75	0,1948	3,62292	5,51
25,1012	624,92	0,1624	3,54777	8,45
26,4739	7394,78	0,1948	3,36685	100,00
27,5450	105,19	0,1948	3,23832	1,42
28,4776	52,74	0,3897	3,13435	0,71
30,1636	378,11	0,0974	2,96289	5,11
31,8029	588,64	0,2598	2,81381	7,96
33,4844	369,84	0,1624	2,67625	5,00
34,1176	91,86	0,1948	2,62802	1,24
36,3796	107,94	0,1299	2,46964	1,46

ODV-OX Form B

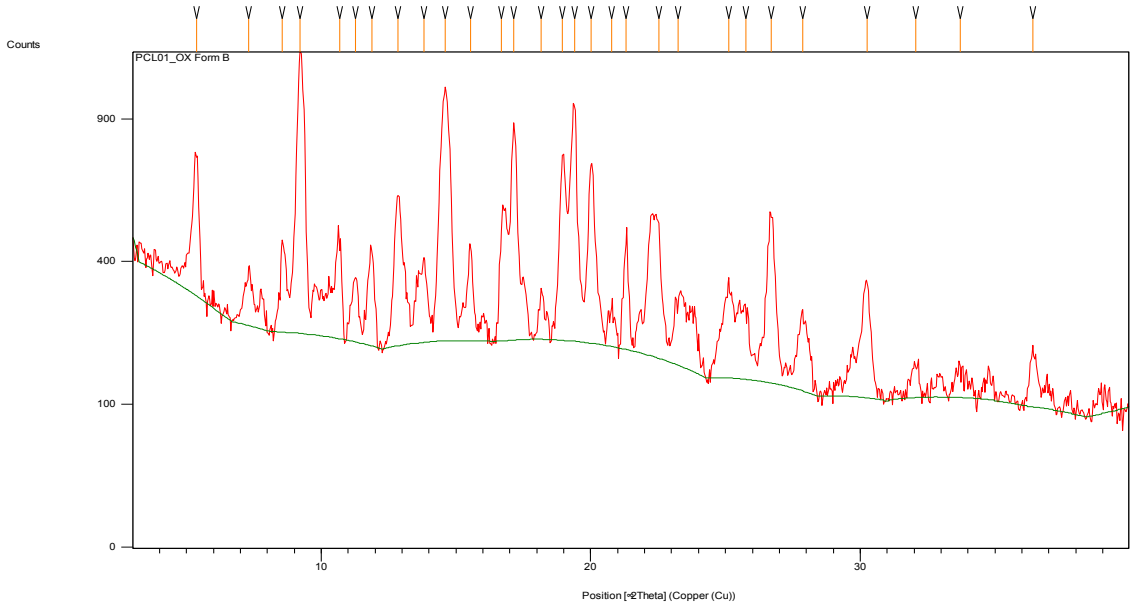

Pos. [°2Th.]	Height [cts]	FWHM [°2Th.]	d-spacing [Å]	Rel. Int. [%]
5,3641	439,54	0,1948	16,47544	46,00
7,2969	135,26	0,2598	12,11504	14,16
8,5593	235,38	0,1624	10,33087	24,63
9,2017	955,53	0,3247	9,61102	100,00
10,6938	252,12	0,1948	8,27310	26,39
11,2577	154,95	0,1948	7,85994	16,22
11,8703	237,62	0,1948	7,45565	24,87
12,8343	406,40	0,2273	6,89774	42,53
13,8200	197,19	0,3897	6,40791	20,64
14,6024	830,27	0,3572	6,06629	86,89
15,5420	230,72	0,1299	5,70159	24,15
16,6848	290,52	0,1948	5,31358	30,40
17,1524	672,62	0,1948	5,16976	70,39
18,1595	103,58	0,2598	4,88525	10,84
18,9482	535,28	0,1624	4,68364	56,02

19,3943	748,29	0,1624	4,57690	78,31
20,0165	515,51	0,1948	4,43603	53,95
20,7798	79,22	0,1948	4,27478	8,29
21,3128	279,49	0,1299	4,16905	29,25
22,5201	341,19	0,1948	3,94820	35,71
23,2400	131,11	0,3247	3,82751	13,72
25,1180	195,56	0,1948	3,54544	20,47
25,7557	140,77	0,3247	3,45908	14,73
26,7095	401,99	0,2922	3,33769	42,07
27,8737	143,24	0,3897	3,20087	14,99
30,2597	232,08	0,2273	2,95370	24,29
32,0673	48,88	0,3247	2,79121	5,12
33,7123	41,46	0,3897	2,65868	4,34
36,4194	90,82	0,2598	2,46703	9,51

ODV-OX Form C

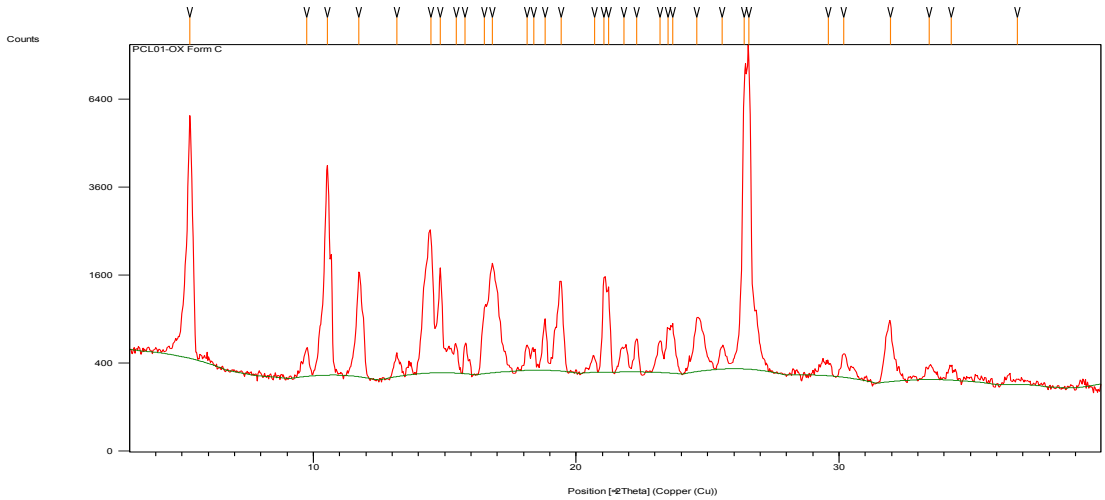

Pos. [°2Th.]	Height [cts]	FWHM [°2Th.]	d-spacing [Å]	Rel. Int. [%]
5,2961	5395,94	0,1624	16,68664	71,65
9,7495	257,33	0,1299	9,07219	3,42
10,5216	3929,64	0,0974	8,40814	52,18
11,7391	1401,52	0,1299	7,53871	18,61
13,1835	185,62	0,2598	6,71580	2,46
14,4702	2021,75	0,1624	6,12142	26,85
14,8339	1413,30	0,1299	5,97214	18,77
15,4394	271,37	0,0974	5,73925	3,60
15,7808	292,54	0,1299	5,61586	3,88
16,4934	662,49	0,1299	5,37480	8,80
16,8009	1497,51	0,1624	5,27710	19,89
18,1278	241,99	0,1299	4,89371	3,21
18,3851	176,62	0,0974	4,82581	2,35
18,8151	575,49	0,0974	4,71647	7,64
19,4207	1157,52	0,1299	4,57076	15,37
20,6912	131,82	0,1624	4,29287	1,75
21,0662	1232,22	0,1299	4,21730	16,36

21,2402	1024,60	0,1299	4,18315	13,61
21,8165	234,32	0,2598	4,07393	3,11
22,2994	330,73	0,1624	3,98679	4,39
23,1901	309,29	0,1299	3,83564	4,11
23,4853	483,46	0,0974	3,78809	6,42
23,6727	531,97	0,1299	3,75853	7,06
24,5807	551,81	0,2273	3,62171	7,33
25,5582	209,83	0,1948	3,48537	2,79
26,4006	6691,82	0,1299	3,37603	88,86
26,5784	7530,57	0,0974	3,35386	100,00
29,6022	114,36	0,3897	3,01779	1,52
30,1896	214,77	0,1624	2,96039	2,85
31,9491	608,43	0,2598	2,80127	8,08
33,4328	104,64	0,3247	2,68027	1,39
34,2782	109,57	0,2598	2,61608	1,46
36,7878	34,86	0,7793	2,44317	0,46

ODV-OX Form D

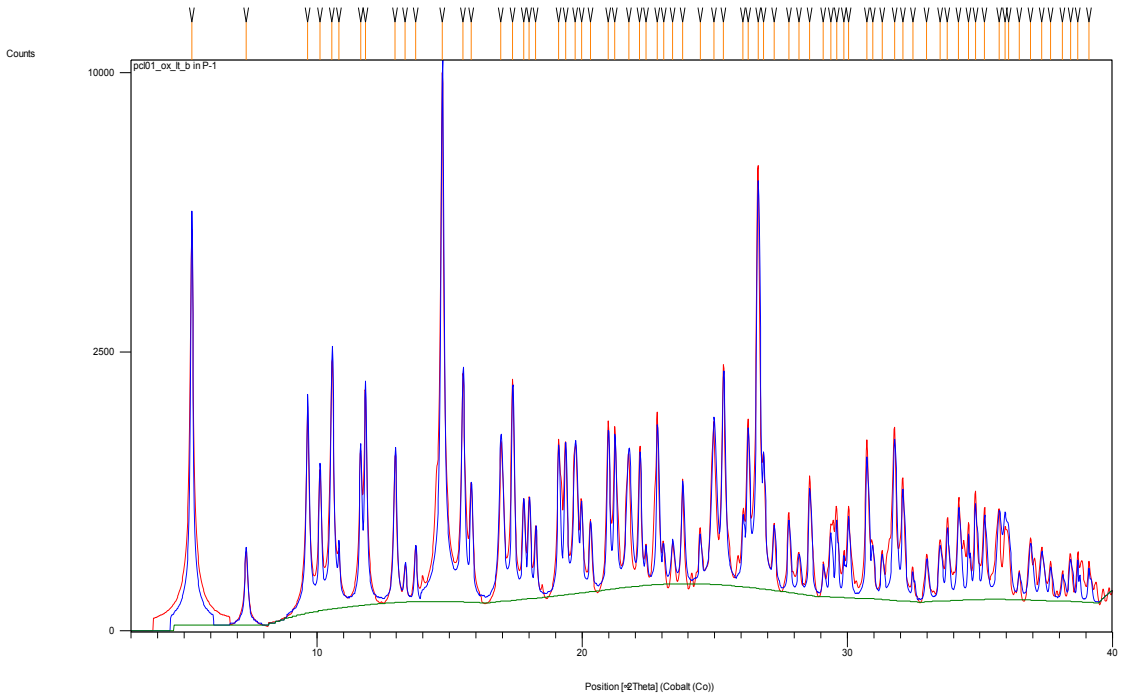

Pos. [°2Th.]	Height [cts]	FWHM [°2Th.]	d-spacing [Å]	Rel. Int. [%]
5,9933	6784,10	0,1004	14,74705	100,00
7,4510	169,33	0,1673	11,86492	2,50
8,6396	212,16	0,1673	10,23503	3,13
9,3377	442,55	0,1673	9,47136	6,52
10,1712	591,61	0,1171	8,69703	8,72
10,9667	1377,86	0,1506	8,06785	20,31
11,3202	165,51	0,1338	7,81672	2,44
11,9003	3456,27	0,1171	7,43691	50,95
12,7210	262,10	0,1004	6,95893	3,86
13,0787	194,35	0,1673	6,76938	2,86
13,5527	62,73	0,1004	6,53370	0,92
14,2075	1560,88	0,1171	6,23399	23,01
14,5834	2237,03	0,1171	6,07414	32,97
14,7491	1971,58	0,1338	6,00629	29,06

15,3062	894,50	0,1673	5,78889	13,19
16,0182	712,46	0,1338	5,53316	10,50
16,3323	218,31	0,1506	5,42745	3,22
16,7051	1036,25	0,1506	5,30714	15,27
17,0828	317,43	0,1338	5,19065	4,68
17,6891	1152,99	0,0669	5,01407	17,00
17,9040	1312,50	0,1004	4,95439	19,35
18,5494	647,40	0,1338	4,78343	9,54
18,9965	971,29	0,1506	4,67186	14,32
19,3387	438,84	0,1506	4,58994	6,47
19,7187	351,89	0,0836	4,50234	5,19
20,3497	2124,19	0,1673	4,36413	31,31
20,9279	1339,29	0,1506	4,24485	19,74
21,4155	492,44	0,1338	4,14930	7,26
22,2480	551,18	0,1338	3,99588	8,12
22,6262	739,99	0,1020	3,92668	10,91
22,7293	694,54	0,0836	3,91234	10,24
23,1464	356,05	0,1004	3,84278	5,25
23,9739	373,17	0,1673	3,71198	5,50
24,7683	174,87	0,1171	3,59470	2,58
25,1096	89,64	0,1338	3,54661	1,32
25,6735	693,97	0,0836	3,46997	10,23
26,0899	212,99	0,1171	3,41553	3,14
26,5592	88,29	0,1004	3,35624	1,30
26,9487	781,15	0,1338	3,30860	11,51
27,5352	579,29	0,1004	3,23945	8,54
28,9533	246,66	0,1673	3,08393	3,64
30,1383	130,98	0,1004	2,96532	1,93

30,4877	100,47	0,1004	2,93212	1,48
30,8740	142,32	0,1673	2,89631	2,10
31,5166	274,34	0,1673	2,83871	4,04
32,8228	177,42	0,1004	2,72867	2,62
33,4907	56,98	0,3346	2,67576	0,84
33,9368	26,85	0,1338	2,64160	0,40
34,4310	102,31	0,2676	2,60481	1,51
35,4317	304,16	0,2007	2,53351	4,48
36,1596	87,17	0,1673	2,48416	1,28
36,5026	122,10	0,1338	2,46160	1,80
37,2102	98,14	0,1673	2,41640	1,45
37,9115	124,71	0,1338	2,37330	1,84
38,6464	46,04	0,1673	2,32984	0,68
39,1466	61,80	0,2007	2,30122	0,91

ODV-OX Form E

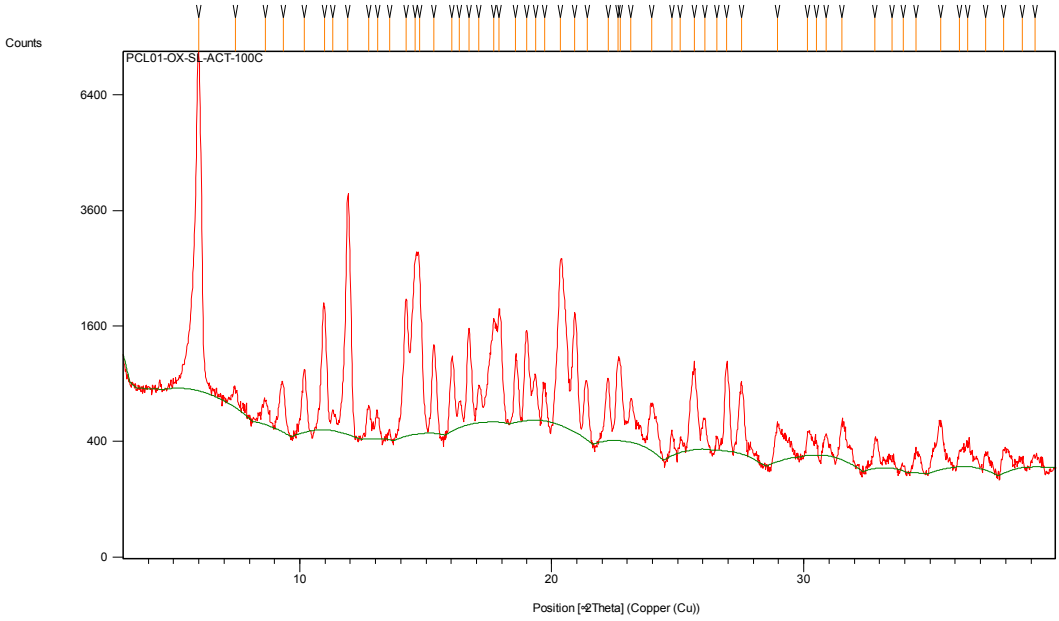

Pos. [°2Th.]	Height [cts]	FWHM [°2Th.]	d-spacing [Å]	Rel. Int. [%]
5,9933	6784,10	0,1004	14,74705	100,00
7,4510	169,33	0,1673	11,86492	2,50
8,6396	212,16	0,1673	10,23503	3,13
9,3377	442,55	0,1673	9,47136	6,52
10,1712	591,61	0,1171	8,69703	8,72
10,9667	1377,86	0,1506	8,06785	20,31
11,3202	165,51	0,1338	7,81672	2,44
11,9003	3456,27	0,1171	7,43691	50,95
12,7210	262,10	0,1004	6,95893	3,86
13,0787	194,35	0,1673	6,76938	2,86
13,5527	62,73	0,1004	6,53370	0,92
14,2075	1560,88	0,1171	6,23399	23,01
14,5834	2237,03	0,1171	6,07414	32,97
14,7491	1971,58	0,1338	6,00629	29,06
15,3062	894,50	0,1673	5,78889	13,19

16,0182	712,46	0,1338	5,53316	10,50
16,3323	218,31	0,1506	5,42745	3,22
16,7051	1036,25	0,1506	5,30714	15,27
17,0828	317,43	0,1338	5,19065	4,68
17,6891	1152,99	0,0669	5,01407	17,00
17,9040	1312,50	0,1004	4,95439	19,35
18,5494	647,40	0,1338	4,78343	9,54
18,9965	971,29	0,1506	4,67186	14,32
19,3387	438,84	0,1506	4,58994	6,47
19,7187	351,89	0,0836	4,50234	5,19
20,3497	2124,19	0,1673	4,36413	31,31
20,9279	1339,29	0,1506	4,24485	19,74
21,4155	492,44	0,1338	4,14930	7,26
22,2480	551,18	0,1338	3,99588	8,12
22,6262	739,99	0,1020	3,92668	10,91
22,7293	694,54	0,0836	3,91234	10,24
23,1464	356,05	0,1004	3,84278	5,25
23,9739	373,17	0,1673	3,71198	5,50
24,7683	174,87	0,1171	3,59470	2,58
25,1096	89,64	0,1338	3,54661	1,32
25,6735	693,97	0,0836	3,46997	10,23
26,0899	212,99	0,1171	3,41553	3,14
26,5592	88,29	0,1004	3,35624	1,30
26,9487	781,15	0,1338	3,30860	11,51
27,5352	579,29	0,1004	3,23945	8,54
28,9533	246,66	0,1673	3,08393	3,64
30,1383	130,98	0,1004	2,96532	1,93
30,4877	100,47	0,1004	2,93212	1,48

30,8740	142,32	0,1673	2,89631	2,10
31,5166	274,34	0,1673	2,83871	4,04
32,8228	177,42	0,1004	2,72867	2,62
33,4907	56,98	0,3346	2,67576	0,84
33,9368	26,85	0,1338	2,64160	0,40
34,4310	102,31	0,2676	2,60481	1,51
35,4317	304,16	0,2007	2,53351	4,48
36,1596	87,17	0,1673	2,48416	1,28
36,5026	122,10	0,1338	2,46160	1,80
37,2102	98,14	0,1673	2,41640	1,45
37,9115	124,71	0,1338	2,37330	1,84
38,6464	46,04	0,1673	2,32984	0,68
39,1466	61,80	0,2007	2,30122	0,91

ODV-OX Form F

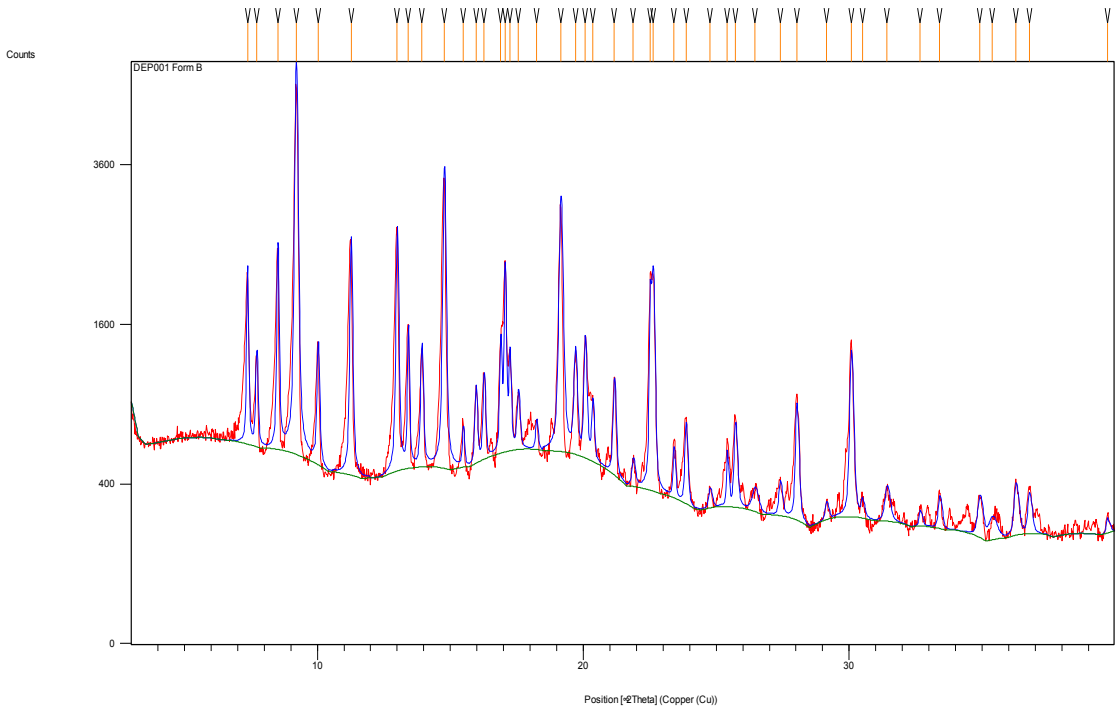

Pos. [°2Th.]	Height [cts]	FWHM [°2Th.]	d-spacing [Å]	Rel. Int. [%]
7,3730	1487,16	0,0836	11,99026	34,31
7,7215	683,63	0,1004	11,44988	15,77
8,5137	1788,29	0,1004	10,38606	41,25
9,2071	4334,96	0,1506	9,60537	100,00
10,0299	869,76	0,1171	8,81923	20,06
11,2693	2030,73	0,1171	7,85193	46,85
13,0015	2148,97	0,1171	6,80945	49,57
13,4206	1077,84	0,0836	6,59770	24,86
13,9285	877,75	0,1171	6,35825	20,25
14,7714	2934,99	0,1338	5,99727	67,71
15,4872	261,62	0,0836	5,72165	6,04
15,9626	530,52	0,1004	5,55232	12,24
16,2689	607,35	0,1004	5,44844	14,01
16,8915	913,00	0,0836	5,24901	21,06

17,0574	1738,08	0,0836	5,19831	40,09
17,2375	778,37	0,0836	5,14443	17,96
17,5584	405,20	0,1171	5,05113	9,35
18,2456	201,61	0,1004	4,86238	4,65
19,1534	2439,25	0,1673	4,63394	56,27
19,7009	766,51	0,1338	4,50637	17,68
20,0695	941,88	0,1171	4,42442	21,73
20,3571	421,26	0,1004	4,36258	9,72
21,1667	678,77	0,1171	4,19751	15,66
21,8812	150,84	0,1338	4,06203	3,48
22,5182	1756,74	0,0836	3,94854	40,52
22,6324	1761,69	0,1004	3,92887	40,64
23,4101	320,55	0,0836	3,80008	7,39
23,8629	506,82	0,1004	3,72900	11,69
24,7699	95,01	0,1338	3,59447	2,19
25,4173	359,74	0,0669	3,50436	8,30
25,7212	513,99	0,1171	3,46365	11,86
26,4636	103,87	0,2676	3,36814	2,40
27,4076	165,78	0,1338	3,25423	3,82
28,0269	742,23	0,1171	3,18372	17,12
29,1487	81,52	0,1338	3,06369	1,88
30,0743	1197,37	0,1338	2,97148	27,62
30,4956	84,06	0,1004	2,93138	1,94
31,4234	155,81	0,2007	2,84691	3,59
32,6729	76,16	0,1004	2,74084	1,76
33,4049	153,79	0,1338	2,68244	3,55
34,9156	168,20	0,2007	2,56976	3,88
35,3807	77,24	0,3346	2,53704	1,78

36,2696	236,59	0,1673	2,47688	5,46
36,7741	195,12	0,1338	2,44405	4,50
39,7162	70,96	0,1004	2,26952	1,64

2.5.4. **FT-IR**

ODV-OX Form A

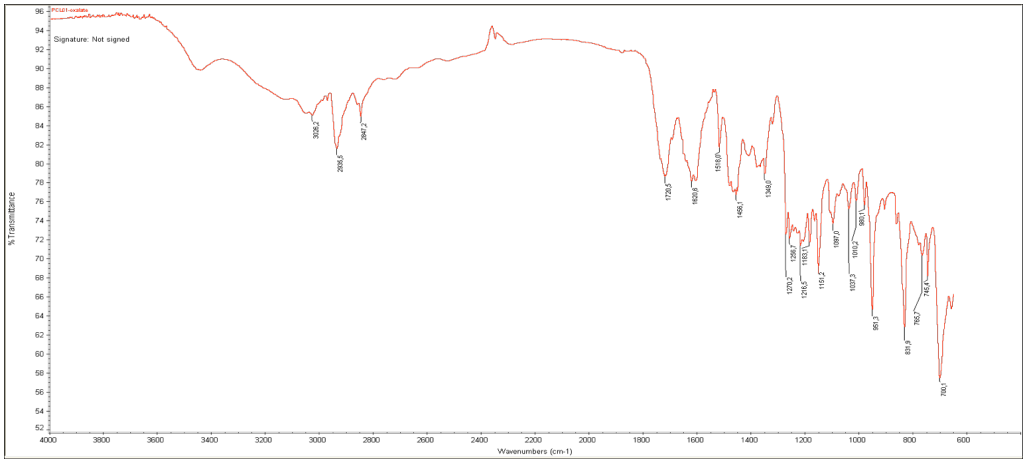

ODV-OX Form B

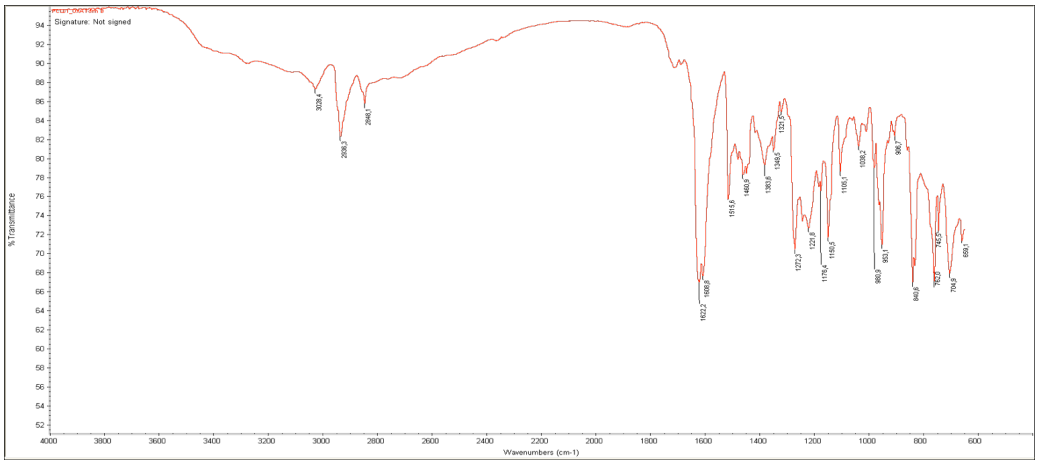

ODV-OX Form F

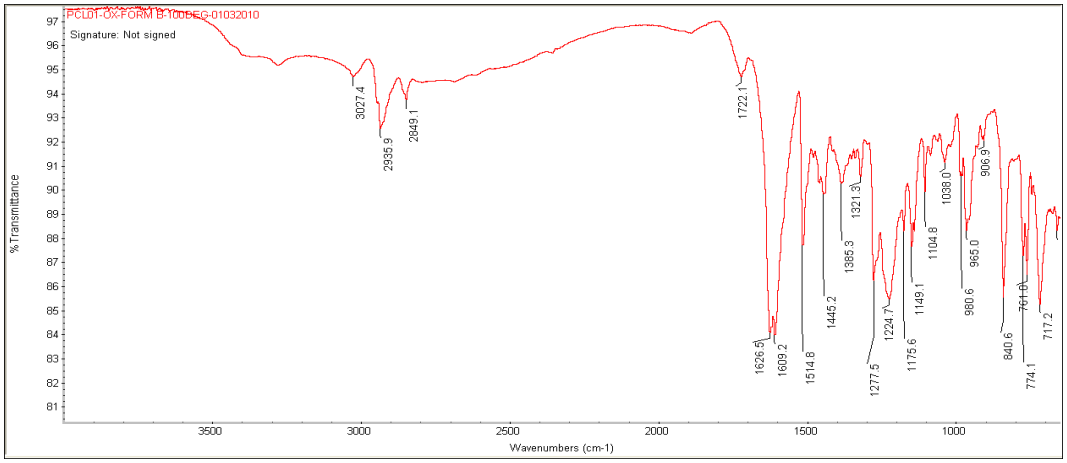

ODV-OX Form C

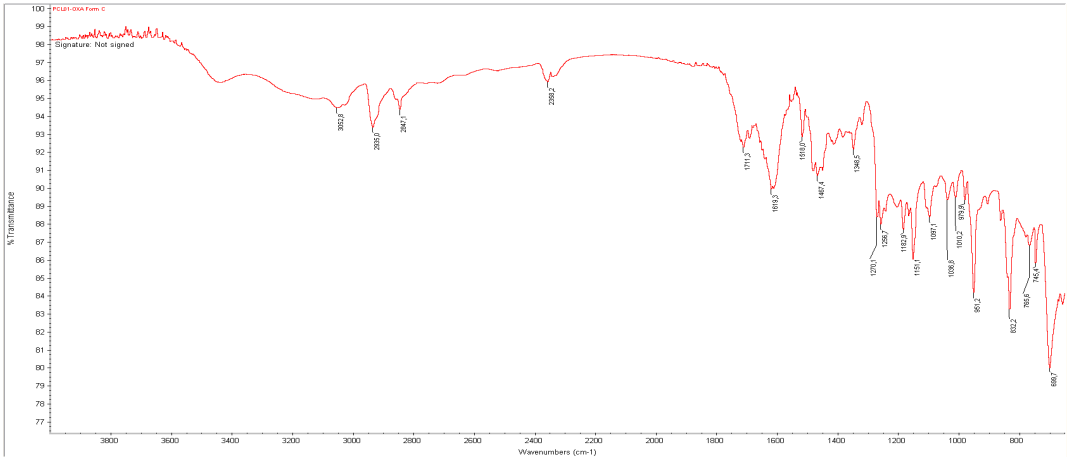

ODV-OX Form D

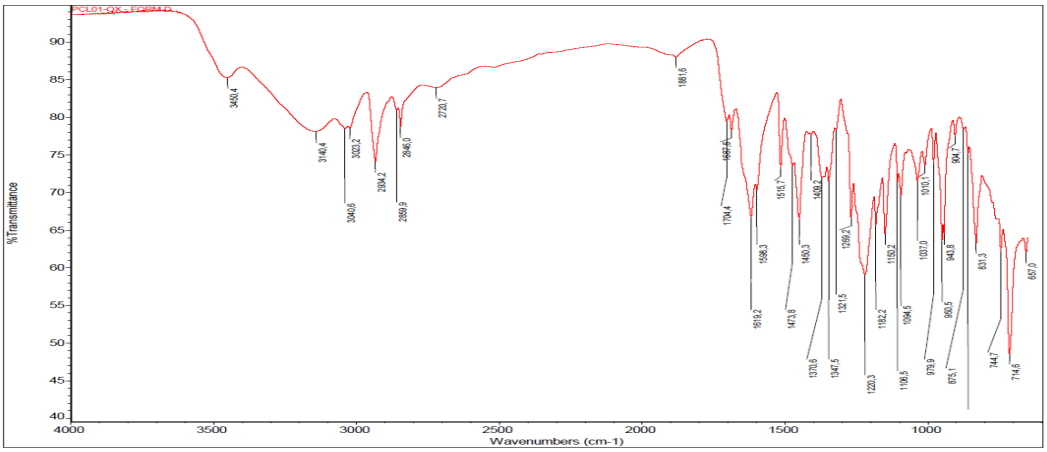

ODV-OX Form E

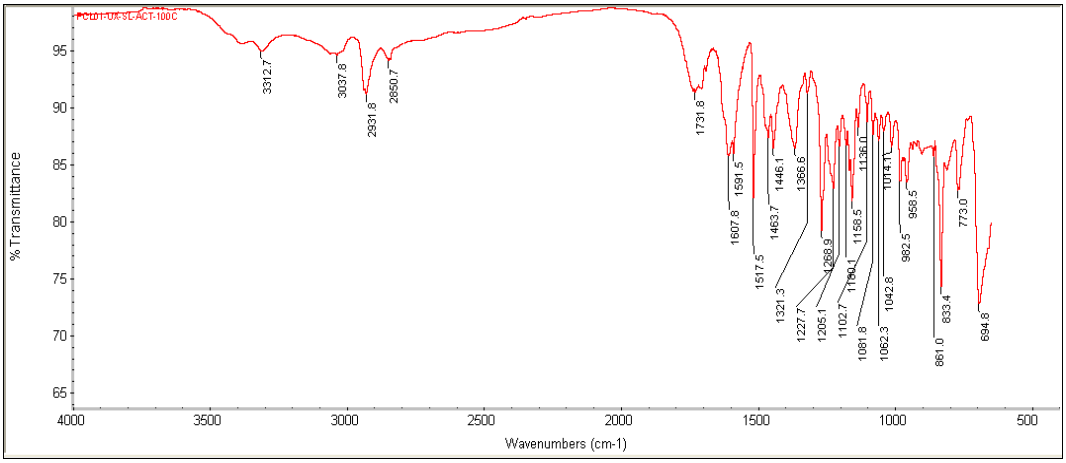

2.5.5. **Dissolution tests**

Calibration curve

The calibration curves were built using four solutions at different concentration for each salt:

1. $1.5*10^{-4}$ mol/L
2. $7.5*10^{-5}$ mol/L
3. $5.0*10^{-5}$ mol/L
4. $3.5*10^{-5}$ mol/L

Instrument Settings

Instrument	Cary 50
Instrument version no.	3.00
Wavelength (nm)	275.0
Ordinate Mode	Abs
Ave Time (sec)	0.1000
Replicates	5
Standard/Sample averaging	OFF
Method Weight	1.0000
Weight units	g
Method Volume	1.000
Volume units	mL

Factor = (Method Wt * Sample Vol)/(Sample Wt * Method Vol)

Fit type	Linear
Min R^2	0.95000
Concentration units	mol/L

Calibration of ODV_OX (Form A)

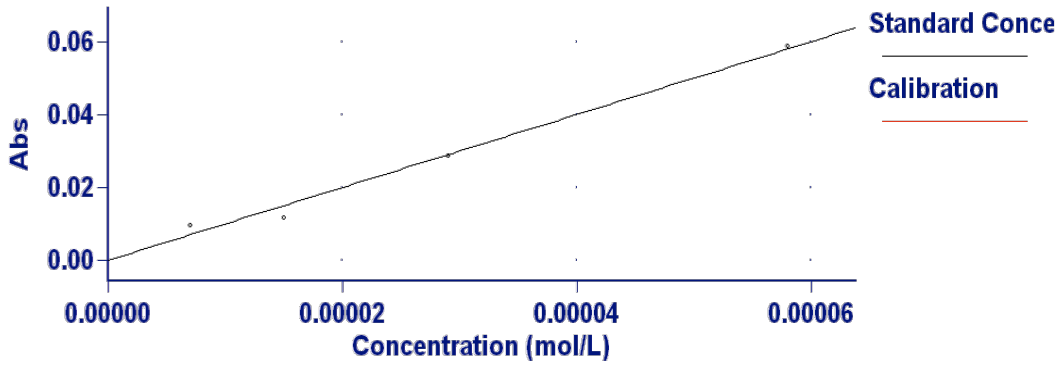

Calibration eqn ***Abs = 1002.4 * Conc***

Correlation Coefficient 0.99189

Calibration time 21/05/2008 10.40.56

Calibration of ODV_SUCC (Form B)

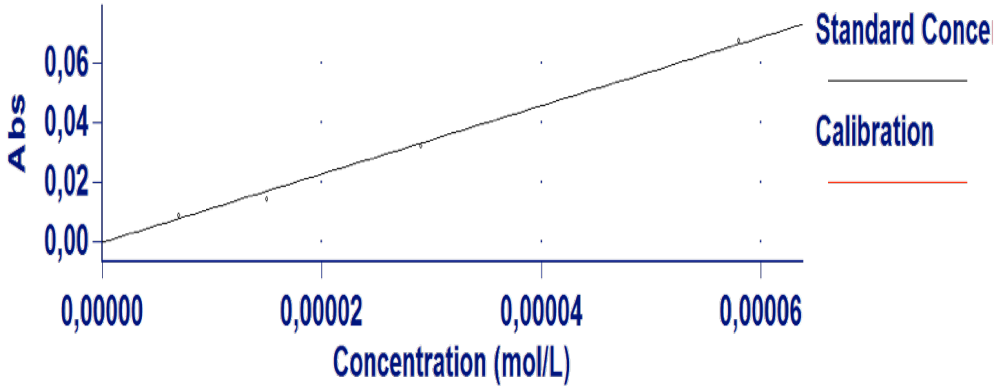

Calibration eqn ***Abs = 1141.4 * Conc***

Correlation Coefficient 0.99638

Calibration time 21/05/2008 10.50.36

2.6. References

1 S.R. Byrn, R.R. Pfeiffer, G. Sthephenson, *Solid State Chemistry of Drugs*, Inc. West Lafayette: SSCI; 1999.

2 M.L. Peterson, M.B. Hickey, M.J. Zaworotko, O. Almarsson, Expanding the scope of crystal form evaluation in pharmaceutical science; *J. Pharm. Scie.*, 2006, **9**, 317-326.

3 C. G. Wermuth, P. H. Stahl Eds, *Handbook of Pharmaceutical Salts: Properties, Selection, and Use*; VHCA and Wiley-VCH: Weinheim, 2008, pp 1-7.

4 A.T.M. Serajuddin, *Advances Drug Delivery Reviews*, 2007, **59**, 603-616.

5 J. Stoimenovski, D.R. MacFarlane, K. Bica, R.D. Rogers, *Pharmaceutical Research*, 2010, **27**,No.4.

6 a)G. R. Desiraju, *J. Chem. Sci,*. 2010*,* **122**, 667-675; b)D. Braga, F. Grepioni, L.Maini, *Chem. Commun.*, 2010, **46**, 6232-6242; c)C. B. Aakeroy, N. R. Champness, C. Janiak, *CrystEngComm,* 2010, **12**, 22-43.

7 a)N. Venu, B. R. Sreekanth, T. Ram, S. Devaraconda, *Acta Cryst.* , 2008, C**64**, 290-292; b)D.C. Deecher, C. E. Beyer, G. Johnston, J. Bray, S. Shah, M. Abou-Gharbia, T.H. Andree, *J. Pharmacol. Exp. Ther.,*2006, **318**, 657-665.

8 a) G. M. Sheldrick, *SHELX97*, *Program for Crystal Structure Determination*; University of Göttingen: Göttingen, Germany, 1997; b) E. Keller, SCHAKAL99, Graphical Representation of Molecular Models, University of Freiburg, Germany, 1999; c)A. L. Speck, PLATON; *ActaCrystallogr*., *Sect*. *A*, 1990, **46**, C34.

3. CHARACTERIZATION OF NEW FOUR ORGANIC SALTS OF LIDOCAINE

3.1. Introduction

Lidocaine (2-diethylamino-N-(2,6-dimethylphenyl)acetamide) is the first amide-type anesthetic synthetized by Nils Löfgren in 1943.[1]

Lidocaine (Scheme 1) is a typical local anesthetic, also known for its treatment in the ventricular tachycardia (a cardiac arhythmia) as an intravenous injection solution (See e.g. U.S. Patent N0. 3,968,205).

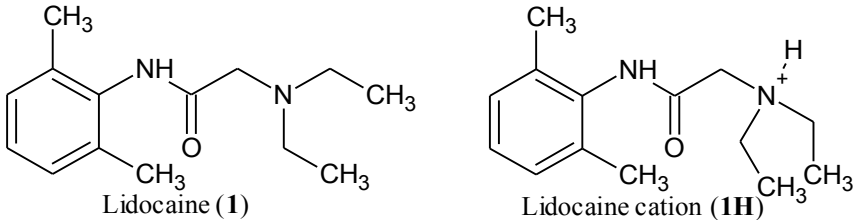

Scheme 1.

Lidocaine is also widely used as a vasoconstrictor to reduce regional blood flow in topical applications or aerosols (such as nasal aerosols to reduce nasal congestion). (See U.S. Pat. No. 5,534,242). In addition, lidocaine is known for its therapeutic effects in reducing post-herpetic neuralgia (PHN), nerve injury pain from shingles (herpes zoster and post herpetic neuralgia) and analogous neuropathies. For example, U.S. Pat. No. RE37,727 discloses methods employing lidocaine intradermal administration by transport of lidocaine from the skin surface, using patches and dressings, into the skin[2].

Lidocaine is present in the European Pharmacopoeia in two forms: the free base, not very stable and characterized by a very low solubility in aqueous solution and the hydrochloride salt, characterized by a very high solubility in aqueous solution and used generally for the preparation of injection solutions.

To improve solubility, stability and therefore efficacy of the free base,

lidocaine is usually made available as salts. In the literature different examples are reported of lidocaine salts with organic acids to improve the properties of the free

base and with other active ingredients to combine different therapeutic effects in the same drug.[3]

Lidocaine is labeled as **1** (Scheme 1) in the neutral form and **1H** in the cationic form.

In this study, four salts of **1** with oxalic, fumaric, malonic and succinic acid were prepared using conventional solution chemistry and using mechanochemical methods by mechanical mixing of the reactants (grinding or kneading).[4]

The powders obtained were characterized by X-ray powder diffraction (XRPD), differential scanning calorimetry (DSC), FT-IR and solid-state NMR (SS NMR). The lidocaine oxalate, fumarate and malonate were also characterized by single crystal X-ray diffraction (SC-XRD). The structure of lidocaine succinate was determined by X-ray powder diffraction. In addition to the synthesis and solid-state characterization, the salts were also subjected to dissolution tests in aqueous solution and the results obtained were compared with thermodynamic and kinetic solubility of lidocaine freebase and lidocaine hydrochloride salt.

3.2. Experimental section

All reactants were purchased from Aldrich and used without further purification. Reagent grade solvents and doubly distilled water were used. For dissolution tests a 0.9%. sodium chloride solution was used.

3.2.1. **Solution synthesis**

All salts were crystallized by room temperature evaporation of a solution obtained dissolving a stoichiometric mixture (1-1) of lidocaine and organic acid in hot methanol 99.8%. The amount of reagent was chosen so that 200-300 mg of solid product could be obtained (see table 1).

3.2.2. **Mechanochemistry**

All salts were quantitatively obtained as polycrystalline materials by grinding or kneading of lidocaine and organic acid in a 1:1 ratio. The experiments were performed with a Retsch MM 200 grinder for 15 minutes at a frequency of 30Hz.

Salts	Lidocaine/mg	Acid/mg
1H oxalate	**200**	**76.8**
1H fumarate	**200**	**99.6**
1H succinate	**200**	**100.7**
1H malonate	**200**	**88.8**

Table1.

3.2.3. **Thermal measurements**

Thermogravimetric analyses were performed using a simultaneus STA 409 PC Luxx® Netzsch equipped with a thermocouple for the direct measurament of DSC signal, and a thermobalance for the measurement of the TGA signal. The samples (5-15 mg) were placed in aluminium pierced pans, and the heating was carried out at 10°C min^{-1} in N_2 atmosphere.

Calorimetric measurements were performed using a DSC 200 *F3 Maia*® differential scanning calorimeter equipped with an intra-cooler. The samples (2–4

mg) were placed in aluminium pierced pans, and the heating was carried out at 10°C min^{-1} in N_2 atmosphere.(See supplementary material)

3.2.4. **Single crystal X-Ray diffraction**

Single-crystal data were collected on an Oxford X'Calibur S CCD diffractometer equipped with a graphite monochromator (MoKα radiation, λ = 0.71073) and operated at room temperature. The structure was solved by direct methods and refined by full-matrix least-squares on F^2 with SHELX97[5a] program package.
A calculated XRPD pattern was generated for Cu radiation using Mercury v 1.4 and the atomic coordinates, space group, and unit cell parameters from the single crystal data.
MERCURY and SCHAKAL99[5b] were used for the graphical representation of the results and PLATON[5c] was used for hydrogen bonding analysis.

3.2.5. **Powder X-Ray diffraction**

Diffraction patterns from 3° to 40° in 2θ were collected on a PANalytical diffractometer with Bragg–Brentano geometry (Cu Kα radiation, detector: X'celerator, step size Δ2θ = 0.0167°, counting time per step = 20 s), using a glass sample holder**.** The tube voltage and amperage were set to 40 kV and 40 mA, respectively.
For the structure solution from X-ray powder diffraction of **1H** succinate crystal phase, diffraction pattern was collected from 5 to 70° in 2θ with a step size of 0.00835° and counting time per step = 50 s. The structure was solved by analogy with the structure of **1H** fumarate phase, and refined by Rietveld analysis. Rietveld refinement was performed with software GSAS.[6]
A Cosine Fourier series with 10 coefficients and a Pseudo-Voigt function (type 3) were used to fit respectively background and peak shape. A spherical harmonics model was used to describe preferred orientation. Soft constraints were applied on bond distances and angles of both molecules. An overall thermal parameter for each atom species was adopted. Refinement converged with χ^2 = 11.04, R_{wp} =

10.84 R_{F2}= 8.96. Figure 1 shows experimental, calculated and difference curves.

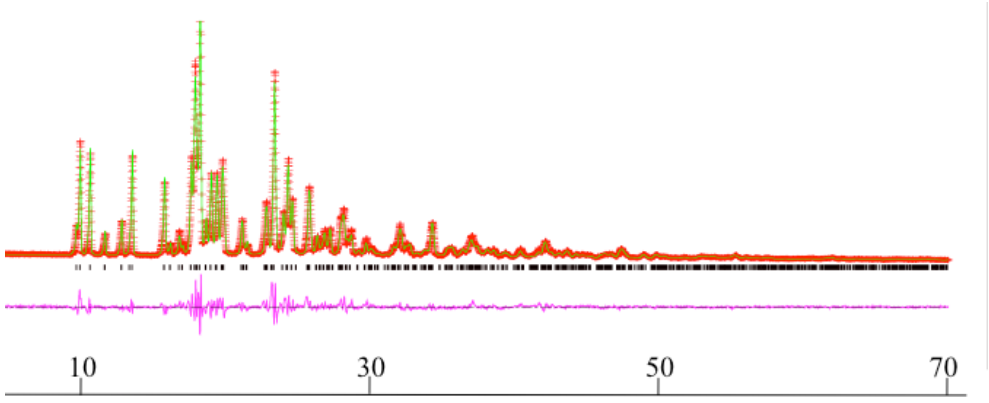

Figure 1. Experimental (red crosses), calculated (green) and difference (purple) curves of **1H** succinate phase.

3.2.6. **FT-IR**

All FT-IR measurements were performed using Nicolet FT-IR 6700 Thermo Fischer equipped with ATR device. The analyses were performed on all samples and for each measurement 32 scans were recorded (See supplemetary material).

3.2.7. **Solid-state Nuclear Magnetic Resonance (SS NMR) spectroscopy**

SS NMR experiments were recorded on a Bruker Avance II 400 instrument. The spactra were collected and interpreted by the Research Group of Prof. Roberto Gobetto at the University of Torino.

3.2.8. **Dissolution tests**

The calibration curve was built by plotting the absorbance against concentrations for four standard solutions of the sample in a sodium chloride solution 0.9% in standard concentrations. The analyses were performed using a dissolution tester and methods as described in the "*European Pharmacopeia section 2.9.3 pg. 267"*. The detector used was a UV-Vis Cary 50 Varian, equipped with an optic fiber. The program used was "*Concentration*" (Cary 50 WinUV Software V.3) and the measurement for each standard was recorded at a fixed λ. The Kinetic solubilities were performed on a Hanson's Vision Classic 6 dissolution tester coupled with a Varian Cary 50 UV-Vis Spectrophotometer. The program used was "*Kinetic"* (Cary 50 WinUV Software V.3), which recorded continuously the absorbance at fixed λ of a sodium chloride solution 0.9% (80mL) under stirring (250 rpm) at 37°C in which were added approx. 10mg of sample. The values obtained were converted from Abs/min into mol/min and for each sample two measurements were recorded. The thermodynamic solubilities were measured by leaving a sodium chloride solution 0.9% of the sample under stirring at 500 rpm for 24 h at 37°C. Then the suspensions were filtered, opportunly diluited and analyzed by UV-Vis Cary 50 Varian equipped with an optic fiber. The results were obtained using the calibration curves built in the first part of the experiment. For each sample two measurements were taken. Dissolution tests details are reported in the supplementary material.

3.3. Results and discussion

In this work four salts of lidocaine were synthesized with carboxylic acids: lidocaine oxalate (**1H**·oxalate), lidocaine fumarate (**1H**·fumarate), lidocaine malonate (**1H**·malonate) and lidocaine succinate (**1H**·succinate). All salts, crystallized by evaporation at room temperature from methanol solution and by grinding or kneading, were investigated with solid state techniques such as X-ray powder diffraction - to determine the diffraction pattern, differential scanning calorimetry - to determine the melting point, FT-IR and SS NMR for a characterization of molecular adducts.

The **1H** oxalate, fumarate and malonate were also characterized by SC-XRD. In these three cases the correspondences, between the structures determined by SC-XRD and those of bulk materials, were checked by comparing calculated and measured patterns (See supplementary material).

In the structure of **1H** fumarate (Figure 2) intermolecular hydrogen bonds are observed. The carboxylate group of the hydrogen fumarate anion forms hydrogen bonds with two molecules of **1H**, one of which with the amide group (N1-H1) and the other with the amino group (N2). The carboxylic group (O100) of the hydrogen fumarate anion forms an hydrogen bond with the carboxylate group (O300) of another anion molecule resulting in chains (Figure 3).

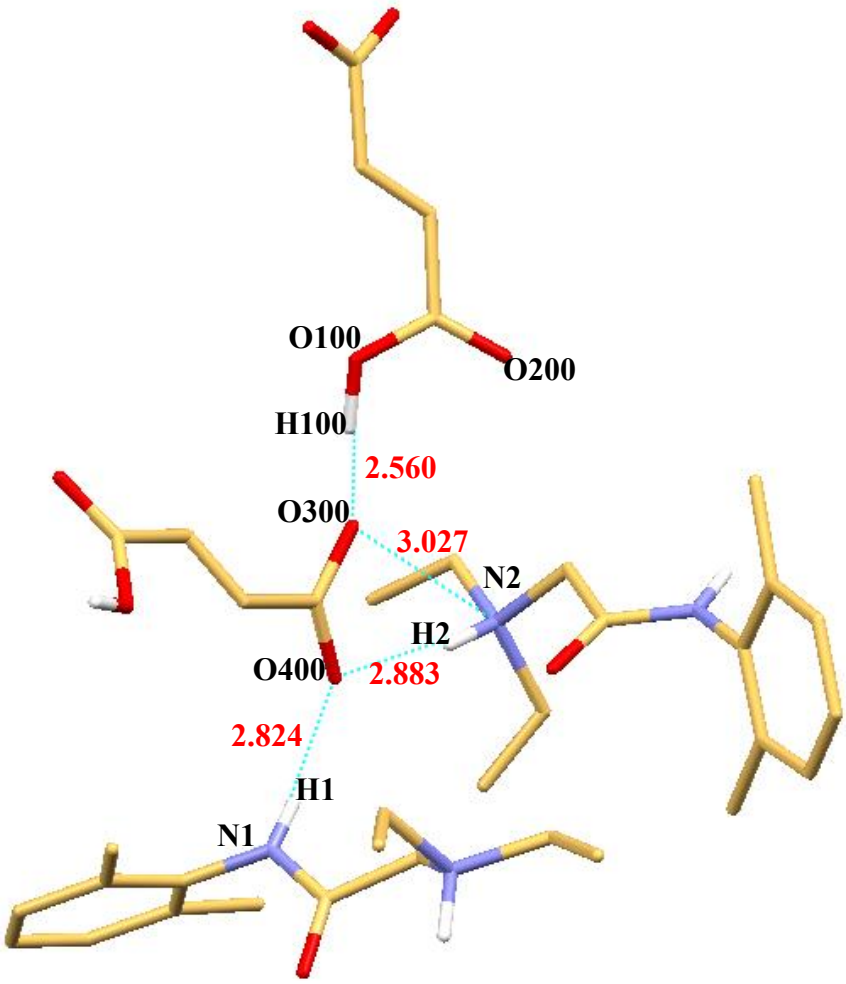

Figure 2. The hydrogen bonds of **1H** fumarate salt.

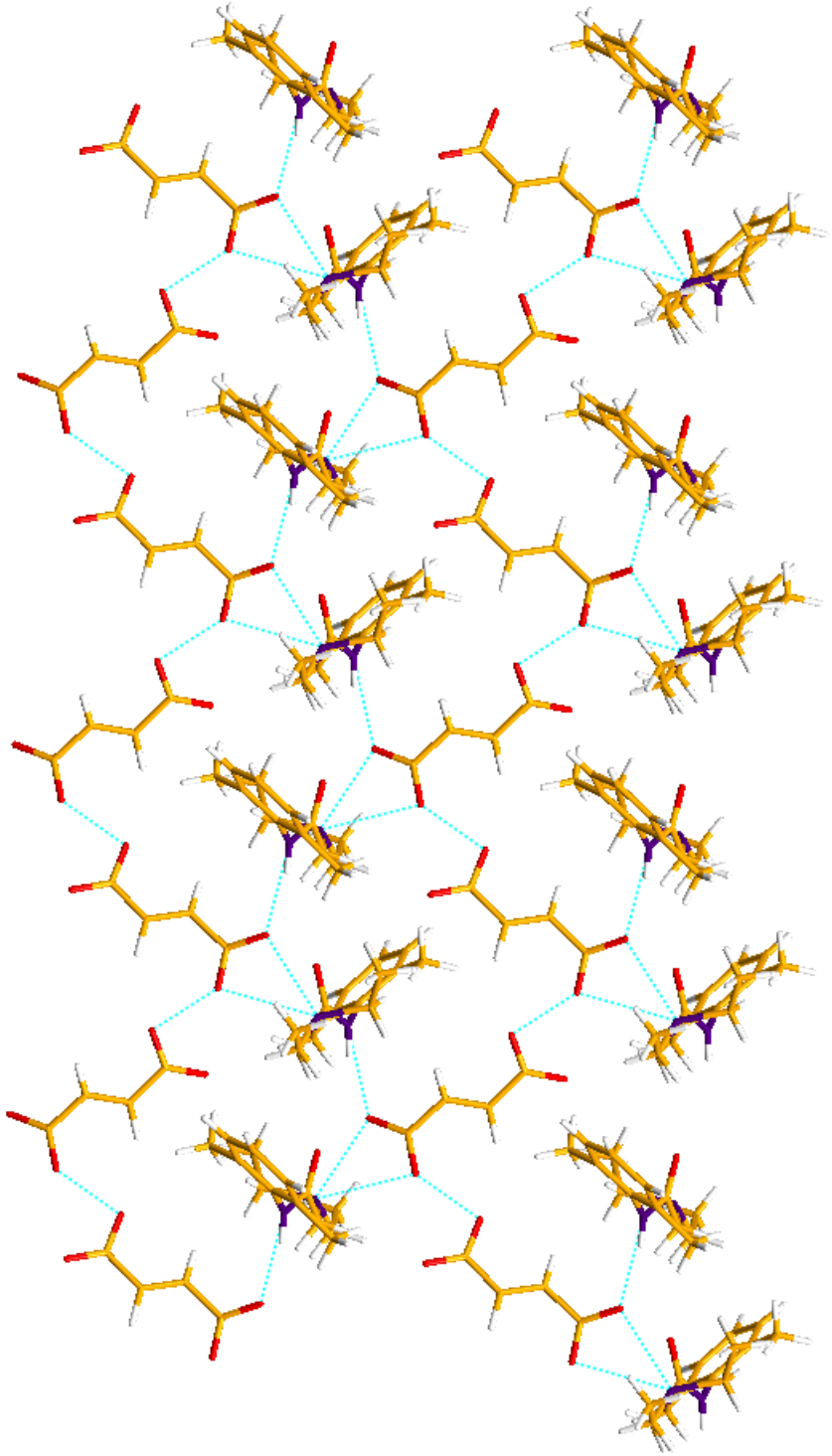

Figure 3. The packing of **1H** fumarate salt.

In the structure of **1H** malonate (Figure 4), the malonate forms one intramolecular (O2···O3) and two intermolecular hydrogen bonds with two molecules of **1H**, one of which with the amide group (N1-H100) and the other with the amino group (N2) (Figure 5).

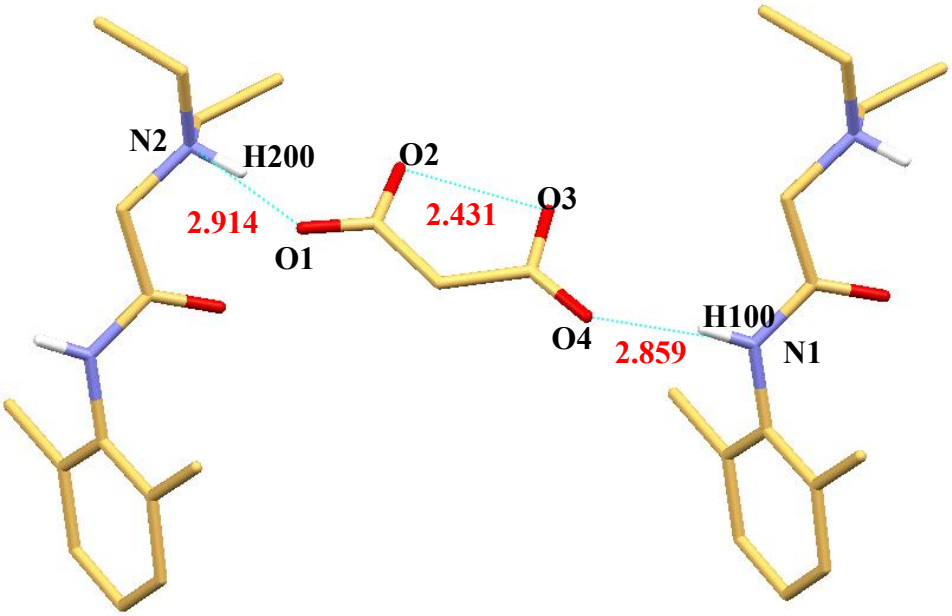

Figure 4. The hydrogen bonds of **1H** malonate salt.

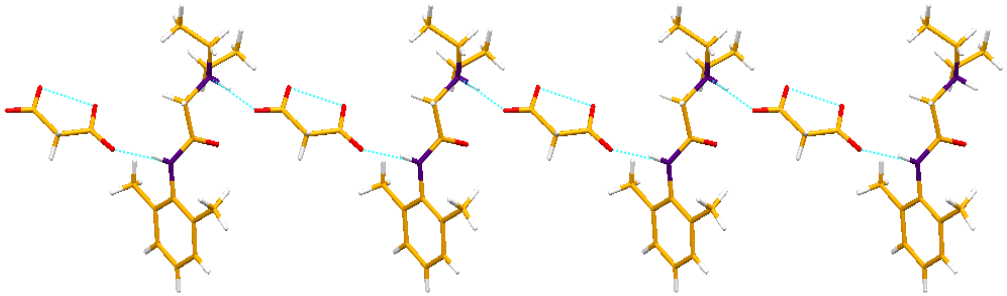

Figure 5. The packing of **1H** malonate salt.

The structure of **1H** oxalate (Figure 6) evidences also the presence of intermolecular hydrogen bonds. There are two hydrogen bonds between the oxalate molecules, which form dimers, and two hydrogen bonds of carboxylate group of hydrogen oxalate anion with two molecules of **1H** one of which with the amide group (N1-H) and the other with the amino group (N2). The dimer, formed by two oxalte molecules and involved between molecules of **1H,** is the motif repeated into the chains which characterizes the structure of the crystal (Figure 7).

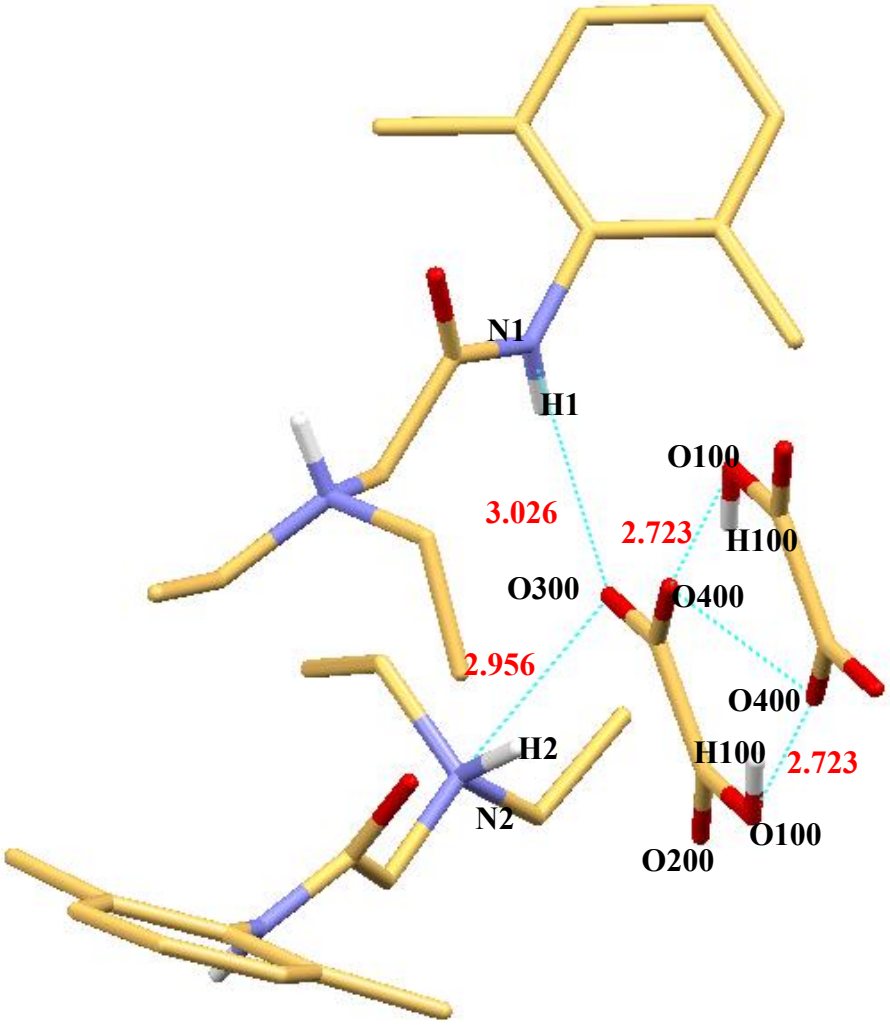

Figure 6. The hydrogen bonds of **1H** oxalate salt.

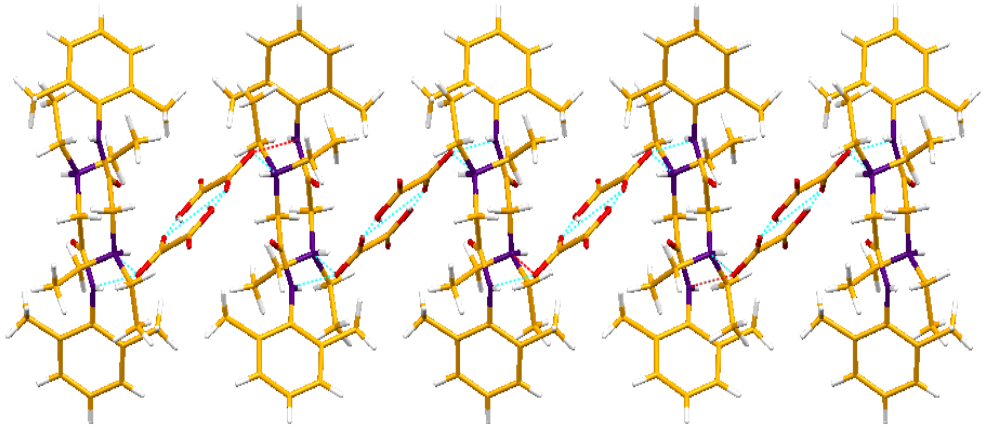

Figure 7. The packing of **1H** oxalate salt.

The structure of **1H** succinate was determined by X-ray powder diffraction, using also the analogy with the structure of **1H** fumarate phase, and was refined by Rietveld analysis.

In the structure of **1H** succinate (Figure 8) the carboxylate group forms hydrogen bonds with two molecules of **1H**, one of which with the amide group (N10) of one molecule of **1H** and the other with the amino group (N5). Furthermore, the carboxylic group (O20) of the succinate anion forms an hydrogen bond with the carboxylate group (O2) of another anion molecule (Figure 9).

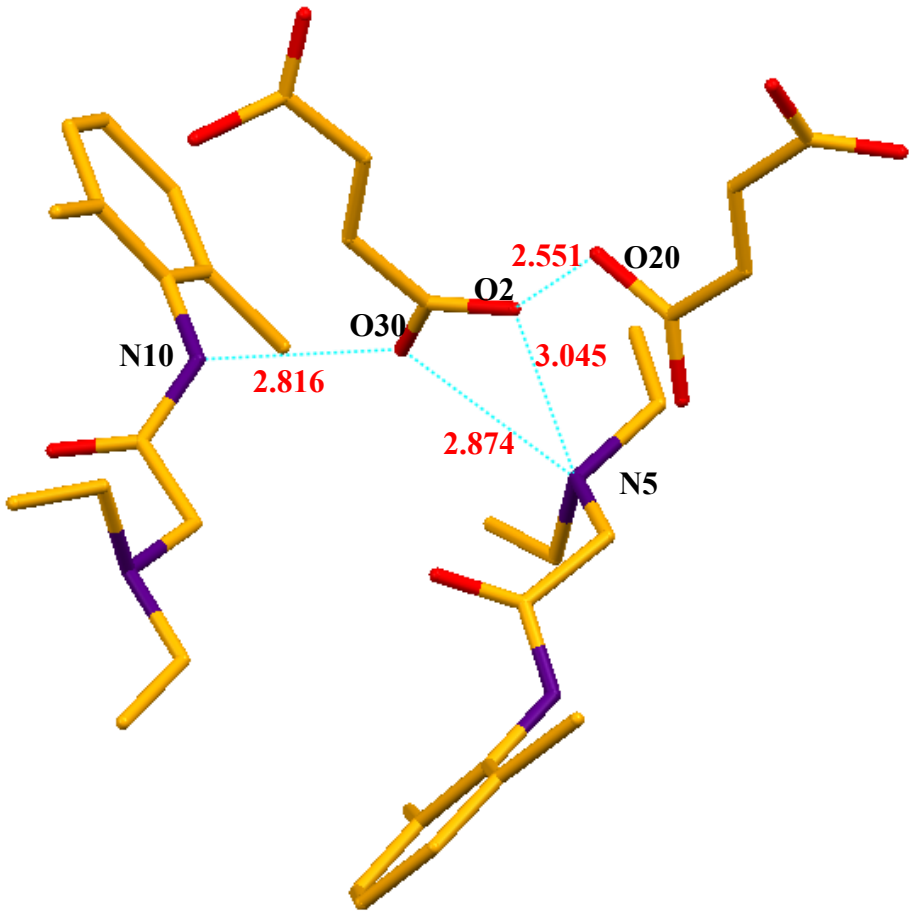

Figure 8. The hydrogen bonds of **1H** succinate salt.

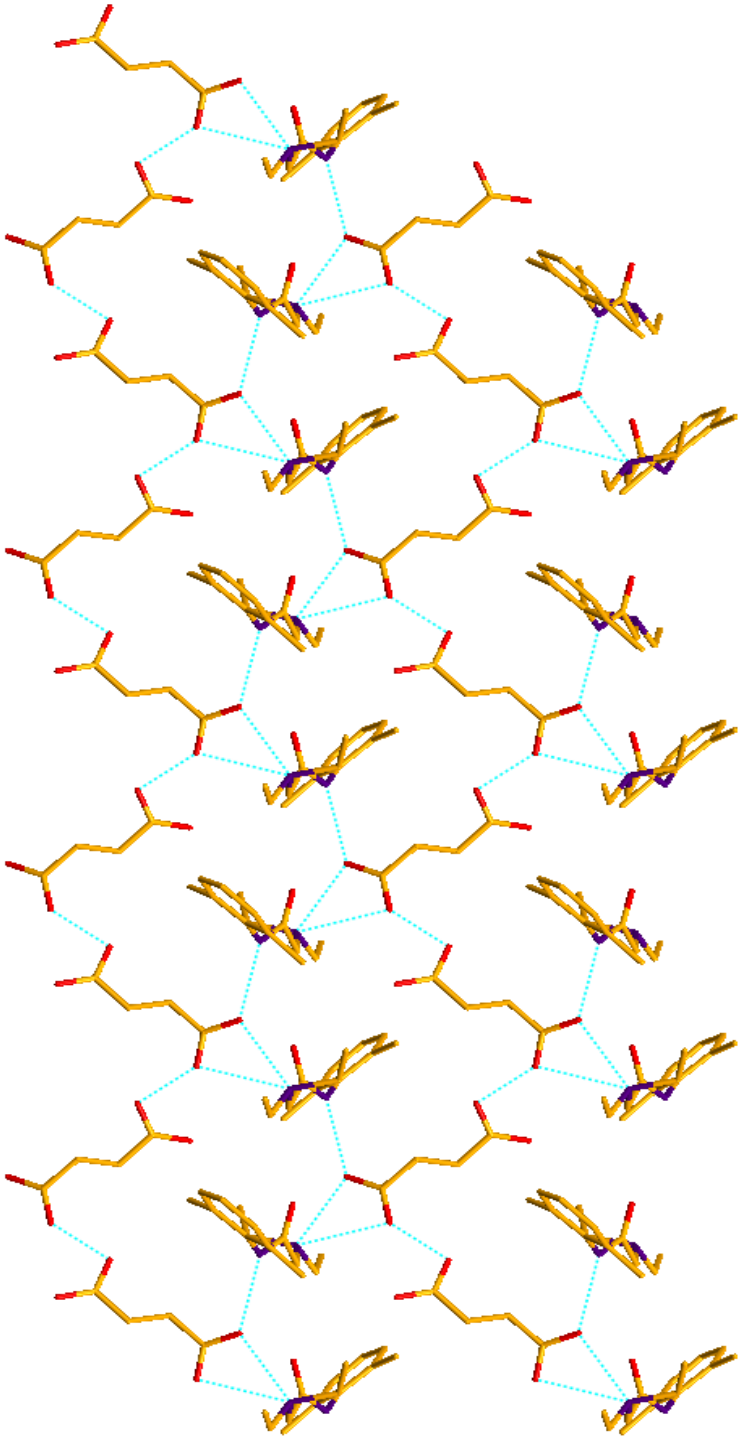

Figure 9. The packing of **1H** succinate salt.

Crystal data and details of measurements for compounds **1H** oxalate, **1H** fumarate, **1H** succinate and **1H** malonate are summarized in table 2.

compound	1H oxalate	1H fumarate	1H malonate	1H succinate
Formula	$C_{16}H_{24}N_2O_5$	$C_{18}H_{26}N_2O_5$	$C_{17}H_{23}N_2O_5$	$C_{18}N_2O_5$
M_r	324.37	350.41	336.38	324.21
system	Monoclinic	Orthorombic	Monoclinic	Orthorombic
space group	$P2_1/c$	$P\ 2_12_12_1$	$P2_1/c$	$P\ 2_12_12_1$
a [Å]	10.5817(8)	10.442(5)	12.317(4)	10.4949(3)
b [Å]	10.3447(5)	16.273(5)	10.503(3)	10.8924(3)
c [Å]	15.3496(1)	24.3454(1)	15.283(4)	16.581(4)
α [°]	90.00	90.00	90.00	90.00
β [°]	102.719(7)	90.00	109.67	90.00
γ[°]	90.00	90.00	90.00	90.00
V [Å³]	1639.01(18)	1862.7(14)	1861.6(9)	1895.4(6)
Z	4	4	4	4
d_{calc}	1.315	1.250	1.200	-
F(000)	696	752	720	-
measured reflns	7219	5838	8906	-
unique reflns	3744	3974	4228	-
refined parameters	226	234	226	-
GOF on F^2	1.032	1.029	1.013	-
R1 [on F, $I>2\sigma(I)$]	0.0784	0.0899	0.0766	-
wR2(onF^2,all data)	0.2002	0.2174	0.1992	-

Table 2. Crystal data of **1H** salts.

The SS NMR technique has been used for the definition of the crystal nature, whether molecular or salts, resulting from the positioning of the acid protons along the O···H···N interactions. Indeed, it is well-known that the ^{13}C chemical shift of the carboxylic carbon atom represents a good indicator of the protonation state of the COOH group[7a-c]. Furthermore, ^{15}N NMR studies on hydrogen-bonded systems have shown that nitrogen protonation or formation of hydrogen bonds results in high- or low-frequency shifts of the nitrogen signal, according to the type of nitrogen atom and to the nature of the interaction.[7d–f, 8]

The analysis of the ^{13}C resonances around 160-179 ppm and of the ^{15}N signal around 14-29 ppm allowed to ascertain the transfer of a single proton from the acid to the lidocaine with formation of one carboxylate and one ammonium group. Thus all adducts can be described as salts (See supplemenatary material).

Differential scanning calorimetry was used to measure the melting point of all compounds and to detect the presence of additional crystalline phases.

To improve their characterization, the salts were also subjected to dissolution tests in aqueous solution and the results obtained are compared with thermodynamic and kinetic solubility of lidocaine free base and lidocaine hydrochloride salt.

In Table 3 the melting points and dissolution results of four carboxylic salts, hydrochloride salt and lidocaine free base are reported.

The results show an increasing of the melting point from free base to lidocaine carboxylic salts, in fact, lidocaine free base and hydrochloride salt show a melting point between 60°C and 70°C, while the salts synthesized show a melting point higher than 100°C.

The malonate salt was also reported in a work of 1994 with other salts of lidocaine (maleate, adipate and tosylate). These salts were characterized using $^{1}HNMR$, IR, MS, UV-Vis. Melting point, tests of skin permeability and apparent partition coefficients were also carried out. The melting points of these salts, as those of samples characterized in this work, have higher melting point than lidocaine and lidocaine hydrochloride.[3e]

The dissolution rates of lidocaine free base and fumarate salt are lower than succinate, oxalate and malonate salts, on the other hand these last three salts show a good thermodynamic solubility more than 120 g/L.

The best value of dissolution rate is showed by the hydrochloride salt, it also has the higher thermodynamic solubility.

The results of kinetic solubilities are reported in Figure 10, this graphic shows a comparison between the dissolution curves (ABS/min) obtained.

Sample	MP(°C)	Thermodynamic Solubility(g\L)	Kinetic Solubility(mol\min)
1H	67.5	3.13	$2.13*10^{-5}$
1H chlorhydrate	75.8	>633	$1.85*10^{-3}$
1H succinate	113.5	>321	$1.5*10^{-4}$
1H malonate	140.2	>279	$1.5*10^{-4}$
1H oxalate	159.2	128.5	$1.05*10^{-4}$
1H fumarate	186.9	71	$7.31*10^{-5}$

Table 3.

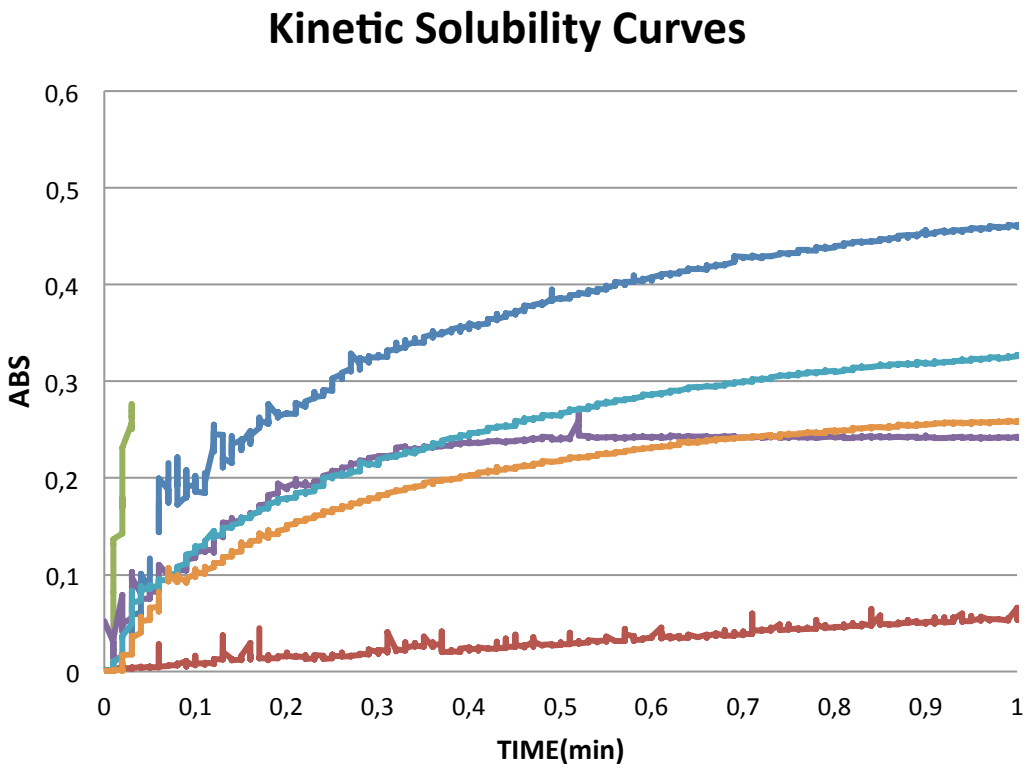

Figure 10: Kinetic profile.

3.4. Conclusion

In this study four lidocaine salts of dicarboxylic acids (oxalate, fumarate, malonate and succinate) were synthesized and characterized by different solid state techniques. SS NMR characterization allowed the distinction between salts or co-crystals obtained: in all compounds a proton-transfer was identified both in solid-state reaction and syntheses solvent assisted. The oxalate, fumarate and malonate salts were also characterized by single crystal XRD while the structure of succinate salt was obtained by powder resolution. All salts show an improvement of chemical-physic stability, in fact, there is an important increasing of the melting points respect to free base and hydrochloride salt. Furthermore, the dissolution tests of the salts obtained show a higher solubility in water in comparison with free base, while, these are lower than hydrochloride salt solubility. The solubility of an API, in fact, is a very important step for its development because before undergoing pharmacological evaluation and other preclinical studies, synthetic or natural active principles must usually be dissolved. However, one must keep in mind that making a drug molecule more water-soluble can also be a drawback. There is a general tendency that the more water-soluble a compound is, the more diffusible it is. This causes it to be less specific in its activity, and more liable to rapid elimination and, therefore, shorter acting.[9]

3.5. Supplementary Material

Legenda

1 = Lidocaine

1H oxalate= Lidocaine oxalate

1H fumarate= Lidocaine fumarate

1H malonate= Lidocaine malonate

1H succinate = Lidocaine succinate

1H chlorhydrate = Lidocaine hydrochloride

3.5.1. **Thermal measuraments**

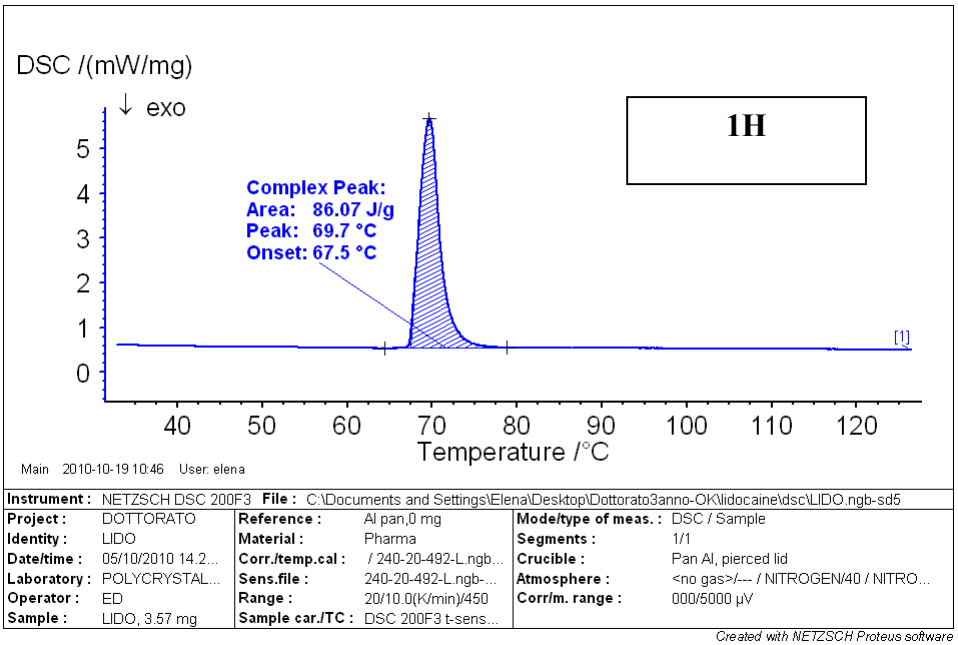

Instrument :	NETZSCH DSC 200F3	**File :**	C:\Documents and Settings\Elena\Desktop\Dottorato3anno-OK\lidocaine\dsc\LIDO.ngb-sd5		
Project :	DOTTORATO	**Reference :**	Al pan,0 mg	**Mode/type of meas. :**	DSC / Sample
Identity :	LIDO	**Material :**	Pharma	**Segments :**	1/1
Date/time :	05/10/2010 14.2...	**Corr./temp.cal :**	/ 240-20-492-L.ngb...	**Crucible :**	Pan Al, pierced lid
Laboratory :	POLYCRYSTAL...	**Sens.file :**	240-20-492-L.ngb-...	**Atmosphere :**	<no gas>/--- / NITROGEN/40 / NITRO...
Operator :	ED	**Range :**	20/10.0(K/min)/450	**Corr/m. range :**	000/5000 µV
Sample :	LIDO, 3.57 mg	**Sample car./TC :**	DSC 200F3 t-sens...		

Created with NETZSCH Proteus software

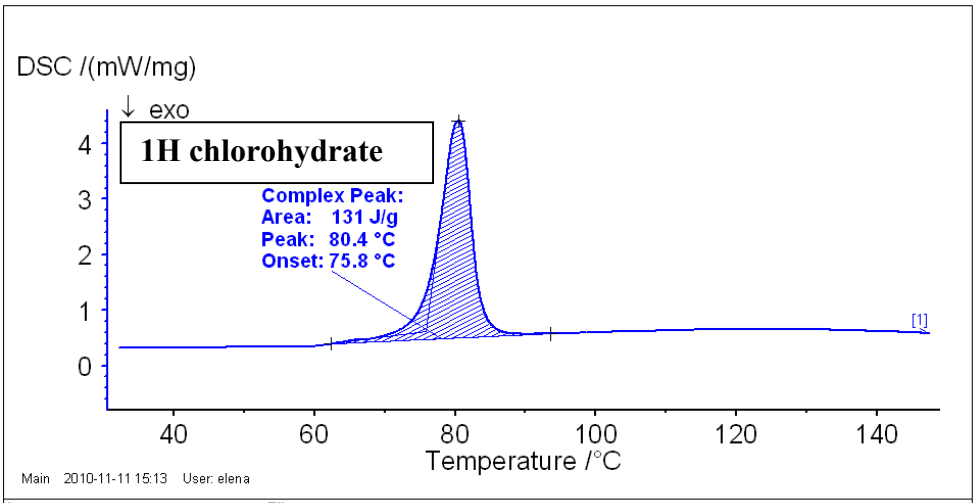

Instrument :	NETZSCH DSC 200F3	**File :**	R:\RAW DATA\THERMAL\DSC\DOTTORATO\LIDO-HCL.ngb-sd5		
Project :	LIDO	**Reference :**	Al pan,0 mg	**Mode/type of meas. :**	DSC / Sample
Identity :	LIDO-HCL	**Material :**	Pharma	**Segments :**	1/1
Date/time :	25/10/2010 11.5...	**Corr./temp.cal :**	/ 240-20-492-L.ngb...	**Crucible :**	Pan Al, pierced lid
Laboratory :	POLYCRYSTAL...	**Sens.file :**	240-20-492-L.ngb-...	**Atmosphere :**	<no gas>/--- / NITROGEN/40 / NITRO...
Operator :	ED	**Range :**	20/10.0(K/min)/450	**Corr/m. range :**	000/5000 µV
Sample :	LIDO-HCL, 4.8 mg	**Sample car./TC :**	DSC 200F3 t-sens...		

Created with NETZSCH Proteus software

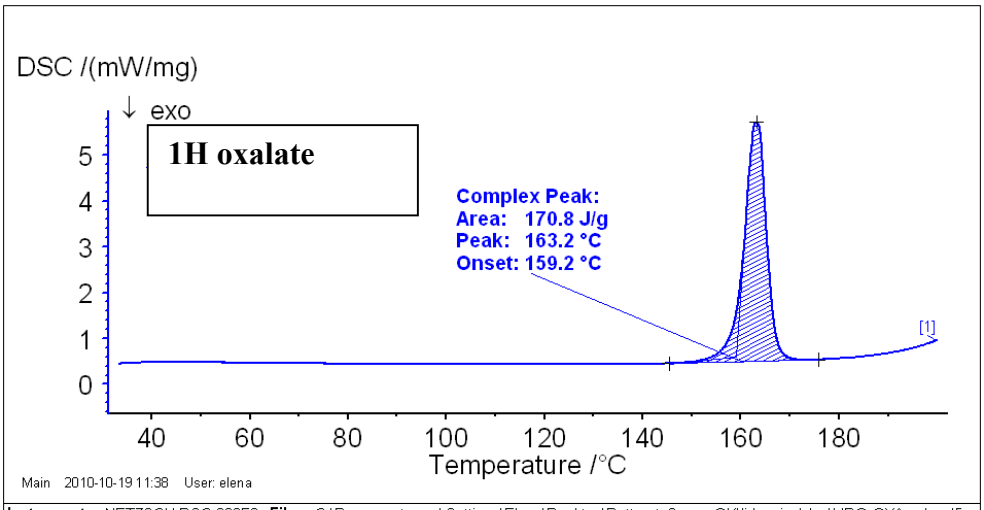

Instrument :	NETZSCH DSC 200F3	**File :**	C:\Documents and Settings\Elena\Desktop\Dottorato3anno-OK\lidocaine\dsc\LIDO-OXA.ngb-sd5		
Project :	DOTTORATO	**Reference :**	Al pan,0 mg	**Mode/type of meas. :**	DSC / Sample
Identity :	LIDO-OXA	**Material :**	Pharma	**Segments :**	1/1
Date/time :	27/09/2010 16.5...	**Corr./temp.cal :**	/ 240-20-492-L.ngb...	**Crucible :**	Pan Al, pierced lid
Laboratory :	POLYCRYSTAL...	**Sens.file :**	240-20-492-L.ngb-...	**Atmosphere :**	<no gas>/--- / NITROGEN/40 / NITRO...
Operator :	ED	**Range :**	20/10.0(K/min)/450	**Corr/m. range :**	000/5000 µV
Sample :	LIDO-OXA, 5.57...	**Sample car./TC :**	DSC 200F3 t-sens...		

Created with NETZSCH Proteus software

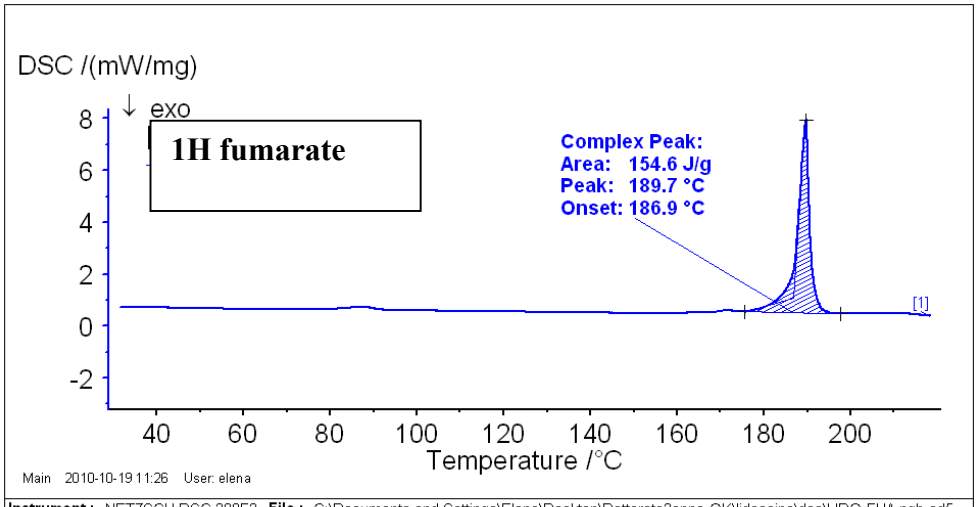

Instrument :	NETZSCH DSC 200F3	**File :**	C:\Documents and Settings\Elena\Desktop\Dottorato3anno-OK\lidocaine\dsc\LIDO-FUA.ngb-sd5		
Project :	DOTTORATO	**Reference :**	Al pan,0 mg	**Mode/type of meas. :**	DSC / Sample
Identity :	LIDO-FUA	**Material :**	Pharma	**Segments :**	1/1
Date/time :	29/09/2010 8.14.38	**Corr./temp.cal :**	/ 240-20-492-L.ngb...	**Crucible :**	Pan Al, pierced lid
Laboratory :	POLYCRYSTAL...	**Sens.file :**	240-20-492-L.ngb-...	**Atmosphere :**	<no gas>/--- / NITROGEN/40 / NITRO...
Operator :	ED	**Range :**	20/10.0(K/min)/450	**Corr/m. range :**	000/5000 µV
Sample :	LIDO-FUA, 3.21...	**Sample car./TC :**	DSC 200F3 t-sens...		

Created with NETZSCH Proteus software

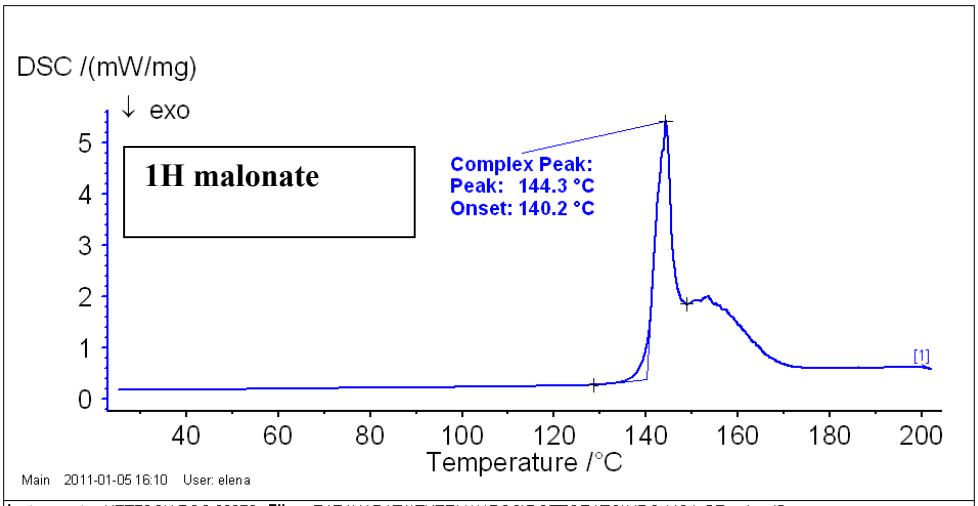

Instrument :	NETZSCH DSC 200F3	**File :**	R:\RAW DATA\THERMAL\DSC\DOTTORATO\LIDO-MOA-GR.ngb-sd5		
Project :	LIDO	**Reference :**	Al pan,0 mg	**Mode/type of meas. :**	DSC / Sample
Identity :	LIDO-MOA-GR	**Material :**	Pharma	**Segments :**	1/1
Date/time :	05/01/2011 11.19.12	**Corr./temp.cal :**	/ 240-20-492-L.ng...	**Crucible :**	Pan Al, pierced lid
Laboratory :	POLYCRYSTALLI...	**Sens.file :**	240-20-492-L.ngb-...	**Atmosphere :**	<no gas>/--- / NITROGEN/40 / NITRO...
Operator :	ED	**Range :**	20/10.0(K/min)/450	**Corr/m. range :**	000/5000 µV
Sample :	LIDO-MOA-GR, 6....	**Sample car./TC :**	DSC 200F3 t-sens...		

Created with NETZSCH Proteus software

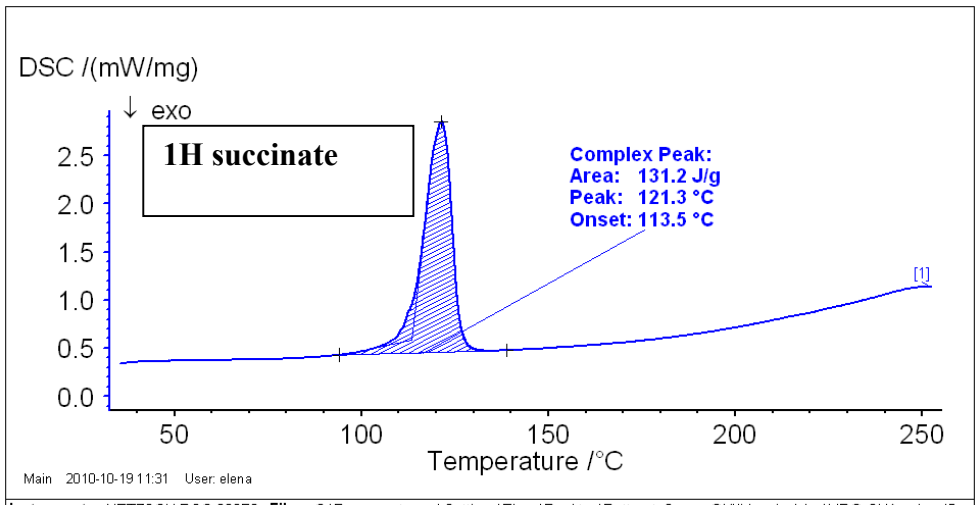

Instrument :	NETZSCH DSC 200F3	**File :**	C:\Documents and Settings\Elena\Desktop\Dottorato3anno-OK\lidocaine\dsc\LIDO-SUA.ngb-sd5		
Project :	DOTTORATO	**Reference :**	Al pan,0 mg	**Mode/type of meas. :**	DSC / Sample
Identity :	LIDO-SUA	**Material :**	Pharma	**Segments :**	1/1
Date/time :	30/09/2010 12.5...	**Corr./temp.cal :**	/ 240-20-492-L.ngb...	**Crucible :**	Pan Al, pierced lid
Laboratory :	POLYCRYSTAL...	**Sens.file :**	240-20-492-L.ngb-...	**Atmosphere :**	<no gas>/--- / NITROGEN/40 / NITRO...
Operator :	ED	**Range :**	20/10.0(K/min)/450	**Corr/m. range :**	000/5000 µV
Sample :	LIDO-SUA, 10.4...	**Sample car./TC :**	DSC 200F3 t-sens...		

Created with NETZSCH Proteus software

3.5.2. **XRPD Patterns**

Comparison between diffraction patterns recorded on products obtained crystallization (red line) and diffraction patterns computed on the basis of the structures resolution (black line).

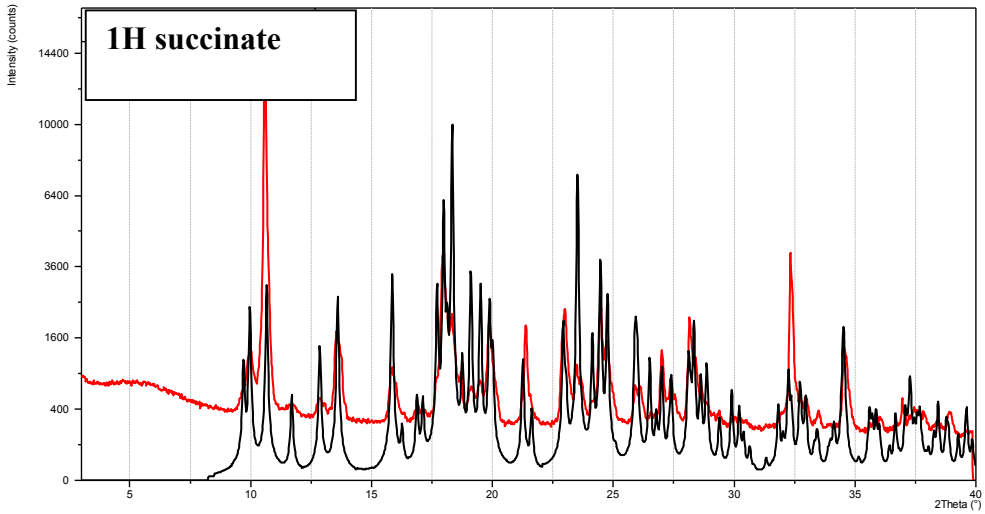

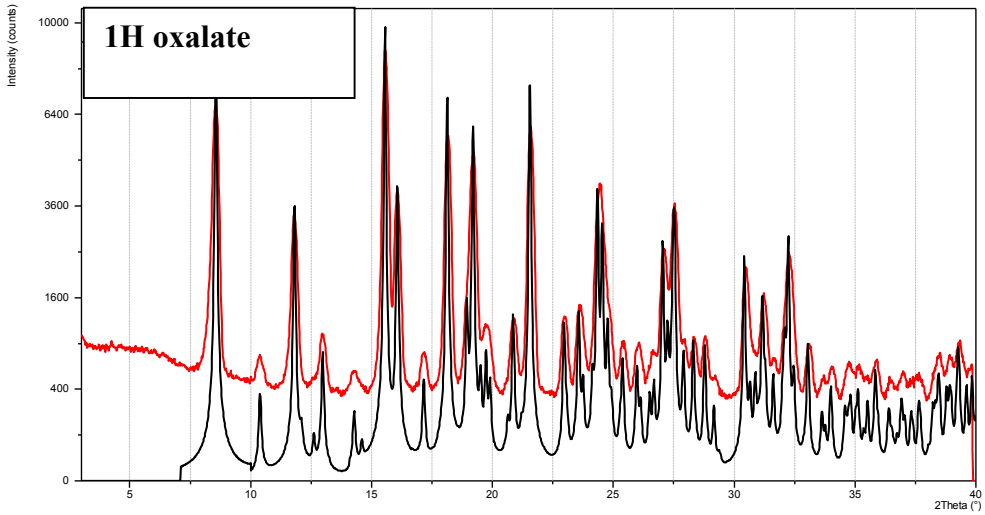

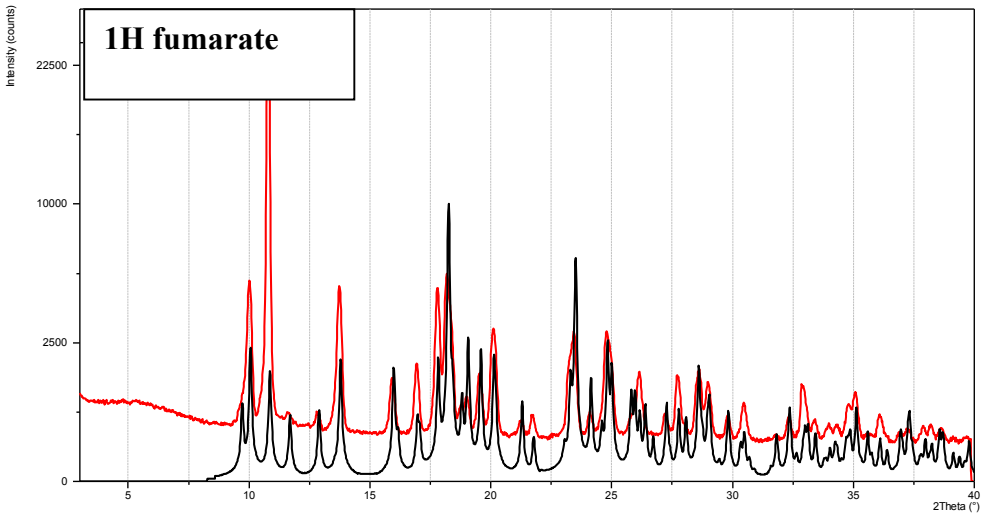
1H fumarate
Intensity (counts)
22500
10000
2500
0
5
10
15
20
25
30
35
40
2Theta (°)

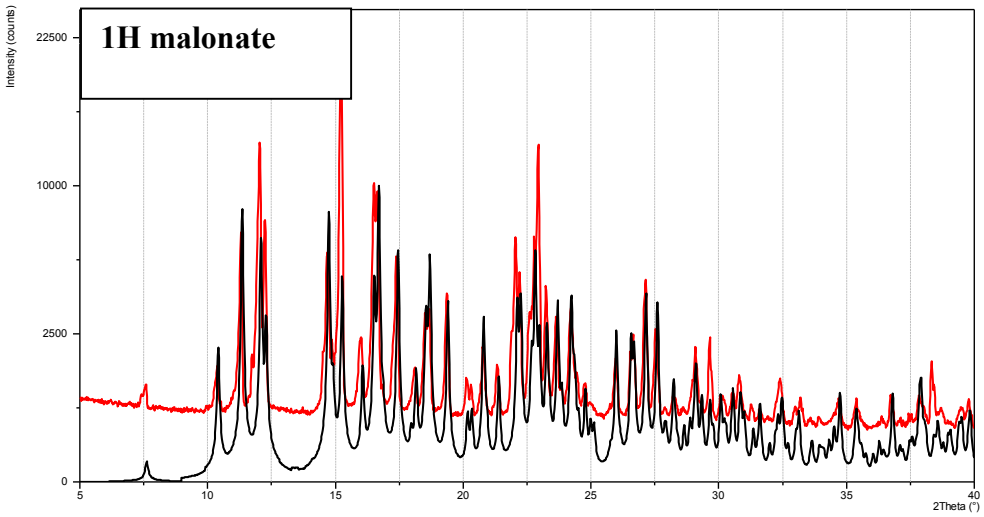
1H malonate
Intensity (counts)
22500
10000
2500
0
5
10
15
20
25
30
35
40
2Theta (°)

3.5.3. **FT-IR**

***1H** oxalate*

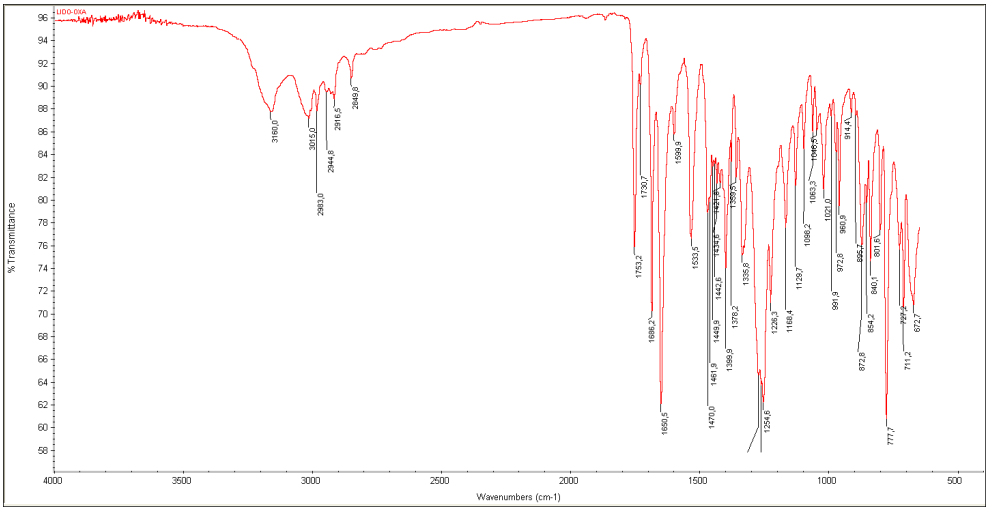

***1H** fumarate*

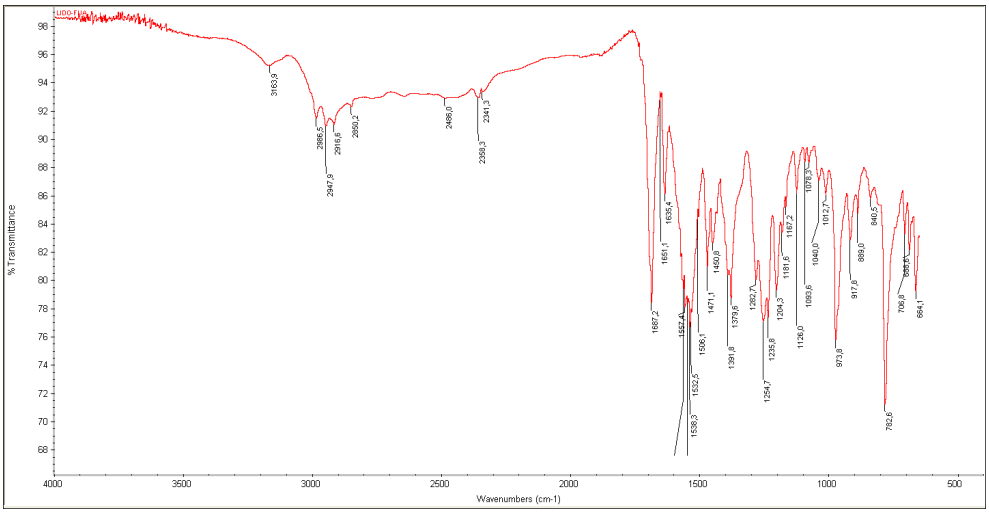

***1H** malonate*

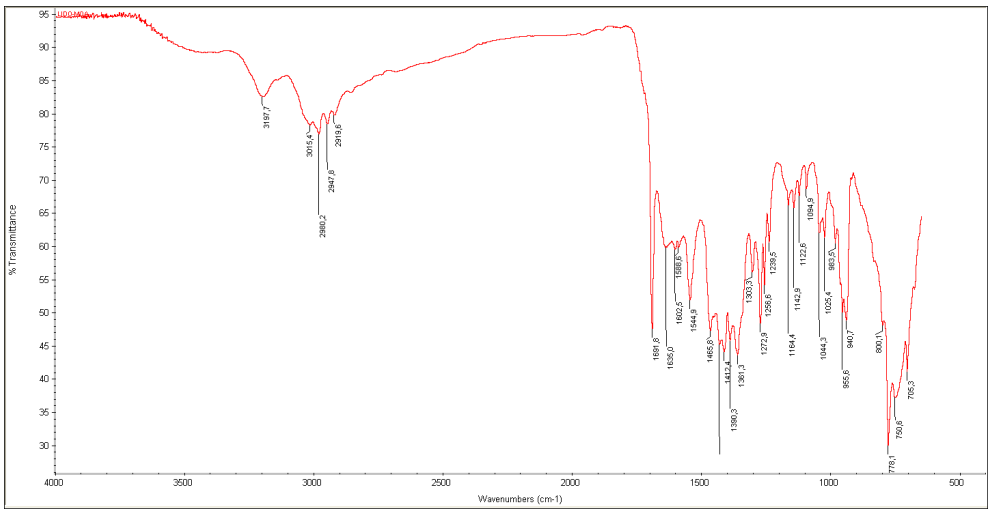

***1H** succinate*

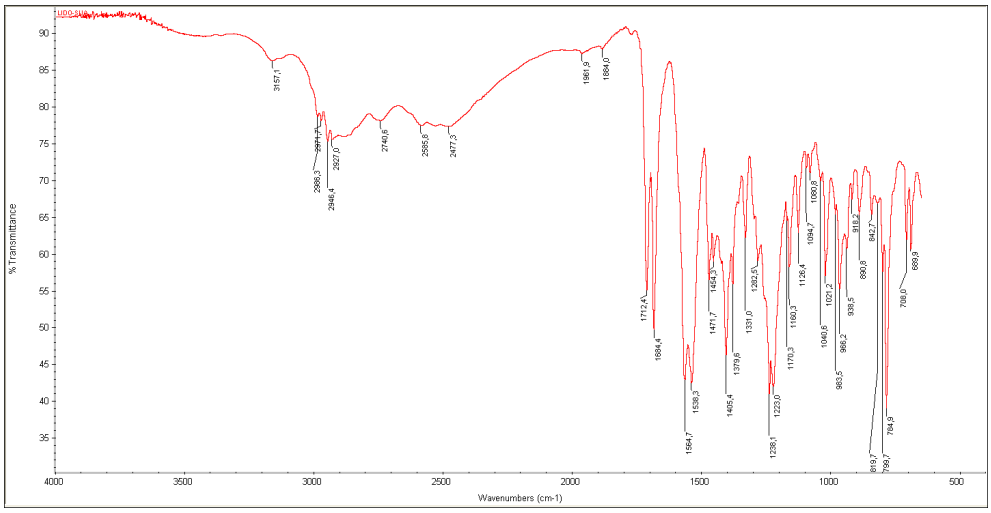

3.5.4. **Dissolution tests**

Calibration curve 1

Instrument Settings

Instrument	Cary 50
Instrument version no.	3.00
Wavelength (nm)	265.0
Ordinate Mode	Abs
Ave Time (sec)	0.1000
Replicates	1
Standard/Sample averaging	OFF
Fit type	Linear
Min R^2	0.95000
Concentration units	mol/L

Calibration

Standard	Concentration (mol/L)	F	Readings
Std 1	0.000643		0.2362
Std 2	0.001285		0.5010
Std 3	0.001928		0.8004
Std 4	0.002570		1.0789

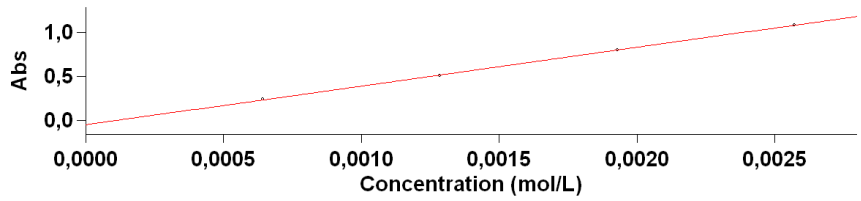

Calibration eqn	Abs = 440.15668*Conc -0.05299
Correlation Coefficient	0.99951
Calibration time	27/10/2010 11.49.16

Calibration curve 1H hydrochloride

Instrument Settings

Instrument	Cary 50
Instrument version no.	3.00
Wavelength (nm)	265.0
Ordinate Mode	Abs
Ave Time (sec)	0.1000
Replicates	1
Standard/Sample averaging	OFF
Fit type	Linear
Min R^2	0.95000
Concentration units	mol/L

Calibration

Standard	Concentration (mol/L)	F Readings
Std 1	0.000446	0.2132
Std 2	0.000892	0.4362
Std 3	0.001339	0.6217
Std 4	0.001785	0.8118

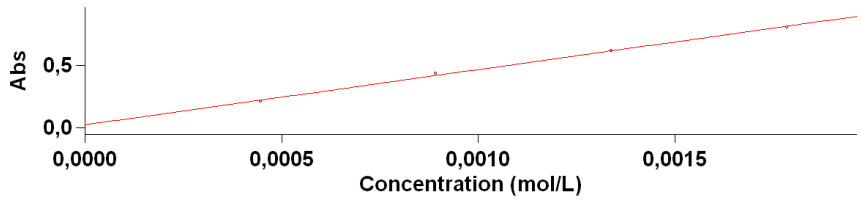

Calibration eqn	Abs = 443.85272*Conc +0.02560
Correlation Coefficient	0.99816
Calibration time	27/10/2010 12.09.08

Calibration curve 1H oxalate

Instrument Settings

Instrument	Cary 50
Instrument version no.	3.00
Wavelength (nm)	265.0
Ordinate Mode	Abs
Ave Time (sec)	0.1000
Replicates	1
Standard/Sample averaging	OFF
Fit type	Linear
Min R^2	0.95000
Concentration units	mol/L

Calibration

Standard	Concentration (mol/L)	F Readings
Std 1	0.000327	0.1187
Std 2	0.000655	0.2830
Std 3	0.000983	0.4609
Std 4	0.001310	0.6054

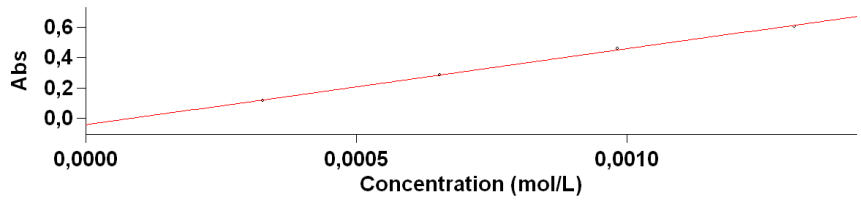

Calibration eqn	Abs = 499.89432*Conc -0.04229
Correlation Coefficient	0.99851
Calibration time	27/10/2010 11.55.37

Calibration curve 1H fumarate

Instrument Settings

Instrument	Cary 50
Instrument version no.	3.00
Wavelength (nm)	265.0
Ordinate Mode	Abs
Ave Time (sec)	0.1000
Replicates	1
Standard/Sample averaging	OFF
Fit type	Linear
Min R^2	0.95000
Concentration units	mol/L

Calibration

Standard	Concentration (mol/L)	F Readings
Std 1	0.000176	0.2246
Std 2	0.000351	0.4372
Std 3	0.000527	0.6428
Std 4	0.000703	0.8829

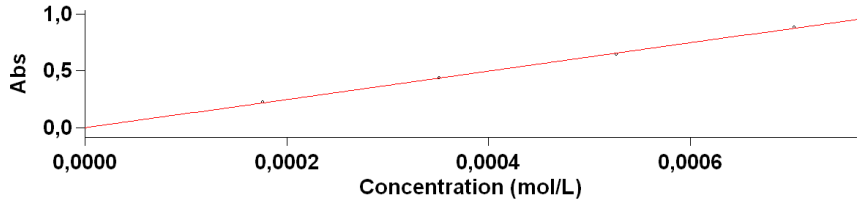

Calibration eqn	Abs = 1241*Conc +0.00174
Correlation Coefficient	0.99889
Calibration time	27/10/2010 12.03.12

Calibration curve 1H malonate

Instrument Settings

Instrument	Cary 50
Instrument version no.	3.00
Wavelength (nm)	265.0
Ordinate Mode	Abs
Ave Time (sec)	0.1000
Replicates	1
Standard/Sample averaging	OFF
Fit type	Linear
Min R^2	0.95000
Concentration units	mol/L

Calibration

Standard	Concentration (mol/L)	F	Readings
Std 1	0.000369	0.1582	
Std 2	0.000738	0.3298	
Std 3	0.001106	0.4710	
Std 4	0.001475	0.6439	

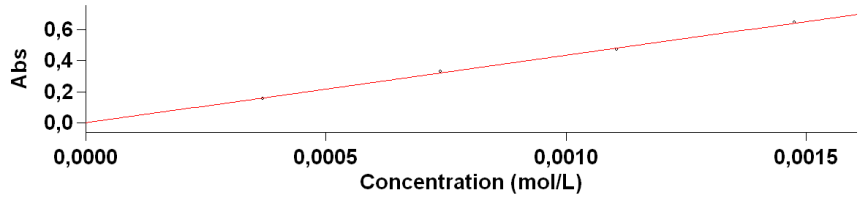

Calibration eqn	Abs = 433.63333*Conc +0.00090
Correlation Coefficient	0.99853
Calibration time	27/10/2010 12.20.45

Calibration curve 1H succinate

Instrument Settings

Instrument	Cary 50
Instrument version no.	3.00
Wavelength (nm)	265.0
Ordinate Mode	Abs
Ave Time (sec)	0.1000
Replicates	1
Standard/Sample averaging	OFF
Fit type	Linear
Min R^2	0.95000
Concentration units	mol/L

Calibration

Standard	Concentration (mol/L)	F Readings
Std 1	0.000425	0.1835
Std 2	0.000850	0.3693
Std 3	0.001275	0.5608
Std 4	0.001700	0.7427

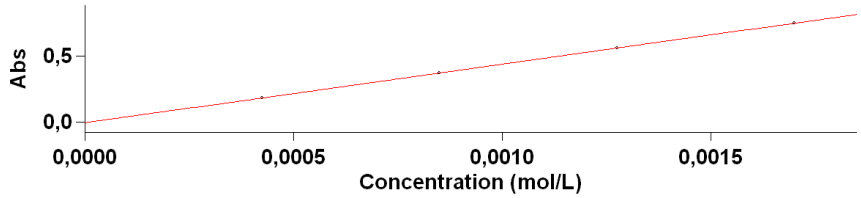

Calibration eqn	Abs = 439.80038*Conc -0.00323
Correlation Coefficient	0.99991
Calibration time	27/10/2010 12.15.34

3.5.5. **Solid state NMR**

The spectra were collected and interpretated by the Research Group of Prof. Roberto Gobetto at the University of Torino.

All ^{13}C spectra (Figure 1) are characterized by a signal at high frequencies (166-169 ppm) typical of carboxylate carbon atom together with a peak around 162-166 ppm attributed to the COOH group. In the ^{15}N CPMAS spectra (Figure 2) the amplitude of the N12 signal shift (from 15-17 ppm to about 25-29 ppm) indicates the complete protonation of the nitrogen atom in agreement with salt nature of the adducts observed by single crystal X-ray diffraction and confirmed by ^{13}C CPMAS spectra.

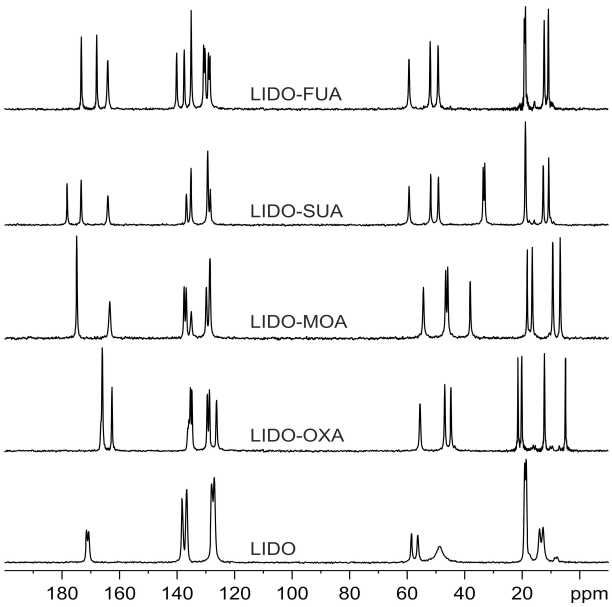

Figure 1. ^{13}C CPMAS spectra of LIDO, LIDO-OXA, LIDO-MOA, LIDO-SUA and LIDO-FUA co-crystals recorded at 100.64 MHz with a spinning speed of 12 kHz.

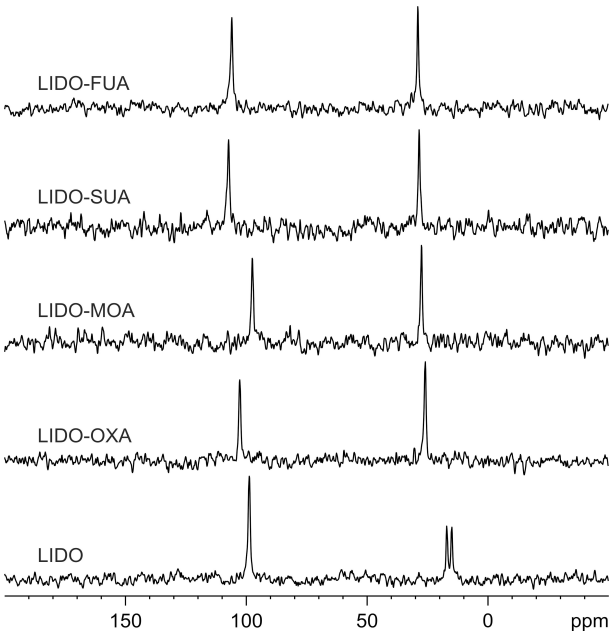

Figure 2. ^{15}N CPMAS spectra of LIDO, LIDO-OXA, LIDO-MOA, LIDO-SUA and LIDO-FUA co-crystals recorded at 40.56 MHz with a spinning speed of 12 kHz.

3.6. References

1 Lofgren, N. M.; Lundquist, B. J. *Alkyl Glycinalnilides. U.S. Patent 2 441 498,* May 11, 1948.

2 Fang-Yu Lee, Shan-Chiung Chen, Bin-Ken Chen, Chiung-Ju Tsai, Yen-Ling Yi, *US Patent 7 166 641 B2*, Jan. 23, 2007.

3 a) Gasparotti, Franca A., *US Patent 4 891 386*, Jan. 2, 1990; b) Fang-Yu Lee, Shan-Chiung Chen, Bin-Ken Chen, Chiung-Ju Tsai, Yen-Ling Yi, *US Patent 7 166 641 B2*, Jan. 23, 2007, c) Umeda Y., Nagase H., Makimura M., Tomono K., Shiro M., Ueda H., *Analytical Sciences*, 2007, **Vol.23**; d) Susan W. Larsen, JesperOstergaard, Sara V. Poulsen, Bjorn Schulz, Claus Larsen, *European Journal of Pharmaceutical Sciences*, 2007, **31**, 172-179; e) OpaVajragupta, Supreeya La-ong, *Drug Development and Industrial Pharmacy*, 1994, **20(17)**, 2671-2684; f) Y. Umeda, T. Fukami, T. Furuishi, T. Suzuki, K. Tanjoh, K. Tomono, Drug Development and Industrial Pharmacy, 2009, **35(7)**, 843-851.

4 a) S.Karki, T. Friscic and W. Jones, *CrystEngComm*, 2009, **11**, 470-481; b) D.R. Weyna, T. Shattock and M. J. Zaworotko, *Cryst. Growth Des.*, 2009, **9**, 1106-1123; c) M. J. Zaworotko, *Cryst. Growth Des..*, 2007, **7(4)**, 616-617; d) D. Braga, G. Palladino, M. Polito, K. Rubini, F. Grepioni, M.R. Chierotti and R. Gobetto, *Chem.-Eur. J.*, 2008, **14**, 1049-10159; e) Andre, D. Braga, F. Grepioni and M. T. Duarte, *Cryst. Growth Des.*, 2009, **9**, 5108-5116; f) T. Frisic and W. Jones, *Cryst. Growth Des.*, 2009, **9**, 1621-1637; g) G. Kaupp, *CrystEngComm*, 2009, **11**, 388-403; h) D. Braga, M. Curzi, E. Dichiarante, S.L. Giaffreda, F. Grepioni, L. Maini, G. Palladino, A. Pettersen, M. Polito, in *Making crystals from crystals: a solid-state route to the engineering of crystalline materials, polymorphs, solvates and co-crystals; considerations on the future of crystal engineering*, ed. L. Addadi, D. Braga and J.J. Novoa, Springer, The Netherlands, 2008, pp.131-156; i) M. R. Chierotti, L. Ferrero, N. Garino, R. Gobetto, L. Pellegrino, D. Braga, F. Grepioni and L. Maini, *Chem.-Eur. J.*, 2010, **16**, 4347-4358.

5 a) G. M. Sheldrick, *SHELX97*, *Program for Crystal Structure Determination*; University of Göttingen: Göttingen, Germany, 1997; b) E. Keller, SCHAKAL99, Graphical Representation of Molecular Models, University of Freiburg, Germany, 1999; c) A. L. Speck, PLATON; *Acta Crystallogr*., *Sect*. *A*, 1990, **46**, C34.

6 A.C. Larson and R.B. Von Dreele, *"General Structure Analysis System (GSAS)"*, Los Alamos National Laboratory Report LAUR 86-748, 2000.

7 a) Z. Gu, A. McDermott, *J. Am. Chem. Soc.*, 1993, **115**, 4282; b) A. Naito, S. Ganapathy, K. Akasaka, C. J. McDowell, *J. Chem. Phys.*, 1981, **74**, 3198; c) D. Braga, L. Maini, G. De Sanctis, K. Rubini, F. Grepioni, M. R. Chierotti, R. Gobetto, *Chem. Eur. J*., 2003, **9**, 5538; d) R. Gobetto, C. Nervi, E. Valfrè, M. R. Chierotti, D. Braga, L. Maini, F. Grepioni, R. K. Harris, P. Y. Ghi, *Chem. Mater*., 2005, **17**, 1457; e) R. O. Duthaler, J. D. Roberts, *J. Magn. Reson.*, 1979, **34**, 129; f) R. E. Botto, J. D. Roberts, *J. Org. Chem.*, 1977, **42**, 2247.

8 a) E. Diez-Pena, I. Quijada-Garrido, J. M. Barrales-Rienda, I. Schnell, H.W. Spiess, *Macromol. Chem. Phys*., 2004, **205**, 430; b) D. Braga, F. Grepioni, M. Polito, M. R. Chierotti, S. Ellena, R. Gobetto, *Organometallics*, 2006, **25**, 4627; c) R. Gobetto, C. Nervi, M. R. Chierotti, D. Braga, L. Maini, F. Grepioni, R. K. Harris, P. Hodgkinson, *Chem. Eur. J*., 2005, **11**, 7461.

9 C. G. Wermuth, P. H. Stahl, *Introduction*. in *Handbook of Pharmaceutical Salts: Properties, Selection, and Use*; P. H. Stahl, C. G. Wermuth , Eds.; VHCA and Wiley-VCH: Weinheim, 2002

4. POLYMORPHS AND SALTS/CO-CRYSTALS SCREENING OF NALIDIXIC ACID

4.1. Introduction

Nalidixic acid (**1**) (1-ethyl-1,4-dihydro-7-methyl-4-oxo-1,8-naphthyridine-3-carboxylic acid) is the first of the synthetic quinolone antibiotics. **1** is an antibacterial agent effective against both gram-positive and gram-negative bacteria. It is especially used in treating urinary tract infections, caused, for example, by *Escherichia coli*, *Proteus*, *Shigella*, *Enterobacter*, and *Klebsiella.*[1]

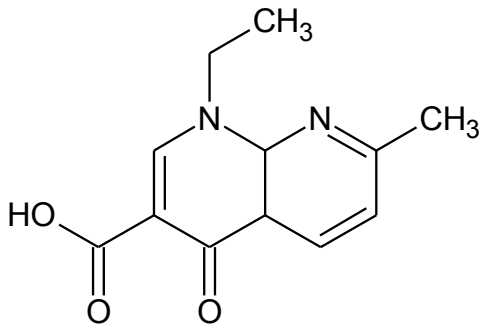

Nalidixic Acid (**1**)

Scheme 1.

1, present in one crystal form (Form I) in CSD, was studied by polymorph and salt/co-crystal screening to identify new crystal forms. Experiments of evaporation and slurry at room temperature were performed in different solvents, and allowed the discovery of a new crystal form, named Form II, obtained by evaporation experiments at room temperature of a dichloromethane solution. The salt/co-crystal screening, performed using as coformer the bases listed in Table 2 in *Preface*, allowed the discovery of two new salts/co-crystals of **1** with diethanolamine (DIETHAN) and pyrrolidine (PYR). The solid products obtained were characterized by X-ray powder diffraction (XRPD), differential scanning calorimetry (DSC), thermogravimetric analysis (TGA), FT-IR, Solid-State NMR (SS NMR) and single crystal X-ray diffraction (SC-XRD). The salt/co-crystal of **1**

with pyrrolidine was also analyzed by evolved gas analysis (EGA) and variable temperature XRPD (VT-XRPD) that led to a new crystal form of **1** named Form III (same form delivered by Sigma Aldrich) characterized by different solid state techniques. The three crystal forms of **1** were also studied by interconversion experiments that allowed identify the only stable crystal form of **1**: **1** Form I.

4.2. Experimental section

4.2.1. **Synthesis of 1 Form II**

1 Form II was obtained by evaporation of a dichloromethane solution of **1** bought from Sigma Aldrich (named **1** Form III). The solution was prepared dissolving 50 mg of **1** as delivered in 4 mL of dichloromethane. The suspension was stirred for 30 min until complete dissolution and filtered with Wathman filter 0.45μm. The solution was left to evaporate at room temperature.

4.2.2. **Synthesis of 1 – PYR**

1-PYR was crystallized by room temperature evaporation of a solution obtained dissolving stoichiometric amounts (1-1) of **1** and PYR in hot methanol 99.8%.

4.2.3. **Synthesis of 1 – DIETHAN**

1-DIETHAN was crystallized by room temperature evaporation of a solution obtained dissolving stoichiometric amounts (1-1) of **1** and DIETHAN in hot acetone.

4.2.4. **Synthesis of 1 Form III**

1 Form III (purchased by Sigma Aldrich) was obtained by VT-XRPD experiment performed on **1**-PYR; Form III was obatined following loss of water and PYR by the salt/co-crystal **1**-PYR, heated to approx. 120°C.

4.2.5. **Thermal measuraments**

Thermogravimetric analyses were performed using a simultaneus STA 409 PC Luxx® Netzsch equipped with a thermocouple for the direct measurament of DSC signal, and a thermobalance for the measurament of TGA signal. The samples (5-15 mg) were placed in aluminium pierced pans, and the heating was carried out at 10°C min^{-1} in N_2 atmosphere.

Calorimetric measurements were performed using a DSC 200 *F3 Maia*® differential scanning calorimeter equipped with an intra-cooler. The samples (2–4 mg) were placed in aluminium pierced pans, and the heating was carried out at 10°C min^{-1} in N_2 atmosphere.(See Supplementary material)

4.2.6. **X-Ray diffraction**

Single-crystal data were collected on an Oxford X'Calibur S CCD diffractometer equipped with a graphite monochromator (MoKα radiation, λ = 0.71073) and operated at room temperature. Data collection and refinement details are reported in ESI. The structure was solved by direct methods and refined by full-matrix least-squares on F^2 with SHELX97[2a] program package.

A calculated XRPD pattern was generated for Cu radiation using Mercury v 1.4 and the atomic coordinates, space group and unit cell parameter from the single crystal data.

MERCURY and SCHAKAL99 [2b] were used for the graphical representation of the results and PLATON [2c] was used for hydrogen bonding analysis.

X-ray powder diffractograms were collected on a Panalytical X'Pert Pro automated Diffractometer equipped with X'Celerator, CuKα, using glass sample holder**.** The tube voltage and amperage were set to 40 kV and 40 mA, respectively. The program used for data collection was set to record only the data points within the range 2θ= 3° - 40°. VT-XRPD analyses were performed equipping the diffractometer with an Anton Paar TTK 450 low-temperature camera that is a non-ambient attachment for powder X-ray diffraction studies in reflection geometry from -193 °C to +450 °C.

4.2.7. **FT-IR**

All FT-IR measurements were performed using Nicolet FT-IR 6700 Thermo Fischer equipped with ATR device. The analyses were performed on all samples and for each measurament 32 scans were performed (See Supplementary material).

4.2.8. **Solid-state Nuclear Magnetic Resonance (SS NMR) spectroscopy**

SS NMR experiments were recorded on a Bruker Avance II 400 instrument. The spactra were collected and interpreted by the Research Group of Prof. Roberto Gobetto at the University of Torino.

4.2.9. **Grinding experiments**

Grinding experiments were performed with a Retsch MM 200 grinder for 10 minutes at a frequency of 30Hz, to verify the stability of crystal forms of **1**.

4.3. Results and discussion

In this work nalidixic acid was studied by polymorph and salt/co-crystal screening to identify new crystal forms. Experiments of evaporation and slurry at room temperature, performed in different solvents, led to the discovery of a new crystal form, named Form II, obtained by evaporation at room temperature from dichloromethane.

The SC-XRD analysis of **1** Form II evidences the presence of four molecules of 1 in the $P2_1/n$ unit cell. As evidenced in the packing - Figure 1 – the structure is characterized by parallel planes while in Form I [3] – Figure 2- the molecules form zig-zag motifs.

The correspondence of the structure determined by SC-XRD and that of bulk material, was checked by comparing the calculated pattern with the experimental one (Figure 3).

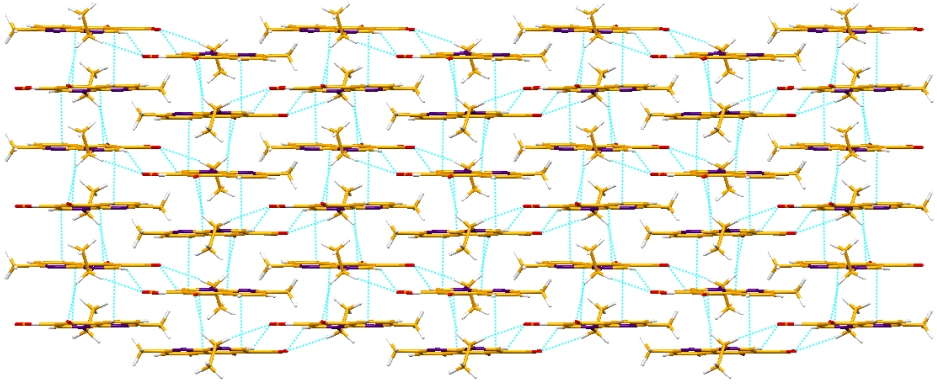

Figure1. Packing of **1** Form II.

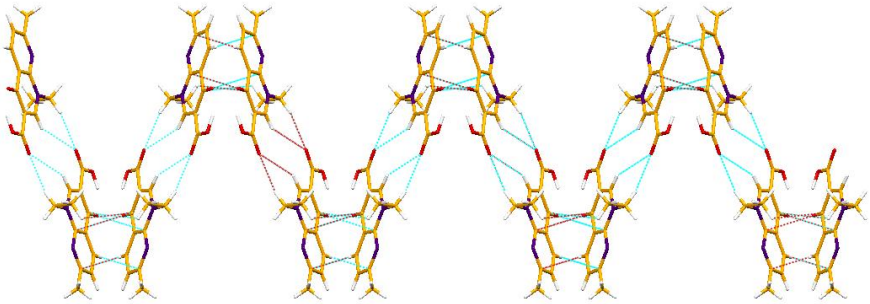

Figure2. Packing of **1** Form I.

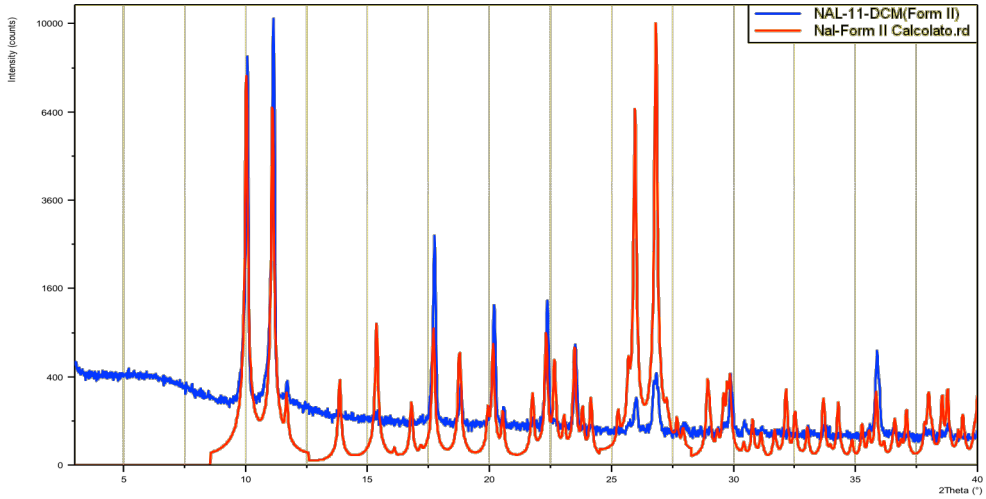

Figure3. Comparison between XRPD patterns of **1** Form II calculated (red line) and measured (blue line)

1 Form II was also characterized by TGA, DSC, FT-IR and SS NMR. The DSC and SS NMR analyses led to the same results of Form I: the two crystal forms show the same SS NMR spectrum – Figure 4 - and the same DSC profile – Figure 5 - with melting point at approx. 228.5°C

1 Form II probably is an unstable crystalline form, which converts into Form I during the analyses.

In fact, Form II heated to 150°C and measured by XRPD showed the XRPD pattern of Form I – Figure 6 - that at high temperature melt; this conversion is also observed by grinding experiment.

This phenomenon is not observed during the DSC analysis, which shows only the endothermic peak associated to the melting of the compound (Form I).

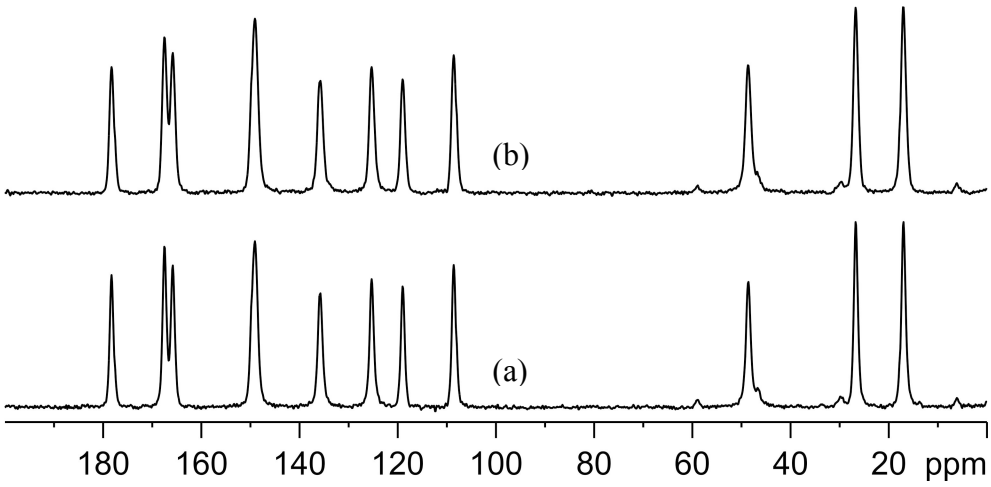

Figure4a. Comparison between SS NMR spectra ^{13}C of **1** Form I (a) and 1 Form II (b).

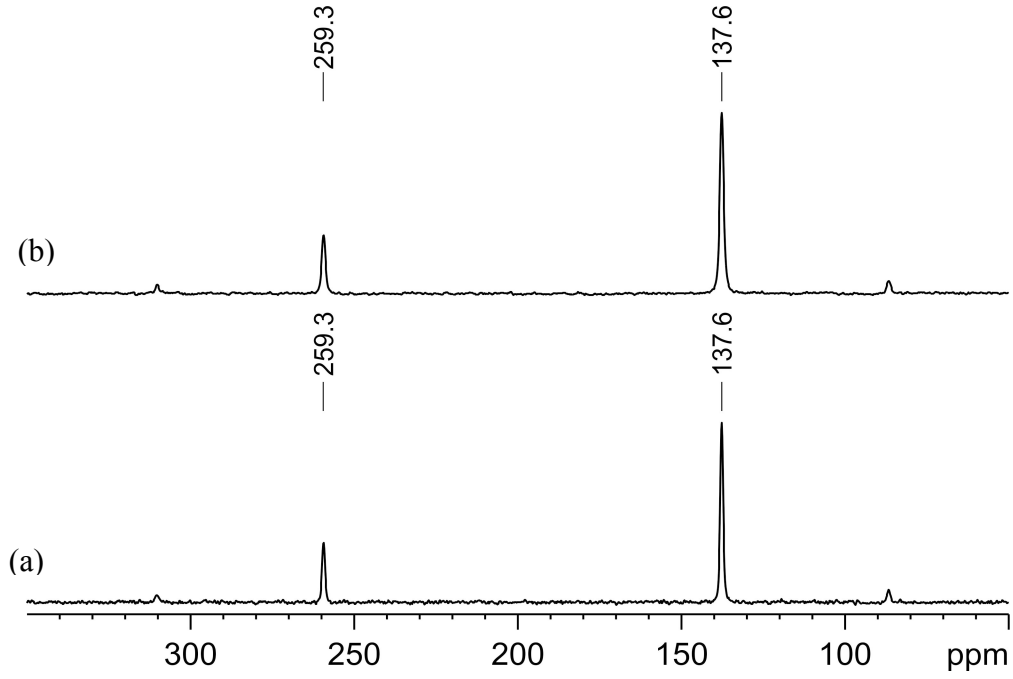

Figure4b. Comparison between SS NMR spectra ^{15}N of **1** Form I (a) and 1 Form II (b).

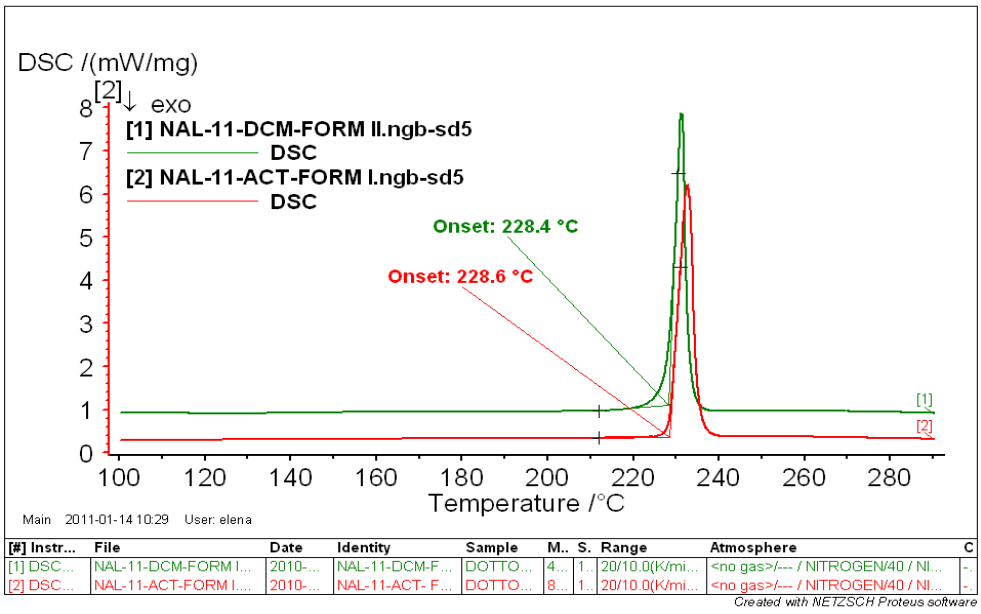

Figure5. Comparison between DSC profile of **1** Form I and 1 Form II.

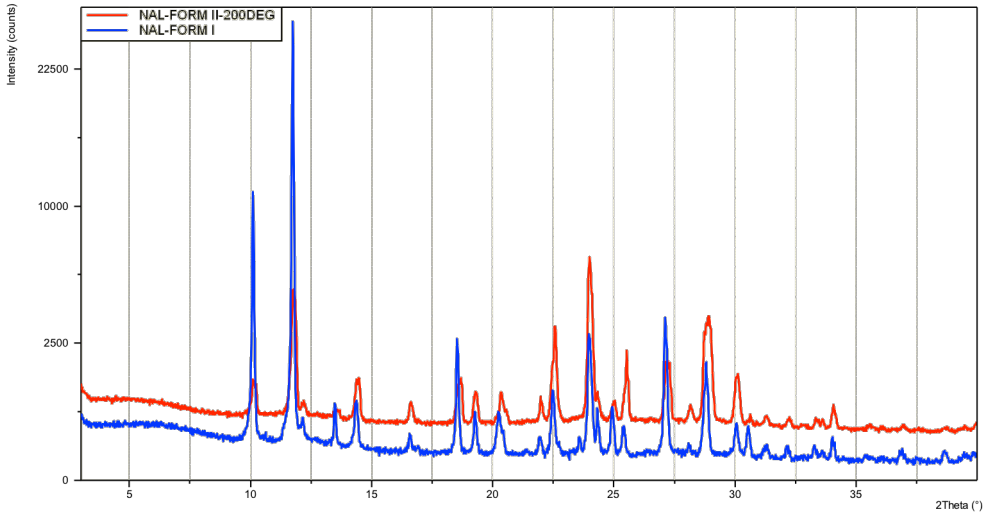

Figure6. Comparison between XRPD patterns of **1** Form I(blue line) and 1 Form II heated to 200°C (red line)

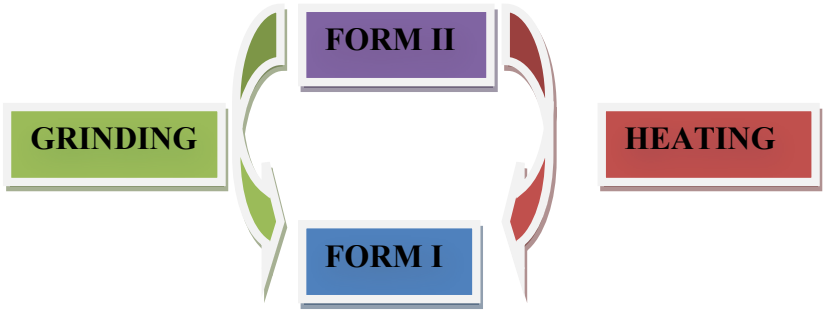

Scheme 2.

The salt/co-crystal screening, performed using as coformer the bases LISTED IN THE Table 2 in the *Preface*, allowed the discovery two new salts/co-crystals of **1**: with diethanolamine (DIETHAN) and pyrrolidine (PYR). The powder obtained were characterized by XRPD and SC-XRD.

The SC-XRD analysis of **1**-DIETHAN evidences the presence of eight molecules of **1** and eight molecules of diethanolamine in the P-1 unit cell. As evidenced in the packing - Figure 7 – the structure is characterized by parallel planes held together by hydrogen bonds between diethanolamine molecules. Each plane is characterized by two chains of **1** and DIETAN alternatively held together through hydrogen bonds (Figure 8).

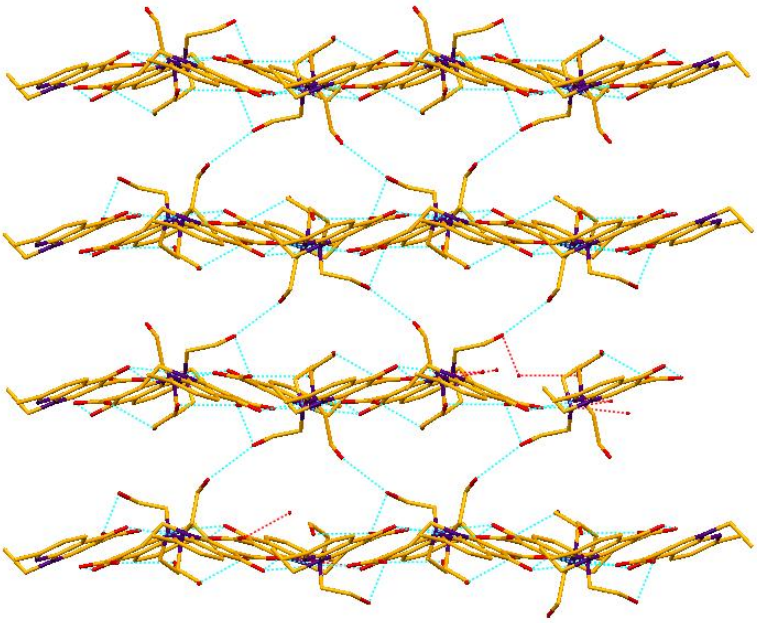

Figure7. Packing of **1**-DIETHAN: the structure is characterized by parallel planes held together by hydrogen bonds between diethanolamine molecules

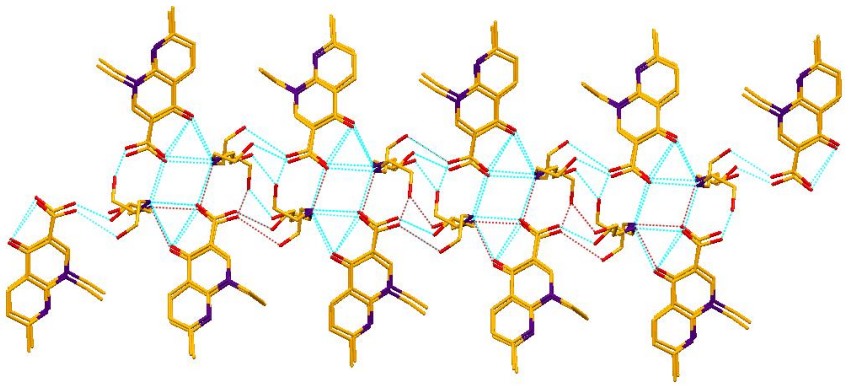

Figure8. Packing of **1**-DIETHAN: each plane are characterized by two chains of 1 and DIETAN alternatively held together through hydrogen bonds

The correspondence of the structure determinate by SC-XRD and that of bulk material, was checked by comparing the calculated pattern with the experimental one (Figure 9).

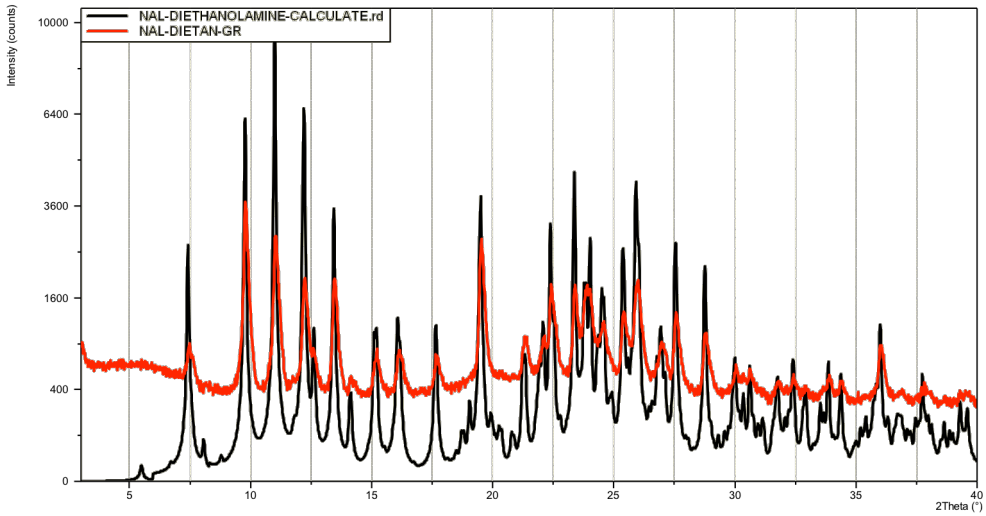

Figure9. Comparison between XRPD patterns of **1** DIETHAN calculated (black line) and measured (red line)

The SC-XRD analysis of 1-PYR evidences the presence of two molecules of **1**, two molecules of pyrrolidine and four molecules of water in the P-1 unit cell. As evidenced in the packing – Figure 10 - the structure is characterized by parallel planes held together by hydrogen bonds between chains and water molecules. Each plane is characterized by two chains of **1** and PYR alternatively held together through hydrogen bonds (Figure 11).

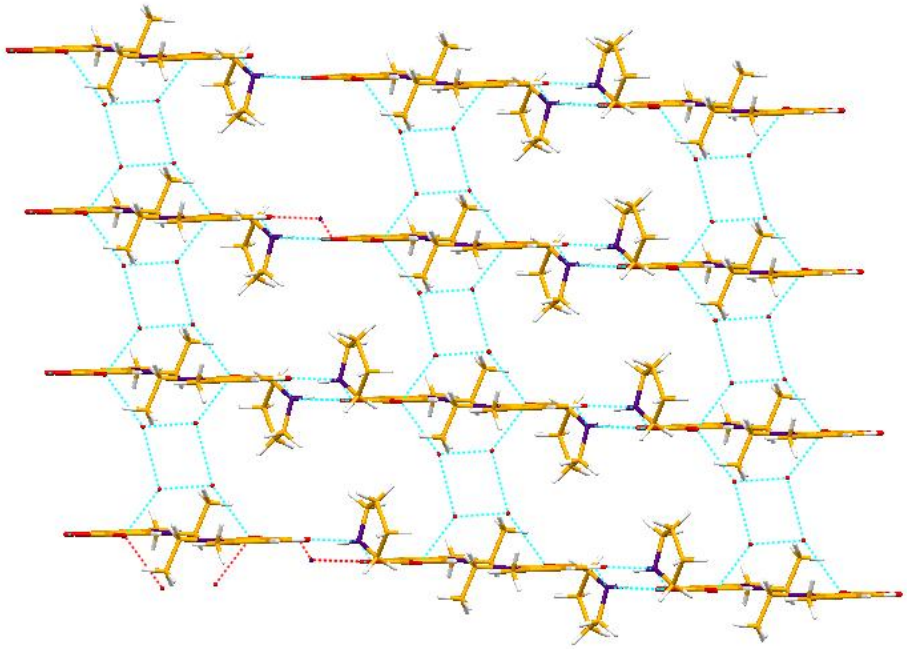

Figure10. Packing of **1**-PYR: the structure is characterized by parallel planes held together by hydrogen bonds between chains and water malecules.

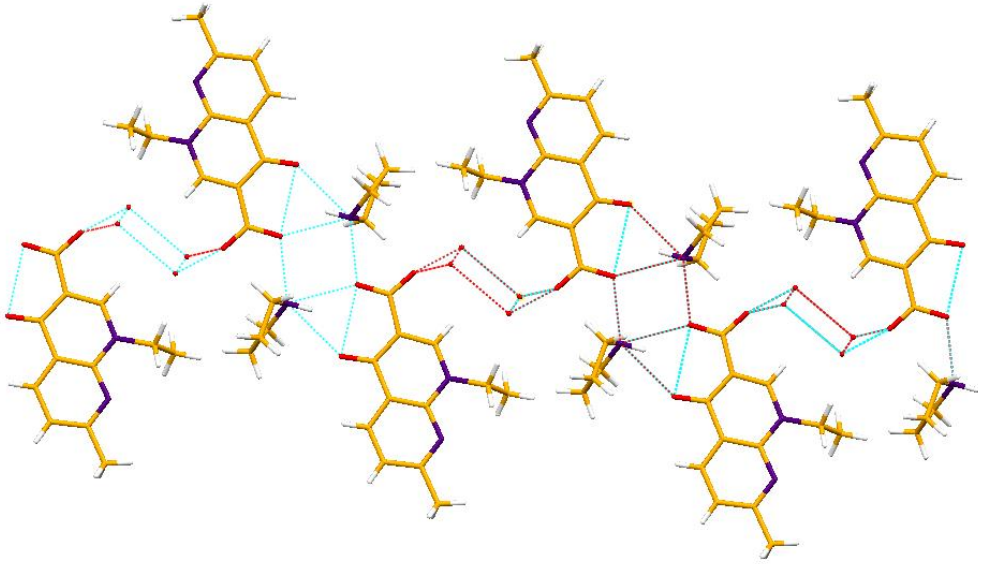

Figure11. Packing of **1**-PYR: each plane are characterized by two chains of **1** and PYR alternatively held together through hydrogen bonds.

The correspondence of the structure determinate by SC-XRD and that of bulk material, was checked by comparing the calculated pattern with the experimental one (Figure 12).

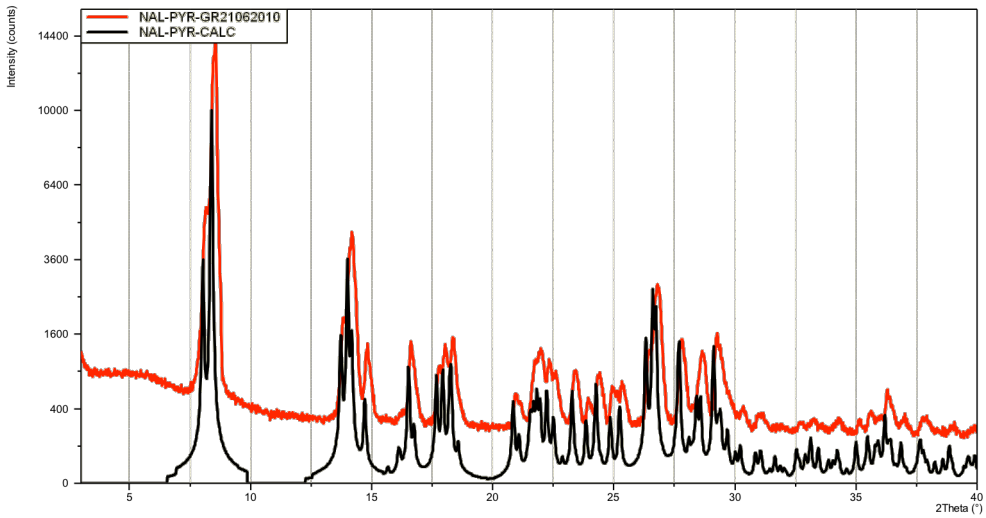

Figure12. Comparison between XRPD patterns of **1** PYR calculated (black line) and measured (red line)

The salt/co-crystal of **1** with pyrrolidine was also analyzed by DSC, TGA, EGA, FT-IR, SS NMR and VT-XRPD.

DSC profile – Figure 13 – evidences three endothermic events before of melt at 228.4°C. The first two peaks are associated in TGA – Figure 14 – with a loss of pyrrolidine and water as showed by EGA analysis (figure 15a, 15b, 15c, 15d).

The third peak is associated to a solid – solid transition of **1** that melts at 228.4°C (melting point of **1** Form I).

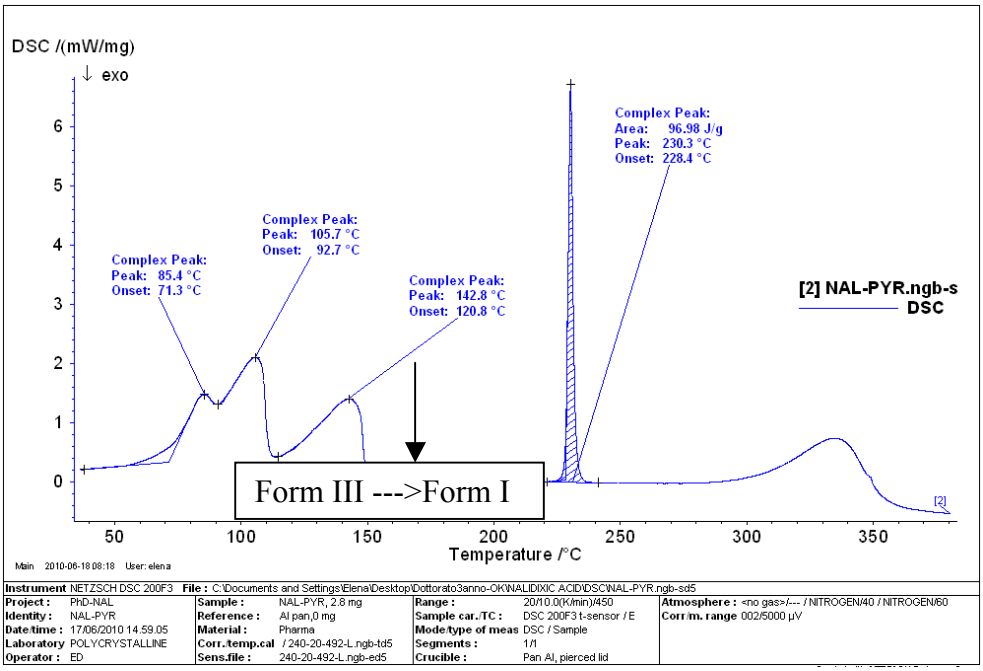

Figure 13. DSC profile of **1**-PYR.

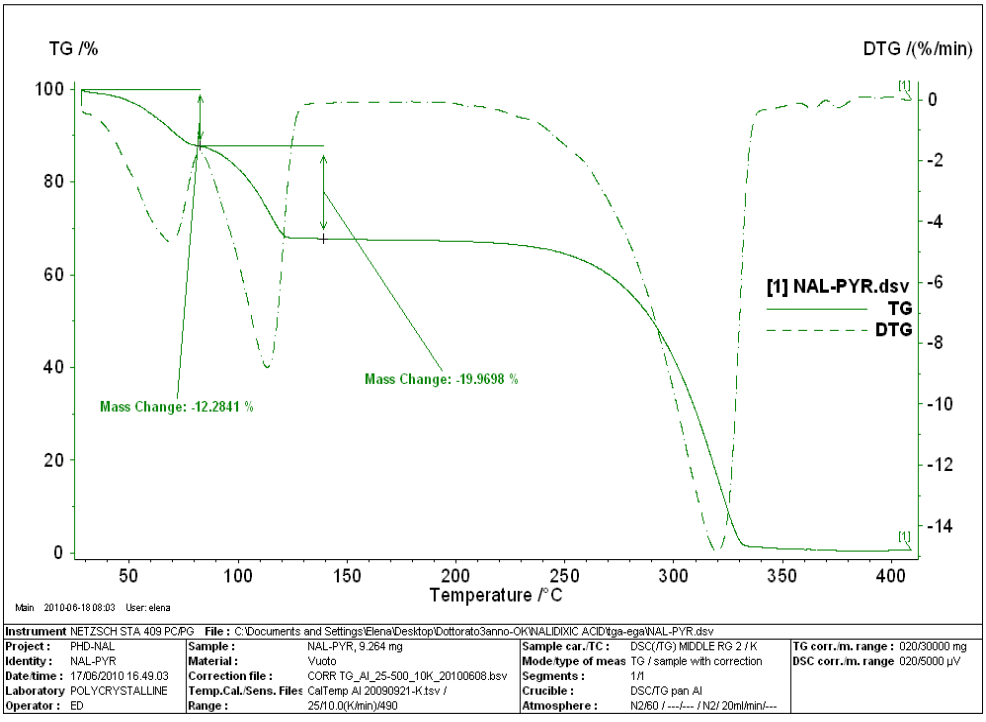

Figure 14. TGA profile of **1**-PYR

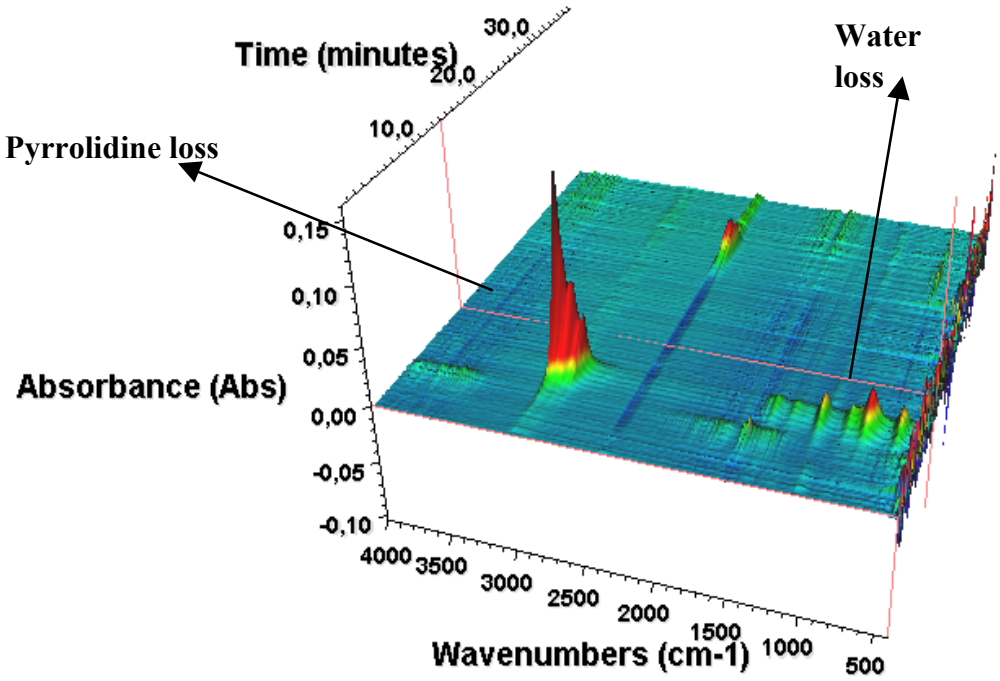

Figure 15a. 3D-EGA profile of **1**-PYR

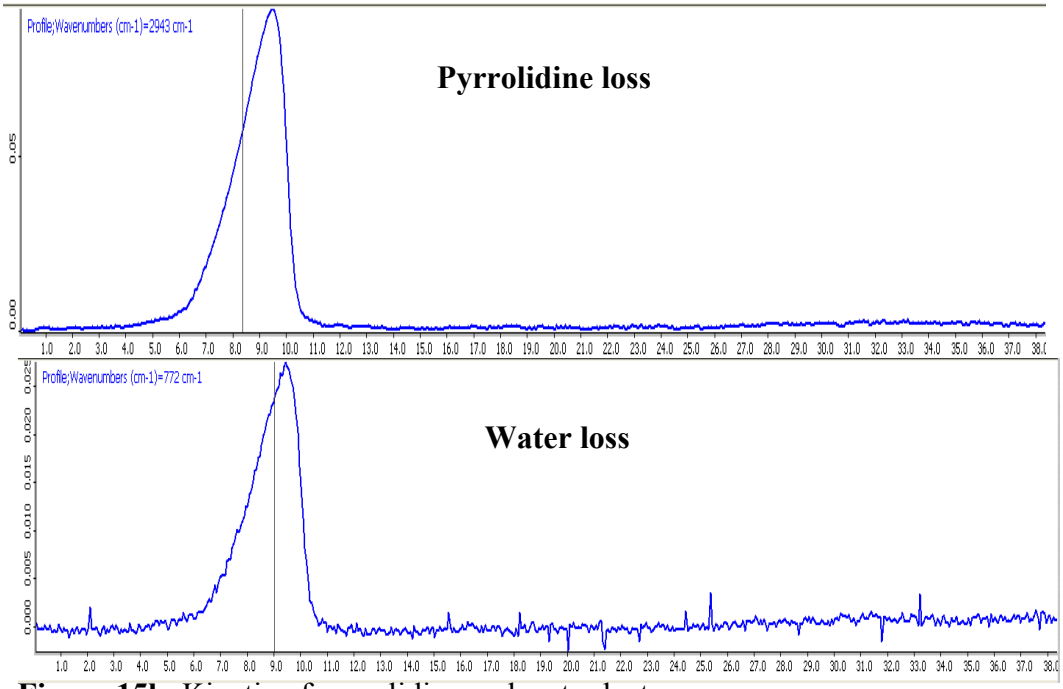

Figure 15b. Kinetic of pyrrolidine and water lost.

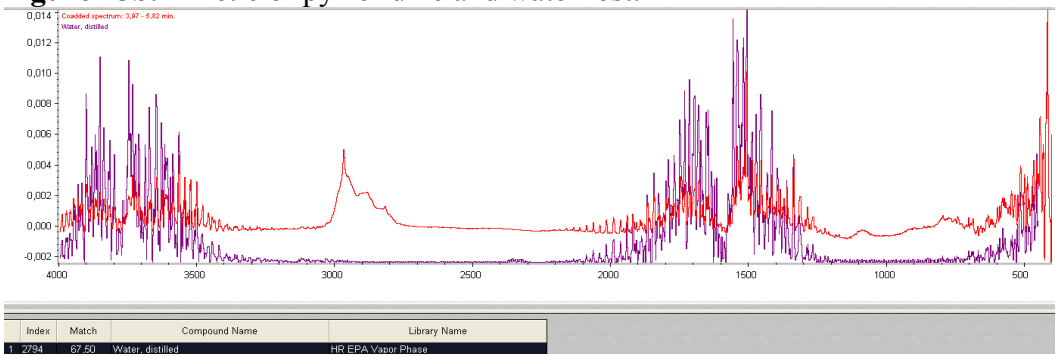

Figure 15c. Comparison between FT-IR spectrum obtained coadded region between 3 and 6 minutes and spectrum of water in data base: match 67.5%

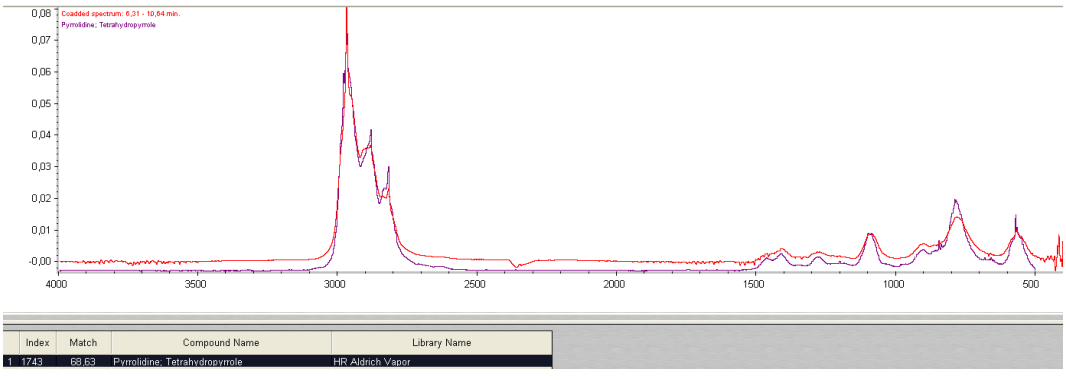

Figure 15d. Comparison between FT-IR spectrum obtained coadded region between 6 and 10 minutes and spectrum of pyrrolidine in data base: match 68.3%

1-PYR was characterized by VT – XRPD. The sample was heated until melt at approx. 230°C and analyzed at different temperature summarized in the Table 1.

FILE NAME	TEMPERATURE	RESULT
1-PYR_30.0°C	30°C	CO-CRYSTAL
1-PYR_50.0°C	50°C	CO-CRYSTAL
1-PYR_76.6°C	76.6°C	MIX 1
1-PYR_85.5°C	85.5°C	MIX 1
1-PYR_93.0°C	93°C	MIX 1
1-PYR_105.7°C	105.7°C	MIX2
1-PYR_119.8°C	119.8°C	MIX2
1-PYR_143.1°C	143.1°C	MIX2
1-PYR_200°C	200°C	1 FORM I
1-PYR_228°C	228°C	AMORPHOUS+PEAK
1-PYR_250°C	250°C	AMORPHOUS

Table 1. VT-XRPD steps of 1-PYR analysis.

The sample shows the same pattern of the co-crystal until 50°C (Figure 16).

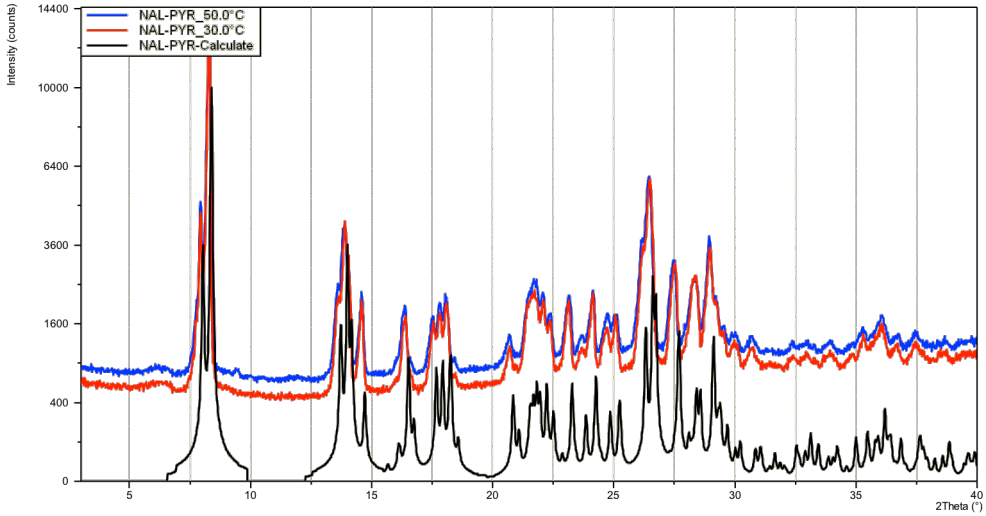

Figure 16. Comparison between XRPD patterns of **1**-PYR calculate (black line), sample analyzed at 30°C and at 50°C.

After 50°C the XRPD pattern begins to change: (Figure 17) the DSC at these temperatures evidences a double peak that in TGA-EGA corresponded to water and pyrrolidine losses in two steps. This pattern was also recorded analyzing a sample obtained by heating the salt/co-crystal to 85°C and also to 105°C in DSC with a heating rate of 10°C\min.

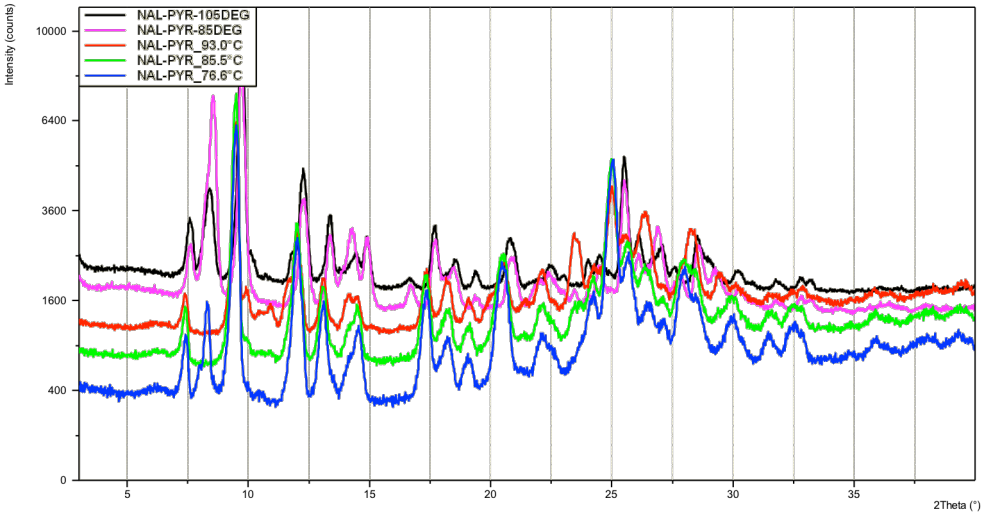

Figure 17. Comparison between XRPD patterns of **1**-PYR sample analyzed at 76.6°C, 85.5°C, 93°C and sample heated to 85°C and 105°C by DSC.

After 100°C the diffraction pattern recorded is the same of **1** Form III. This pattern was also recorded analyzing a sample obtained by heating the sample to 120°C with a heating rate of 10°C\min (Figure 18) and left the sample at 120°C for 5 min to obtain the complete conversion of the co-crystal into **1** Form III (Figure 19).

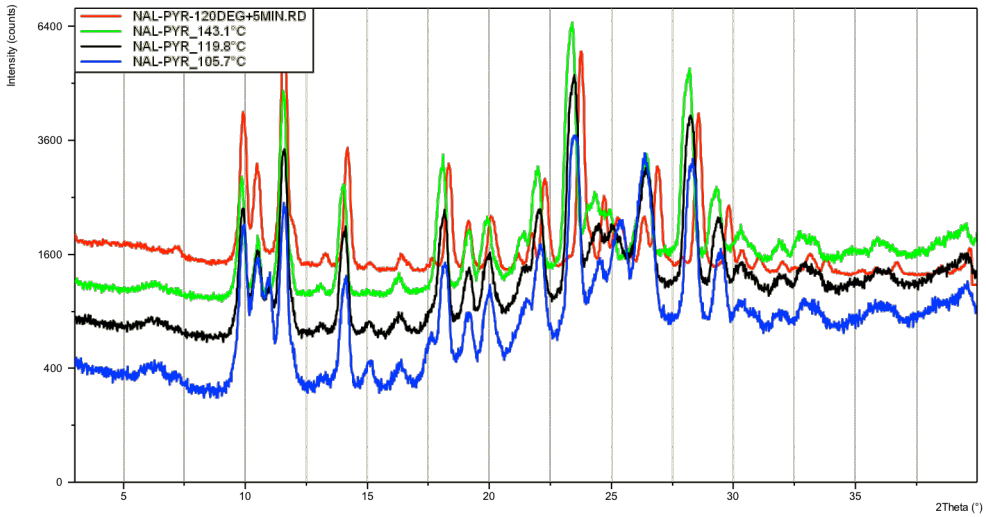

Figure 18. Comparison between XRPD patterns of **1**-PYR sample analyzed at 105.7°C, 119.8°C, 143.1°C and sample heated to 120°C for 5 minutes.

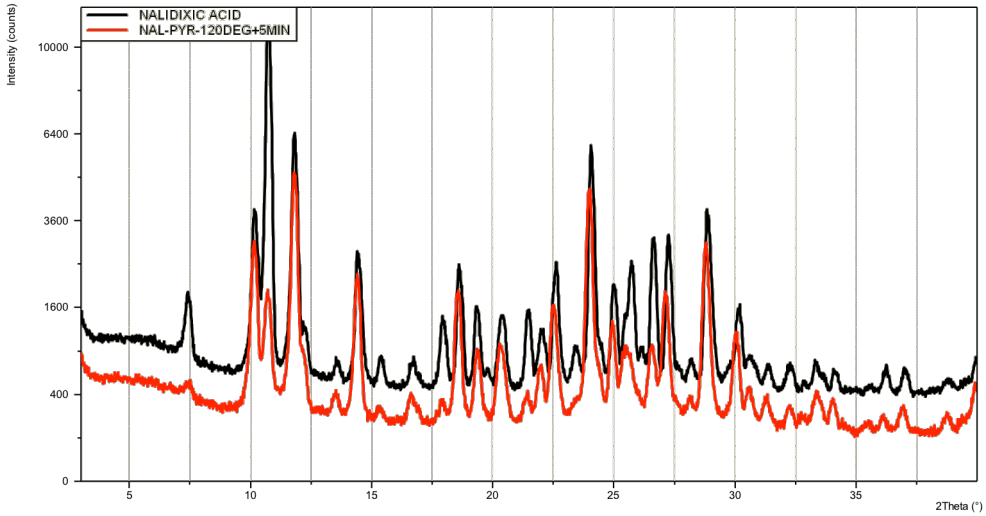

Figure 19. Comparison between XRPD patterns of **1**-PYR heated to 120°C for 5 minutes and **1** as delivered by Sigma Aldrich (Form III)

After 120°C a solid - solid transition, associated in DSC with an endothermic peak, is observed: **1** Form III converts into 1 Form I. This pattern is also recorded analyzing a sample obtained by heating the salt/co-crystal to 170°C and 200°C with a heating rate of 10°C\min (Figure 20).

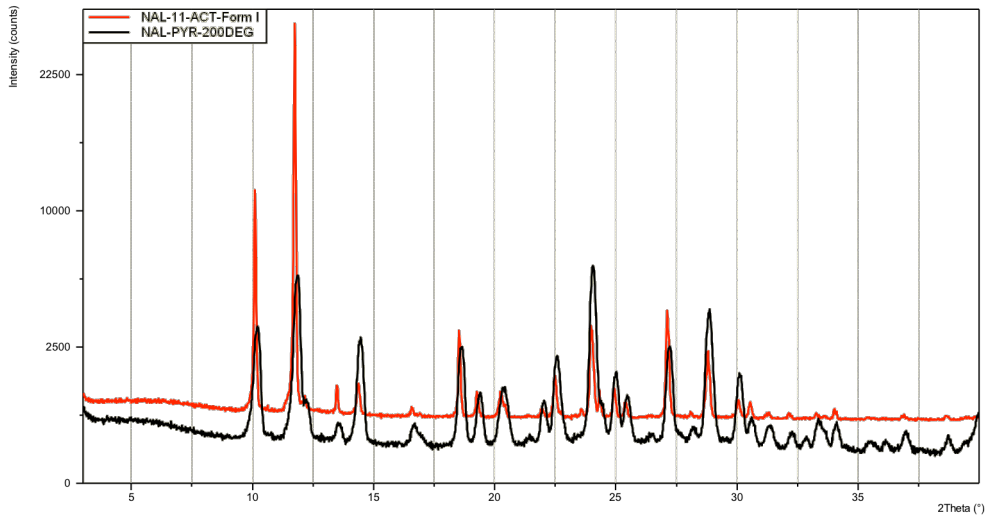

Figure 20. Comparison between XRPD patterns of Form I (red line) and **1**-PYR heated to 200°C.

1 Form III, obtained by VT-XRPD, shows the same XRPD pattern of **1** as delivered by Sigma Aldrich. The sample was also characterized by TGA, DSC, FT-IR and SS NMR. The DSC and SS NMR analyses led to the same results obtained for the Form I: the two crystal forms show the same SS NMR spectrum – Figure 21 - and the same DSC profile – Figure 22 - with melting point at approx. 228.5°C. In the NMR spectrum of **1** Form III there are some peaks, probably of form III, that are too intense to be assigned.

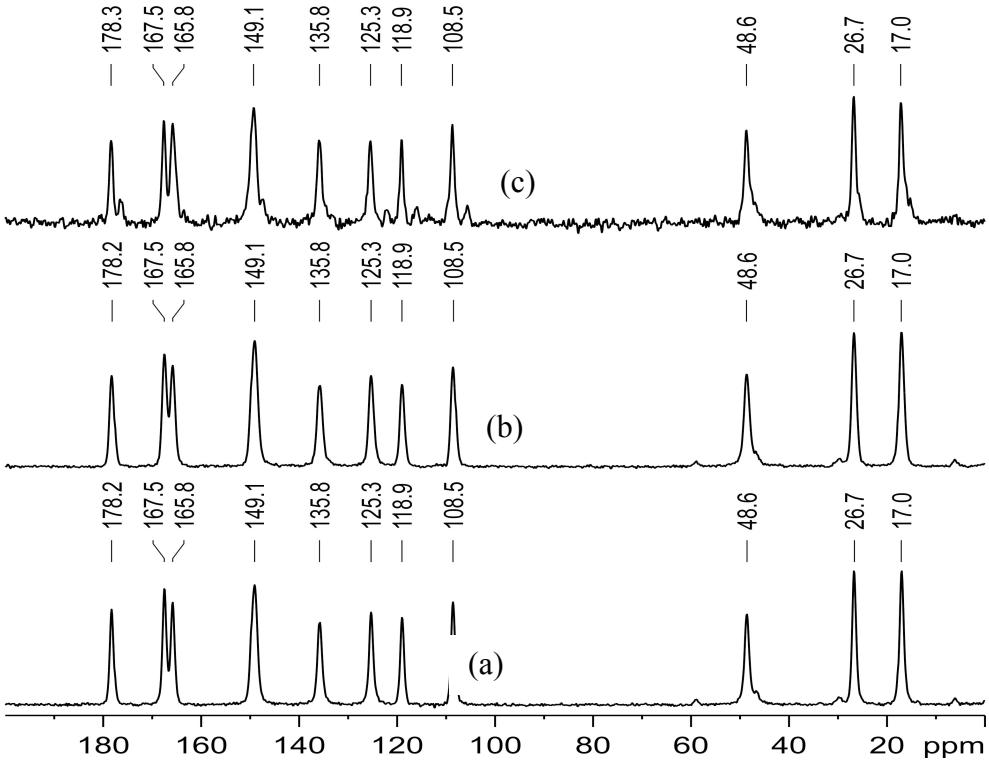

Figure21. Comparison between SS NMR spectra ^{13}C of **1** Form I (a), Form II (b) that during the analysis converts into Form I and **1** Form III (c).

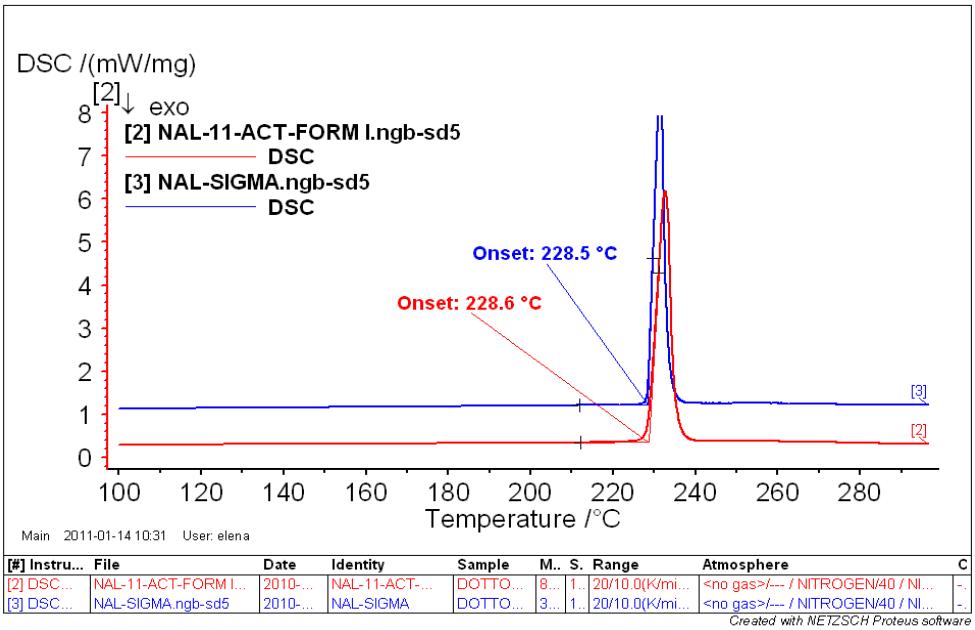

Figure22. Comparison between DSC profiles of **1** Form I and **1** Form III.

Form III is an unstable crystalline form, which converts into Form I upon heating or grinding.

In fact, Form III, heated to 200°C and then measured by XRPD, shows the XRPD pattern of Form I – Figure 23 - that at high temperature melts; this conversion was observed also by a grinding experiment.

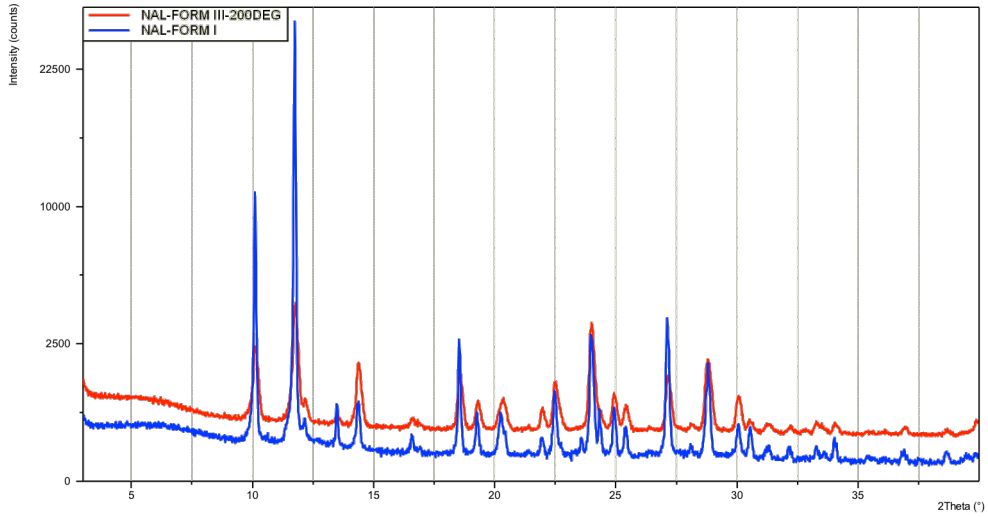

Figure23. Comparison between XRPD patterns of **1** Form I(blue line) and **1** Form III heated at 200°C (red line).

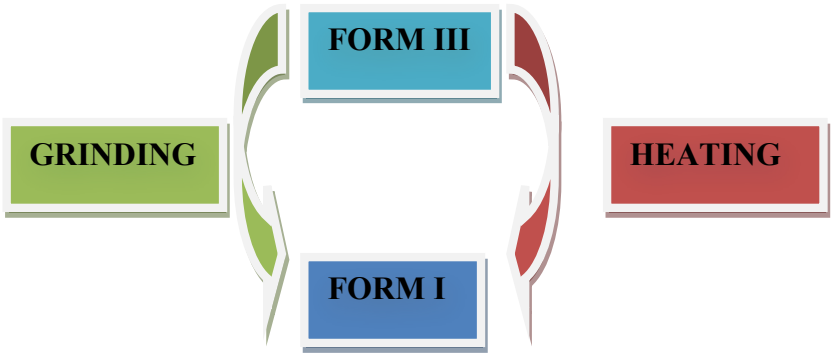

Scheme 3.

4.4. Conclusion

In conclusion in this work we have subjected nalidixic acid to experiments of evaporation and slurry at room temperature and to salt/co-crystal screening using as coformer the bases listed in the table 2 in *Preface*.

A new crystal form, named Form II, was obtained by evaporation at room temperature from dichloromethane.

Salt/co-crystal screening led to the discovery of two new salts-co-crystals of **1** with diethanolamine and pyrrolidine.

The new form obtained were characterized by XRPD, DSC, TGA, FT-IR, SS NMR and SC-XRD. The salt/co-crystal of **1** with pyrrolidine was also analyzed by EGA and VT-XRPD, this last techinique allows us to identify a new crystal form of **1** named Form III. This new form shows the same XRPD pattern of the sample as delivered by Sigma Aldrich. The three crystal forms of **1** were also studied by interconversion experiments that led to identify the stable crystal form of **1**: **1** Form I. In fact Form II and Form III convert into Form I through grinding and heating experiments.(Sheme 4)

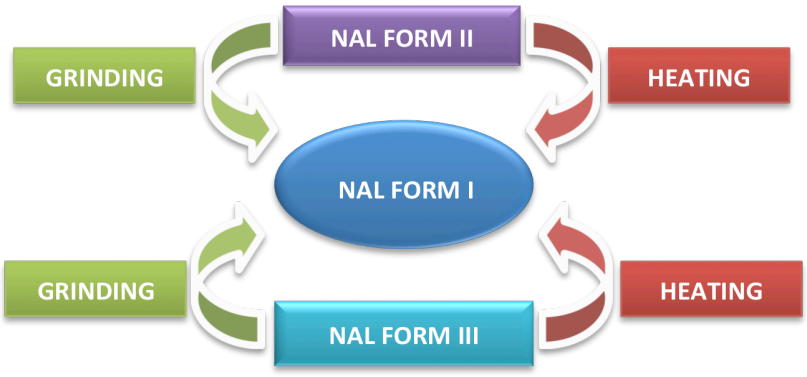

Scheme 4

4.5. Supplementary Material

Legenda

1 = Nalidixic Acid

1 - PYR = Nalidixic Acid – Pyrrolidine Salt/Co-crystal

1 - DIETHAN = Nalidixic Acid – Diethanolamine Salt/Co-crystal

---

4.5.1. **Crystal structure determination**

Crystal data and details of measurements are summarized in Table 1.

Table 1. Crystal Data and Details of Measurements for compounds **1** Form II, **1**-PYR, **1**-DIETHAN.

Compound	1 Form II	1-PYR	1-DIETHAN
Formula	C13 H17 N2 O2	C16 H21 N3 O3	C16 H21 N3 O5
M_r	232.23	303.36	335.36
system	Monoclinic	Triclinic	Triclinic
space group	$P2_1/n$	P-1	P-1
a [Å]	10.072	7(6)	14.184
b [Å]	7.041	12(14)	15.214
c [Å]	15.229	13(15)	17.130
α [°]	90	116(12)	77.34
β [°]	96.30	98(8)	71.63
γ [°]	90	102(9)	74.81
V [Å^3]	1073.5	903(1680)	3347.7
Z	4	2	4
d_{calc} [Mg mm^{-3}]	1.443	0.665	1.116
F(000)	500	712	324
$\mu(Mo_{K\alpha})$ [mm^{-1}]	0.098	0.050	0.078
θ_{max} [°]	25	25	28.98
measured reflns	4638	30.776	7374
unique reflns	2435	15197	4103
refined parameters	69	901	221
GOF on F^2	0.923	0.688	0.832
*R*1 [on *F*, $I > 2\sigma(I)$]	0.0757	0.0589	0.0734
*wR*2(onF^2,all data)	0.2473	0.1575	0.1968

4.5.2. **Thermal measuraments**

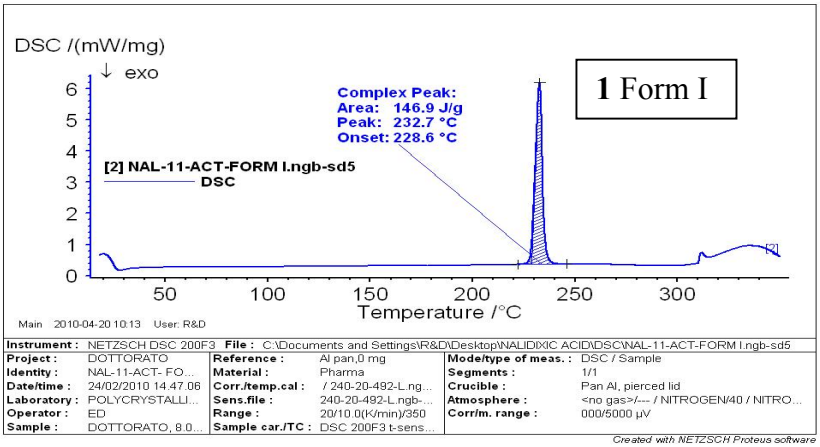

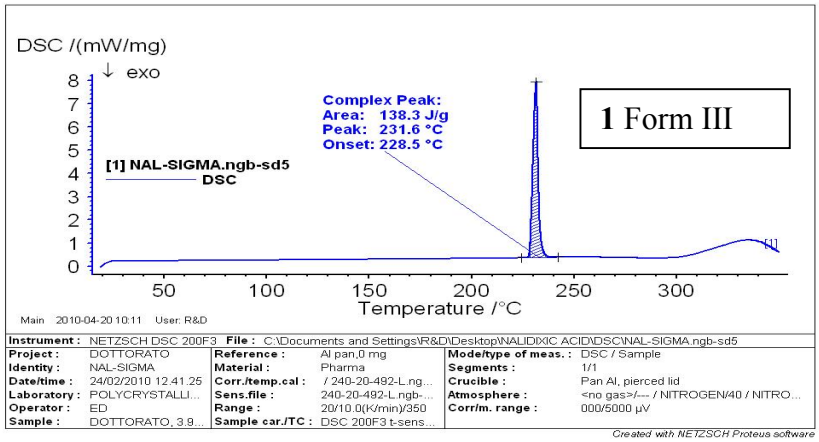

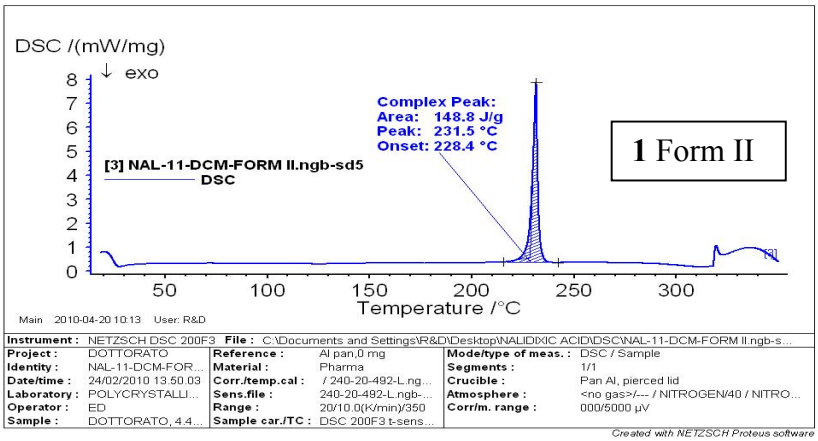

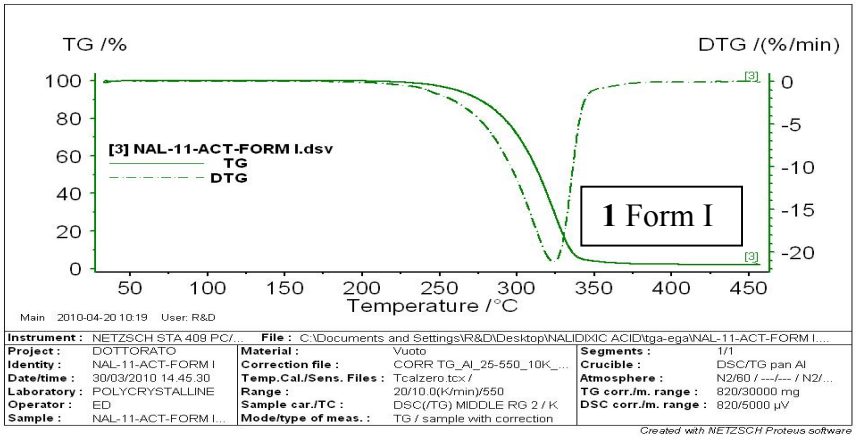

Instrument :	NETZSCH STA 409 PC/...	**File :**	C:\Documents and Settings\R&D\Desktop\NALIDIXIC ACID\tga-ega\NAL-11-ACT-FORM I....		
Project :	DOTTORATO	**Material :**	Vuoto	**Segments :**	1/1
Identity :	NAL-11-ACT-FORM I	**Correction file :**	CORR TG_AI_25-550_10K_...	**Crucible :**	DSC/TG pan Al
Date/time :	30/03/2010 14:45:30	**Temp.Cal./Sens. Files :**	Tcalzero.tcx /	**Atmosphere :**	N2/60 / ---/--- / N2/...
Laboratory :	POLYCRYSTALLINE	**Range :**	20/10.0(K/min)/550	**TG corr./m. range :**	820/30000 mg
Operator :	ED	**Sample car./TC :**	DSC(/TG) MIDDLE RG 2 / K	**DSC corr./m. range :**	820/5000 µV
Sample :	NAL-11-ACT-FORM I...	**Mode/type of meas. :**	TG / sample with correction		

Created with NETZSCH Proteus software

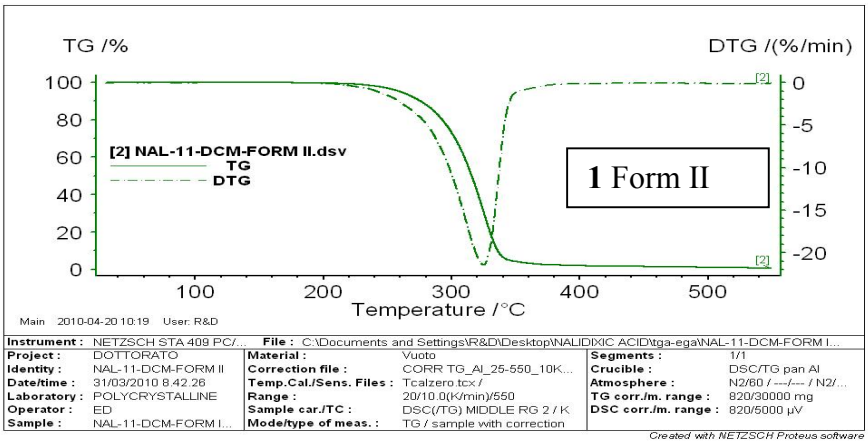

Instrument :	NETZSCH STA 409 PC/...	**File :**	C:\Documents and Settings\R&D\Desktop\NALIDIXIC ACID\tga-ega\NAL-11-DCM-FORM I...		
Project :	DOTTORATO	**Material :**	Vuoto	**Segments :**	1/1
Identity :	NAL-11-DCM-FORM II	**Correction file :**	CORR TG_AI_25-550_10K...	**Crucible :**	DSC/TG pan Al
Date/time :	31/03/2010 8:42:26	**Temp.Cal./Sens. Files :**	Tcalzero.tcx /	**Atmosphere :**	N2/60 / ---/--- / N2/...
Laboratory :	POLYCRYSTALLINE	**Range :**	20/10.0(K/min)/550	**TG corr./m. range :**	820/30000 mg
Operator :	ED	**Sample car./TC :**	DSC(/TG) MIDDLE RG 2 / K	**DSC corr./m. range :**	820/5000 µV
Sample :	NAL-11-DCM-FORM I...	**Mode/type of meas. :**	TG / sample with correction		

Created with NETZSCH Proteus software

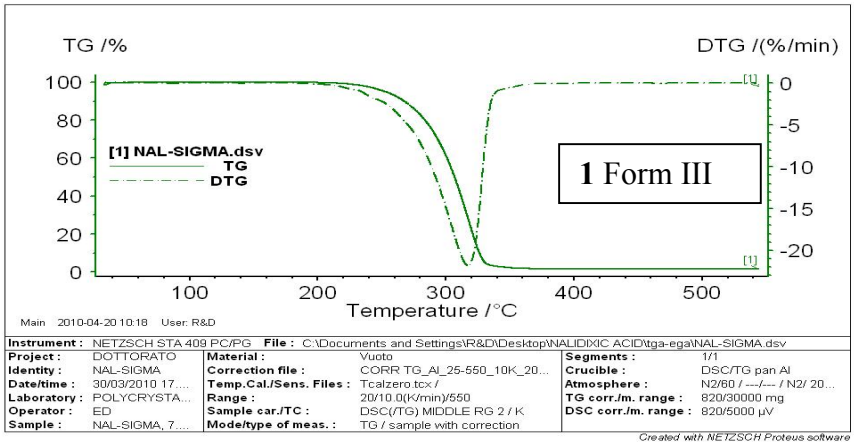

Instrument :	NETZSCH STA 409 PC/PG	**File :**	C:\Documents and Settings\R&D\Desktop\NALIDIXIC ACID\tga-ega\NAL-SIGMA.dsv		
Project :	DOTTORATO	**Material :**	Vuoto	**Segments :**	1/1
Identity :	NAL-SIGMA	**Correction file :**	CORR TG_AI_25-550_10K_20...	**Crucible :**	DSC/TG pan Al
Date/time :	30/03/2010 17:...	**Temp.Cal./Sens. Files :**	Tcalzero.tcx /	**Atmosphere :**	N2/60 / ---/--- / N2/ 20...
Laboratory :	POLYCRYSTA...	**Range :**	20/10.0(K/min)/550	**TG corr./m. range :**	820/30000 mg
Operator :	ED	**Sample car./TC :**	DSC(/TG) MIDDLE RG 2 / K	**DSC corr./m. range :**	820/5000 µV
Sample :	NAL-SIGMA, 7....	**Mode/type of meas. :**	TG / sample with correction		

Created with NETZSCH Proteus software

4.5.3. **FT-IR**

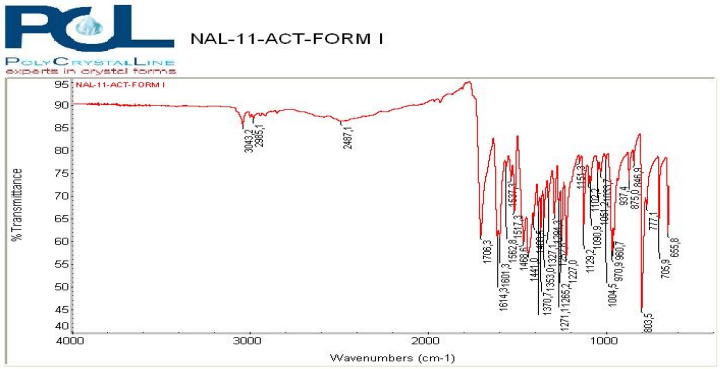

Detector: DTGS KBr
Beamsplitter: KBr
Source: IR

Number of sample scans: 32
Number of background scans: 32
Resolution: 4,000
Sample gain: 4,0
Optical velocity: 0,6329
Aperture: 100,00

1 Form I

Tue Apr 20 09:54:05 2010 (GMT+02:00)
FIND PEAKS:
Spectrum: NAL-11-ACT-FORM I
Region: 4000,0 400,0
Absolute threshold: 87,179
Sensitivity: 80
Peak list:

Position:	655,8	Intensity:	61,565
Position:	705,9	Intensity:	64,834
Position:	777,1	Intensity:	67,687
Position:	803,5	Intensity:	44,610
Position:	846,9	Intensity:	77,056
Position:	875,0	Intensity:	73,295
Position:	937,4	Intensity:	73,164
Position:	960,7	Intensity:	61,072
Position:	970,9	Intensity:	57,617
Position:	1004,5	Intensity:	77,858
Position:	1033,7	Intensity:	74,871
Position:	1051,2	Intensity:	75,078
Position:	1090,9	Intensity:	73,147
Position:	1102,2	Intensity:	72,395
Position:	1129,2	Intensity:	63,151
Position:	1151,3	Intensity:	77,600
Position:	1227,0	Intensity:	56,621
Position:	1252,8	Intensity:	60,313
Position:	1265,2	Intensity:	68,806
Position:	1271,1	Intensity:	68,643
Position:	1294,3	Intensity:	65,575
Position:	1327,1	Intensity:	69,236
Position:	1353,0	Intensity:	64,623
Position:	1370,7	Intensity:	62,142
Position:	1384,5	Intensity:	66,377
Position:	1409,5	Intensity:	65,278
Position:	1441,0	Intensity:	57,210
Position:	1468,6	Intensity:	59,565
Position:	1517,3	Intensity:	66,512
Position:	1537,3	Intensity:	73,721
Position:	1562,8	Intensity:	76,279
Position:	1601,3	Intensity:	60,639
Position:	1614,3	Intensity:	60,803
Position:	1706,3	Intensity:	61,126
Position:	2487,1	Intensity:	86,355
Position:	2985,1	Intensity:	86,941
Position:	3043,2	Intensity:	85,669

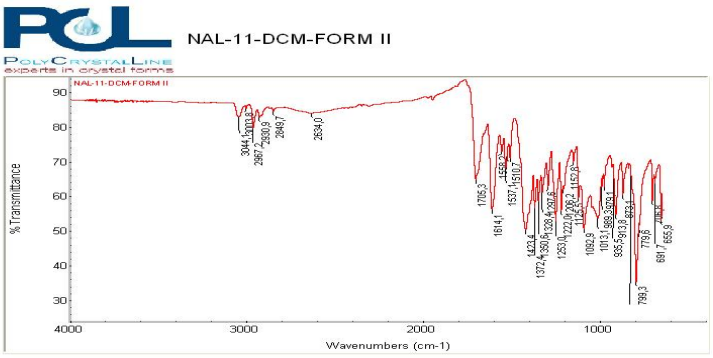

Detector: DTGS KBr
Beamsplitter: KBr
Source: IR

Number of sample scans: 32
Number of background scans: 32
Resolution: 4,000
Sample gain: 4,0
Optical velocity: 0,6329
Aperture: 100,00

1 Form II

Tue Apr 20 09:57:08 2010 (GMT+02:00)
FIND PEAKS:
Spectrum: NAL-11-DCM-FORM II
Region: 4000,0 400,0
Absolute threshold: 85,610
Sensitivity: 80
Peak list:

Position:	655,9	Intensity:	52,833
Position:	691,7	Intensity:	63,487
Position:	706,8	Intensity:	57,912
Position:	779,6	Intensity:	51,511
Position:	799,3	Intensity:	34,860
Position:	839,6	Intensity:	67,789
Position:	873,1	Intensity:	59,993
Position:	913,8	Intensity:	54,373
Position:	935,5	Intensity:	68,330
Position:	979,1	Intensity:	62,535
Position:	989,3	Intensity:	62,841
Position:	1013,1	Intensity:	53,411
Position:	1092,9	Intensity:	50,370
Position:	1125,5	Intensity:	58,949
Position:	1152,8	Intensity:	69,537
Position:	1206,2	Intensity:	61,841
Position:	1222,0	Intensity:	55,428
Position:	1253,0	Intensity:	52,678
Position:	1297,6	Intensity:	62,481
Position:	1328,4	Intensity:	60,935
Position:	1350,6	Intensity:	58,370
Position:	1372,4	Intensity:	56,372
Position:	1423,4	Intensity:	50,189
Position:	1510,7	Intensity:	70,846
Position:	1537,1	Intensity:	67,818
Position:	1558,2	Intensity:	72,822
Position:	1614,1	Intensity:	55,950
Position:	1705,3	Intensity:	64,682
Position:	2634,0	Intensity:	83,828
Position:	2849,7	Intensity:	84,457
Position:	2930,9	Intensity:	82,618
Position:	2967,2	Intensity:	79,488
Position:	3003,8	Intensity:	85,296
Position:	3044,1	Intensity:	82,787

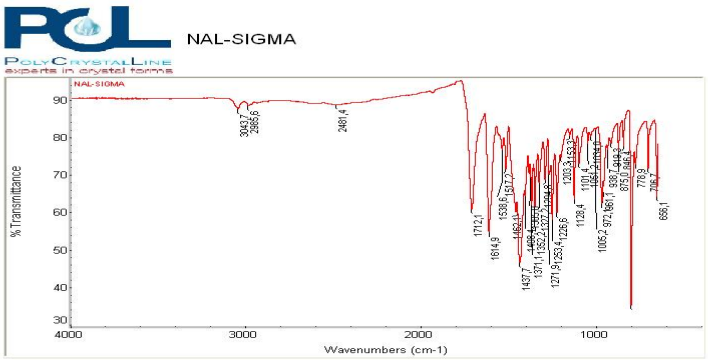

Detector: DTGS KBr
Beamsplitter: KBr
Source: IR

Number of sample scans: 32
Number of background scans: 32
Resolution: 4,000
Sample gain: 4,0
Optical velocity: 0,6329
Aperture: 100,00

1 Form III

Tue Apr 20 09:51:53 2010 (GMT+02:00)
FIND PEAKS:
Spectrum: NAL-SIGMA
Region: 4000,0 400,0
Absolute threshold: 89,306
Sensitivity: 80
Peak list:

Position:	656,1	Intensity:	63,931
Position:	706,7	Intensity:	71,138
Position:	778,9	Intensity:	72,664
Position:	803,8	Intensity:	34,809
Position:	846,4	Intensity:	77,576
Position:	875,0	Intensity:	76,279
Position:	919,3	Intensity:	78,270
Position:	938,7	Intensity:	76,628
Position:	961,1	Intensity:	66,624
Position:	972,1	Intensity:	62,196
Position:	1005,2	Intensity:	81,851
Position:	1034,0	Intensity:	80,179
Position:	1051,2	Intensity:	78,256
Position:	1101,4	Intensity:	72,896
Position:	1128,4	Intensity:	63,226
Position:	1153,3	Intensity:	80,293
Position:	1203,3	Intensity:	74,625
Position:	1226,6	Intensity:	59,712
Position:	1253,4	Intensity:	57,848
Position:	1271,9	Intensity:	69,637
Position:	1294,8	Intensity:	68,261
Position:	1327,2	Intensity:	67,584
Position:	1352,2	Intensity:	61,417
Position:	1371,1	Intensity:	61,807
Position:	1385,0	Intensity:	70,039
Position:	1408,4	Intensity:	64,178
Position:	1437,7	Intensity:	46,335
Position:	1462,1	Intensity:	59,938
Position:	1517,2	Intensity:	71,461
Position:	1538,6	Intensity:	76,620
Position:	1614,9	Intensity:	54,435
Position:	1712,1	Intensity:	60,727
Position:	2481,4	Intensity:	88,614
Position:	2985,6	Intensity:	88,381
Position:	3043,7	Intensity:	87,471

4.6. Refereces

1. Turk J Chem 30 (2006) , 193 202,us4207418,jp61243020,photochemistry and photobiology, 2006,82: 254-261
2. *(a)* G. M. Sheldrick, *SHELX97*, *Program for Crystal Structure Determination*; University of Göttingen: Göttingen, Germany, 1997; *(b)* E. Keller, SCHAKAL99, Graphical Representation of Molecular Models, University of Freiburg, Germany, 1999; *(c)* A. L. Speck, PLATON; *Acta Crystallogr*., *Sect*. *A*, 1990, 46, C34.
3. C. P. Huber, D.S.S. Gowda, K.R. Acharya, *Acta Cryst.,* **1980,** *B36,* 497-499.

5. CHARACTERIZATION OF NEW SALTS AND CO-CRYSTAL OF SULFADIAZINE

5.1. Introduction

The sulfadiazine is a sulfonamide antibiotic. The sulfonamides are a class of antibacterial drugs used in treatment of urinary tract infection: they eliminate bacteria that cause infections stopping the production of folic acid inside the bacterial cell.[1-4]

In this drug class the molecule contains multiple hydrogen bonds, donor and acceptor functions allowing the use of these molecules as co-crystallization partners with other drugs.[5-6]

Sulfadiazine (Scheme 1), as all sulfonamide drugs, contains two important functional groups: one acidic moiety (NH) and one basic moiety (NH_2). The amine nitrogen atom is able to gain a proton, while the amide nitrogen atom is able to release a proton under specific pH conditions.[7]

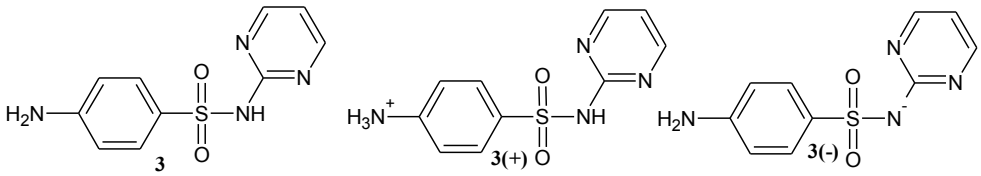

Scheme 1.

Sulfadiazine is labeled as **3** in the neutral form, **3(-)** in the anionic form and **3(+)** in the cationic form (Scheme 1).

Sulfadiazine, present in one crystal form (Form I) in the CSD[8], was studied by polymorph and salt/co-crystal screening to identify new crystal forms.

The salt/co-crystal screening was performed using as co-former the bases and acids listed in Table 2 in the *Preface*.

The API was made to react with a co-former (solid or liquid) through different methods: crystallization by solution, grinding, kneading and solid-gas reactions.[9]

The screening allowed the discovery of six new salts and one co-crystal characterized by X-ray powder diffraction (XRPD), differential scanning calorimetry (DSC), thermogravimetric analysis (TGA), evolved gas analysis (EGA), FT-IR. The salts of **3** with pyrrolidine (PYR) and methanesulfonic acid (MSA) were also characterized by single crystal X-ray diffraction (SC-XRD).

5.2. Experimental section

All reactants were purchased from Sigma Aldrich and used without further purification. Reagent grade solvents and doubly-distilled water were used.

5.2.1. **Solution synthesis**

All salts/co-crystals were crystallized by room temperature evaporation of a solution obtained dissolving a stoichiometric mixture (1-1) of **3** and acid or base in hot acetone.

5.2.2. **Mechanochemistry**

The salts of **3** with PYR, KOH and H_3PO_4 were quantitatively obtained as polycrystalline materials by grinding or kneading experiments (**3** and acid or base are in a 1:1 ratio). The experiments were performed with a Retsch MM 200 grinder for 15 minutes at frequency of 30Hz.

5.2.3. **Solid-gas reaction**

The salt/co-crystal of **3** with formic acid was also obtained after 3 days of exposure to the acid vapor.

5.2.4. **Thermal measurements**

Thermogravimetric analyses were performed using a simultaneus STA 409 PC Luxx® Netzsch equipped with a thermocouple for the direct measurament of DSC signal, and a thermobalance for the measurement of the TGA signal. The samples (5-15 mg) were placed in aluminium pierced pans, and the heating was carried out at 10°C min^{-1} in N_2 atmosphere (See supplementary material).

Calorimetric measurements were performed using a DSC 200 *F3 Maia*® differential scanning calorimeter equipped with an intra-cooler. The samples (2–4 mg) were placed in aluminium pierced pans, and the heating was carried out at 10°C min^{-1} in N_2 atmosphere. (See supplementary material).

5.2.5. **Single crystal X-Ray diffraction**

Single-crystal data were collected on an Oxford X'Calibur S CCD diffractometer equipped with a graphite monochromator (MoKα radiation, λ = 0.71073) and operated at room temperature. The structure was solved by direct methods and refined by full-matrix least-squares on F^2 with SHELX97[10a] program package.

A calculated XRPD pattern was generated for Cu radiation using Mercury v 1.4 and the atomic coordinates, space group, and unit cell parameters from the single crystal data.

MERCURY and SCHAKAL99[10b] were used for the graphical representation of the results and PLATON[10c] was used for hydrogen bonding analysis.

5.2.6. **Powder X-Ray diffraction**

Diffraction patterns from 3° to 40° in 2θ were collected on a PANalytical diffractometer with Bragg–Brentano geometry (Cu Kα radiation, detector: X'celerator, step size Δ2θ = 0.0167°, counting time per step = 20 s), using a glass sample holder**.** The tube voltage and amperage were set to 40 kV and 40 mA, respectively.

5.2.7. **FT-IR**

All FT-IR measurements were performed using Nicolet FT-IR 6700 Thermo Fischer equipped with ATR device. The analyses were performed on all samples and for each measurement 32 scans were recorded (See supplementary material).

5.3. Results and discussion

In this work **3** was studied by polymorph and salt/co-crystal screening to identify new crystal forms.

The screening allowed the discovery of six salts and one co-crystal (with formic acid) – Scheme 2, 3- characterized by X-ray powder diffraction (XRPD), differential scanning calorimetry (DSC), thermogravimetric analysis (TGA), evolved gas analysis (EGA), FT-IR (See supplementary material). The salts of **3** with PYR and MSA were also characterized by single crystal X-ray diffraction (SC-XRD).

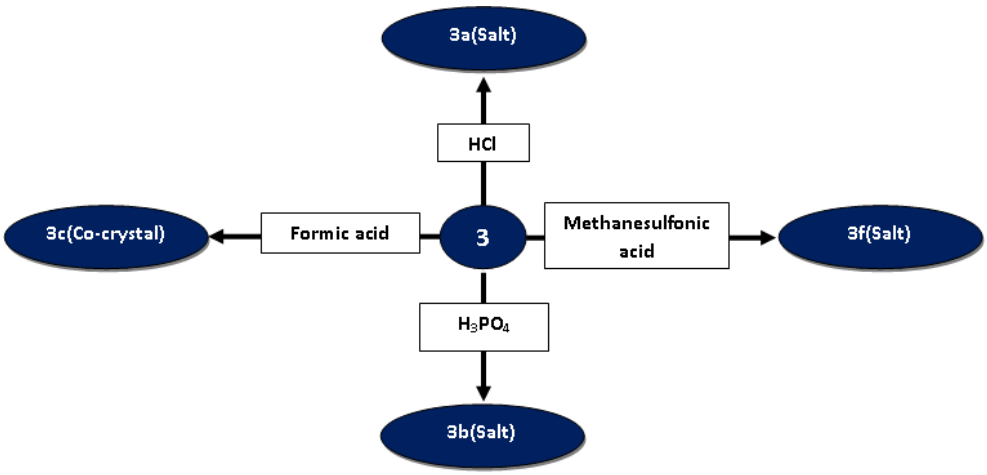

Scheme 2. Reaction of **3** with acids.

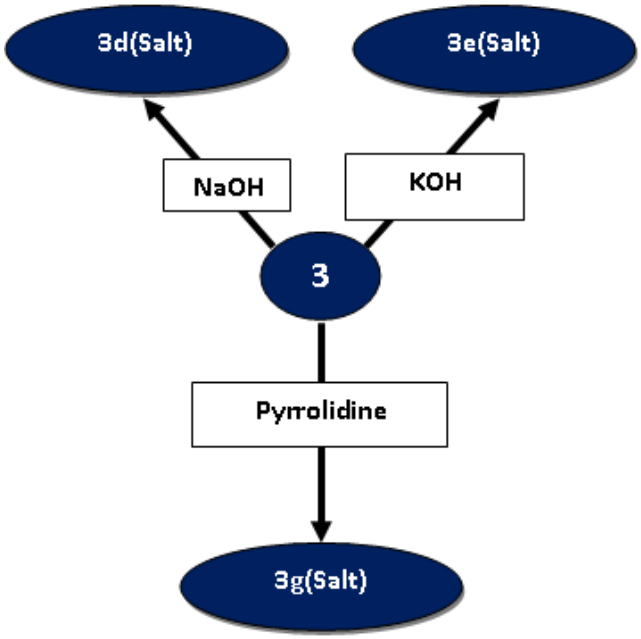

Scheme 3. Reaction of **3** with bases.

The API was made to react with a co-former (solid or liquid) through different methods: crystallization from solution, grinding, kneading and solid-gas reactions. The results obtained are summarized in Table 1.

Table 1. Methods used to obtained salts or co-crystals (the co-crystal 3c was also obtained by solid-gas reaction.

SAMPLE	SOLUTION SYNTHESIS	GRINDING-KNEADING
3a	SALT	-
3b	SALT	SALT
3c	COCRYSTAL	-
3d	SALT	-
3e	SALT	SALT
3f	SALT	-
3g	SALT	SALT

In the figure 1 is showed a comparison of diffraction patterns of salts and co-crystal obtained by screening and pattern of **3** for comparison.

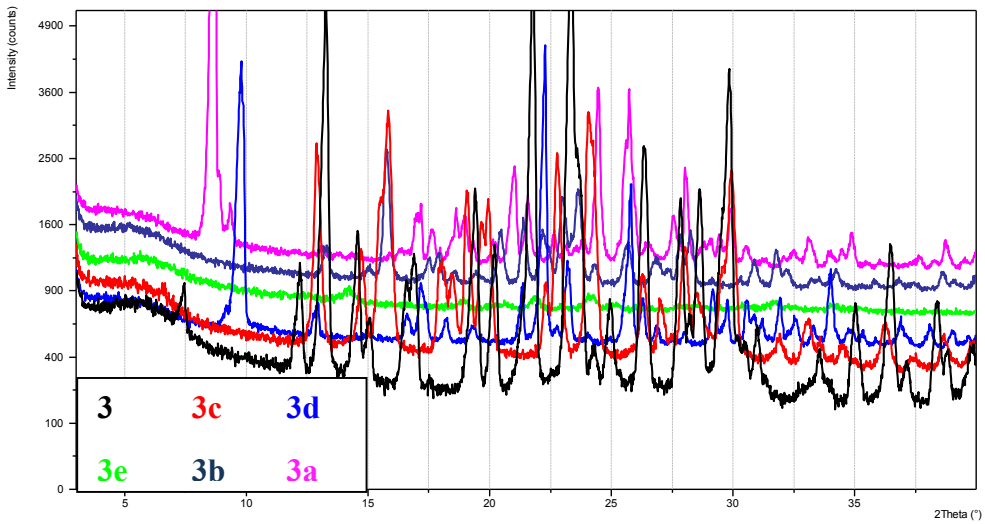

Figure 1 . Comparison between diffraction patterns of different salts and co-crystals obtained by screening.

Differential scanning calorimetry was used to measure the melting point of all compounds and to detect the presence of additional crystalline phases.

Thermogravimetric analysis (TGA) was used to measure possible solvent loss. This tecnique was associated with evolved gas analysis (EGA) that measured IR spectra and the kinetic profile of solvent loss during the TGA.
In Table 2 are summarized the onset and the solvent loss measured with EGA of **3** and of new compounds synthesized.

Table 2

Sample	Onset(°C)	Solvent Loss
3	261.8	-
3a	63.7 159.5	Water- HCl
3b	139.7	-
3c	263.2	Formic acid
3d	27.4 259.7	-
3e	52.3 93.2 166.9 260	Water
3g	200.7	Pyrrolidine

The SC-XRD analysis of **3g** evidences the presence of four ions of **3(-)** and four pyrrolidine cations in the $Pna2_1$ unit cell. As evidenced in the Figure 2 the compound obtained is a salt, in fact, PYR is in cationic form and the **3** is in anionic form **3**(-): there is the proton transfer from the amide (N1) group of **3** to N5 of PYR that forms an hydrogen bond with N1 of one molecule of **3(-)** and two hydrogen bonds with N4 and O2 of another molecule of **3(-)**. The amino group (N2) of **3(-)** forms a hydrogen bond with O1 of another molecule of **3(-)**.

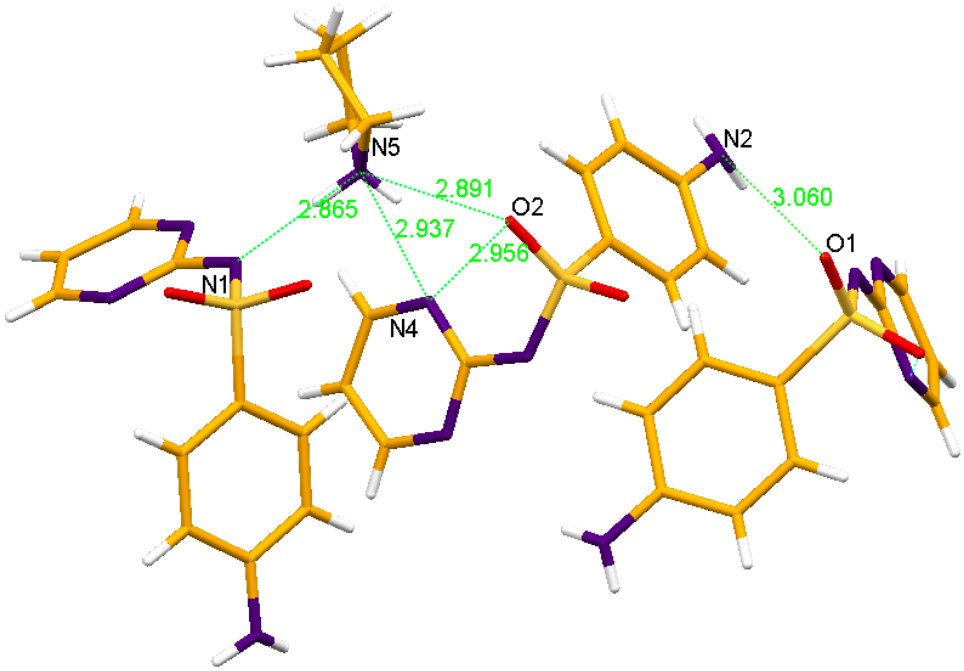

Figure 2. Hydrogen bonds in **3g** salt.

The correspondence, of the structure, determined by SC-XRD, and that of bulk material was checked by comparing the calculated pattern with the experimental one (Figure 3).

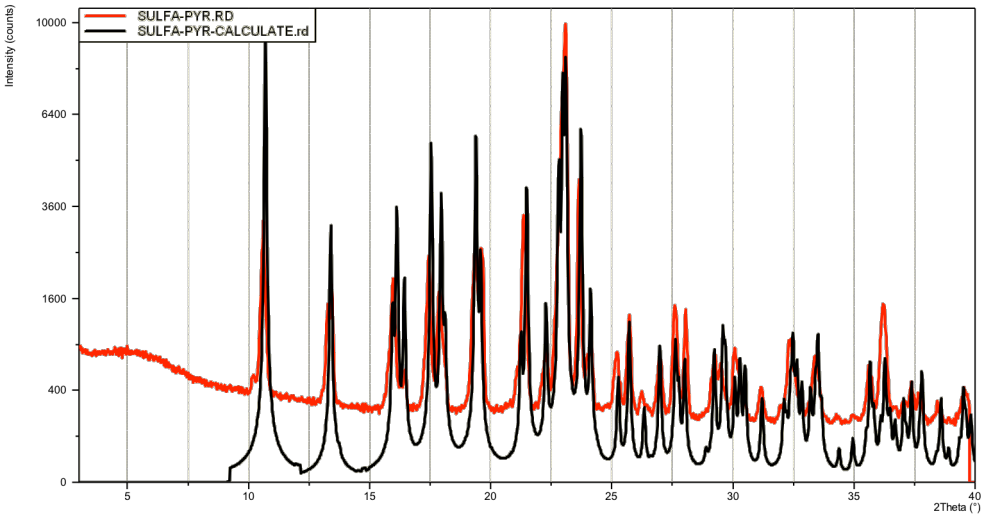

Figure 3. Comparison between XRD patterns of **3g** salt calculate (black line) and experimental (red line).

The SC-XRD analysis of **3f** evidences the presence of two ions **3(+)**, two methanesulfonate anions and two water molecules in P-1 unit cell. As evidenced in figure 4 the compound obtained is a salt, in fact, the MSA is in anionic form and the **3** is in cationic form **3(+)**: there is the proton transfer from the acid to the amino (N1) group of **3**. N1 amino group of **3(+)** form three hydrogen bond with O3, O4 and O5 of three molecules of acid and one hydrogen bond with a molecule of water that forms two hydrogen bonds with two molecules of acid. N2 and N4 groups of **3(+)** form two hydrogen bonds with another ions of 3**(+)**.

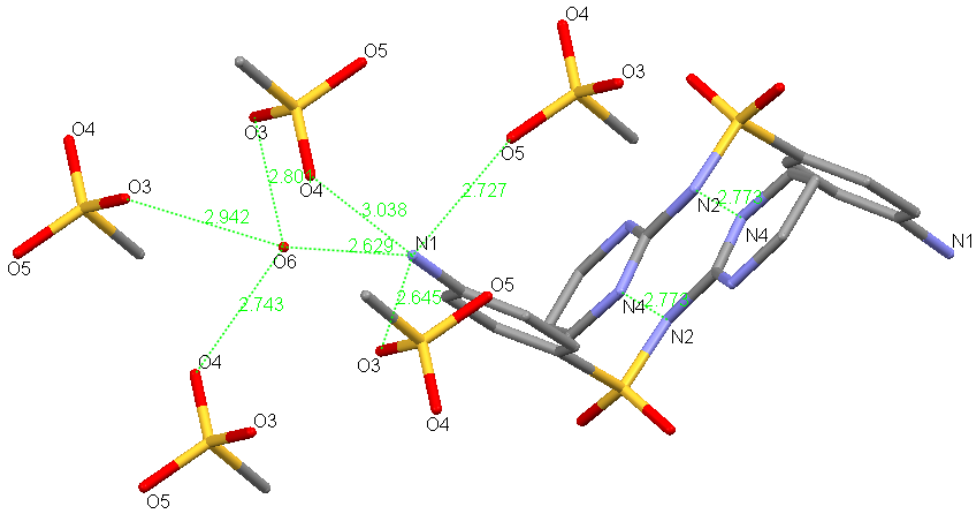

Figure 4. Hydrogen bonds in **3f** salt.

The correspondence, of the structure, determined by SC-XRD, and that of bulk material was checked by comparing the calculated pattern with the experimental one (Figure 5).

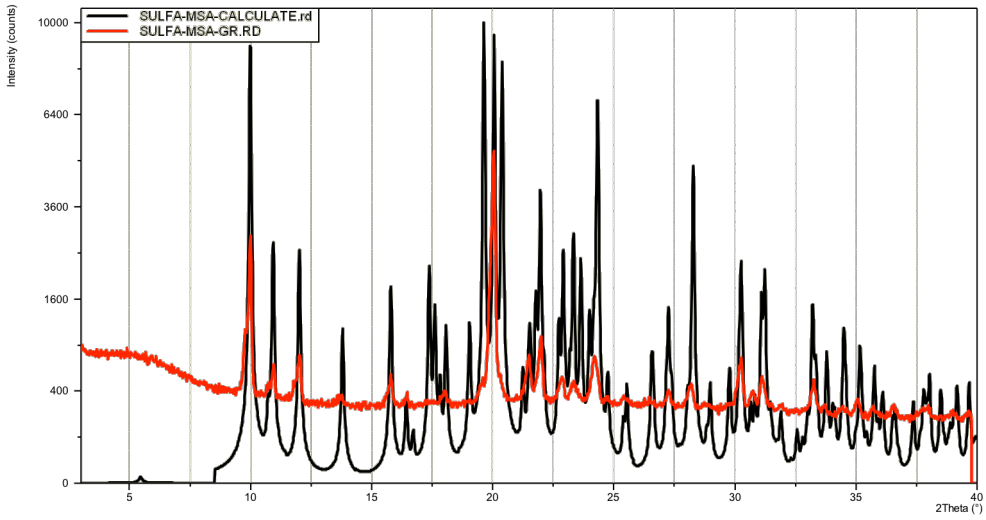

Figure 5. Comparison between XRD patterns of **3f** salt calculate (black line) and experimental (red line).

Crystal data and details of measurements for compounds **3g** and **3f** are summarized in table 3.

Table 3. Crystal data of **3** salts.

compound	**3g**	**3f**
Formula	C14 H19 N5 O2 S	C11 H14 N4 O5 S2
M_r	321.40	346.38
system	ORTHOROMBIC	TRICLINIC
space group	$Pna2_1$	P-1
a [Å]	10.9847(5)	5(6)
b [Å]	12.8697(5)	9(1)
c [Å]	10.7788(4)	16(2)
α [°]	90	82(1)
β [°]	90	86(1)
γ[°]	90	78(1)
V [Å³]	1523.80(1)	784.148
Z	4	2
d_{calc}	1.401	1.467
F(000)	680	360
measured reflns	4366	5833
unique reflns	2255	3502
refined parameters	216	268
GOF on F²	0.931	0.911
R1 [on F, I>2σ(I)]	0.0334	0.0439
wR2(onF²,all data)	0.0670	0.1047

5.4. Conclusion

In this work **3** was studied by polymorph and salt/co-crystal screening to identify new crystal forms. The API was made to react with a co-former (solid or liquid) through different methods: crystallization by solution, grinding, kneading and solid-gas reactions The screening allowed the discovery of six salts and one co-crystal (**3c** with formic acid) – Scheme 4, 5 - characterized by X-ray powder diffraction (XRPD), differential scanning calorimetry (DSC), thermogravimetric analysis (TGA), evolved gas analysis (EGA), FT-IR (See supplementary material). The salts **3f** and **3g** were also characterized by single crystal X-ray diffraction (SC-XRD).

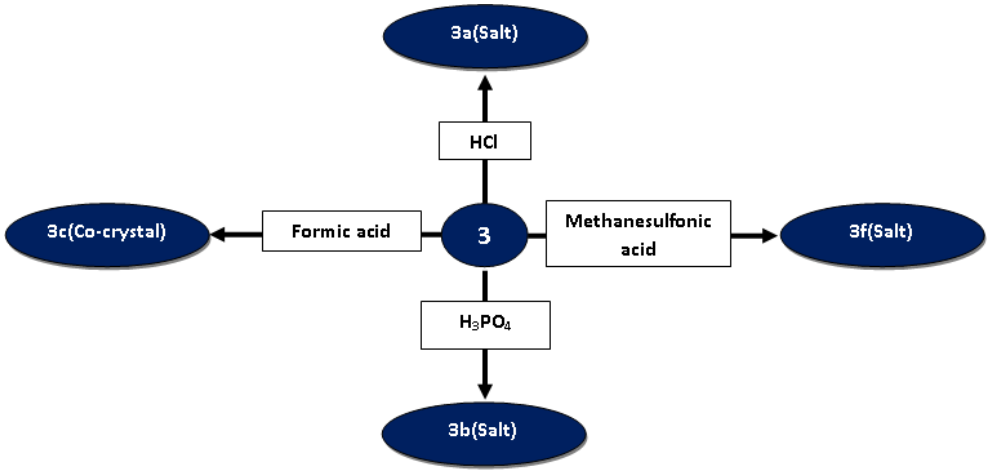

Scheme 4. Reaction of **3** with acids.

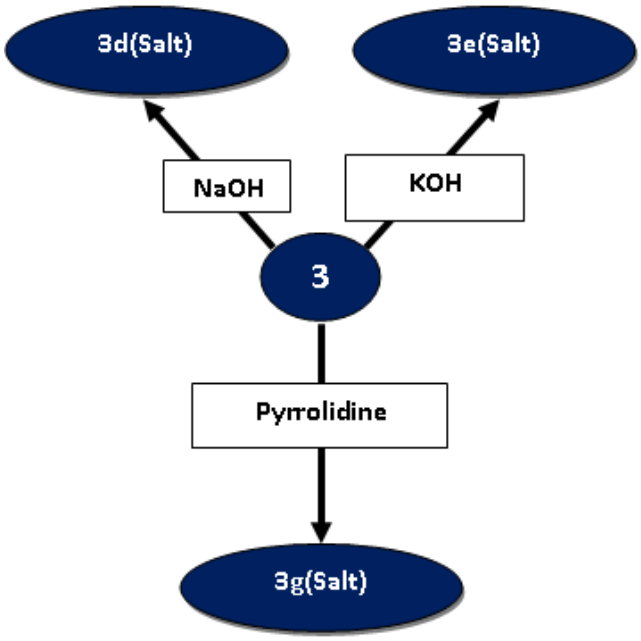

Scheme 5. Reaction of **3** with bases.

5.5. Supplementary Material

Legenda

3 = SULFADIAZINE

3a = Salt obtained by reaction of **3** with HCl

3b= Salt obtained by reaction of **3** with H_3PO_4

3c= Co-crystal obtained by reaction of **3** with formic acid

3d= Salt obtained by reaction of **3** with NaOH

3e= Salt obtained by reaction of **3** with KOH

3g= Salt obtained by reaction of **3** with pyrrolidine

5.5.1. **Thermal measuraments**

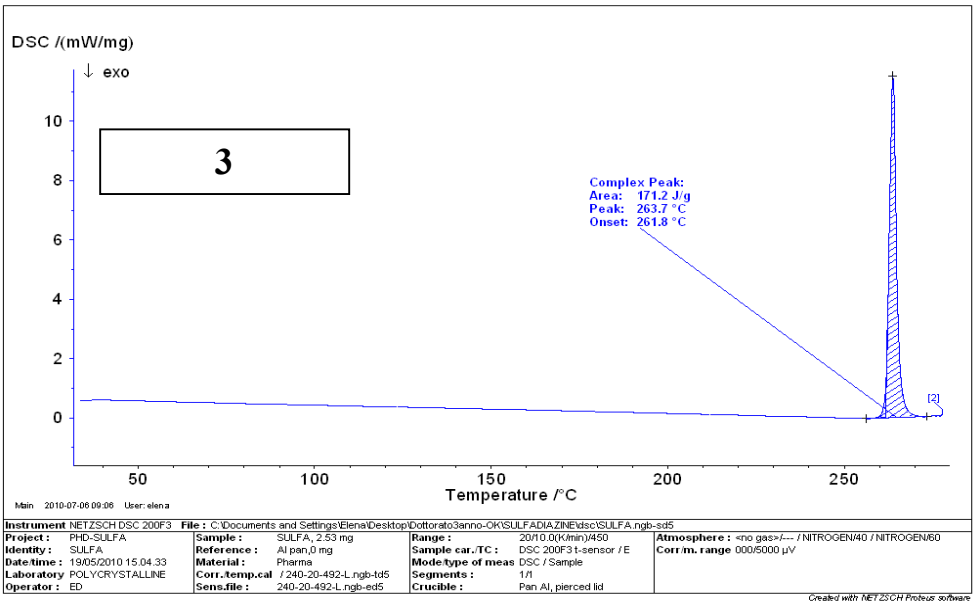

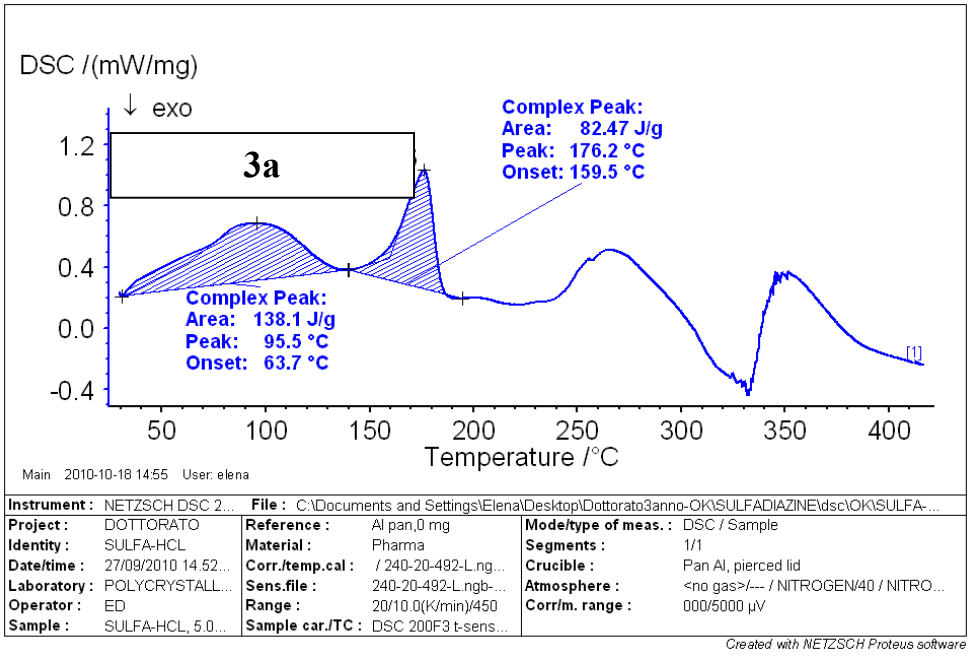

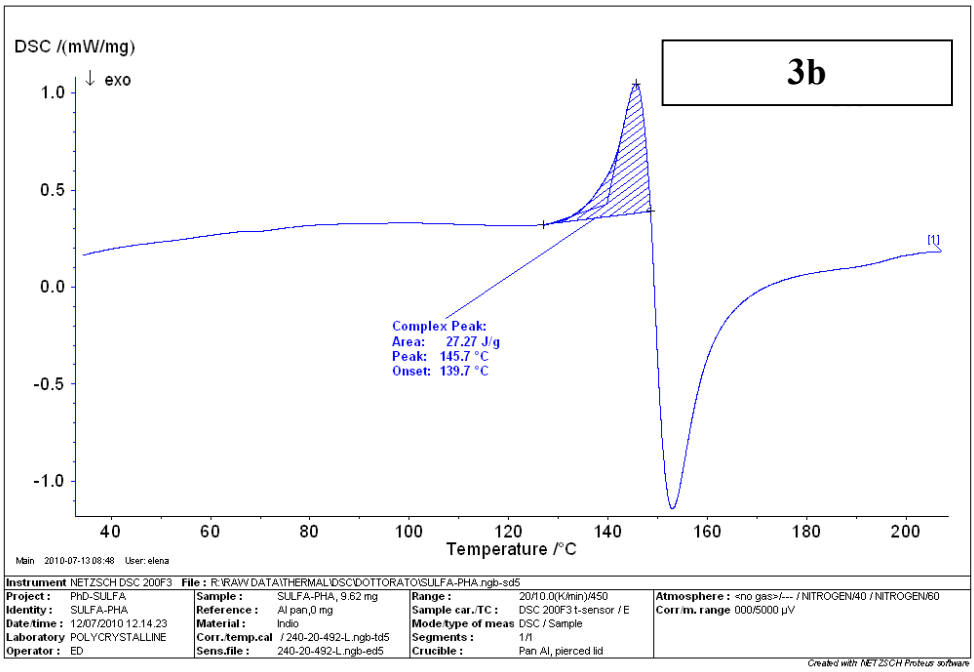
DSC /(mW/mg)
↓ exo
3b
1.0
0.5
0.0
-0.5
-1.0
Complex Peak:
Area: 27.27 J/g
Peak: 145.7 °C
Onset: 139.7 °C
40
60
80
100
120
140
160
180
200
Temperature /°C
Main 2010-07-13 08:48 User: elena
Instrument NETZSCH DSC 200F3 File : R:\RAW DATA\THERMAL\DSC\DOTTORATO\SULFA-PHA.ngb-sd5
Project : PhD-SULFA
Identity : SULFA-PHA
Date/time : 12/07/2010 12.14.23
Laboratory POLYCRYSTALLINE
Operator : ED
Sample : SULFA-PHA, 9.62 mg
Reference : Al pan,0 mg
Material : Indio
Corr./temp.cal / 240-20-492-L.ngb-td5
Sens.file : 240-20-492-L.ngb-ed5
Range : 20/10.0(K/min)/450
Sample car./TC : DSC 200F3 t-sensor / E
Mode/type of meas DSC / Sample
Segments : 1/1
Crucible : Pan Al, pierced lid
Atmosphere : <no gas>/--- / NITROGEN/40 / NITROGEN/60
Corr/m. range 000/5000 µV
Created with NETZSCH Proteus software

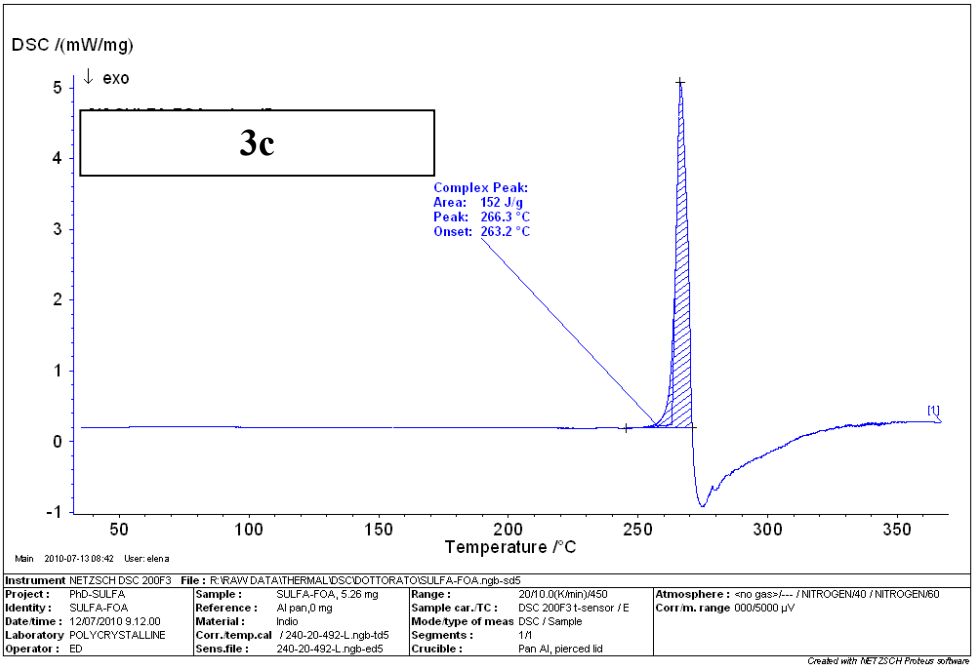
DSC /(mW/mg)
↓ exo
3c
5
4
3
2
1
0
-1
Complex Peak:
Area: 152 J/g
Peak: 266.3 °C
Onset: 263.2 °C
50
100
150
200
250
300
350
Temperature /°C
Main 2010-07-13 08:42 User: elena
Instrument NETZSCH DSC 200F3 File : R:\RAW DATA\THERMAL\DSC\DOTTORATO\SULFA-FOA.ngb-sd5
Project : PhD-SULFA
Identity : SULFA-FOA
Date/time : 12/07/2010 9.12.00
Laboratory POLYCRYSTALLINE
Operator : ED
Sample : SULFA-FOA, 5.26 mg
Reference : Al pan,0 mg
Material : Indio
Corr./temp.cal / 240-20-492-L.ngb-td5
Sens.file : 240-20-492-L.ngb-ed5
Range : 20/10.0(K/min)/450
Sample car./TC : DSC 200F3 t-sensor / E
Mode/type of meas DSC / Sample
Segments : 1/1
Crucible : Pan Al, pierced lid
Atmosphere : <no gas>/--- / NITROGEN/40 / NITROGEN/60
Corr/m. range 000/5000 µV
Created with NETZSCH Proteus software

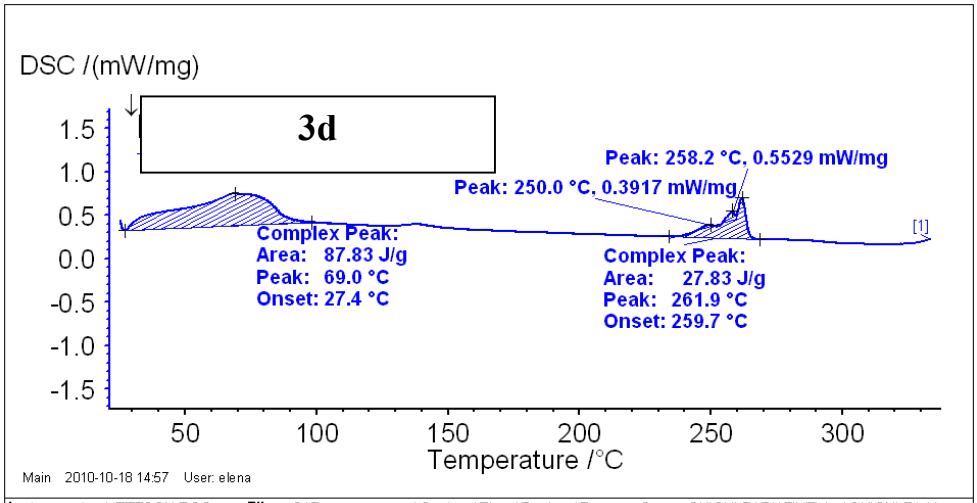

Instrument :	NETZSCH DSC...	**File :**	C:\Documents and Settings\Elena\Desktop\Dottorato3anno-OK\SULFADIAZINE\dsc\OK\SULFA-N...		
Project :	DOTTORATO	**Reference :**	Al pan,0 mg	**Mode/type of meas. :**	DSC / Sample
Identity :	SULFA-NAOH	**Material :**	Pharma	**Segments :**	1/1
Date/time :	27/09/2010 15.58.45	**Corr./temp.cal :**	/ 240-20-492-L.ng...	**Crucible :**	Pan Al, pierced lid
Laboratory :	POLYCRYSTALLI...	**Sens.file :**	240-20-492-L.ngb-...	**Atmosphere :**	<no gas>/--- / NITROGEN/40 / NITRO...
Operator :	ED	**Range :**	20/10.0(K/min)/450	**Corr/m. range :**	000/5000 µV
Sample :	SULFA-NAOH, 5.7...	**Sample car./TC :**	DSC 200F3 t-sens...		

Created with NETZSCH Proteus software

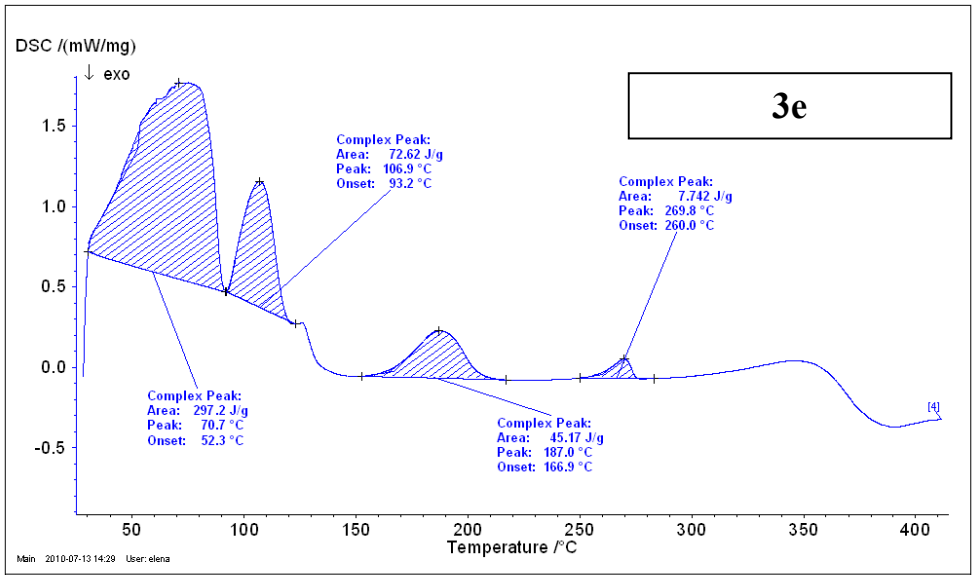

Instrument	NETZSCH DSC 200F3	**File :**	R:\RAW DATA\THERMAL\DSC\DOTTORATO\SULFA-KOH-PA.ngb-sd5				
Project :	PhD-SULFA	**Sample :**	SULFA-KOH-PA, 9.84 mg	**Range :**	20/10.0(K/min)/450	**Atmosphere :**	<no gas>/--- / NITROGEN/40 / NITROGEN/60
Identity :	SULFA-KOH-PA	**Reference :**	Al pan,0 mg	**Sample car./TC :**	DSC 200F3 t-sensor / E	**Corr/m. range**	000/5000 µV
Date/time :	13/07/2010 10.56.29	**Material :**	Indio	**Mode/type of meas**	DSC / Sample		
Laboratory	POLYCRYSTALLINE	**Corr./temp.cal**	/ 240-20-492-L.ngb-td5	**Segments :**	1/1		
Operator :	ED	**Sens.file :**	240-20-492-L.ngb-ed5	**Crucible :**	Pan Al, pierced lid		

Created with NETZSCH Proteus software

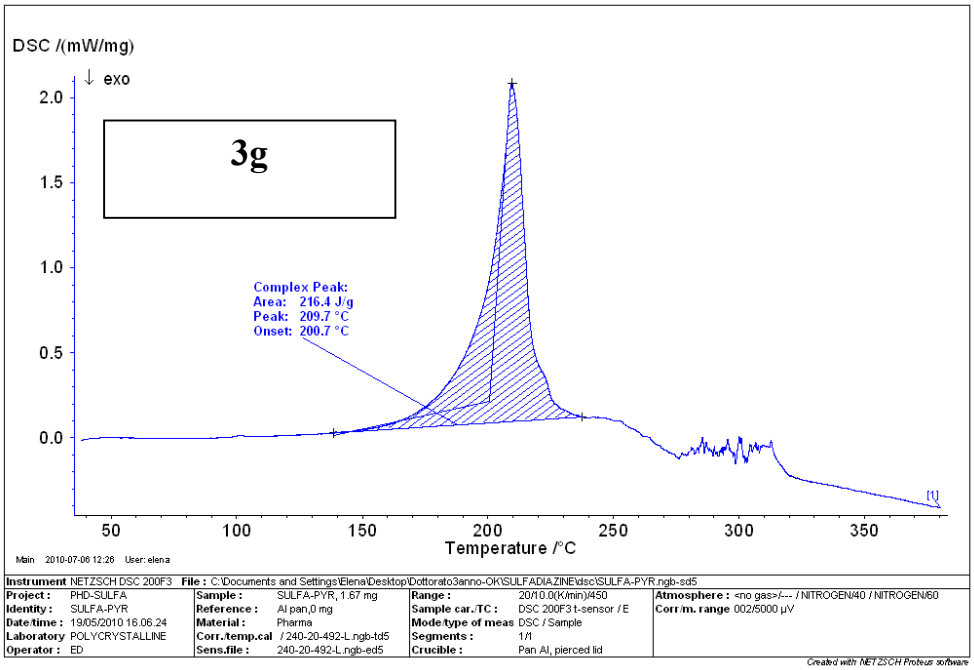
DSC /(mW/mg)
↓ exo
3g
Complex Peak:
Area: 216.4 J/g
Peak: 209.7 °C
Onset: 200.7 °C
Temperature /°C
Main 2010-07-06 12:26 User: elena
Instrument NETZSCH DSC 200F3 File : C:\Documents and Settings\Elena\Desktop\Dottorato3anno-OK\SULFADIAZINE\dsc\SULFA-PYR.ngb-sd5
Project : PHD-SULFA
Identity : SULFA-PYR
Date/time : 19/05/2010 16.06.24
Laboratory POLYCRYSTALLINE
Operator : ED
Sample : SULFA-PYR, 1.67 mg
Reference : Al pan,0 mg
Material : Pharma
Corr./temp.cal / 240-20-492-L.ngb-td5
Sens.file : 240-20-492-L.ngb-ed5
Range : 20/10.0(K/min)/450
Sample car./TC : DSC 200F3 t-sensor / E
Mode/type of meas DSC / Sample
Segments : 1/1
Crucible : Pan Al, pierced lid
Atmosphere : <no gas>/--- / NITROGEN/40 / NITROGEN/60
Corr/m. range 002/5000 µV
Created with NETZSCH Proteus software

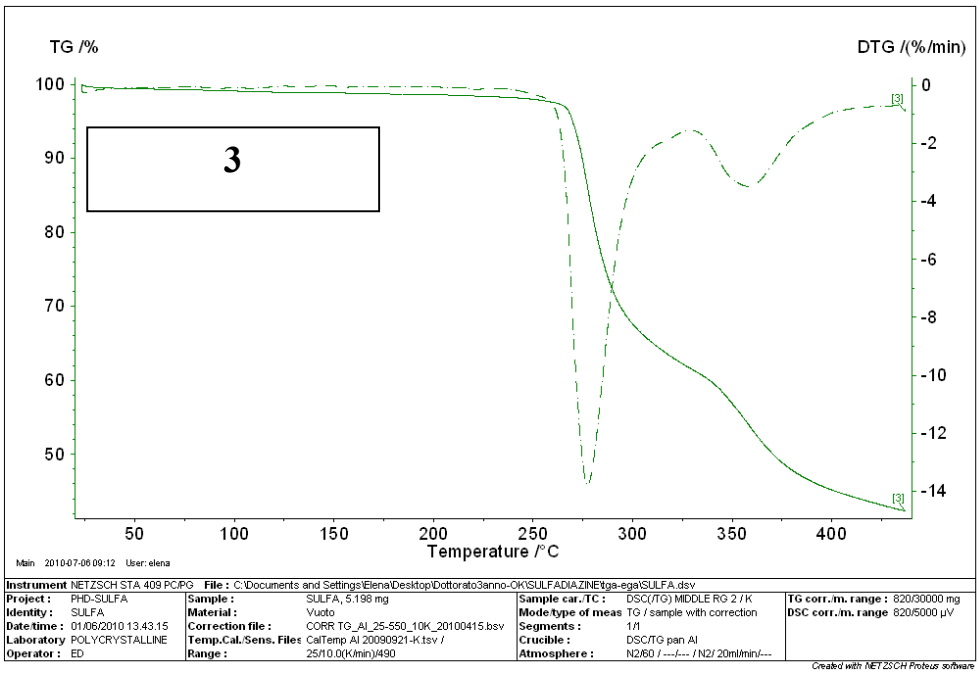
TG /%
DTG /(%/min)
3
Temperature /°C
Main 2010-07-06 09:12 User: elena
Instrument NETZSCH STA 409 PC/PG File : C:\Documents and Settings\Elena\Desktop\Dottorato3anno-OK\SULFADIAZINE\tga-ega\SULFA.dsv
Project : PHD-SULFA
Identity : SULFA
Date/time : 01/06/2010 13.43.15
Laboratory POLYCRYSTALLINE
Operator : ED
Sample : SULFA, 5.198 mg
Material : Vuoto
Correction file : CORR TG_Al_25-550_10K_20100415.bsv
Temp.Cal./Sens. File: CalTemp Al 20090921-K.tsv /
Range : 25/10.0(K/min)/490
Sample car./TC : DSC(/TG) MIDDLE RG 2 / K
Mode/type of meas TG / sample with correction
Segments : 1/1
Crucible : DSC/TG pan Al
Atmosphere : N2/60 / ---/--- / N2/ 20ml/min/---
TG corr./m. range : 820/30000 mg
DSC corr./m. range 820/5000 µV
Created with NETZSCH Proteus software

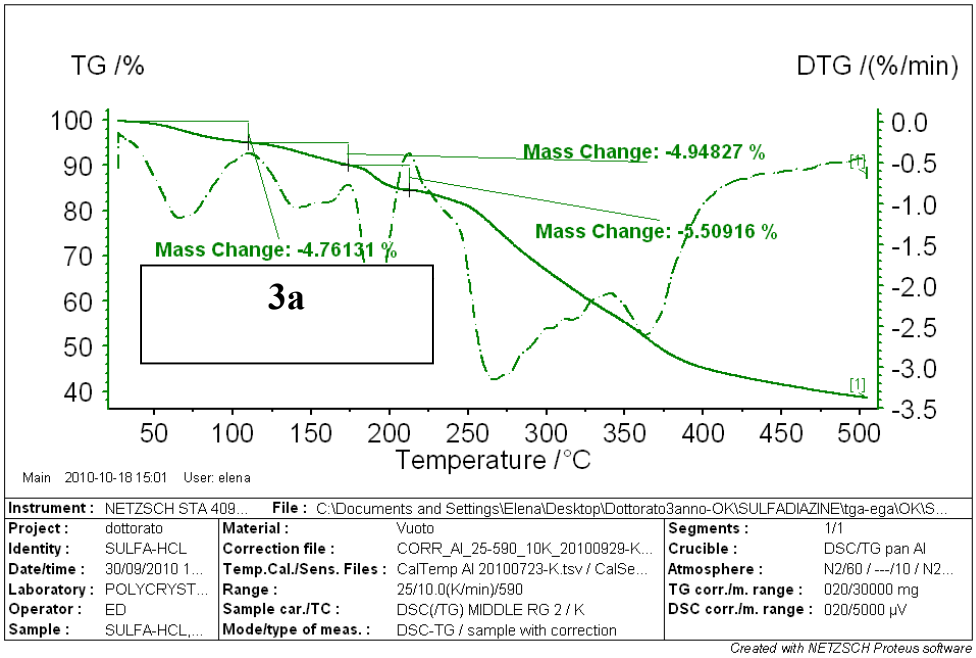

Instrument :	NETZSCH STA 409...	**File :**	C:\Documents and Settings\Elena\Desktop\Dottorato3anno-OK\SULFADIAZINE\tga-ega\OK\S...		
Project :	dottorato	**Material :**	Vuoto	**Segments :**	1/1
Identity :	SULFA-HCL	**Correction file :**	CORR_Al_25-590_10K_20100929-K...	**Crucible :**	DSC/TG pan Al
Date/time :	30/09/2010 1...	**Temp.Cal./Sens. Files :**	CalTemp Al 20100723-K.tsv / CalSe...	**Atmosphere :**	N2/60 / ---/10 / N2...
Laboratory :	POLYCRYST...	**Range :**	25/10.0(K/min)/590	**TG corr./m. range :**	020/30000 mg
Operator :	ED	**Sample car./TC :**	DSC(/TG) MIDDLE RG 2 / K	**DSC corr./m. range :**	020/5000 µV
Sample :	SULFA-HCL,...	**Mode/type of meas. :**	DSC-TG / sample with correction		

Created with NETZSCH Proteus software

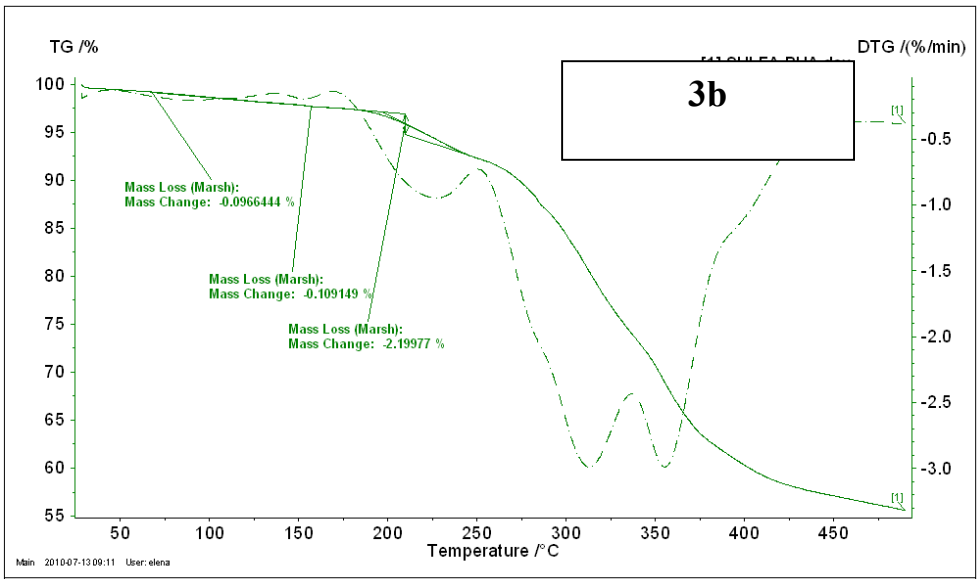

Instrument	NETZSCH STA 409 PC/PG	**File :**	R:\RAW DATA\THERMAL\TGA\DOTT ELENA\SULFA\SULFA-PHA.dsv				
Project :	SULFA	**Sample :**	SULFA-PHA, 21.920 mg	**Sample car./TC :**	DSC(/TG) MIDDLE RG 2 / K	**TG corr./m. range :**	420/30000 mg
Identity :	SULFA-PHA	**Material :**	Vuoto	**Mode/type of meas**	TG / sample with correction	**DSC corr./m. range**	420/5000 µV
Date/time :	12/07/2010 12.22.32	**Correction file :**	CORR TG_Al_25-500_10K_20100708.bsv	**Segments :**	1/1		
Laboratory	POLYCRYSTALLINE	**Temp.Cal./Sens. Files**	CalTemp Al 20090921-K.tsv /	**Crucible :**	DSC/TG pan Al		
Operator :	ED	**Range :**	25/10.0(K/min)/490	**Atmosphere :**	N2/60 / ---/--- / N2/ 20ml/min/---		

Created with NETZSCH Proteus software

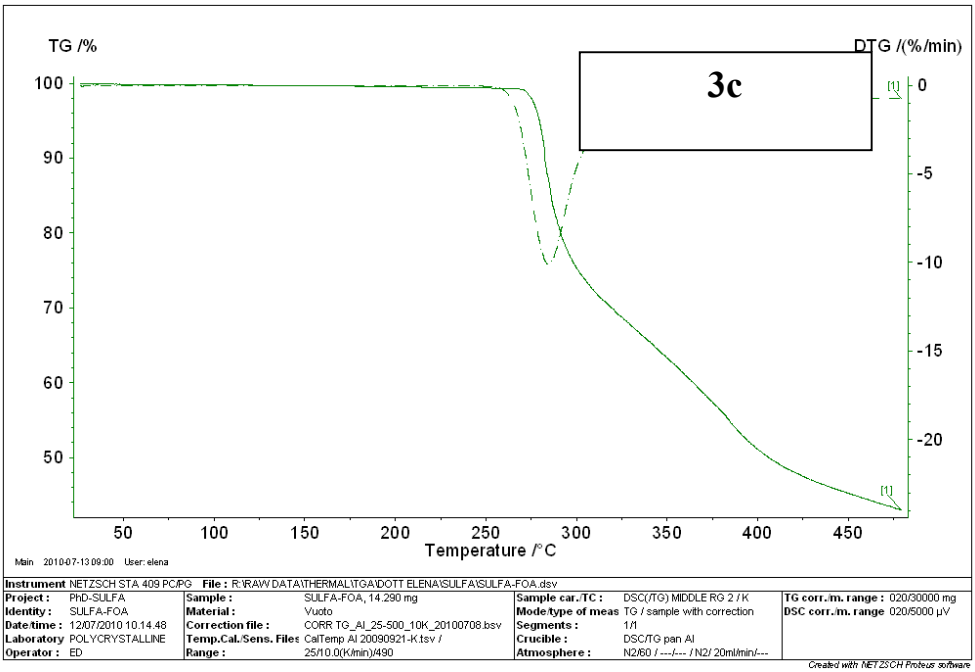
TG /%
DTG /(%/min)
3c
Temperature /°C
Main 2010-07-13 09:00 User: elena
Instrument NETZSCH STA 409 PC/PG File : R:\RAW DATA\THERMAL\TGA\DOTT ELENA\SULFA\SULFA-FOA.dsv
Project : PhD-SULFA
Identity : SULFA-FOA
Date/time : 12/07/2010 10.14.48
Laboratory POLYCRYSTALLINE
Operator : ED
Sample : SULFA-FOA, 14.290 mg
Material : Vuoto
Correction file : CORR TG_Al_25-500_10K_20100708.bsv
Temp.Cal./Sens. Files CalTemp Al 20090921-K.tsv /
Range : 25/10.0(K/min)/490
Sample car./TC : DSC(/TG) MIDDLE RG 2 / K
Mode/type of meas TG / sample with correction
Segments : 1/1
Crucible : DSC/TG pan Al
Atmosphere : N2/60 / ---/--- / N2/ 20ml/min/---
TG corr./m. range : 020/30000 mg
DSC corr./m. range 020/5000 µV
Created with NETZSCH Proteus software

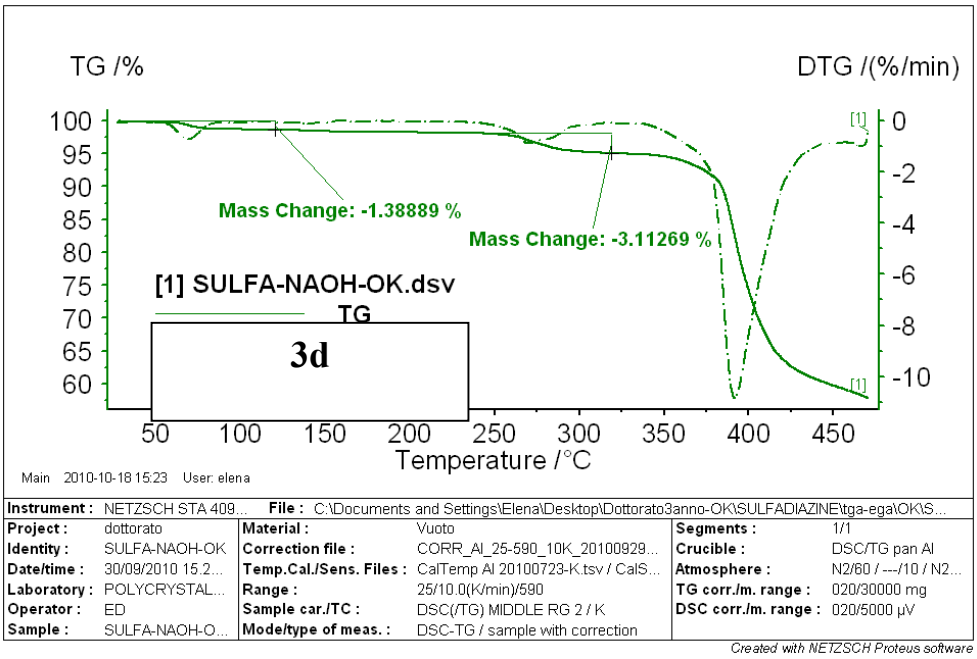
TG /%
DTG /(%/min)
Mass Change: -1.38889 %
Mass Change: -3.11269 %
[1] SULFA-NAOH-OK.dsv
TG
3d
Temperature /°C
Main 2010-10-18 15:23 User: elena
Instrument : NETZSCH STA 409... File : C:\Documents and Settings\Elena\Desktop\Dottorato3anno-OK\SULFADIAZINE\tga-ega\OK\S...
Project : dottorato
Identity : SULFA-NAOH-OK
Date/time : 30/09/2010 15.2...
Laboratory : POLYCRYSTAL...
Operator : ED
Sample : SULFA-NAOH-O...
Material : Vuoto
Correction file : CORR_Al_25-590_10K_20100929...
Temp.Cal./Sens. Files : CalTemp Al 20100723-K.tsv / CalS...
Range : 25/10.0(K/min)/590
Sample car./TC : DSC(/TG) MIDDLE RG 2 / K
Mode/type of meas. : DSC-TG / sample with correction
Segments : 1/1
Crucible : DSC/TG pan Al
Atmosphere : N2/60 / ---/10 / N2...
TG corr./m. range : 020/30000 mg
DSC corr./m. range : 020/5000 µV
Created with NETZSCH Proteus software

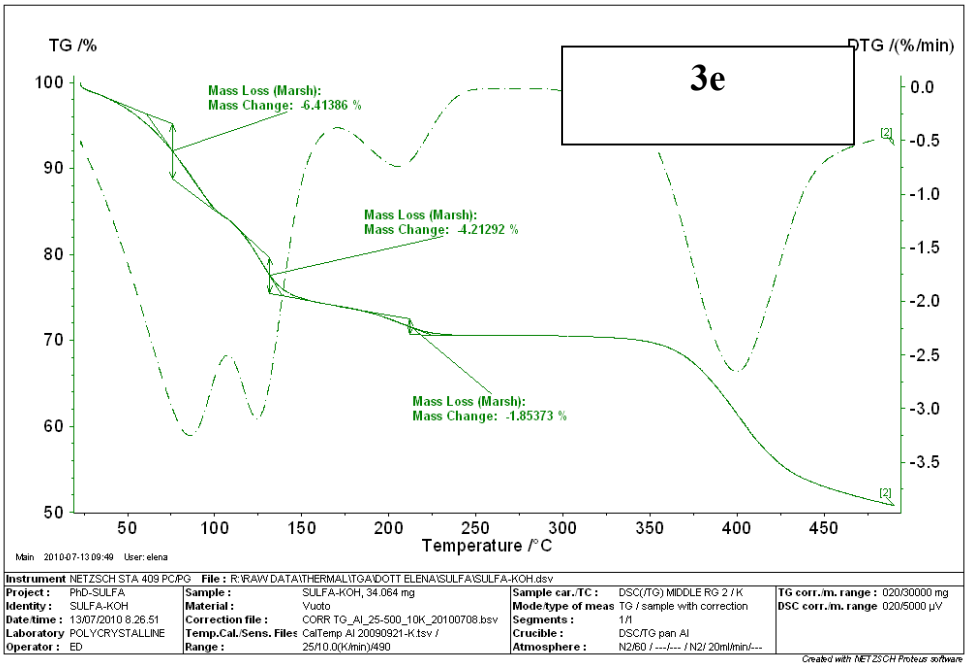
TG /%
DTG /(%/min)
3e
Mass Loss (Marsh):
Mass Change: -6.41386 %
Mass Loss (Marsh):
Mass Change: -4.21292 %
Mass Loss (Marsh):
Mass Change: -1.85373 %
Temperature /°C
Main 2010-07-13 09:49 User: elena
Instrument NETZSCH STA 409 PC/PG File : R:\RAW DATA\THERMAL\TGA\DOTT ELENA\SULFA\SULFA-KOH.dsv
Project : PhD-SULFA
Identity : SULFA-KOH
Date/time : 13/07/2010 8.26.51
Laboratory POLYCRYSTALLINE
Operator : ED
Sample : SULFA-KOH, 34.064 mg
Material : Vuoto
Correction file : CORR TG_Al_25-500_10K_20100708.bsv
Temp.Cal./Sens. Files CalTemp Al 20090921-K.tsv /
Range : 25/10.0(K/min)/490
Sample car./TC : DSC(/TG) MIDDLE RG 2 / K
Mode/type of meas TG / sample with correction
Segments : 1/1
Crucible : DSC/TG pan Al
Atmosphere : N2/60 / ---/--- / N2/ 20ml/min/---
TG corr./m. range : 020/30000 mg
DSC corr./m. range 020/5000 µV
Created with NETZSCH Proteus software

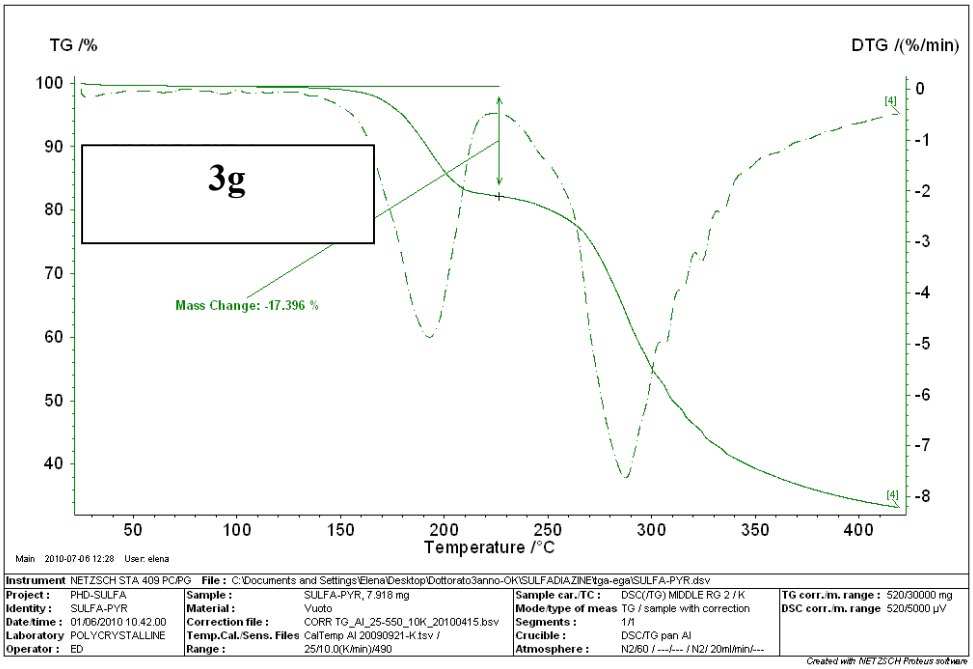
TG /%
DTG /(%/min)
3g
Mass Change: -17.396 %
Temperature /°C
Main 2010-07-06 12:28 User: elena
Instrument NETZSCH STA 409 PC/PG File : C:\Documents and Settings\Elena\Desktop\Dottorato3anno-OK\SULFADIAZINE\tga-ega\SULFA-PYR.dsv
Project : PHD-SULFA
Identity : SULFA-PYR
Date/time : 01/06/2010 10.42.00
Laboratory POLYCRYSTALLINE
Operator : ED
Sample : SULFA-PYR, 7.918 mg
Material : Vuoto
Correction file : CORR TG_Al_25-550_10K_20100415.bsv
Temp.Cal./Sens. Files CalTemp Al 20090921-K.tsv /
Range : 25/10.0(K/min)/490
Sample car./TC : DSC(/TG) MIDDLE RG 2 / K
Mode/type of meas TG / sample with correction
Segments : 1/1
Crucible : DSC/TG pan Al
Atmosphere : N2/60 / ---/--- / N2/ 20ml/min/---
TG corr./m. range : 520/30000 mg
DSC corr./m. range 520/5000 µV
Created with NETZSCH Proteus software

5.5.2. **FT-IR**

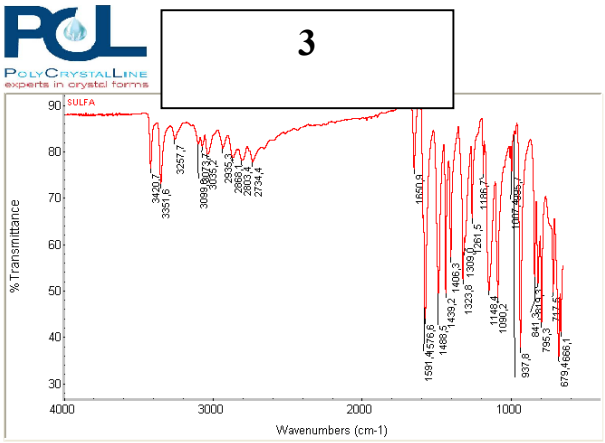

Detector: DTGS KBr
Beamsplitter: KBr
Source: IR

Number of sample scans: 32
Number of background scans: 32
Resolution: 4,000
Sample gain: 4,0
Optical velocity: 0,6329
Aperture: 100,00

Thu Jul 15 16:14:16 2010 (GMT+02:00)
FIND PEAKS:
Spectrum: SULFA
Region: 4000,0 400,0
Absolute threshold: 83,727
Sensitivity: 80
Peak list:

Position:	666,1	Intensity:	40,653
Position:	679,4	Intensity:	35,414
Position:	717,5	Intensity:	49,506
Position:	795,3	Intensity:	42,656
Position:	819,3	Intensity:	51,300
Position:	841,3	Intensity:	52,722
Position:	937,8	Intensity:	37,297
Position:	972,3	Intensity:	83,566
Position:	995,7	Intensity:	75,587
Position:	1007,4	Intensity:	78,368
Position:	1090,2	Intensity:	48,042
Position:	1148,4	Intensity:	49,877
Position:	1186,7	Intensity:	74,662
Position:	1261,5	Intensity:	65,424
Position:	1309,0	Intensity:	60,147
Position:	1323,8	Intensity:	52,026
Position:	1406,3	Intensity:	56,891
Position:	1439,2	Intensity:	49,059
Position:	1488,5	Intensity:	49,307
Position:	1576,6	Intensity:	43,480
Position:	1591,4	Intensity:	65,509
Position:	1650,9	Intensity:	76,103
Position:	2734,4	Intensity:	77,657
Position:	2803,4	Intensity:	77,907
Position:	2868,1	Intensity:	78,547
Position:	2935,3	Intensity:	80,581
Position:	3035,2	Intensity:	79,275
Position:	3073,7	Intensity:	80,924
Position:	3099,6	Intensity:	81,514
Position:	3257,7	Intensity:	82,543
Position:	3351,6	Intensity:	73,005
Position:	3420,7	Intensity:	76,230

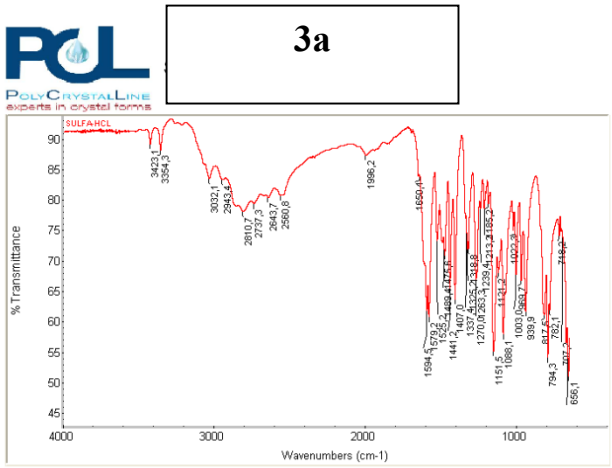

Detector: DTGS KBr
Beamsplitter: KBr
Source: IR

Number of sample scans: 32
Number of background scans: 32
Resolution: 4,000
Sample gain: 4,0
Optical velocity: 0,6329
Aperture: 100,00

Wed Jul 14 08:42:24 2010 (GMT+02:00)
FIND PEAKS:
Spectrum: SULFA-HCL
Region: 4000,0 400,0
Absolute threshold: 89,498
Sensitivity: 80
Peak list:

Position:	656,1	Intensity:	50,832
Position:	670,3	Intensity:	56,185
Position:	707,2	Intensity:	74,721
Position:	718,2	Intensity:	73,915
Position:	782,1	Intensity:	61,675
Position:	794,3	Intensity:	53,917
Position:	817,5	Intensity:	60,868
Position:	939,9	Intensity:	61,474
Position:	969,7	Intensity:	66,563
Position:	1003,0	Intensity:	67,550
Position:	1022,3	Intensity:	74,901
Position:	1088,1	Intensity:	57,725
Position:	1121,2	Intensity:	67,798
Position:	1151,5	Intensity:	55,021
Position:	1185,2	Intensity:	79,212
Position:	1213,2	Intensity:	78,417
Position:	1239,4	Intensity:	78,399
Position:	1263,3	Intensity:	67,110
Position:	1270,0	Intensity:	66,580
Position:	1318,8	Intensity:	71,887
Position:	1325,2	Intensity:	71,681
Position:	1337,4	Intensity:	76,769
Position:	1407,0	Intensity:	63,344
Position:	1441,2	Intensity:	65,295
Position:	1475,6	Intensity:	70,755
Position:	1489,4	Intensity:	72,894
Position:	1525,2	Intensity:	73,127
Position:	1579,2	Intensity:	60,633
Position:	1594,5	Intensity:	61,624
Position:	1650,4	Intensity:	83,733
Position:	1996,2	Intensity:	87,252
Position:	2560,8	Intensity:	80,627
Position:	2643,7	Intensity:	80,299
Position:	2737,3	Intensity:	79,294
Position:	2810,7	Intensity:	77,981
Position:	2943,4	Intensity:	83,210
Position:	3032,1	Intensity:	83,348
Position:	3354,3	Intensity:	88,121
Position:	3423,1	Intensity:	89,097

3b

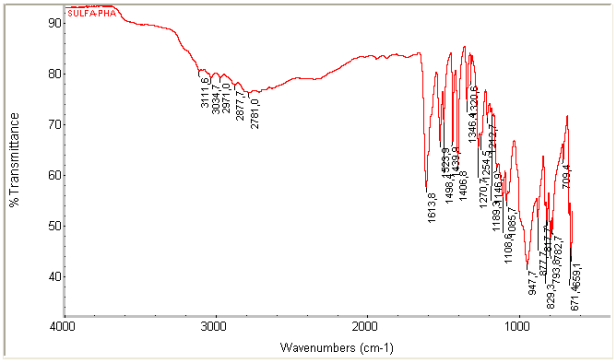

Detector: DTGS KBr
Beamsplitter: KBr
Source: IR

Number of sample scans: 32
Number of background scans: 32
Resolution: 4,000
Sample gain: 4,0
Optical velocity: 0,6329
Aperture: 100,00

Thu Jul 15 15:46:50 2010 (GMT+02:00)
FIND PEAKS:
Spectrum: SULFA-PHA
Region: 4000,0 400,0
Absolute threshold: 81,858
Sensitivity: 80
Peak list:

Position:	659,1	Intensity:	43,733
Position:	671,4	Intensity:	51,853
Position:	709,4	Intensity:	63,011
Position:	782,7	Intensity:	49,072
Position:	793,8	Intensity:	47,423
Position:	817,7	Intensity:	50,615
Position:	829,3	Intensity:	53,672
Position:	877,7	Intensity:	51,279
Position:	947,7	Intensity:	42,251
Position:	1085,7	Intensity:	54,686
Position:	1108,6	Intensity:	55,583
Position:	1146,9	Intensity:	61,269
Position:	1189,3	Intensity:	72,323
Position:	1212,7	Intensity:	71,106
Position:	1254,5	Intensity:	67,612
Position:	1270,7	Intensity:	65,250
Position:	1320,6	Intensity:	78,513
Position:	1346,4	Intensity:	74,518
Position:	1406,8	Intensity:	61,415
Position:	1439,9	Intensity:	66,258
Position:	1498,4	Intensity:	70,238
Position:	1523,9	Intensity:	66,407
Position:	1613,8	Intensity:	57,379
Position:	2781,0	Intensity:	76,065
Position:	2877,7	Intensity:	77,640
Position:	2971,0	Intensity:	79,065
Position:	3034,7	Intensity:	78,964
Position:	3111,6	Intensity:	80,256

3c

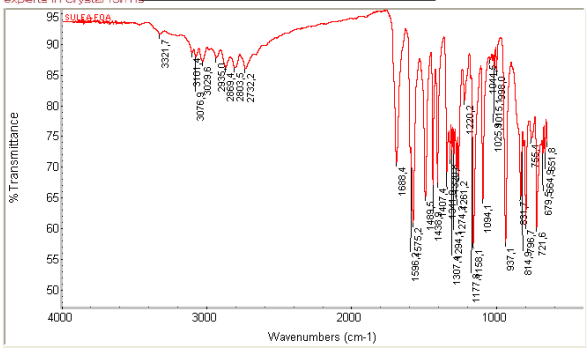

Detector: DTGS KBr
Beamsplitter: KBr
Source: IR

Number of sample scans: 32
Number of background scans: 32
Resolution: 4,000
Sample gain: 4,0
Optical velocity: 0,6329
Aperture: 100,00

Wed Jul 14 08:38:26 2010 (GMT+02:00)
FIND PEAKS:
Spectrum: SULFA-FOA
Region: 4000,0 400,0
Absolute threshold: 91,672
Sensitivity: 80
Peak list:

Position:	651,8	Intensity:	73,895
Position:	664,9	Intensity:	72,229
Position:	679,5	Intensity:	72,005
Position:	721,6	Intensity:	59,995
Position:	755,4	Intensity:	74,512
Position:	796,7	Intensity:	60,400
Position:	814,9	Intensity:	73,074
Position:	831,7	Intensity:	65,021
Position:	937,1	Intensity:	57,665
Position:	998,0	Intensity:	85,398
Position:	1015,1	Intensity:	86,033
Position:	1025,9	Intensity:	87,278
Position:	1044,5	Intensity:	87,445
Position:	1094,1	Intensity:	64,497
Position:	1158,1	Intensity:	57,105
Position:	1177,8	Intensity:	84,303
Position:	1220,2	Intensity:	80,778
Position:	1261,2	Intensity:	68,437
Position:	1274,2	Intensity:	69,822
Position:	1294,1	Intensity:	71,958
Position:	1307,4	Intensity:	72,687
Position:	1320,8	Intensity:	71,104
Position:	1341,8	Intensity:	69,037
Position:	1407,4	Intensity:	67,197
Position:	1438,9	Intensity:	66,905
Position:	1489,5	Intensity:	65,013
Position:	1575,2	Intensity:	60,783
Position:	1596,2	Intensity:	72,074
Position:	1688,4	Intensity:	70,610
Position:	2732,2	Intensity:	85,883
Position:	2803,5	Intensity:	86,085
Position:	2869,4	Intensity:	86,105
Position:	2935,0	Intensity:	87,687
Position:	3029,6	Intensity:	87,051
Position:	3076,9	Intensity:	87,846
Position:	3101,4	Intensity:	88,492
Position:	3321,7	Intensity:	91,486

3d

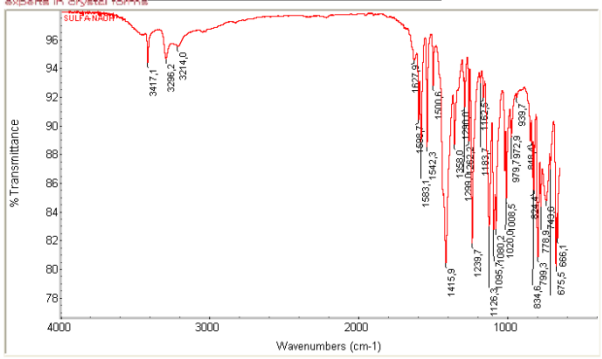

Detector: DTGS KBr
Beamsplitter: KBr
Source: IR

Number of sample scans: 32
Number of background scans: 32
Resolution: 4,000
Sample gain: 4,0
Optical velocity: 0,6329
Aperture: 100,00

Thu Jul 15 15:45:26 2010 (GMT+02:00)
FIND PEAKS:
Spectrum: SULFA-NAOH
Region: 4000,0 400,0
Absolute threshold: 95,881
Sensitivity: 80
Peak list:

Position:	666,1	Intensity:	81,971
Position:	675,5	Intensity:	80,052
Position:	714,8	Intensity:	86,881
Position:	743,6	Intensity:	84,704
Position:	778,9	Intensity:	84,269
Position:	799,3	Intensity:	80,705
Position:	824,4	Intensity:	85,262
Position:	834,6	Intensity:	87,109
Position:	848,4	Intensity:	88,873
Position:	939,7	Intensity:	91,891
Position:	972,9	Intensity:	89,539
Position:	979,7	Intensity:	89,111
Position:	1008,5	Intensity:	84,885
Position:	1020,0	Intensity:	86,792
Position:	1080,2	Intensity:	82,706
Position:	1095,7	Intensity:	82,652
Position:	1126,3	Intensity:	82,911
Position:	1162,5	Intensity:	91,921
Position:	1183,7	Intensity:	92,890
Position:	1239,7	Intensity:	81,736
Position:	1262,2	Intensity:	88,588
Position:	1290,0	Intensity:	91,272
Position:	1299,0	Intensity:	92,995
Position:	1358,0	Intensity:	88,621
Position:	1415,9	Intensity:	80,383
Position:	1500,6	Intensity:	92,717
Position:	1542,3	Intensity:	88,396
Position:	1583,1	Intensity:	88,813
Position:	1598,7	Intensity:	90,355
Position:	1627,9	Intensity:	94,550
Position:	3214,0	Intensity:	95,480
Position:	3296,2	Intensity:	94,623
Position:	3417,1	Intensity:	94,360

3e

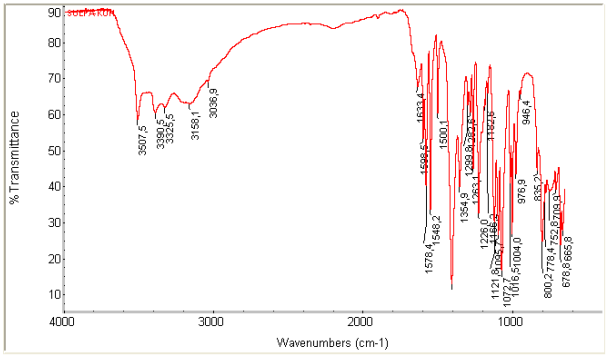

Detector: DTGS KBr
Beamsplitter: KBr
Source: IR

Number of sample scans: 32
Number of background scans: 32
Resolution: 4,000
Sample gain: 8,0
Optical velocity: 0,6329
Aperture: 100,00

Thu Jul 15 15:48:58 2010 (GMT+02:00)
FIND PEAKS:
Spectrum: SULFA-KOH
Region: 4000,0 400,0
Absolute threshold: 74,965
Sensitivity: 80
Peak list:

Position:	665,8	Intensity:	27,489
Position:	678,8	Intensity:	23,385
Position:	709,9	Intensity:	38,850
Position:	752,8	Intensity:	38,494
Position:	778,4	Intensity:	37,750
Position:	800,2	Intensity:	24,440
Position:	835,2	Intensity:	44,229
Position:	946,4	Intensity:	65,371
Position:	976,9	Intensity:	42,734
Position:	1004,0	Intensity:	25,809
Position:	1016,5	Intensity:	40,582
Position:	1072,7	Intensity:	16,223
Position:	1095,7	Intensity:	26,322
Position:	1121,8	Intensity:	29,821
Position:	1166,2	Intensity:	65,695
Position:	1182,6	Intensity:	62,323
Position:	1226,0	Intensity:	32,155
Position:	1263,1	Intensity:	44,689
Position:	1282,6	Intensity:	60,461
Position:	1299,8	Intensity:	62,535
Position:	1354,9	Intensity:	39,552
Position:	1407,3	Intensity:	12,656
Position:	1500,1	Intensity:	59,997
Position:	1548,2	Intensity:	33,196
Position:	1578,4	Intensity:	39,254
Position:	1598,5	Intensity:	53,051
Position:	1633,4	Intensity:	67,436
Position:	3036,9	Intensity:	68,688
Position:	3158,1	Intensity:	62,698
Position:	3325,5	Intensity:	61,571
Position:	3390,5	Intensity:	60,214
Position:	3507,5	Intensity:	58,276

PolyCrystalLine
experts in crystal forms

3g

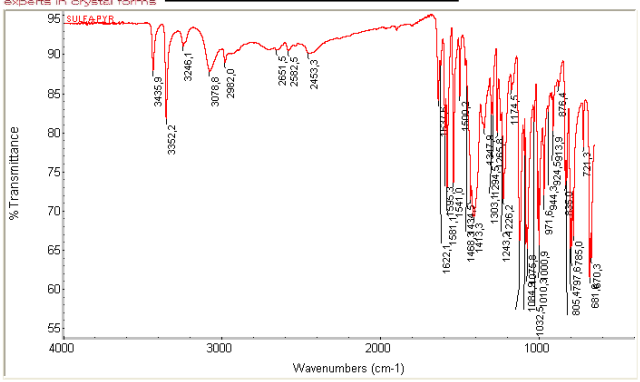

Detector: DTGS KBr
Beamsplitter: KBr
Source: IR

Number of sample scans: 32
Number of background scans: 32
Resolution: 4,000
Sample gain: 4,0
Optical velocity: 0,6329
Aperture: 100,00

Thu Jul 15 16:13:16 2010 (GMT+02:00)
FIND PEAKS:
Spectrum: SULFA-PYR
Region: 4000,0 400,0
Absolute threshold: 91,788
Sensitivity: 80
Peak list:

Position:	670,3	Intensity:	83,628
Position:	681,6	Intensity:	81,053
Position:	721,3	Intensity:	78,093
Position:	785,0	Intensity:	66,682
Position:	797,6	Intensity:	65,204
Position:	805,4	Intensity:	64,747
Position:	825,5	Intensity:	74,104
Position:	835,0	Intensity:	73,116
Position:	876,4	Intensity:	85,809
Position:	913,9	Intensity:	80,072
Position:	924,5	Intensity:	84,438
Position:	944,3	Intensity:	82,544
Position:	971,6	Intensity:	71,862
Position:	1000,9	Intensity:	65,426
Position:	1010,3	Intensity:	70,190
Position:	1032,5	Intensity:	81,247
Position:	1075,8	Intensity:	64,970
Position:	1084,9	Intensity:	65,085
Position:	1098,0	Intensity:	78,060
Position:	1123,4	Intensity:	66,032
Position:	1174,5	Intensity:	85,396
Position:	1226,2	Intensity:	71,394
Position:	1243,2	Intensity:	81,408
Position:	1265,8	Intensity:	79,604
Position:	1294,5	Intensity:	82,012
Position:	1303,1	Intensity:	82,165
Position:	1347,9	Intensity:	80,352
Position:	1413,3	Intensity:	69,074
Position:	1434,5	Intensity:	71,302
Position:	1468,3	Intensity:	88,458
Position:	1500,2	Intensity:	84,600
Position:	1541,0	Intensity:	73,563
Position:	1581,1	Intensity:	72,868
Position:	1595,3	Intensity:	79,569
Position:	1622,1	Intensity:	88,527
Position:	1637,6	Intensity:	83,920
Position:	2453,3	Intensity:	89,991
Position:	2562,5	Intensity:	90,370
Position:	2651,5	Intensity:	90,449
Position:	2982,0	Intensity:	88,847
Position:	3078,8	Intensity:	87,743
Position:	3246,1	Intensity:	91,015
Position:	3352,2	Intensity:	81,615
Position:	3435,9	Intensity:	87,782

5.6. References

1. T. Owa, T. Nagasu, *Expert Opin. Ther. Pat.* **2000**, *10*, 1725-1740.
2. W. Haasnoot, G. Cazemier, J. D. Pre, A. Kemmers-Voncken, M. Bienenmann-Ploum, R. Verheijen, *Food Agric. Immunol.,***2000**, *12*, 15-30.
3. K. Suganya, S. Kabilan, *Acta A*, **2004**, *60*, 1225-1228.
4. P. Patel, S. Korgaokar, K. Parikh, H. Parekh, *Indian J. Chem.B*, **1999**, *38,* 696-700.
5. M. R. Caira, *Molecular Pharmaceutics,* **2007**, *Vol.4, No. 3,* 310-316.
6. D. A. Adsmond, D. J. W. Grant, *Journal of Pharmaceutical Sciences,* **2001**, *Vol.90, No. 12,* 2058
7. S. Sanly, Y. Altun, N. Sanli, G. Alsancak, J. L. Beltran, *J. Chem. Eng. Data,***2009**, *54*, 3014-3021.
8. M. K. Kokila, Puttarja, M. V. Kulkarni, S. Thampi, *ActaCrystallogr., Sect. C: Cryst.Struct.Commun.,***1995**, *51*, 333.
9. D. Braga, M. Curzi, E. Dichiarante, S. L. Giaffreda, F. Grepioni, L. Maini, G. Palladino, A. Pettersen, M. Polito in *Engineering of CrystallineMaterialsProperties*(Eds. J. J. Novoa, D. Braga, L. Addadi), Springer*,* **2008**, pp. 131-156.
10. *(a)* G. M. Sheldrick, *SHELX97*, *Program for Crystal Structure Determination*; University of Göttingen: Göttingen, Germany, 1997; *(b)* E. Keller, SCHAKAL99, Graphical Representation of Molecular Models, University of Freiburg, Germany, 1999; *(c)* A. L. Speck, PLATON; *ActaCrystallogr*., *Sect*. *A*, 1990, 46, C34.